Molecular and functional analysis of novel regulators of defense hormone signaling

Marciel Pereira Mendes

Molecular and functional analysis of novel regulators of defense hormone signaling
PhD thesis
Marciel Pereira Mendes, September 2019
Utrecht University - Plant-Microbe Interactions

ISBN: 978-90-393-7176-3

Cover: Marciel Pereira Mendes
Layout: Anna Bleeker | persoonlijkproefschrift.nl
Printing: Ridderprint BV | www.ridderprint.nl

Molecular and functional analysis of novel regulators of defense hormone signaling

Moleculaire en functionele analyse van nieuwe regulatoren van
afweer-gerelateerde hormoonsignalering
(met een samenvatting in het Nederlands)

Proefschrift

ter verkrijging van de graad van doctor aan de Universiteit Utrecht op gezag van de rector magnificus, prof.dr. H.R.B.M. Kummeling, ingevolge het besluit van het college voor promoties in het openbaar te verdedigen op dinsdag 24 september 2019 des ochtends te 10.30 uur

door

Marciel Pereira Mendes

geboren op 6 november 1989
te Dourados, Brazilië

Promotor:	Prof. dr. ir. C.M.J. Pieterse
Copromotoren:	Dr. S.C.M. van Wees
	Dr. R. Hickman

This thesis was partly accomplished with financial support from Brazilian Federal Government, Science Without Borders program.

CONTENTS

1

General Introduction

1. HORMONAL SIGNALING IN THE PLANT HOLOBIONT

Biological structures in living organisms are often delineated as a network consisting of intricate interactions between biological components, such as genes, proteins, and metabolites. Because plants in nature are constantly interacting with their biotic and abiotic environment, they evolved a highly sophisticated environmental signaling network to be able to swiftly adapt to their, often hostile, environment. A relatively small number of pathogenic microbes untune this network to start a pathogenic relationship with their hosts. Although such successful pathogens can have devastating effects on plant survival in both agricultural and ecological settings, the majority of the microbes that interact with plants are neutral or beneficial. Like pathogens, beneficial microbes can also tune the environmental signaling network to their own advantage and start a long-term mutually beneficial relationship with their host. The collective association of plants with their interacting organisms is called "the holobiont" (Vandenkoornhuyse et al., 2015). The gene regulatory networks within and between the interacting organisms in the plant holobiont are coupled in a super interaction network that micromanages the plant-microbe interactions in the system (Nobori et al., 2018).

1.1. The plant immune system

To survive and establish themselves in a holobiont context, plants need to be able to defend themselves against microbial pathogens and insect herbivores. For that, plants evolved a sophisticated immune system. Unlike animals, plants do not have a circulating immune system. Instead, each single plant cell has the capacity to build up an effective immune response against possible harmful invaders (Couto and Zipfel, 2016). To realize this, plants utilize a recognition system that identifies non-self or modified-self molecules using protein immune receptors localized in the plasma membrane. At the external part of the plant cell, receptor kinases and receptor-like proteins (RLPs) work as pattern-recognition receptors (PRRs) to perceive conserved non-self microbial molecules, such as bacterial flagellin or fungal chitin – so called pathogen/microbe associated molecular patterns (PAMPs/MAMPs) – or modified-self molecules – so called damage-associated molecular patterns (DAMPs). The plant receptor network is composed of receptor kinases with an ectodomain committed in ligand binding, a single transmembrane domain, and an intracellular kinase domain mediating intracellular signaling. Other types of PRRs are RLPs that have the same canonical structure, but miss the intracellular kinase signaling domain (Couto and Zipfel, 2016; Boutrot and Zipfel, 2017). As a consequence, RLPs often depend on other components of the receptor network to transmit ligand recognition into the intracellular immune signaling network (Gust and Felix, 2014). Upon recognition of PAMPs by PRRs, a downstream immune

signaling network is activated resulting in PAMP-triggered immunity (PTI). This first line of defense wards off most of the non-adapted pathogens and prevents infection of the plant (Dangl et al., 2013). Adapted pathogens evolved to circumvent PTI as they can deliver effectors in the host cells that hinder PTI. To counteract this, plants deploy a second layer of immunity called effector-triggered immunity (ETI). During ETI, intracellular nucleotide-binding site leucine-rich repeat proteins (NLRs; also known as NBS-LRRs) recognize pathogen-secreted virulence effectors, setting off downstream ETI signaling, which often results in a hypersensitive response that arrests the invading pathogen (Cui et al., 2015; Berens et al., 2017). Downstream of PTI or ETI activation, intracellular Ca^{2+} and ROS levels rise, and MAPK signaling cascades are activated (Boller and Felix, 2009). These signals together lead to the production of phytohormones, which can trigger extensive transcriptional reprogramming, resulting in an efficient defense response.

1.2 Phytohormones in plant defense

Diverse plant hormones act as central players in modulating the plant immune signaling network (Pieterse et al., 2012). Pathogen infection stimulates the plant to synthesize one or more hormonal signals depending on the type of attacker. Analogous to animal hormones, plant hormones were originally recognized as regulators of growth and development (Santner & Estelle 2009). Hence, it is not surprising that the plant immune signaling network is not only coupled to adaptive plant responses to pathogen or insect attack, but also to developmental processes, such growth and flowering (Greene and Dong, 2018). By finely tuning the plant immune signaling network with the network that regulates growth and development, plants are able to utilize their scarce resources in an economic manner and therewith maximize their survival (Heil and Baldwin, 2002; Vos et al., 2013a).

Historically, salicylic acid (SA), jasmonic acid (JA), and ethylene (ET) were identified as the main phytohormones with important regulatory roles in the plant immune signaling network (Pieterse et al., 2009). SA and the major immune regulator PHYTOALEXIN-DEFICIENT 4 (PAD4) are often associated with defense against biotrophic pathogens, while JA and ET with defense against necrotropic pathogens and insect herbivores, although this generalization does not always hold up (Mur et al., 2006; Spoel et al., 2007; Liu et al., 2016). In the past decade, several other phytohormones, including abscisic acid (ABA), gibberellic acid, auxin, cytokinin and brassinosteroids, were shown to have specific modulating roles in plant immunity (Robert-Seilaniantz et al., 2011; Pieterse et al., 2012; Spoel and Dong, 2012). Extensive research on the role of hormones in plant immunity revealed that hormones act together in a synergistic or antagonistic manner.

During this so-called hormone crosstalk, plants finely tune their defense responses to the invader encountered, therewith maximizing the effectiveness of their immune system, while managing growth and defense in a cost-efficient manner (Spoel and Dong, 2008; Vos et al., 2013a; Caarls et al., 2015).

When PTI or ETI is locally activated at the site of pathogen infection, a systemic defense response is often triggered in distal plant parts to protect these undamaged tissues against subsequent invasion by the pathogen. This long-lasting and broad-spectrum induced disease resistance is called systemic acquired resistance (SAR) (Fu and Dong, 2013). The onset of SAR is accompanied by increased accumulation of SA. SA signaling is controlled by the redox-regulated protein NONEXPRESSOR OF PR GENES1 (NPR1). Upon activation by SA, NPR1 acts as a transcriptional coactivator of a large set of *PR* genes, many of which encode pathogenesis-related proteins with antimicrobial properties (Van Loon et al., 2006). In non-induced cells, NPR1 is sequestered in the cytoplasm as an oligomer through intermolecular disulfide bonds. SA-induced changes in the cellular redox state facilitate monomerization of NPR1, after which it translocates to the nucleus (Tada et al., 2008; Spoel and Dong, 2012). In SA-activated cells, NPR1 interacts with members of the TGA family of transcription factors that bind to the promoters of many SA-responsive genes, like WRKY transcription factors and other downstream transcriptional regulators, to up-regulate downstream defense-related genes (Tsuda and Somssich, 2015). In the past decade, many details of the local and systemic players in the SA sector of the plant immune signaling network have been uncovered and described in a series of excellent reviews (Fu and Dong, 2013; Klessig et al., 2018).

In response to infection by a necrotrophic pathogen or infestation by a herbivorous insect, JA and its derivatives, collectively called jasmonates (JAs), accumulate rapidly. The amino acid conjugate JA-isoleucine (JA-Ile) is the most bioactive JA derivative amongst the JAs (Fonseca et al., 2009). The F-box protein CORONATINE INSENSITIVE1 (COI1) in the E3 ubiquitin ligase SCF^{COI1} complex, and the JASMONATE-ZIM DOMAIN (JAZ) repressor proteins act as JA-Ile co-receptors (Howe and Yoshida, 2019). Upon JA-Ile perception, JAZ repressor proteins are targeted by COI1 for degradation via the 26S proteasome, which leads to de-repression of transcription factors (TFs), like the master regulator MYC2, and subsequent induction of JA-responsive genes, many of which encode proteins with roles in defense against necrotrophic pathogens or insect herbivores. Also, for the local and systemic players in the JA sector of the plant immune signaling network many details have been uncovered in the past decades, which have been excellently captured in a series of reviews (Chini et al., 2016; Wasternack and Song, 2017; Zhang et al., 2017a; Howe et al., 2018).

ET emerged as an important modulator of plant responses to wounding and pathogen attack, therewith fine tuning the defense responses that are initiated by other hormone-regulated defense pathways. ET-responses are mainly regulated by the TF ETHYLENE INSENSITIVE3 (EIN3). Protein-DNA binding data revealed extensive connectivity between EIN3 and the hormone pathways regulated by JA, auxin and ABA (Chang et al., 2013). Such interplay between hormone pathways has a pivotal role in the regulation of plant immune responses and helps the plant to "decide" which defensive strategy to follow, depending on the attacker encountered. The antagonistic effects of hormonal interactions, often referred to as hormone crosstalk, is essential for the cost-efficient regulation of plant development under different stress conditions (Spoel and Dong, 2008; Pieterse et al., 2009; Pieterse et al., 2012; Vos et al., 2013a; Caarls et al., 2015). Interestingly, specialized pathogens evolved to utilize plant hormone crosstalk as a decoy mechanism to obscure the hormone-regulated plant immune signaling network for their own advantage (Robert-Seilaniantz et al., 2011; Pieterse et al., 2012; Howe et al., 2018). Hence, the hormone-regulated plant immune signaling network is vital for plant defense but can also be manipulated by pathogens to increase virulence on their host (Gimenez-Ibanez et al., 2014; Xin et al., 2018).

1.3 Plant interactions with beneficial rhizosphere microbes

Although microbial pathogens have been the focal point of plant immune signaling research for a long time, it becomes more and more clear that the plant immune system also plays an important role in interactions with beneficial microbes (Berendsen et al., 2012; Bakker et al., 2014; Pieterse et al., 2014; Raaijmakers and Mazzola, 2016; Hacquard et al., 2017). Most members of the plant holobiont reside in the rhizosphere, which is highly enriched in microorganisms (Mendes et al., 2013). Members of the rhizosphere microbiome can be beneficial, like plant growth-promoting rhizobacteria (PGPR), or pathogenic, like *Fusarium*, *Pythium*, or *Phytophthora* spp. These soil-borne pathogens infect the plant via the roots causing devastating diseases in economically important crops. Soil-borne pathogens can penetrate roots through natural apertures present at the junction between the main and lateral roots such as epidermal cracks or through young growing tissues which lack secondary cell walls (De Coninck et al., 2015). The detection of MAMPs by PRRs during microbe colonization and the onset of PTI, the first layer of plant immunity, has been extensively described for leaves but is also active in roots (Millet et al., 2010; Berendsen et al., 2012). Application of the bacterial flagellin epitope flg22, or fungal elicitors such as peptidoglycan or chitin to *Arabidopsis thaliana* (hereafter Arabidopsis) roots induced root immune responses (Millet et al., 2010; Stringlis et al., 2018). These MAMP-induced root responses seem mainly modulated by ET signaling, and to a lesser extent by SA and JA (Millet et al.,

2010). Recent studies of the rhizosphere microbiome show that many root microbiota members are engaged in beneficial plant-microbe interactions (Berendsen et al., 2012; Hacquard et al., 2017; Bakker et al., 2018; Cordovez et al., 2019). Many beneficial microbes have developed mechanisms to circumvent PTI defense responses and to form a harmonic interaction with their plant host (Millet et al., 2010; Stringlis et al., 2018). Moreover, selected beneficial microbes have been shown to systemically prime the plant immune system, conferring a broad-spectrum disease resistance referred to as induced systemic resistance (ISR) (Pieterse et al., 2014). ISR requires intact JA and ET signaling pathways, highlighting that also interactions with soil-borne beneficial microbes call upon the hormone-regulated plant immune signaling network.

In the next part, I will review recent findings in research on the gene regulatory networks that are related to plant-microbe interactions in the plant holobiont (Figure 1), with special focus on the regulatory role of phytohormones in this process.

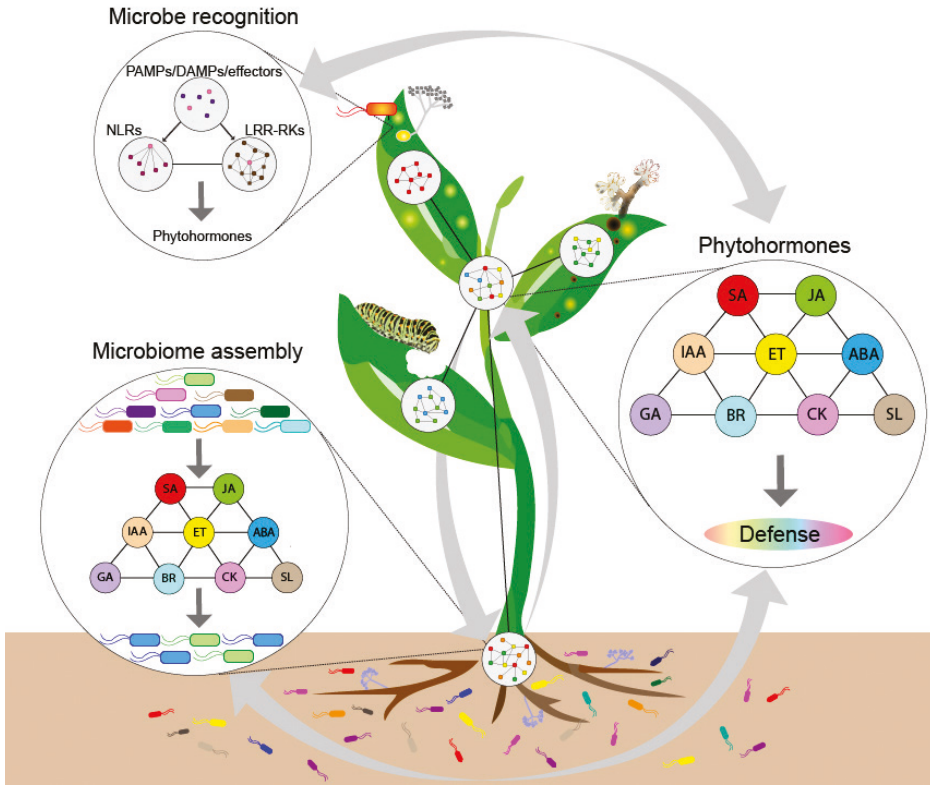

Figure 1. Interconnected sub-networks in the plant immune signaling network of the plant holobiont.

Pathogen and insect pests are recognized by receptor networks, including leucine-rich repeat receptor kinases (LRR-RKs), nucleotide-binding domain and leucine-rich repeat-containing proteins (NLRs). Activation of receptor networks by damage-associated molecular patterns (DAMPs)/pathogen-associated molecular patterns (PAMPs) and effectors leads to activation of the immune signaling network in which phytohormones play an important regulatory role. The plant immune signaling network also interacts with microbiota in the rhizosphere, either in microbial community assembly or in the response to beneficial microbes that prime the plant immune system and/or promote plant growth. SA, salicylic acid; JA, jasmonic acid; IAA, auxin; ET, ethylene; ABA, abscisic acid; GA, gibberellic acid; BR, brassinosteroid; CK, cytokinin; SL, strigolactone.

2. HORMONE-REGULATED IMMUNE SIGNALING NETWORK

The core of the plant immune signaling network consists of cell surface-localized PRRs, mainly leucine-rich repeat receptor kinases (LRR-RKs), that function in a LRR-RK interaction network to recognize MAMPs and DAMPs and activate the plant immune system (Boutrot and Zipfel, 2017; Smakowska-Luzan et al., 2018). The biosynthesis of defense hormones is among the early immune responses when plants recognize a

pathogen or insect. Plants have evolved a collection of hormones that guide the plant to adapt to its environment (Wang et al., 2015a). By exploring the evolution of the defense hormone signaling networks, Berens et al. (2017) provided evidence that the evolution of the signaling pathways regulated by the major defense-related hormones SA and JA coincides with their colonization of land and may, thus, have been a likely requirement for plant survival in more harsh terrestrial environments that included threats caused by microbial pathogens.

In the past decades, the defense signaling pathways regulated by SA and JA have been subject of intense study, culminating in an insightful view of how both hormones regulate downstream defense responses in the plant immune signaling network (for informative reviews see: (Pieterse et al., 2009; Robert-Seilaniantz et al., 2011; Pieterse et al., 2012; Chini et al., 2016; Berens et al., 2017; Howe et al., 2018; Klessig et al., 2018; Wasternack and Feussner, 2018). For SA, a new model for its perception was recently proposed. In this model, the SA master regulator NPR1 and its paralogues NPR3 and NPR4 act as SA receptors. Depending on the cellular SA concentration, NPR1 on the one hand, and NPR3 and NPR4 on the other hand, act in an antagonistic manner to finely control the downstream SA response (Ding et al., 2018; Kazan, 2018). For the JA pathway, the discovery of JAZ repressor proteins accelerated the progress in our understanding of how the biosynthesis of JA and its bioactive form JA-Ile is coupled to transcriptional activation of JA-responsive genes. Basic helix-loop-helix (bHLH) TFs, such as the master regulators MYC2, MYC3 and MYC4, emerged as important binding partners of JAZs and when they become released after 26S proteasome-mediated degradation of the JAZs, they bind to G-box motifs in JA-responsive promoters to regulate the expression a large portion of JA-responsive genes in the JA sector of the plant immune signaling network (Kazan and Manners, 2013). Structural analysis of JAZ9-MYC3 complexes indicated that JAZs competitively inhibit MYC TF binding to the activator interacting domain of MED25 of the Mediator complex, which is a conserved, multiprotein complex that bridges DNA-bound transcription factors and RNA polymerase II, and integrates transcription with a wide variety of cellular signals (Zhang et al., 2015a).

The SA and JA signaling pathways interact with each other in a synergistic or antagonistic manner, depending on the context and activity of other hormones (Pieterse et al., 2009; Robert-Seilaniantz et al., 2011). Crosstalk between defense-related and development-related hormones is implicated in fine-tuning the growth-defense trade-off. Activation of SA and JA pathway can suppress growth to temporarily prioritize defense responses. For instance, SA was shown to inhibit the auxin signaling pathway through stabilization of AUX/IAA repressor proteins (Wang et al., 2007), therewith arresting growth, while

prioritizing defense. Moreover, hormone crosstalk is also thought to help the plant to fine tune its defense response to a single biotic stress, or in prioritizing specific defenses when coping with multiple attackers (Pieterse et al., 2009; Robert-Seilaniantz et al., 2011; Caarls et al., 2015).

2.1 Complexity in hormone network regulation during pathogen attack

The hormone-regulated immune signaling network is complex and in recent years its architecture and dynamics has been studied by analyzing the behavior of gene regulatory networks in single, double, triple and quadruple hormone mutants. This elegant approach allows to dissect the complexity of the network through the genetic removal of specific network sectors and to study the remaining functionality of the plant immune system. In this approach, the network can stepwise reconstruct and assign functions to individual network modules (Windram and Denby, 2015). To this end, all possible combinations of Arabidopsis mutants (from single to quadruple) defective in signaling modules regulated by SA, JA, ET or PAD4 were created, making possible stepwise reconstruction of the four signaling sectors and their interplay in the network (Tsuda et al., 2009). PAD4 contributes to SA biosynthesis and also modulates an SA-independent part of the plant immune system, called the PAD4 sector. Expression of marker genes for each sector and the growth of *Pseudomonas syringae* pv. *tomato* DC3000 (*Pto*) and *P. syringae* pv. *maculicola* ES4326 (*Pma*) in all possible combinations of mutants allowed the development of a plant regression model that characterizes the signal interactions and fluxes in the SA, JA, ET, and PAD4 signaling network during PTI (Kim et al., 2014). The model predicted a central role for ET in the robustness and tunability of the plant immune signaling network via its inhibition of the JA sector (Kim et al., 2014). Moreover, the model predicted an unexpected positive regulatory role of the JA sector on the SA sector, which was experimentally confirmed on the basis of SA level measurements in the JA biosynthesis mutant *dde2*.

The network reconstruction was also applied to dissect the complex regulation of the Arabidopsis transcriptome in response to flg22 induction via SA, JA, ET and PAD4 signaling. Statistical modeling of the role of the specific signaling sectors ranged over 5000 differentially expressed genes and showed that the flg22-induced changes were not entirely dependent on unique signaling sectors, but often on multi-sector interactions. This network analysis highlighted that MAMP-induced transcriptional responses are highly buffered, suggesting that the plant immune signaling network is robust and that different signaling sectors can take over each other's "tasks" when one fails or is inhibited, e.g. by pathogen effectors (Hillmer et al., 2017). The combination of network reconstruction and statistical modeling also unveiled mechanisms of

transcriptional regulation that could not be detected in classical genetic studies, pinpointing the added value of global network approaches to decipher functioning of the plant immune system.

During PTI and ETI, both the SA and the JA pathway are often initially activated. However, during the onset of the downstream immune response, interactions between both pathways are decisive in which sectors of the plant immune signaling network eventually become activated. Knowledge of the biological implications of SA/JA crosstalk predominantly point to the antagonistic interaction between SA and JA in the context of the prioritization of defense responses depending on the lifestyle of the invading pathogen (Pieterse et al., 2012). Several key players in the regulation of SA/JA crosstalk have been identified, including NPR1 and TFs, such as ORA59 and members from the TGA and WRKY TF families (Van der Does et al., 2013; Zander et al., 2014; Caarls et al., 2015). The PTI signaling network model described above inferred an unexpected additional function of SA/JA crosstalk in which JA, in addition to PAD4, is important for the activation of SA signaling during PTI. In a follow-up study, Mine et al. (2017a) confirmed this hypothesis by showing that JA represses flg22-induced SA accumulation via suppression of *PAD4* gene expression, and consequently repression of the PAD4-regulated SA translocation gene *EDS5*. However, if PAD4 is not functional, then JA can activate via MYC2 directly *EDS5*, thereby providing robustness to the SA subnetwork. Additionally, Liu et al. (2016) demonstrated that SA can activate JA signaling though disease resistance protein RPS2-mediated ETI. In response to ETI-induced SA accumulation, NPR3 and NPR4 interact with JAZ proteins leading to their degradation and subsequent activation of the JA pathway. Activation of both SA- and JA-signaling pathways during ETI is thought to be a defense strategy against biotrophic pathogens without making them more vulnerable to necrotrophic pathogens (Liu et al., 2016).

These examples showcase how SA and JA can interact at multiple levels in the plant immune signaling network. Recently, yet another example of the biological significance of SA/JA crosstalk was demonstrated (Betsuyaku et al., 2018). During ETI in Arabidopsis, SA starts to accumulate around the site of pathogen infection in leaf tissue that eventually undergoes HR cell death. Interval time-lapse imaging of the promoter activity of the SA marker gene *PR1* and the JA marker gene *VSP1* during the course of *Pto* AvrRpt2-triggered ETI showed that JA signaling was activated in a spatially separated domain around the HR area at early stages of the infection. This was followed by SA signaling in the region between the HR and JA-activated domains. This temporally dynamic and spatially separated activation of SA and JA signaling during ETI may be a SA/JA antagonism-based plant strategy that limits runaway cell death in the zone of SA-

activated HR cells, while creating a zone of JA-activated cells around the HR lesion that hamper potential secondary infections by necrotrophic pathogens that might benefit from the necrotizing tissue. This study also emphasizes the importance of temporal dynamic and spatial analysis of plant immune responses to better understand the role of hormones and their interplay in the plant immune signaling network.

2.2 Effector-mediated modulation of the hormone network

While plants evolved defense hormone signaling to finely tune their plant immune signaling network, pathogens on the other hand evolved to hamper plant immunity by targeting different features of the hormone signaling network (Kazan and Lyons, 2014; Shen et al., 2018). Hormone crosstalk directed towards the suppression of SA signaling (JA/SA, ABA/SA and auxin/SA) is frequently utilized by biotrophic pathogens that are sensitive to SA-mediated immunity. The bacterial pathogen *Pto* is an excellent example of this. During infection, *Pto* produces the JA-Ile mimic coronatine as a virulence factor, which in turn suppresses stomatal and apoplastic immunity by repressing SA accumulation and/or inactivating MAPKs (Mine et al., 2017b; Yang et al., 2017). The production of coronatine or coronatine-like molecules has also been observed in other bacterial pathogens, indicating that the production of JA-Ile mimicking molecules might be a widespread mechanism for bacteria to suppress host immunity (Zhang et al., 2017a). *Pto* also produces a suite of effector proteins that target hormone signaling pathways to suppress SA-dependent defenses. For instance, *Pto* effectors AvrB, HopX1, HopZ1a and HopBB1 apply several mechanisms to degrade JAZ repressor proteins and set off JA responses to dampen SA-mediate immunity (Jiang et al., 2013; Gimenez-Ibanez et al., 2014; Zhou et al., 2015; Yang et al., 2017). *Pto* effector AvrPtoB induces ABA accumulation and effector AvrRpt2 enhances auxin signaling, both leading to the reduction of SA-dependent defenses and the promotion of pathogen virulence (Chen et al., 2007; Torres-Zabala et al., 2007).

Several other examples showcase the role of phytohormone-mimicking molecules that are produced by pathogens as virulence factors. For instance, *Pto* can produce the auxin indole-3-acetic acid (IAA) to modulate plant auxin signaling. Mutation of the IAA biosynthesis genes *aldA* and *aldB* in *Pto* results in the suppression of bacterial virulence in susceptible plants because the mutants are less well capable of suppressing SA-dependent defenses. This indicates that hijacking auxin signaling through the production of microbial auxin can be a successful virulence system (McClerklin et al., 2018). Interestingly, some bacterial pathogens are known to produce SA, but the biological significance of this during interaction with host plants is currently unknown (Bakker et al., 2014). Detailed knowledge of the mechanisms of pathogenicity and its

interplay with the (hormone-regulated) plant immune system is essential to re-wire plant immune signaling networks for future disease-resistant crops. Pioneering work on the crystal structure of the receptor-ligand of JA, COI1, demonstrated that it is possible to engineer COI1 such that it prevents binding to the virulence factor coronatine while the binding capacity for the plant hormone JA-Ile remains (Zhang et al., 2015b). This example showcases that discoveries on important components of the plant immune signaling network hold great promise for biotechnological innovations in future disease resistant crops.

2.3 Dynamics of SA and JA gene regulatory networks

For many years, scientists worked on the elucidation of the mechanisms by which NPR1 regulates SA signaling. In the Arabidopsis *npr1* mutant, expression of the SA marker gene *PR1* is abolished, indicating that NPR1 is a positive regulator of SA signaling (Cao et al., 1994). During SA signaling, NPR1 moves to the nucleus where it interacts with a class of bZIP transcription factors called TGAs (Zhang et al., 1999). TGAs regulate other defense-related genes, therewith contributing to plant immunity (Kazan, 2018). NPR1 has two paralogues, NPR3 and NPR4, which interact with TGAs as well. But in contrast to the *npr1* single mutant, *npr3 npr4* double mutants show elevated *PR* gene expression, suggesting that NPR3/NPR4 act as negative regulators of SA signaling. Previously, it was shown that both NPR3 and NPR4 can bind to SA with low and high affinity, respectively, while NPR1 could not (Fu et al., 2012), although others reported contrasting findings (Wu et al., 2012). In a more recent paper, it was shown that all three NPR proteins are likely SA receptors. In the updated model of the SA pathway, NPR1 and NPR3/NPR4 act in an antagonistic manner in regulating SA-mediated disease resistance (Ding et al., 2018). According to this model, NPR3 and NPR4 bind to TGA transcription factors and repress their transcriptional activity in the nucleus when cellular SA levels are low. After pathogen attack, SA levels rise, after which SA binds to NPR3 and NPR4, which stops the transcriptional repression on TGAs. In parallel, SA binds to NPR1 which promotes transcription activation of TGAs and their downstream SA-responsive, defense-related genes (Ding et al., 2018).

NPR1 is a master regulator in the activation of the SA sector of the plant immune signaling network. It is not only required for the onset of SA-dependent defenses and SAR, it also functions at the crossroad of SA/JA crosstalk, therewith playing an important role in regulating the dynamics of the plant immune signaling network (Spoel et al., 2003; Spoel and Dong, 2012). With its central role, NPR1 is in theory an attractive target for pathogens to manipulate host immunity (Sun et al., 2018). Recently, the *Pto* effector AvrPtoB was shown to interact with NPR1 in the presence of SA, therewith facilitating

NPR1 poly-ubiquitination and degradation via the 26S proteasome, which disrupts the SA sector of the plant immune signaling network and thus increases susceptibility to *Pto* (Chen et al., 2017).

JA-mediated defense responses are activated in response to pathogen or insect attack and lead to a transcriptional and metabolic reprogramming towards the production of specific defense-related compounds that help to combat the invaders. In Arabidopsis, two major branches of the JA signaling network are recognized: the MYC branch and the ERF branch (Pieterse et al., 2012). The MYC branch is controlled by MYC-type transcription factors, such as MYC2, MYC3 and MYC4 (Dombrecht et al., 2007). The ERF branch is regulated by members of the APETALA2/ETHYLENERESPONSE FACTOR (AP2/ERF) family of transcription factors, such as ERF1 and ORA59 (Lorenzo and Solano, 2005; Pré et al., 2008). The ERF branch requires both JA and ET signaling, while the MYC branch is regulated by both JA and ABA. In general, the ERF branch is associated with enhanced resistance to necrotrophic pathogens, whereas the MYC branch is associated with defense against insect herbivory (Pieterse et al., 2012; Howe et al., 2018). The ERF and the MYC branch of the JA pathway act antagonistically on each other: when in response to necrotrophic pathogen infection JAs and ET start to accumulate, the ERF branch becomes activated, while the MYC branch is suppressed. Conversely, when upon insect herbivory JA and ABA start to accumulate, the MYC branch is activated, while the ERF branch becomes suppressed (Verhage et al., 2010; Verhage et al., 2011; Vos et al., 2013b).

Most studies on the role of hormones in the immune signaling network have been conducted using bilateral interactions between a single pathogen isolate and a single plant genotype. In order to capture the variation of responses in the plant immune signaling network within a single pathogen species, Zhang et al. (2017b) monitored defense-related phenotypes and transcriptome responses in diverse Arabidopsis SA- and JA- mutants, each challenged with 96 different *Botrytis cinerea* isolates. The authors identified four gene regulatory networks that were related to the genetic interaction between host and pathogen. These networks included genes related to camalexin production and to SA and JA signaling. Furthermore, the authors also identified a network involved in photosystem I, with the uncharacterized transcript *YFC2* acting as a hub, and another network with nuclear-encoded chloroplast-localized proteins involved in photosynthesis and reactive oxygen species production (Zhang et al., 2017b). However, it remains unknown how these networks function in defense against *B. cinerea.*

It is known that plants can swiftly adjust their gene regulatory networks to changes in their biotic and abiotic environment (Coolen et al., 2016). Berens et al. (2019) recently provided evidence that biotic and abiotic stress responses are differentially prioritized in Arabidopsis leaves of different ages. Abiotic stress suppressed immune responses in the older leaves through ABA, whereas this antagonistic effect on immunity was blocked in younger leaves by PBS3, a component of the SA pathway. Plants defective in *PBS3* showed enhanced abiotic stress tolerance at the cost of decreased fitness under combined stress. Hence, with this role of PBS3 in spatial regulation of plant immunity, yet a new layer of complexity is added to the control of the plant immune signaling network.

3. INTERACTIONS OF THE PLANT IMMUNE SIGNALING NETWORK WITH THE UNDERGROUND

Like leaves, roots are also capable of perceiving the presence of pathogens and to subsequently trigger PTI. A wide range of defense elicitors, including flg22, fusaric acid, peptidoglycan, and JA were shown to elicit PTI in roots (Millet et al., 2010; Koroney et al., 2016). Like leaves, roots possess PRRs, like the flagellin receptor FLS2 (Wyrsch et al., 2015), which is present in all root tissues, but different levels of expression are displayed in the different root cell types (Beck et al., 2014). Studies on immune responses in roots show that PTI in root tissue includes molecular events like production of ROS (Poncini et al., 2017), transcriptional reprogramming (Stringlis et al., 2018), callose deposition, and cell wall modification (Millet et al., 2010; Plancot et al., 2013; Tran et al., 2016). The phytohormones SA, JA, and ET are also implicated in root defenses that are triggered by soil-borne pathogens (Papadopoulou et al., 2018). However, the response to these hormones in roots does not always follow the same behavior as in leaves (Attard et al., 2010). For instance in rice, the expression of *PR1* and *PR10* is rapidly activated in early stages of root infections, while in leaves these genes become only highly expressed during later stages of infection (Marcel et al., 2010). In *Brassica rapa*, *PR-1* also shows differential regulation in response to hormonal elicitation in shoots and roots (Papadopoulou et al., 2018). The same holds true for other hormone-responsive marker genes, such as the JA marker gene *PDF1.2* and the ET biosynthesis gene *ACO.* Hence, the hormone-regulated plant immune signaling network might function different in roots than in shoots.

3.1 Root-microbe interaction networks

One of the reasons why roots respond differently to defense elicitors than shoots is likely because roots are continuously exposed to a mesmerizing diversity of microbes in

the root microbiome (Berendsen et al., 2012). Many bacterial and fungal soil microbiota possess MAMPs like flagellin and chitin and are thus a source of defense elicitors that potentially trigger PTI responses in plant roots. PTI aims to eliminate potential pathogenic invasions but also has a downside because defense responses typically result in a negative effect on plant growth (Gomez-Gomez and Boller, 2000). Hence, if plant roots would continuously activate PTI responses upon recognition of MAMPs from root microbiota members, it would be impossible for plants to grow. Therefore, the root immune system must possess sophisticated mechanisms to distinguish beneficial microbes from pathogenic microbes. In order to establish a mutually beneficial relationship, beneficial microbes must circumvent recognition by root immune receptors. Indeed, the plant-beneficial rhizobacteria *Pseudomonas simiae* WCS417 (WCS417) and *Bacillus subtilis* FB17 were found to be able to suppress root immune responses and at the same time promote growth of the host plant (Millet et al., 2010; Lakshmanan et al., 2012; Stringlis et al., 2018). Time series RNA-seq to investigate the early transcriptional responses of Arabidopsis roots to living plant growth-promoting and ISR-inducing WCS417 bacteria in comparison to its MAMP flg22^{417} showed that the root immune response to flg22^{417} is highly similar to that of fungal chitin (Stringlis et al., 2018). Transcriptional changes inflicted by living WCS417 overlapped largely with those mediated by the MAMPs, but about half of the MAMP-induced transcriptional changes were suppressed by living WCS417 cells. The MAMP-repressed genes that were not affected by WCS417 have a strong auxin signature, highlighting the dual role of auxin in finely balancing growth and defense responses, which is involved in shaping the root microbiome and root responses.

Modulation of plant immunity either by pathogens or beneficial microbes is essential for the establishment of plant-microbe interactions. The typical defense-related hormones SA and JA also play a role in modulating the root immune signaling network (Zamioudis and Pieterse, 2012; Gourion et al., 2015). For instance, mycorrhizal fungi have been shown to use effector proteins that target the JA signaling pathway in host roots, therewith facilitating a mutually beneficial symbiosis with the host plant. Also, the plant-beneficial soil-borne fungus *Trichoderma* interacts with the root's hormone signaling network to benefit its host. *Trichoderma*-colonized roots of tomato hinder nematode performance both locally and systemically at multiple stages of parasitism. First, *Trichoderma* primes the roots for enhanced SA-regulated defenses, therewith limiting nematode invasion. Then, *Trichoderma* enhances JA-regulated defenses, therewith antagonizing the deregulation of JA-dependent immunity by the nematodes during invasion of the roots (Martinez-Medina et al., 2017). Modulation of plant immune responses by beneficial microbes such as mycorrhizal fungi and nitrogen-fixing rhizobia

has been shown to be mediated by effectors to facilitate a long-lasting mutually beneficial association (Zamioudis and Pieterse, 2012; Okazaki et al., 2013; Plett et al., 2014). However, in comparison to the role of pathogen effectors in the plant immune signaling network, the research field is still in its infancy.

3.2 Hormonal regulation of induced systemic resistance elicited by root-associated microbes

Besides interfering locally with the root immune system, several genera of the rhizosphere microbiota have been shown to systemically prime the above-ground plant tissues for enhanced immunity. This phenomenon is called induced systemic resistance (ISR) and is effective against a broad spectrum of plant pathogens and insects (Pieterse et al., 2014; Martinez-Medina et al., 2016). Many studies have reported on the ability of plant growth-promoting rhizobacteria (PGPR) and fungi (PGPF) to promote plant health via ISR. These studies mainly involved *Pseudomonas*, *Serratia*, and *Bacillus* PGPR strains, nonpathogenic *F. oxysporum*, *Trichoderma*, and *Piriformospora indica* PGPF strains, and symbiotic arbuscular mycorrhizal fungi (Kloepper et al., 2004; Pozo and Azcon-Aguilar, 2007; Stein et al., 2008; Shoresh et al., 2010; Pieterse et al., 2014). Using Arabidopsis mutants defective in JA or ET signaling, it was demonstrated that JA and ET are central players in the regulation of rhizobacteria-mediated ISR, although there are also examples of beneficial PGPR and PGPF that activate systemic immunity via the SA-dependent SAR pathway (Pieterse et al., 2014). In accordance with its dependency of JA and ET signaling, rhizobacteria-mediated ISR was shown to be effective against attackers that are sensitive to JA/ET-dependent defenses, including necrotrophic pathogens and insect herbivores. However, negative effects of beneficial microbes on plant-insect interactions have been reported as well (Pineda et al., 2013; Haney and Ausubel, 2015).

3.3 Role of phytohormones in microbiome assembly

Because phytohormones are important regulators of the biosynthetic pathways of secondary metabolites that are secreted in the rhizosphere by plant roots, they also influence the microbial community in the rhizosphere (Bakker et al., 2018; Stringlis et al., 2019). The phytohormones SA and JA have both been implicated in this process (Carvalhais et al., 2013; Lebeis et al., 2015). Moreover, activation of the plant immune signaling network in the leaves, can result in changes in the root microbiome. Recently, Berendsen et al. (2018) demonstrated that infection of Arabidopsis leaves with the SA-inducing downy mildew pathogen *Hyaloperonospora arabidopsidis* resulted in the recruitment of a consortium of beneficial microbes to the root system, that in turn were capable of activating ISR that was effective against downy mildew infection. A similar phenomenon was observed with *Pto* on Arabidopsis (Yuan et al., 2018). Together, this

indicates that the plant immune signaling network and the network of microbiota in the root microbiome are functionally linked.

4. TOWARDS ELUCIDATING PLANT IMMUNE SIGNALING NETWORKS IN THE PLANT HOLOBIONT

Temporal control of transcription networks enables organisms to swiftly adapt to a changing environment. Above, I explained the immense complexity of the immune signaling network that has different hormone-controlled sectors that respond differently to environmental cues and that also influence each other. This complexity demands a systems approach, in which the order of TFs and their interaction with target genes is reconstructed to map the architecture of the underlying gene regulatory network. For that, many studies have been using *de novo* network inference approaches (Rodriguez et al., 2019). However, a major challenge of these systems biology approaches is the genome-wide validation of the predictions, and the accuracy of the predictive power of the resulting gene regulatory networks. This is largely due to the lack of dynamic information on expression over time and of methods for rapidly validating the inferred TF-target interactions *in vivo*. Recently, enormous progress has been made toward developing algorithms to modeling high-resolution time series RNA expression data sets (Breeze et al., 2011; Windram et al., 2012; Lewis et al., 2015). Gene regulatory networks can be constructed linking transcription regulators to a specific short sequence in the regulatory region (*cis*-element) of a target gene in a set of co-expressed genes (Windram and Denby, 2015). Gene regulatory networks are also often used to predict new functions for genes or gene products. Using the guilt-by-association strategy, genes belonging to the same cluster are predicted to have similar functions. Regulators, like TFs, in a cluster may be crucial for the expression behavior of the other gene members in the same cluster. In addition, using the temporal expression behavior of genes, from which enrichment in *cis*-elements at certain phases in the dynamic network can be determined, the TF(s) responsible for changed expression level can be derived. These hubs in the network can be experimentally validated *in planta*.

A prerequisite for TFs to function is their accessibility to the regulatory region of their target genes, which is determined by the chromatin structure in the target promoters. Altering the activity of specific regulatory components in TF-DNA complexes can make the plant immune regulatory network more tunable for different signals and improve the interaction between plant and microbes to the advantage of the plant (Foo et al., 2018). Recently developed high-throughput technologies and data analyses are helping to increase our molecular understanding of the regulatory landscape of the

plant genome. The DNA binding sequences that are represented in TF DNA binding datasets have often been determined in *in vitro* assays (Franco-Zorrilla and Solano, 2017). The DNA affinity purification sequencing (DAP-seq) database offers the *in vitro* DNA binding sites of over 327 Arabidopsis TF-binding sites. It was shown that DNA methylation within a TF-binding motif can alter the binding of 76% of the tested TFs, in most cases leading to an inhibition of TF binding (O'Malley et al., 2016).

Refining assays with new chromatin accessibility and TF-DNA binding strategies to better predict target genes will allow new approaches to study whole genome transcriptional regulation in plants. These achievements will enable reconstruction of the gene regulatory networks in a holobiont context, allow discovery of multimeric TF complexes, and establish transcriptional hierarchies in the networks. Undoubtedly, the computational integration of all the DNA-protein interaction data derived from these technological advances, as well as information on chromatin states, DNA methylation, and protein-protein interactions involved in cooperative binding will impose a huge challenge on future biologists. Further development of computational tools will definitely be essential in order to characterize the plant immune gene regulatory network in a holobiont context.

5. OUTLINE OF THIS THESIS

Hormones are central regulators of plant immunity. They can trigger large-scale reprogramming of the plant's transcriptome, and influence each other in an antagonistic or synergistic manner. To better understand the complexity of SA- and JA-mediated transcriptional reprogramming, we performed high-resolution RNA-seq time series in Arabidopsis leaves to define the transcriptional effects elicited by SA and JA. The overall aim of my PhD project was to advance our understanding of the SA- and JA- controlled immune signaling networks in Arabidopsis and discover novel master regulators of hormone-regulated plant immunity. To this end, we used the systems approach of high-density time series RNA-seq to unravel in detail the dynamics and architecture of the gene regulatory network that is activated in Arabidopsis in response to SA and JA.

In Chapter 2, we used high-density time series RNA-seq to investigate the architecture and dynamics of the JA gene regulatory network. Using this approach, we uncovered several TFs, including MYB59 and bHLH27, as early network components with a role in pathogen and insect resistance. Analysis of subnetworks surrounding the TFs ORA47, MYB59 and bHLH27, using a combination of transcriptome profiling of mutants,

plant bioassays with pathogens and insects, and protein-protein interaction studies highlighted their specific regulatory roles in defined modules of the JA network.

In Chapter 3, we used high-density time series RNA-seq to unravel the architecture and dynamics of the SA gene regulatory network. Important roles for the so far unidentified TFs ANAC061 and ANAC090 in SA-mediated immunity was unveiled using mutants in bioassays and transcriptome studies.

In Chapter 4, we used a bioinformatics pipeline to identify groups of related proteins whose genes were responsive to SA, as determined by RNA-seq in Ch3, but as yet had no previously characterized function in plant immunity. One of these families consisted of eight genes encoding small proteins that contain a cysteine-rich transmembrane domain, which we named pathogen-induced cysteine-rich transmembrane proteins (PCMs). Stable PCM-overexpressing Arabidopsis lines displayed enhanced resistance against biotrophic pathogens confirming a role for members of this gene family in plant immunity.

In Chapter 5, I provide a summarizing discussion on the outcomes of my PhD research and a reflection on the questions that remain for future research.

2

Architecture and dynamics of the jasmonic acid gene regulatory network

Marciel Pereira Mendes[1], Marcel C. Van Verk[1,2], Saskia C.M. Van Wees[1], Richard Hickman[1]

[1]Plant-Microbe Interactions, Department of Biology, Science4Life, Utrecht University, P.O. Box 800.56, 3508 TB, Utrecht, the Netherlands

[2]Bioinformatics, Department of Biology, Science4Life, Utrecht University, P.O. Box 800.56, 3508 TB, Utrecht, the Netherlands

Adapted from:

Hickman R.J., Van Verk, M.C., Van Dijken, A.J.H., Pereira Mendes, M., Vroegop-Vos, I.A., Caarls, L., Steenbergen, M., Van der Nagel, I. Wesselink, G.J., Jironkin, A., Talbot, A., Rhodes, J., De Vries, M., Schuurink, R.C., Denby, K., Pieterse, C.M.J. and Van Wees, S.C.M. (2017). Architecture and dynamics of the jasmonic acid gene regulatory network *The Plant Cell* 29:2086-2105 (DOI: 10.1105/tpc.16.00958)

The work described in Hickman et al., (2017) is a large study with important contributions of different authors. Chapter 2 is an adapted version of Hickman et al. (2017). Besides the core of the story, it highlights the contributions of Marciel Pereira-Mendes, which includes the validation of the transcription factors bHLH27, ERF16, MYB48, MYB59, and ANAC056 (Fig. 1), and additional transcription factors using bioassays (Supplemental Fig. S2, S3 and S4), validation of the ORA47 subnetwork (Fig. 4), transcriptome analyses of bhlh27 and myb48/my59 (Fig. 5), yeast two-hybrid analysis (Fig. 6 and Table 1).

ABSTRACT

Jasmonic acid (JA) is a critical hormonal regulator of plant growth and defense. To advance our understanding of the architecture and dynamic regulation of the JA gene regulatory network, we performed a high-resolution RNA-Seq time series of methyl JA-treated *Arabidopsis thaliana* at 15 time points over a 16-h period. Computational analysis showed that MeJA induces a burst of transcriptional activity, generating diverse expression patterns over time that partition into distinct sectors of the JA response targeting specific biological processes. The presence of transcription factor (TF) DNA-binding motifs correlated with specific TF activity during temporal MeJA-induced transcriptional reprogramming. Insight into the underlying dynamic transcriptional regulation mechanisms was captured in a chronological model of the JA gene regulatory network. Several TFs, including MYB59 and bHLH27, were uncovered as early network components with a role in pathogen and insect resistance. Analysis of subnetworks surrounding the TFs ORA47, MYB59 and bHLH27, using transcriptome profiling of overexpressors and mutants, provided insights into their regulatory role in defined modules of the JA network. Collectively, our work illuminates the complexity of the JA gene regulatory network, pinpoints and validates previously unknown regulators, and provides a valuable resource for functional studies on JA signaling components in plant defense and development.

INTRODUCTION

In nature, plants are subject to attack by a broad range of harmful pests and pathogens. To survive, plants have evolved a sophisticated immune signaling network that enables them to mount an effective defense response upon recognition of invaders. The phytohormone jasmonic acid (JA) and its derivatives are key regulators in this network and are typically synthesized in response to insect herbivory and infection by necrotrophic pathogens (Wasternack, 2015). Enhanced JA production mediates large-scale reprogramming of the plant's transcriptome, which is influenced by the antagonistic or synergistic action of other hormones produced during parasitic interactions, such as salicylic acid (SA), ethylene (ET) or abscisic acid (ABA) (Pieterse et al., 2012; Campos et al., 2014; Wasternack, 2015). The JA signaling network coordinates the production of a broad range of defense-related proteins and secondary metabolites, the composition of which is adapted to the environmental context and nature of the JA-inducing condition (Pieterse et al., 2012; Campos et al., 2014; Wasternack, 2015).

In the past decade, major discoveries in the model plant Arabidopsis have greatly advanced our understanding of the JA signaling pathway. In the absence of an invader, when JA levels are low, activation of JA-responsive gene expression is constrained by repressor proteins of the JASMONATE ZIM-domain (JAZ) family that bind to specific JA-regulated transcription factors (TFs). The conserved C-terminal JA-associated (Jas) domain of JAZs competitively inhibits interaction of the TF MYC3 with the MED25 subunit of the transcriptional Mediator complex (Zhang et al., 2015a). Moreover, JAZs recruit the TOPLESS corepressor, either directly or through the NOVEL INTERACTOR OF JAZ (NINJA) adapter, which epigenetically inhibits expression of TF target genes. In response to pathogen or insect attack, bioactive JA-Isoleucine (JA-Ile) is synthesized, and promotes the formation of the coreceptor complex of JAZ (via its Jas domain) with CORONATINE INSENSITIVE1 (COI1), the F-box protein of the E3 ubiquitin-ligase Skip-Cullin-F-box complex SCF^{COI1}. Upon perception of JA-Ile, JAZ repressor proteins are targeted by SCF^{COI1} for ubiquitination and subsequent proteasomal degradation (Chini et al., 2007; Thines et al., 2007; Sheard et al., 2010). This degradation leads to the release of the JAZ-mediated repression of TFs and to subsequent induction of JA-responsive gene expression.

Several groups of TFs are known to be important for regulation of the JA pathway. Upon degradation of JAZs, MYC2 acts in concert with the closely related bHLH TFs MYC3 and MYC4 in activating a large group of JA-responsive genes by directly targeting their promoters (Dombrecht et al., 2007; Cheng et al., 2011; Fernández-Calvo et al., 2011).

While current evidence indicates that MYC2, MYC3 and MYC4 act as master regulators of the onset of JA responsive gene expression, additional factors are required for further fine-regulation of the JA signaling circuitry. Several other bHLH TFs, such as JASMONATE-ASSOCIATED MYC2-LIKE1 (JAM1)/bHLH017, JAM2/bHLH013, JAM3/bHLH003 and bHLH014 act redundantly to repress JA-inducible genes by competitive binding to *cis*-regulatory elements, possibly to control the timing and magnitude of the induced JA response (Nakata et al., 2013; Sasaki-Sekimoto et al., 2013; Song et al., 2013). Another important family of regulators that shapes the JA response is the APETALA2/ETHYLENE RESPONSE FACTOR (AP2/ERF) family of TFs. AP2/ERF-type TFs, such as ERF1 and ORA59 (OCTADECANOID-RESPONSIVE ARABIDOPSIS AP2/ERF-DOMAIN PROTEIN59), integrate the JA and ET response pathways and act antagonistically on MYC2-, MYC3-, and MYC4-regulated JA-responsive genes (Lorenzo et al., 2003; Pré et al., 2008; Zhu et al., 2011; Pieterse et al., 2012). In general, AP2/ERF-regulated JA responses in the ERF branch of the JA pathway are associated with enhanced resistance to necrotrophic pathogens (Berrocal-Lobo et al., 2002; Lorenzo et al., 2003), whereas the MYC TF-regulated JA responses in the MYC branch of the JA pathway are associated with wound response and defense against insect herbivores (Lorenzo et al., 2004; Kazan and Manners, 2008; Verhage et al., 2011).

A detailed understanding of how responsiveness to JA is regulated is important in order to find leads that can improve crop resistance to pathogens and insects, while maintaining plant growth. Previously, several microarray-based transcriptome profiling studies revealed important information on the regulation of JA-responsive gene expression (Goda et al., 2008; Pauwels et al., 2008). However, because these studies analyzed this response at limited temporal resolution, much has remained unknown about the architecture and dynamics of the JA gene regulatory network. Here, we performed an in-depth, high-throughput RNA sequencing (RNA-Seq) study in which we generated a high-resolution time series of the JA-mediated transcriptional response in leaf number 6 of Arabidopsis plants. Computational analysis of the JA-induced transcriptional landscape provided insight into the structure of the JA gene regulatory network at an unprecedented level of detail. We accurately identified distinct JA-induced expression profiles, and used these to predict and validate the biological function of several previously unknown regulators of the JA immune regulatory network. We resolved the sequence of transcriptional events that take place following induction of the JA response, constructed a dynamic model of the JA gene regulatory network, and identified and validated subnetworks surrounding several JA-induced TFs, confirming the suitability of our systems approach to obtain detailed knowledge on regulation of the JA response pathway.

RESULTS

A time course of MeJA-elicited transcriptional reprogramming

A key step towards a systems-level understanding of the architecture of the JA signaling network is to obtain comprehensive and accurate insight into the dynamic transcriptional reprogramming that takes place in plants following JA stimulation. To go beyond earlier studies that analyzed the JA transcriptional response with a limited number of time points, we generated a high-resolution time series of JA-mediated transcriptional reprogramming in Arabidopsis leaves. Previously, similar types of dense time series experiments with Arabidopsis have been successfully utilized to help decipher gene regulatory networks underpinning a variety of biological processes, such as senescence and responsiveness to infection by *Botrytis cinerea* and *Pseudomonas syringae* (Breeze et al., 2011; Windram et al., 2012; Lewis et al., 2015). Here, we used RNA-Seq technology to profile whole-genome transcriptional expression in Arabidopsis leaves just before the treatments (t = 0 h), and over 14 consecutive time points within 16 h following application of methyl JA (MeJA, which is readily converted to JA) or a mock solution to the leaves of intact plants (Supplemental Dataset 1). At all time points and for each treatment, one leaf (true leaf number 6) was sampled in quadruplicate from four independent 5-week-old Col-0 plants, yielding 116 samples in total (Supplemental Dataset 1). Read counts were normalized for differences in sequencing depth between samples (Supplemental Dataset 2) and a generalized linear model was employed to identify genes whose transcript levels differed significantly over time between MeJA and mock treatments (see Van Verk et al. (2013) and Methods for details). This analysis yielded a set of 3611 differentially expressed genes (DEGs; Supplemental Dataset 3).

Our high-resolution temporal transcriptome data captured a diverse set of dynamic responses to MeJA stimulation (Supplemental Figure 1). The majority of expression changes in individual genes followed a clear single-pulse (impulse) pattern, which is often observed in responses to environmental stress in eukaryotic cells and coordinates the temporal regulation of specific gene expression programs (Yosef and Regev, 2011). By monitoring the transcriptional changes in leaf number 6, we maximally synchronized the onset of the JA response in intact plant tissue. Hence, the resulting information-rich time series of MeJA-responsive gene expression profiles are highly suited to computational approaches that can generate biological insights into the regulation of the underlying JA transcriptional network.

Process-specific gene clusters

To begin to decode the JA gene regulatory network, the time series–clustering algorithm SplineCluster was used to partition the set of 3611 DEGs into clusters of co-expressed genes that share similar expression dynamics. This yielded 27 distinct clusters with distinct response patterns (Figure 1A, Supplemental Figure 1, Supplemental Dataset 4), which broadly fell into two major groups: those that showed increased expression in response to application of MeJA (clusters 1–14), and those that exhibited reduced expression (clusters 15–27). The cluster analysis highlighted a global burst of MeJA-induced up- or down-regulation of gene transcription, generally starting within 1 h and peaking within 2 h after treatment. Most clusters showed a clear pulse-like, transient change in transcript levels (e.g. clusters 8 and 18, up- and down-regulation, respectively). A largely sustained induction throughout the time course was displayed in for example clusters 1 and 2. More complex expression patterns were also revealed; cluster 14 presented two consecutive pulses of activation.

The genes in each cluster were tested for overrepresented functional categories using Gene Ontology (GO) term enrichment analysis to investigate the biological significance of the distinct dynamic expression patterns (Supplemental Dataset 5). This analysis showed that clusters representing up-regulated genes were, as expected, overrepresented for functional terms associated with JA defense responses. Broad annotations such as 'Response to wounding' and 'Response to herbivory' were present in multiple up-regulated clusters, while in contrast the more specific functional categories were linked to distinct clusters. For example, cluster 6 was specifically enriched for the annotation term 'Anthocyanin-containing compound biosynthetic process', cluster 8 for 'Tryptophan biosynthetic process', and cluster 14 for 'Glucosinolate biosynthetic process'. Each of these clusters contained many of the genes previously implicated in these secondary metabolite biosynthesis pathways, but also uncharacterized genes that may have an important function in these specific processes (Supplemental Dataset 5). The significant enrichment of distinct gene clusters for a specific biological process indicates that the dynamic expression profiles generated in this study possess information that is sufficiently detailed to capture discrete sectors of the JA-controlled gene network that control specific processes. These sectors are likely subject to distinct regulation encoded within the promoters of the genes in the respective clusters.

To facilitate the use of the expression data for the research community, a searchable (by gene ID) figure has been made available that visualizes coexpression relationships in time for all DEGs in the individual clusters (Supplemental File 1).

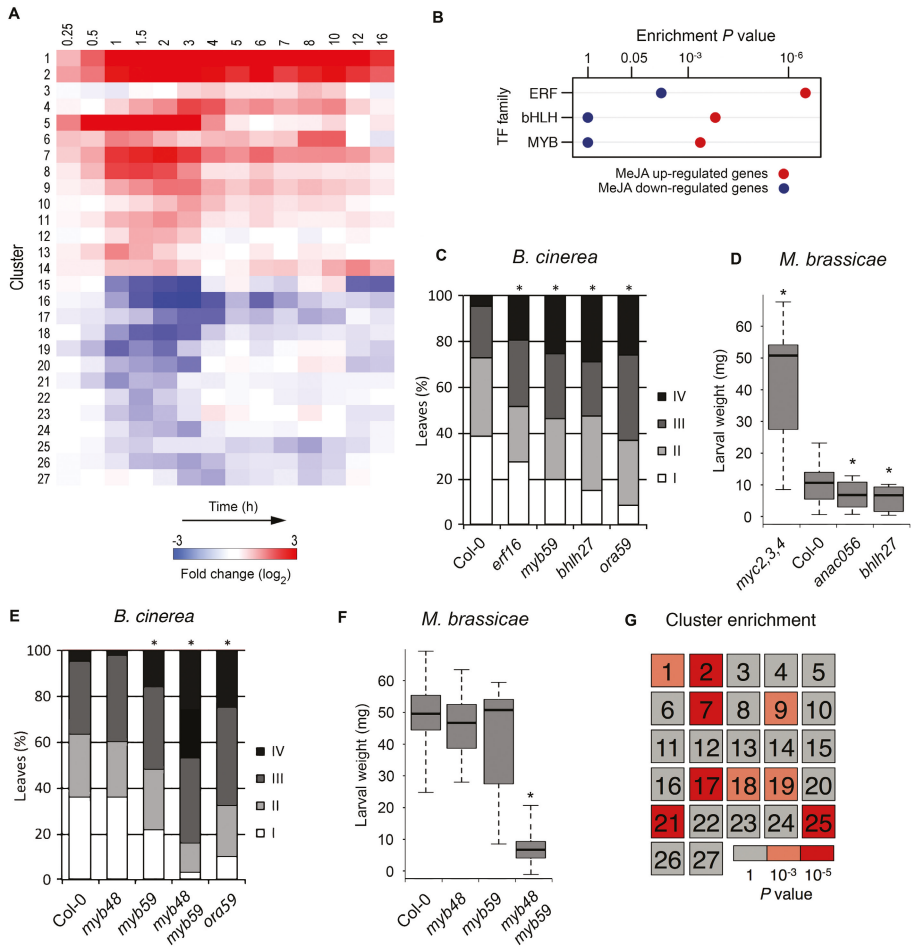

Figure 1. Clustering of co-expressed genes in the JA gene regulatory network and identification of novel components of JA-dependent resistance.

(**A**) The set of 3611 genes showing differential expression in Arabidopsis leaves following exogenous application of MeJA was partitioned into 27 distinct co-expressed gene clusters using SplineCluster. The heatmap shows the mean gene expression profile for each cluster, with red and blue indicating up-regulation and down-regulation of expression (log_2-fold change (MeJA/mock)), respectively. (**B**) Significantly overrepresented TF families within clusters of genes up-regulated (clusters 1-14; red) or down-regulated (clusters 15-27; blue) in response to MeJA treatment (hypergeometric test; $P \leq 0.001$). (**C**) Quantification of disease symptoms of wild-type Col-0, highly susceptible ERF TF mutant *ora59,* and T-DNA insertion lines for selected genes *ERF16, MYB59,* and *bHLH27* (members of coexpression clusters 2, 4 and 1, respectively) at 3 days after inoculation with *B. cinerea*. Disease severity of inoculated leaves was scored in four classes ranging from restricted lesion (class I), non-spreading lesion (class II), spreading lesion (class III), up to severely spreading lesion (class IV). The percentage of leaves in each class was calculated per plant (n > 20). Asterisk indicates statistically significant difference from Col-0 (Chi-squared test; $P \leq 0.05$).

(**D**) Performance of *M. brassicae* larvae on Col-0, highly susceptible triple bHLH TF mutant *myc2,3,4* and T-DNA insertion lines for selected genes *ANAC056* (coexpression cluster 13) and *bHLH27.* The larval fresh weight was determined after 8 days of feeding. Asterisk indicates statistically significant difference from Col-0 (two-tailed Student's *t* test for pairwise comparisons; $P \leq 0.05$; n=30; error bars are SE). (**E**) Quantification of disease symptoms of Col-0*, myb48, myb59, myb48 myb59* and *ora59* mutant lines at 3 days after inoculation with *B. cinerea*. Disease severity of inoculated leaves was scored as described in (C) (n > 20). Asterisk indicates statistically significant difference from Col-0 (Chi-squared test; $P \leq 0.05$). (**F**) Performance of *M. brassicae* larvae on Col-0 and *myb48, myb59* and *myb48 myb59* mutant lines. The larval fresh weight was determined after 12 days of feeding. Asterisk indicates statistically significant difference from Col-0 (two-tailed Student's *t* test for pairwise comparisons; $P \leq 0.05$; n=30; error bars are SD). (**G**) Heatmap indicating hypergeometric enrichment *P* value of genes differentially expressed in *myb48 myb59* (compared to Col-0) in each MeJA-induced coexpression cluster.

Discovery of defense regulators

Since TFs are the main drivers of transcriptional networks, we mapped the TF families that are enriched in the 27 clusters of MeJA-responsive DEGs. Within the up-regulated clusters, genes encoding members of the bHLH, ERF and MYB TF families were most significantly overrepresented (Figure 1B), suggesting that these TF families dominate the onset of JA-induced gene expression.

The early up-regulated gene clusters 1 and 2 (61 and 165 genes, respectively) were enriched for known JA-related genes such as the herbivory markers *VSP1* and *VSP2*, as well as the regulators *JAZ1*, *2*, *5*, *7, 8*, *9*, *10* and *13*, *MYC2*, *ANAC019*, *ANAC055*, *RGL3*, and *JAM1* (Wasternack and Hause, 2013). In addition, TF genes with no previously reported roles in the JA response pathway were present in these clusters, which implies that they may also have regulatory functions in the JA response relevant to plant defense. To test this hypothesis, we selected 7 uncharacterized TF genes from clusters 1 and 2 and supplemented this set with 5 uncharacterized TF genes from other clusters displaying a similarly rapid response to MeJA treatment. The respective Arabidopsis T-DNA knockout lines were functionally analyzed for their resistance against the necrotrophic fungus *Botrytis cinerea* and the generalist insect herbivore *Mamestra brassicae*, which are both controlled by JA-inducible defenses (Pieterse et al., 2012). Mutants in the TF genes *bHLH27*, *ERF16* and *MYB59* displayed a significant increase in disease susceptibility to *B. cinerea* compared to wild-type Arabidopsis Col-0, approaching the disease severity level of the highly susceptible control mutant *ora59* (Figure 1C; full results in Supplemental Figure 1 and additional mutant alleles in Supplemental Figure 3). Weight gain of *M. brassicae* larvae was significantly reduced on mutants of *ANAC056* and *bHLH27*, while on none of the tested mutants larval weight was enhanced, as was the case on the susceptible control mutant *myc2,3,4* (Figure 1D; full results and additional mutant alleles in Supplemental Figure 3 and 4). Thus, for 4 of the 12 tested MeJA-responsive, previously uncharacterized TF genes a predicted role in the JA response could be functionally validated for either *B. cinerea* or *M. brassicae* resistance, demonstrating

the value of using information-rich time series data to accurately identify co-expressed genes that may have novel functions in the JA pathway.

Contrasting roles in pathogen and insect defense for redundant gene pair *MYB48/ MYB59*

Many TFs originate from duplication events and have overlapping or even redundant functionality, so that their single mutants may not display the full effects on host immunity in the above-described analyses. Therefore, we additionally assayed a double mutant of a pair of genetically unlinked paralogous genes, *MYB48* and *MYB59* (Bolle et al., 2013) to uncover phenotypes not seen in either single mutant. This approach can provide further insight into the functionality of such TFs. The TF gene *MYB59* was upregulated within 30 minutes after application of MeJA and although the single mutant *myb59* displayed enhanced susceptibility to *B. cinerea* (Figure 1C and 1E), it was unaffected in resistance to *M. brassicae* (Figure 1D and 1F). *MYB48* was transiently downregulated by MeJA, but the single mutant *myb48* did not show altered resistance to either *B. cinerea* or *M. brassicae* (Figure 1E and 1F). By contrast, the *myb48 myb59* double mutant was highly resistant to *M. brassicae*, reducing the larval growth 5-fold in comparison to Col-0 and the single mutants. Moreover, the double mutant displayed significantly more severe disease symptoms following infection by *B. cinerea* than either of the single mutants. This suggests that MYB48 and MYB59 function in concerted action as negative regulators of insect resistance and positive regulators of necrotrophic pathogen resistance.

To gain insight into the biological processes contributing to the differentially altered attacker performance on *myb48 myb59,* we performed RNA-Seq analysis on the double mutant. A total of 399 genes were differentially expressed between non-stimulated *myb48 myb59* and Col-0 leaves (168 were up-regulated and 231 were down-regulated in the double mutant; Supplemental Dataset 6). Functional category analysis showed that in the up-regulated DEG set of the mutant compared to Col-0, processes like 'Response to wounding' and 'Response to jasmonic acid stimulus' were enriched (Supplemental Dataset 7). This finding is in accordance with these *myb48 myb59*-upregulated DEGs being overrepresented in coexpression clusters 1, 2, 7 and 9 of the MeJA-responsive DEGs (Figure 1G). Genes that showed enhancement of expression by both MeJA treatment and the *myb48 myb59* mutation were for example the JA biosynthetic genes *AOC2* and *OPR3*, and TF gene *MYC2*. Also, the downstream herbivore defense marker gene *VSP2* showed > 50-fold higher expression in the mutant. This up-regulation suggests prioritization of the JA pathway towards the anti-insect MYC branch in *myb48 myb59*, explaining its enhanced resistance to *M. brassicae*. However, MYC

branch-mediated antagonism of the ERF branch of the JA pathway, which would explain the reduction of defense against the necrotrophic pathogen *B. cinerea*, is not apparent from our transcriptome data. It may be that *MYB48/MYB59*-regulated genes that are enriched for 'Secondary metabolite biosynthetic processes' (represented by clusters 17–19, 21 and 25) and are down-regulated in the mutant are important for resistance to *B. cinerea*. This example highlights that higher-order mutants can reveal important gene regulatory functions that would otherwise be masked by genetic redundancy.

Chronology of MeJA-mediated transcriptional reprogramming

Next, we utilized the temporal information in our RNA-Seq time series to resolve the chronology of gene expression events in the JA gene regulatory network. First, we divided the genes into sets of up- and down-regulated DEGs and sorted them according to the time at which they first became differentially expressed (Supplemental Figure 5; see Methods for details). From this analysis, it became clear that a massive onset of gene activation precedes that of gene repression, and that different waves of coordinated gene expression changes can be identified in the time series. The majority of all DEGs became first differentially expressed within 2–4 h after MeJA treatment, which indicates engagement of relatively short transcriptional cascades, allowing for a rapid response to an external signal (Alon, 2007). Up- and down-regulated DEGs were then further separated into two additional sets based on their predicted function as transcriptional regulators (termed regulator genes) or as having a different function (termed regulated genes; Supplemental Dataset 3). We were specifically interested in identifying time points where coordinated switches in transcriptional activity take place, reasoning that pairs of adjacent time points that display a weaker correlation indicate important points of coordinated switches in transcriptional activity (see Methods and Supplemental Figure 6 for details). Therefore, within each of the four mutually exclusive gene sets, we examined the pairwise correlations of expression levels between all pairs of time points. Clustering of the resulting correlation matrices revealed six distinct phases in transcriptional activation, and four phases in transcriptional repression (Figure 2). The first two phases of up-regulation (phase Up1 and Up2) started within 0.5 h after MeJA treatment in the set of regulator genes, while at 1.5 h a third phase of up-regulation of regulator genes ensued (phase Up4). For the regulated genes, the first phase of up-regulation started at 1 h after MeJA treatment (phase Up3), which was clearly later than the first onset of the regulator genes. A similar sequence of events could be observed in the down-regulated regulator and regulated genes, although the start was delayed compared to the activation of up-regulated genes.

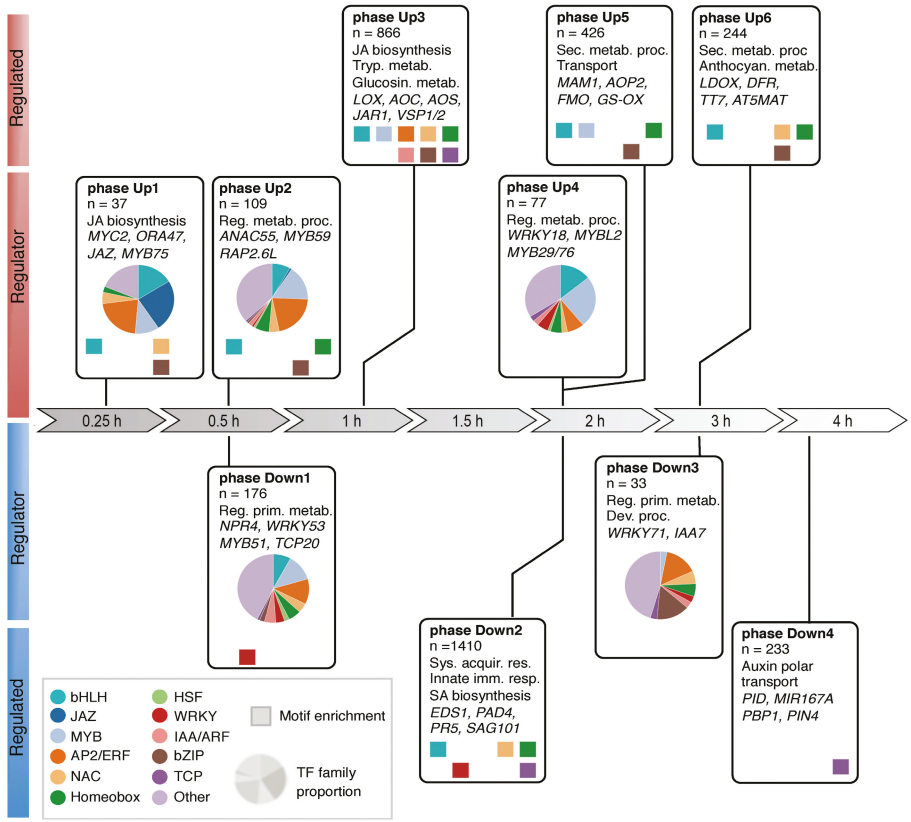

Figure 2. Chronology of changes in the MeJA-triggered gene regulatory network.

Analysis of the major transcriptional phases in the JA gene regulatory network. Transcriptional phases are indicated by boxes, aligned on the timeline. DEGs are assigned to the phases according to the time point where they become first differentially expressed; indicated are overrepresented functional categories and representative genes. Colored squares indicate known TF DNA-binding motifs overrepresented in gene promoters (hypergeometric distribution; $P \leq 0.001$). Pie charts indicate the proportion of TF gene families.

Our time series captured the temporal association between the changes in transcript abundance of transcriptional regulators and downstream targets encoding proteins responsible for the biochemical reactions that represent the defensive outputs of the JA response. To explore the biological significance and directionality in the regulation of the identified transcriptional phases in the JA gene regulatory network, all DEGs were assigned to the phase in which they first became differentially expressed (see Methods and Supplemental Figure 6 for details). The resulting gene lists of the 10 transcriptional phases were tested for overrepresentation of functional categories and promoter motifs (Figure 2; Supplemental Dataset 11–14). Phase Up1 represented the immediate transcriptional response, with genes encoding bHLHs, JAZs, MYBs, ERFs, and

other transcriptional regulators associated with JA biosynthesis. These early regulator genes may play a role in the induction of other regulator-encoding genes present in phases Up2 and 4, and of regulated genes present in phases Up3, 5 and 6, which are linked to defense responses such as glucosinolate, tryptophan and anthocyanin biosynthesis (Figure 2; Supplemental Dataset 12). In support of this relationship, in the promoters of DEGs in phase Up3, DNA motifs that could be bound by TFs transcribed in previous phases Up1 and 2, like bHLH-, ERF- and MYB-binding motifs, were enriched. In phase Up3, genes involved in JA biosynthesis were also enriched, suggesting that this process is one of the first targets of JA-mediated transcriptional reprogramming. Overall, induction of the JA pathway showed a clear chronology of up-regulated gene expression events, starting with the activation of genes encoding specific classes of TFs and of JA biosynthesis enzymes, followed by genes encoding enzymes involved in the production of important defensive secondary metabolites.

The first wave of transcriptional repression by MeJA was also marked by genes encoding transcriptional regulators, and began at 1 h after MeJA treatment, after which phases Down2, 3 and 4 followed at 2, 3 and 4 h after MeJA treatment, respectively (Figure 2; Supplemental Dataset 11). These groups of down-regulated genes highlight the antagonistic effects of JA on other hormone signaling pathways and defense responses in the first two phases. Phase Down1 for instance was characterized by the repression of different defense-related genes such as *NPR4* and *MYB51*, which encode regulators that promote SA responses and indolic glucosinolate biosynthesis, respectively (Gigolashvili et al., 2007; Fu et al., 2012). Accordingly, *MYC2*, which was induced by MeJA in phase Up1, was previously shown to suppress the accumulation of indolic glucosinolates (Dombrecht et al., 2007). Phase Down2 was also enriched for genes associated with SA-controlled immunity, including the key immune-regulators *EDS1* and *PAD4* (Feys et al., 2001). In line with these observations, there was an overrepresentation for WRKY-binding motifs in the promoters of genes present in phase Down 1 and 2, suggesting that their repressed expression was mediated by an effect of MeJA on WRKY action. Later phases of transcriptional repression (phases Down3 and 4) were marked by an overrepresentation of genes related to growth and development, including primary metabolism and auxin signaling, and an enrichment of DNA motifs recognized by TCP TFs, which conceivably reflects an effort by the plant to switch energy resources from growth to defense (Attaran et al., 2014). A general observation that can be made from this chronological analysis of the JA gene regulatory network is that despite the overall relatively short transcriptional cascades controlling gene activation or repression, distinctive transcriptional signatures, associated with specific biological processes, were initiated at different phases in time.

Inference of regulatory interactions reveals ORA47 as a key regulator of JA biosynthesis

Next, we made use of the TF DNA-binding motif information of the genes in the temporally separated transcriptional phases to construct a gene regulatory network that predicted directional interactions between the JA responsive TF genes and all genes associated with the different transcriptional phases (Supplemental Dataset 15). The JA gene regulatory network generated via this analysis is shown in Figure 3, in which a differentially expressed TF gene (represented by a circular node in the network) is connected by an edge to a transcriptional phase (represented by a rectangle in the network) when the corresponding DNA-binding motif was overrepresented in that phase. The generated network model showed TFs that were predicted to regulate expression of genes at either single or multiple transcriptional phases. The early phases likely contained key regulators of subsequent phases. Phase Up1 contained the TFs MYC2 and JAM1, which were among the most active TFs, as their cognate DNA-binding motifs (both share the same consensus, CACGTG) were enriched in the promoters of genes assigned to a large fraction of the up-regulated transcriptional phases. This prediction is in line with recent reports suggesting that the positive regulator MYC2 and the negative regulator JAM1 cooperate to balance JA responses by competitive binding to their shared target sequences (Nakata et al., 2013; Sasaki-Sekimoto et al., 2013). What determines the different timing by these regulators to effectively activate or repress transcription awaits further investigation. Phases Up1 and Up2 also contained the TF genes *bHLH27, ERF16, ANAC056* and *MYB59*, of which corresponding mutants showed altered resistance levels to *B. cinerea* infection and/or *M. brassicae* infestation (Figure 1C and 1D). Cognate DNA-binding motifs of these TF families were enriched in genes that were induced in multiple subsequent transcriptional phases (Figure 2 and 3).

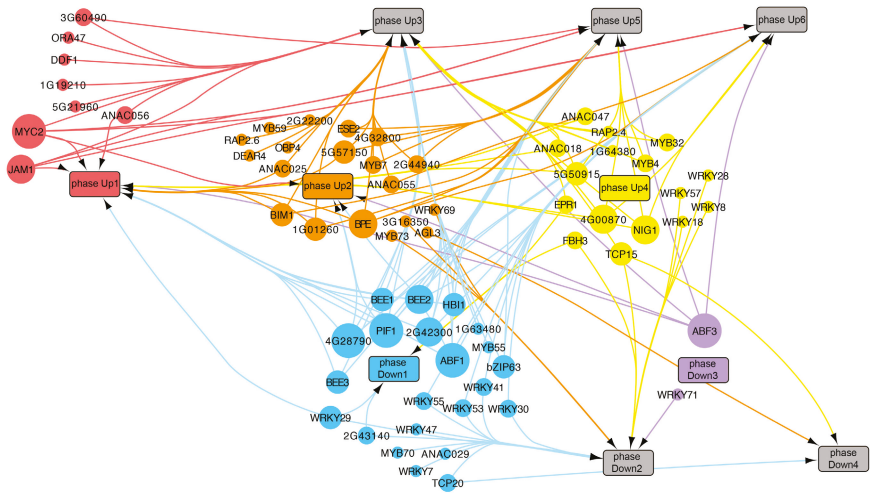

Figure 3. Predicted directional interactions in the JA gene regulatory network.

Network plot of inferred connections between MeJA-induced TFs and genes in transcriptional phases. The promoter sequences of genes associated with a transcriptional phase were tested for overrepresentation of DNA motifs shown to be bound to TFs that are differentially transcribed following MeJA treatment. Each TF with a known motif is represented by a colored circle, and is plotted at the time point that its corresponding gene is first differentially expressed. Each transcriptional phase is represented by a rectangle and plotted in time according to its onset. An edge between a TF and a phase indicates significant enrichment of the corresponding binding motif in that phase. The size of each TF node is proportional to the number of phases in which its binding site is overrepresented. To aid interpretation of the network, nodes are grouped and colored according to the transcriptional phase where they first become differentially expressed.

Phase Up1 also contained TF genes that were predicted to have a more limited regulatory scope, such as the ERF TF gene *ORA47*, for which the binding motif (consensus, CCG(A/T)CC) was overrepresented only in the promoters of genes assigned to phase Up3. These genes included the JA biosynthesis genes *LOX2*, *AOS*, *AOC1*, *AOC2*, *AOC3*, *ACX* and *OPR3*, thus suggesting that this *cis*-element and its cognate TF ORA47 may play a role in regulating JA production, which reflects the positive feedback loop that is known to maintain and boost JA levels upon initiation of the JA response (Wasternack, 2015). Focusing on this predicted subnetwork (Figure 4A), we found that *ORA47* and several of the JA biosynthesis genes were predicted to be targets of MYC2, suggesting that MYC2 together with ORA47 regulates JA biosynthesis in Arabidopsis. Figure 4B shows that the presence of the ORA47-binding motif was conserved between the promoters of *AOS*, *AOC2*, *OPR3* and *LOX3* orthologs of field mustard (*Brassica rapa*), grape (*Vitis vinifera*), and poplar (*Populus trichocarpa*), pointing to a role for ORA47 and its cognate binding element in the regulation of JA biosynthesis genes. Moreover, in stimulated β-estradiol-inducible *ORA47* plants, expression of *LOX2*, *LOX3*, *AOS*, *AOC1*, *AOC2* and

OPR3 was increased and accumulation of JA and JA-Ile was also enhanced (Figure 4C and 4D), which is in line with and extends previous findings (Pauwels et al., 2008; Chen et al., 2016). We did not observe a significant increase in expression of *JAR1*, encoding the enzyme responsible for catalyzing conjugation of JA with isoleucine, suggesting that basal JAR1 levels are sufficient for the conversion of excess JA into biologically active JA-Ile. Taken together, these experimental results supported our model prediction that ORA47 is an important regulator of JA biosynthesis and highlight the potential of combining time series expression data with motif analysis to infer key regulators and their targets in gene regulatory networks.

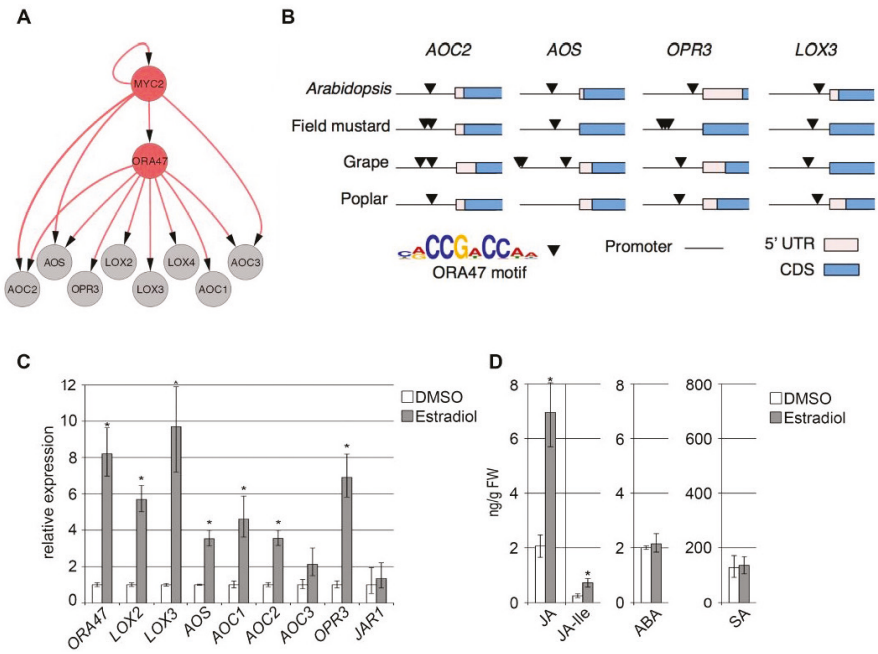

Figure 4. Prediction and functional analysis of ORA47-controlled subnetwork.

(**A**) Expanded sub-network extracted from the global JA gene regulatory network, indicating inferred regulation of JA biosynthesis genes by ORA47. Nodes indicating TFs and JA biosynthesis genes are colored grey and orange, respectively. Directed edges indicate occurrence of TF-binding sites in the promoter of the target gene. (**B**) Evolutionary conservation of ORA47 DNA-binding motif. Occurrences of the ORA47 motif (consensus, CCG(A/T)CC) were identified in promoters of an orthologous gene from each of the indicated JA biosynthesis genes (top row). Black arrows indicate a significant match within a gene promoter to the ORA47 motif. 5'UTR, 5-prime untranslated region; CDS, coding sequence. (**C**) Induction of genes encoding JA biosynthesis enzymes in estradiol-inducible *ORA47* plants. Expression levels of JA biosynthesis genes were measured in leaves 8 h after application of either estradiol or DMSO (mock) using quantitative RT-PCR (qRT-PCR). Shown are the mean expression levels of five biological replicates with mock treatments set at 1.

Asterisk indicates significant differences between mock- and estradiol-treated plants (Student's *t* test; $P \leq 0.05$; error bars are SE). (**D**) Production of JA, JA-Ile, ABA, and SA in estradiol-inducible *ORA47* lines. Compound levels were measured from the same leaf tissue harvested for the qRT-PCR analysis described in C. Asterisk indicates significant difference between mock- and estradiol-treated plants (Student's *t* test; $P \leq 0.05$; error bars are SE).

Inference of regulatory interactions reveals key regulators of JA subnetworks

For the vast majority of TFs in our chronological model, it was unclear which specific JA-responsive genes they regulate. To validate and extend our chronological network model further, we made use of transcriptome data sets of three Arabidopsis lines that are perturbed in TFs that were predicted by our model to regulate downstream subnetworks. First, we investigated the effect of the TFs MYB48 and MYB59 by studying their target genes in the *myb48 myb59* double mutant line. As described above (Figure 1G; Supplemental Dataset 6), 399 genes were differentially expressed compared to the wild type and the overlap between MeJA-responsive and MYB48/59-regulated genes was highly significant (164 DEGs, $P < 2.2e\text{-}16$; hypergeometric test). The vast majority of these genes were first differentially expressed after induction of *MYB48* and *MYB59* by MeJA treatment (Figure 5A). This pattern suggests that these DEGs may be downstream targets of MYB48/MYB59 activity during induced JA signaling. The likelihood of such targeting was confirmed by the enrichment of the MYB-binding motif in the promoter sequences of the down-regulated DEG set, while the enrichment in the up-regulated DEGs for the bHLH-binding motif suggests a role for MYB48/MYB59 in attenuation of the MYC branch of the JA pathway.

We also investigated the effect of the TF bHLH27 by studying their target genes in the *bhlh27* mutant. Transcriptional profiling of leaves from the *bhlh27* mutant under non-stress conditions, led to the identification of 197 DEGs (Supplemental Dataset 16). Of these, a significant portion (52 DEGs; $P < 4.93e\text{-}6$; hypergeometric test) was also differentially expressed in the MeJA time series. Projecting the common set of DEGs onto the transcriptional network model revealed that >95% of these genes were present in transcriptional phases that were temporally downstream of the phase containing *bHLH27* (phase Up2, Figure 5B). Analysis of the overlap between *bhlh27* DEGs and the MeJA-induced coexpression clusters from the present study revealed a specific enrichment for bHLH27 targets in cluster 7, 12, 19, 21 and 25, which are overrepresented for genes associated with JA-related responses such as JA biosynthesis, biological regulation and pigment metabolic process, suggesting a role for bHLH27 in the JA gene regulatory network, which may impact the resistance levels to *B. cinerea* positively and to *M. brassicae* negatively (Figure 1).

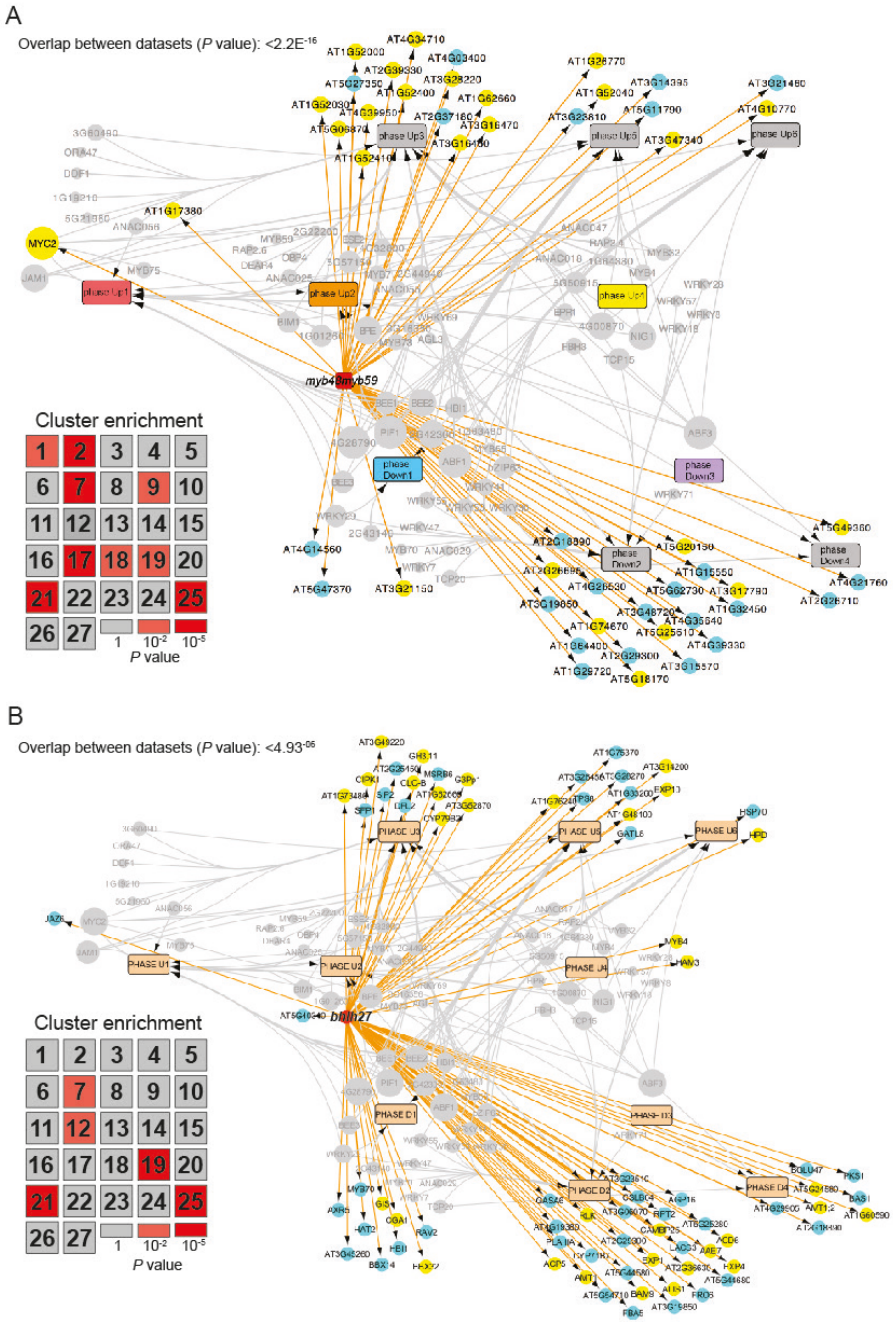

Figure 5. Projection of MYB48/MYB59 and bHLH27 target genes on the JA network model.

Genes that are differentially expressed in the *myb48myb59* double mutant line (**A**) and *bhlh27* (**B**) were overlaid on the network described in Figure 3. Due to space limitations, shown are the top 50 most significant differentially expressed overlapping genes.

DEGs are indicated by nodes and positioned according to phase membership. Direction of misregulation in the mutants is indicated by color; yellow, up-regulated; cyan, down-regulated. Edges are drawn out from a red-colored square node, representing *myb48 myb59* (**A**) or *bhlh27* (**B**); the *myb48 myb59* double mutant is situated between MYB59 in phase Up2 and MYB48 in phase Down1 (**A**), and the *bhlh27* mutant is situated in phase Up2 (**B**). Inset: heatmap indicating hypergeometric enrichment *P* value of bHLH27 target genes in each MeJA-induced coexpression cluster. A similar figure for MYB48/59 target genes is shown in Figure 1G.

Collectively, analysis of the transcriptomes of *myb48 myb59* and *bhlh27* suggests that in the context of the JA gene regulatory network, the studied TFs regulate specific subsets of genes and are associated with distinct biological processes. Thus, these examples demonstrate the value of leveraging TF perturbation transcriptome data with our information-rich MeJA-induced dataset to begin to explore specific transcriptional subnetworks, which better define the mechanistic function of individual TFs, and aids the holistic understanding of the JA gene regulatory network.

bHLH27 interactome network

Interactions between TFs with other proteins can strongly influence TF functionality. To identify binding partners of bHLH27, we conducted yeast two-hybrid (Y2H) screens for Arabidopsis proteins that interact with bHLH27. Fusion of bHLH27 to the Gal4 DNA binding domain (BD) showed substantial auto activation when used as bait, indicating that bHLH27 could activate transcription of the reporter gene. Therefore, we generated a series of eight different versions of bHLH27 that were truncated at different positions (Figure 6A). Only bHLH27Δ58, which is truncated at the N-terminus, displayed no auto activation in yeast when used as bait (Figure 6B).

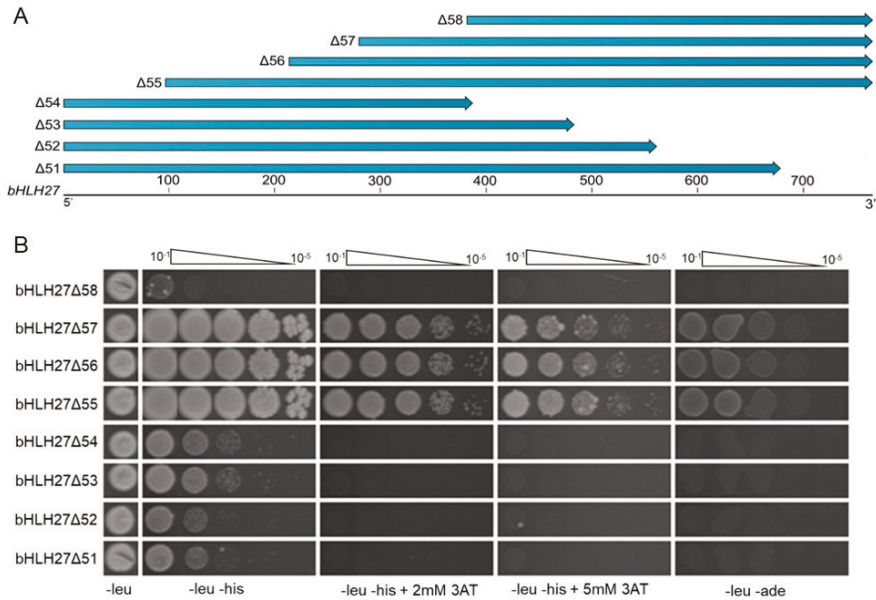

Figure 6. Screening of truncated versions of *bHLH27* for auto activation-negative Y2H bait constructs.

(**A**) The *bHLH27* coding sequence (cDNA) was truncated at eight different position (Δ51 to Δ58) at both 5' and 3' of the gene. The amplified fragments were cloned into Y2H bait vectors. (**B**) bHLH27 auto activation in yeast. Deletion fragments of the bHLH27 were assayed for auto activation in the Y2H system. Spots range 10^{-1} to 10^{-5} dilution in different auto activation selection media.

Y2H screens using bHLH27Δ58 as bait recovered nine potential targets, which are annotated with diverse molecular functions (Table 1). Three of the putative interacting proteins were annotated as regulators of transcription, including the TFs TCP13 and TCP21/CHE. These candidates are particularly interesting because the interactions between the MeJA-regulated bHLH27 with TCP family TFs may represent a mechanism of crosstalk between JA and transcriptional regulation by these TCPs, which regulate photomorphogenesis (Baba et al., 2001) and circadian clock (Pruneda-Paz et al., 2009), respectively).

The screen also revealed two candidate proteins that are involved in MAP kinase signaling, NDPK3 and CKL3, which have been associated with programmed cell death (Baek et al., 2004; Hammargren et al., 2008) and blue light signaling (Tan et al., 2013), respectively. Also, two candidates related to protein degradation were detected: a predicted component of the ubiquitin system, and enzyme CLPP4 that has endopeptidase functionality. Thus, these data suggest multiple points in the cellular

signaling cascade where bHLH27 may act through interaction with other proteins, thereby influencing JA responsiveness and functioning in different biological processes.

Table 1. Selected candidate binding partners for bHLH27Δ58.

AGI	Gene symbol	Description
AT4G11010	NDPK3	nucleoside diphosphate kinase
AT1G72340		translation initiation factor
AT4G28880	CKL3	protein serine/threonine kinase
AT5G45390	CLPP4	serine-type endopeptidase
AT3G02150	PTF1/TCP13	TF
AT5G08330	CHE/TCP21	TF
AT1G03130	PSAD-2	photosystem I reaction center subunit
AT4G38170	FRS9	transcriptional regulator
AT5G32440		ubiquitin system component

DISCUSSION

Our computational analyses of high-density time series of RNA-Seq data obtained from Arabidopsis leaves of the same developmental stage (leaf number 6) allowed us to provide an unprecedentedly detailed insight into the architecture and dynamics of the JA gene regulatory network. Previously, studies on phytohormone-induced transcriptional responses have typically included only a limited number of time points or focused on the effect of perturbation of specific regulatory proteins on transcriptional activity in hormone-controlled gene regulatory networks (Tsuda et al., 2009; Nakata et al., 2013). Our time series study shows that MeJA induces a burst of transcriptional activity that generates a variety of detailed temporal expression patterns that partition into specific gene clusters representing different biological processes (Figure 1, 2 and 4; Supplemental Figure 1 and 5). Differential expression analysis yielded a considerably more comprehensive MeJA-responsive gene set compared to previous transcriptomic studies, including a significant number of genes not represented on microarrays. In turn, this information yielded insights into the chronology and regulation of the biologically relevant JA response.

Network-informed discovery of players in the JA response

Using a dynamic network approach, we systematically determined how the diverse positive and negative regulatory components in the JA gene regulatory network function over time. MeJA-induced gene activation or repression was shown to be controlled

by short transcriptional cascades, yet yield distinctive transcriptional signatures that corresponded to specific sets of genes and biological processes (Figure 1). In general, it appears that bHLH TFs are master regulators controlling the majority of the MeJA-inducible genes, while ERF and MYB TFs fine-tune the expression of dedicated sets of target genes in specific sectors of the gene regulatory network (Figure 1, 2 and 3). Besides the known regulators of the JA pathway, several other TFs, whose functions were not previously linked to JA responses, were identified in the network. By using a guilt-by-association approach, twelve early MeJA-induced TFs with unknown roles in the JA response were selected for validation of their biological function in pathogen or insect resistance. Four of these (bHLH27, ERF16, MYB59, and ANAC056) were found to play a role in resistance against the pathogen *B. cinerea* and/or the insect *M. brassicae* (Figure 1), highlighting the high success rate of our approach in the discovery of biological functions of genes in the JA network. Collectively, our gene perturbation data provide an important starting point for the characterization of so-far unexplored components of the JA gene regulatory network, while numerous other early- and late-expressed TF or enzyme-encoding genes still await further exploration for functionality.

Mutants in bHLH27 and the double mutant lacking MYB48 and MYB59 were more susceptible to *B. cinerea*, yet more resistant to *M. brassicae* (Figure 1). Although this necrotrophic pathogen and chewing insect both stimulate JA biosynthesis, many subsequently induced changes in JA-responsive gene expression are specifically directed to the different attackers and hence engage different TFs and downstream targets. This differential response is coordinated by the mutually antagonistic ERF branch of the JA pathway, which is co-regulated by ET, and the MYC branch of the JA pathway, which is co-regulated by ABA (Pieterse et al. 2012). Several TFs have been documented to differentially affect MYC versus ERF branch-controlled gene expression and associated defenses. The best-known example of such a regulator is MYC2, a key positive regulator of MYC branch genes and associated defenses against chewing insects (e.g. *Helicoverpa armigera*, *Spodoptera littoralis*) (Dombrecht et al., 2007; Fernández-Calvo et al., 2011). By contrast, MYC2 negatively regulates defenses against necrotrophic pathogens (e.g. *B. cinerea*, *Plectosphaerella cucumerina*) (Lorenzo et al., 2004; Nickstadt et al., 2004). JA-inducible NAC TF family paralogs ANAC019 and ANAC055 show the same effect: they positively regulate MYC branch-associated genes and defenses to *S. littoralis*, while they antagonize ERF branch-associated resistance to *B. cinerea* (Bu et al., 2008; Schweizer et al., 2013). Oppositely, a positive regulator of the ERF branch, ORA59, controls defenses to *B. cinerea* while it antagonizes MYC branch defenses, and ORA59 overexpression lines become more attractive to *P. rapae* larvae (Pré et al., 2008; Verhage et al., 2011). Our data suggest that bHLH27 functions as a negative regulator of the MYC branch, which

may enhance ERF branch activation, thereby influencing resistance to *B. cinerea*. Other bHLH TFs (so called JAMs) have also been reported to antagonize MYC2-activated gene expression and defense to insects (Nakata et al., 2013; Sasaki-Sekimoto et al., 2013), but by contrast, ERF branch defense marker genes and resistance against *B. cinerea* were enhanced by the quadruple mutant lacking bHLH3 bHLH13 bHLH14 bHLH17 (Song et al. 2013). This finding indicates different underlying mechanisms of the different repressive bHLHs. MYB48 and MYB59 also antagonize the MYC branch as evidenced by the finding that the *myb48 myb59* mutant showed not only enhanced resistance to *M. brassicae*, but also enhanced expression of MYC branch-associated genes (Figure 1E–G; Supplemental Datasets 6 and 7). The transcriptome analysis of *myb48 myb59* did not suggest that the reduced resistance to *B. cinerea* is due to MYB48/MYB59-mediated antagonism of ERF branch. It may be that down-regulation of gene clusters enriched in specific secondary metabolism contributes towards compromised immunity in this mutant, but this awaits further functional analysis.

Uncovering redundant function by double mutant analysis

Reverse genetic screens are an important approach in the study of gene functions in Arabidopsis, but when additional genes have either fully or partially redundant functions, which is often the case with TF genes, their utility can be limited (Bolle et al., 2011). Redundancy may partially explain why 8 out of the 12 T-DNA insertion lines of the predicted JA-responsive TF genes that were tested in this study did not display significant changes in JA-associated immunity. By specifically targeting the highly similar TF-encoding gene pair *MYB48* and *MYB59*, we generated a double mutant that displayed a more severe perturbation of JA-associated gene expression and immunity compared to either single mutant (Figure 1E–G and Supplemental Figure 9). Use of higher-order mutants can be critical to understand TF gene regulatory functions.

Network reconstruction enables prediction of regulatory interactions

Our time series data discerned a chronology of 10 transcriptional phases, showing that the onset of up-regulation preceded that of down-regulation, and that the first phase that was initiated within 15 minutes was represented by transcriptional regulators (Figure 2). JA biosynthesis is shown to be a first target for activation, followed by secondary metabolism, including activation of the tryptophan, glucosinolate and anthocyanin biosynthesis pathways. This latter observation correlates with the later activation of many MYB TF genes, which are important regulators of secondary metabolism, and the enrichment of MYB DNA-binding motifs in the up-regulated genes in later phases. Down-regulated genes showed enrichment in WRKY TF-binding motifs, which is linked with the suppressed expression of SA-associated defense genes.

Integrating TF DNA-binding motif enrichment data with our chronological JA network model predicted putative causal regulations between TFs and downstream JA-regulated subnetworks (Figure 3, 4 and 5). Although subsets of the regulatory predictions were supported by the literature and by experimental validation in this study, the presented network model is not without limitations. Our approach does not consider potential nonlinear relationships between gene expression profiles, and has limited ability to account for expression of genes that strongly depend on the joint activity of more than one TF. Thus, a future extension of the work presented here could be to utilize these data with more formal modeling approaches that better account for combinatorial regulation of targets and/or are capable of capturing nonlinear characteristics of the regulatory system, such as approaches based on mutual information or dynamic Bayesian networks (Margolin et al., 2006; Penfold and Wild, 2011). Even when focusing on transcriptional networks as we have done here, it is important to note that some TFs may not be regulated transcriptionally themselves and hence are absent from our analysis. Additional techniques such as ChIP-seq and Y1H will help incorporate such regulators into the JA gene regulatory network model (Windram et al., 2014).

Dataset integration validates TF-specific regulatory functions

Exploring the regulatory predictions between TF regulators and their target genes highlighted a local regulatory module centered around the early JA-responsive AP2/ERF TF ORA47. Based on the occurrence of the ORA47 DNA-binding motif in their core promoters, we predicted that this TF targets a large fraction of genes encoding enzymes involved in JA biosynthesis in Arabidopsis (Figure 4A) and evolutionarily distant species (Figure 4B). Indeed, yeast one-hybrid experiments confirmed that ORA47 binds to promoter elements of JA biosynthesis genes (Supplemental Figure 7). Using transgenic lines that allow for the conditional expression of *ORA47* upon β-estradiol treatment, we showed that induction of *ORA47* expression significantly increases levels of JA and bioactive JA-Ile, indicating that ORA47 is an important activator of JA biosynthesis (Figure 4D). Recently, it was demonstrated that ORA47 could bind to the promoters of many of the JA biosynthesis genes reported here (Chen et al., 2016); however, the consequence for the expression of its target genes was only reported for a small subset. Using the β-estradiol conditional overexpression system allowed us to demonstrate that induction of *ORA47* expression indeed leads to the activation of all 7 important JA biosynthesis genes investigated (Figure 4C). Our *in silico* predictions combined with experimental validation underscore ORA47 as a central regulator of JA biosynthesis, which may form part of an evolutionarily conserved JA amplification loop (Figure 4B).

For many known and unknown JA-responsive TFs, their exact role in the JA gene regulatory network has remained unresolved. We show how integrating either existing or novel transcriptome data with our models of MeJA-mediated gene expression can generate hypotheses regarding the roles of specific transcriptional regulators in the context of the JA response. In particular, transcriptional profiling of a mutant line of the MeJA-responsive TF bHLH27 and subsequent overlay of the gene expression data onto our coexpression clusters led to the hypothesis that within the JA gene regulatory network bHLH27 plays a role in the regulation of JA biosynthesis-associated genes (Figure 5B). A similar approach, using the stress-associated TF MYB48/MYB59 (highlighted in this study), confirmed and extended the predicted regulatory interactions with distinct downstream targets in the JA network model (Figure 5A). Specific co-expressed gene clusters in the JA network were shown to be affected in the TF-perturbed lines, highlighting the strength of our clustering analysis for inferring functional regulation mechanisms. A similar transcriptome overlay approach could be used in future studies to further define the roles of other JA-inducible TFs in the diverse JA subnetworks.

Interplay of transcriptome and interactome network

Using Y2H screens we provided evidence that bHLH27 can interact with several different functional classes of protein, including proteins involved in signaling, transcriptional regulation, and protein degradation. Among these detected interactions where the TFs TCP13 and TCP21/CHE. Several members of the TCP family have been implicated in cross-TF family interactions (Bemer et al., 2017) and interestingly have also been identified as hubs in a large-scale protein-protein interaction screen (Arabidopsis Interactome Mapping, 2011). CHE (*CCA1 HIKING EXPEDITION*) is a well-known regulator of the circadian clock that has been shown to interact with TFs from the MYB, bZIP families. It is well established that the circadian clock regulates JA levels and JA-modulated defences; therefore, assessing the regulatory relationship between CHE and bHLH27, and the resulting effect on circadian regulation of JA signalling is an important next step. However, as with the other candidate bHLH27 interaction partners identified in this screen, it will be important to confirm the interaction between CHE and bHLH27 *in planta* (e.g., using bimolecular fluorescence complementation).

Summary

This study provides detailed insight into the dynamics and architecture of the JA gene regulatory network that is activated in Arabidopsis upon treatment with MeJA, and rapidly develops a range of transient or longer-lasting expression changes in specific groups of co-expressed genes with distinct biological functions. Our information-rich data set offers a potentially high success rate for the discovery of genes with so-far

unknown functions in JA-regulated responses related to plant immunity, growth and development. Future use of these time series data could include integration with additional transcriptome data across diverse environmental conditions, together with other 'omics' datasets, which will aid in building a comprehensive picture of the JA response.

METHODS

Plant materials and growth conditions

All wild-type, mutant, and transgenic *Arabidopsis thaliana* plants used in this study are in the Columbia ecotype (Col-0) background. The following T-DNA insertion mutants and transgenic lines were obtained from the Nottingham Arabidopsis Stock Centre: *ofp1* (At5g01840; SALK_111492C), *myb59* (At5g59780; GK-627C09), *anac056* (At3g15510; SALK_137131C), *rap2.6* (At1g43160; SAIL_1225G09), *erf16(-1)* (At5g21960; SALK_053563C), *erf16-2* (At5g21960; SALK_096382C), *at1g10586* (At1g10586; SALK_027725C), *bhlh19* (At2g22760; GABI_461E05), *bhlh27(-1)* (At4g29930; SALK_049808C), *bhlh27-2* (At4g29930; SALK_149244C), *bhlh35* (At5g57150; SALK_100300C), *bhlh92* (At5g43650; SALK_033657C), *bhlh113* (At3g19500; GK_892H04), *myb48* (At3g46130; SALK_103847), *ora59* (Zander et al., 2014) (At1g06160; GK-061A12.16), and *ORA47* β-estradiol-inducible TRANSPLANTA line (Coego et al., 2014) (N2101685). The *myb48* and *myb59* mutants were crossed to generate the *myb48 myb59* double mutant. The *myc2 myc3 myc4* (*myc2,3,4*) triple mutant (At1g32640/At5g46760/At4g17880) has been described previously (Fernández-Calvo et al., 2011). Seeds were stratified for 48 h in water at 4°C prior to sowing on river sand. After 2 weeks, the seedlings were transferred to 60-mL pots containing a soil:river sand mixture (12:5) that had been autoclaved twice for 1 h. Plants were cultivated in standardized conditions under a 10-h day (75 µmol/m^2/s^1) and 14-h night cycle at 21°C and 70% relative humidity. Plants were watered every other day and received modified half-strength Hoagland nutrient solution containing 10 mM Sequestreen (CIBA-GEIGY GmbH, Frankfurt, Germany) once a week. To minimize within-chamber variation, all the trays, each containing a mixture of plant genotypes or treatments, were randomized throughout the growth chamber once a week. Mutants or treatments were indicated by colored labels of which the code was unknown by the experimenter. T-DNA insertion lines were confirmed homozygous for the T-DNA in the relevant genes with PCR using the gene-specific primers listed in Supplemental Table 1.

RNA-Seq experimental setups

For the MeJA time series, 5-week-old Arabidopsis Col-0 plants were treated by dipping the rosette leaves into a mock or MeJA (Duchefa Biochemie BV, Haarlem, The Netherlands) solution. The mock solution contained 0.015% (v/v) Silwet L77 (Van Meeuwen Chemicals BV, Weesp, The Netherlands) and 0.1% ethanol. The MeJA solution contained 0.015% (v/v) Silwet L77 and 0.1 mM MeJA, which was added from a 1,000-fold stock in 96% ethanol. For time series expression analysis, leaf number 6 (counted from oldest true leaf to youngest leaf) was harvested from individual Arabidopsis plants and snap frozen in liquid nitrogen for each treatment and time point as indicated in Supplemental Dataset 1. Each individual leaf corresponds to one biological replicate and four biological replicates for each treatment and time point combination were sequenced (see below). For the comparison of the *myb48 myb59* mutant with wild-type Col-0, two mature leaves (number 6 and 7) were harvested per plant from two 5-week-old plants per genotype, resulting in two biological replicates.

Induction of the *ORA47* β-estradiol-inducible line and hormone analysis

Five-week-old *ORA47* inducible overexpression lines were treated by dipping the rosette leaves into a mock or β-estradiol (Sigma-Aldrich, Steinheim, Germany) solution. The mock solution contained 0.015% (v/v) Silwet L77 and 0.1% DMSO. The β-estradiol solution contained 0.015% (v/v) Silwet L77 and 10 µM β-estradiol, which was added from a 1,000-fold stock in DMSO.

Hormone analysis was performed as described previously (Vos et al., 2013b). Briefly, for JA, JA-Ile, SA, and ABA quantification, 0.5 g of leaf tissue was ground to a fine powder using liquid nitrogen. Samples were homogenized in 0.5 ml of 70% methanol using a Precellys24 tissue homogenizer (Bertin Technologies) by shaking at 6,000 rpm for 40 s. The resulting homogenates were centrifuged at 10,000 x *g* for 20 min at 4°C. Hormone levels were analyzed by liquid chromatography-mass spectrometry (LC-MS) on a Varian 320 Triple Quad LC-MS/MS. JA and JA-Ile levels were calculated by correcting for the internal standard of JA and for leaf weight. ABA and SA levels were calculated by correcting for leaf weight and their respective internal standards.

Insect performance and disease bioassays

Botrytis cinerea disease resistance was determined essentially as described previously (Van Wees et al., 2013). In brief, *B. cinerea* was grown on half-strength Potato Dextrose Agar (PDA; Difco BD Diagnostics, Franklin Lakes, NJ, USA) plates for 2 weeks at 22°C. Harvested spores were incubated in half-strength Potato Dextrose Broth (PDB; Difco) at a final density of 5 x 10^5 spores/mL for 2 h prior to inoculation. Five-week-old plants

were inoculated by placing a 5-µL droplet of spore suspension onto the leaf surface. Five leaves were inoculated per plant. Plants were maintained under 100% relative humidity with the same temperature and photoperiod conditions. Disease severity was scored 3 days after inoculation in four classes ranging from restricted lesion (<2 mm; class I), non-spreading lesion (2 mm) (class II), spreading lesion (2-4 mm; class III), up to severely spreading lesion (>4 mm; class IV). The distribution of disease categories between genotypes were compared using a Chi-squared test.

Mamestra brassicae eggs were obtained from the laboratory of Entomology at Wageningen University where they were reared as described previously (Pangesti et al., 2015). Per 5-week-old Arabidopsis plant one freshly hatched first-instar (L1) larva was directly placed on a leaf using a fine paintbrush. Larval fresh weight was determined after 8–12 days of feeding. To confine the larvae, every plant was placed in a cup that was covered with an insect-proof mesh. Significant differences in larval weight between genotypes were determined using a two-tailed Student's *t* test.

High-throughput RNA-sequencing

Arabidopsis leaves were homogenized for 2 x 1.5 min using a mixer mill (Retsch, Haan, Germany) set to 30 Hz. Total RNA was extracted using the RNeasy Mini Kit (Qiagen) including a DNaseI treatment step in accordance with manufacturer's instructions. Quality of RNA was checked by determining the RNA Integrity Number (RIN) using an Agilent 2100 Bioanalyzer and RNA 6000 Nano Chips (Agilent, Santa Clara, United States). For Illumina TruSeq RNA library preparation (see below) only RNA samples with a RIN value of ≥ 9 were used.

For the time series experiment, RNA-Seq library preparation and sequencing was performed by the UCLA Neuroscience Genomics Core (United States). Sequencing libraries were prepared using the Illumina TruSeq mRNA Sample Prep Kit, and sequenced on the Illumina HiSeq2000 platform with read lengths of 50 bases. In total, 12 randomized samples were loaded per lane of a HiSeq2000 V3 flowcell, and each mix of 12 samples was sequenced in 4 different lanes over different flow cells to account for technical variation. A complete scheme of all biological replicates, technical replicates, barcoding used per sample, lane and flow cell usage is provided in Supplemental Dataset 1. For each of the 15 time points, 4 biological replicates were sequenced in 4 technical replicates, resulting in ~60 million reads per sample with a read length of 50 bp single end. Complete sequencing setup details can be found in Supplemental Dataset 1.

Basecalling was performed using the Casava v1.8.2. pipeline with default settings except for the additional argument '--use-bases-mask y50,y6n', to provide an additional Fastq file containing the barcodes for each read in each sample. Sample demultiplexing was performed by uniquely assigning each barcode to sample references, allowing for a maximum of 2 mismatches (the maximum allowed by the barcode) and only considering barcode nucleotides with a quality score of 28 or greater.

For the analysis of the *myb48 myb59* double mutant and the *bhlh27-2* mutant, RNA-Seq library preparation and sequencing was performed by the Utrecht Sequencing Facility (the Netherlands). Sequencing libraries were prepared using the Illumina Truseq mRNA Stranded Sample Prep Kit, and sequenced on the Illumina NextSeq5000 platform with read lengths of 75 bases.

The raw RNA-Seq read data are deposited in the Short Read Archive (http://www.ncbi.nlm.nih.gov/sra/) and are accessible through accession numbers PRJNA224133 (time course of MeJA and mock treatment) and PRJNA395645 (*myb48 myb59* mutant and Col-0 wild type).

Processing of RNA-Seq data

Read alignment, summarization and normalization followed the pipeline as previously described (Van Verk et al., 2013). Reads were aligned to the Arabidopsis genome (TAIR version 10) using TopHat v2.0.4 (Trapnell et al., 2009) with the parameter settings: 'transcriptome-mismatches 3', 'N 3', 'bowtie1', 'no-novel-juncs', 'genome-read-mismatches 3', 'p 6', 'read-mismatches 3', 'G', 'min-intron-length 40', 'max-intron-length 2000'. Aligned reads were summarized over annotated gene models using HTSeq-count v0.5.3p9 (Anders et al., 2015) with settings: '-stranded no', '-i gene_id'. Sample counts were depth-adjusted using the median-count-ratio method available in the DESeq R package (Anders and Huber, 2010).

Differential gene expression analysis

Genes that were significantly differentially expressed after MeJA treatment compared to mock were identified using a generalized linear model (GLM) with a log link function and a negative binomial distribution. Within this model we considered both the time after treatment and the treatment itself as factors. To assess the treatment effect on the total read count for each gene, a saturated model (total counts ~ treatment + time + treatment:time) was compared to a reduced model considering time alone (total counts ~ time) using ANOVA with a Chi-squared test. For all genes, the *P* values obtained from the Chi-squared test were corrected for multiple testing using a Bonferroni correction.

All genes that did not meet the following requirement were omitted from further analysis: a minimum 2-fold difference in expression on at least one of the 14 time points, supported by a minimum of 10 counts in the lowest expressed sample, and a *P* value ≤ 0.01 for that time point. Remaining genes with Bonferroni-corrected *P* value ≤ 0.05 were called as differentially expressed genes (DEGs). All statistics associated with testing for differential gene expression were performed with R (http://www.r-project.org).

Of all the DEGs, the time point of first differential expression was predicted. To this end the significance of the treatment effect at each time point was obtained from the GLM, represented by its *z* score. These values were used as a basis to interpolate the significance of the treatment effect in between the sampled time points. This was done using the interpSpline function in R using 249 segments. The first time point of differential expression was set where the *z* score was higher than 2.576 (equivalent of *P* value 0.01) for up-regulation or lower than -2.576 for down-regulation.

Differentially expressed genes between Col-0 and *myb48 myb59* and *bhlh27* ($|\log_2$-fold change$|$ >1; FDR ≤0.05) were identified using DESeq (Anders and Huber, 2010).

Clustering of gene expression profiles

Clustering of DEGs was performed using SplineCluster (Heard et al., 2006) on the profiles of $\log_2$-fold changes at each time point (MeJA-treated versus mock), with a prior precision value of 10^{-4}, the default normalization procedure and cluster reallocation step (Heard, 2011). All other optional parameters remained as default.

TF family and promoter motif analyses

To determine which TF families were enriched among the genes differentially expressed in response to application of MeJA, we tested for overrepresentation of 58 TF families described in the TF database PlantTFDB version 3.0 (Jin et al., 2014). Overrepresentation of TF families within a set of genes was analyzed using the cumulative hypergeometric distribution, with the total number of protein coding genes (TAIR version 10) as the background. *P* values were corrected for multiple testing with the Bonferroni method.

For promoter motif analysis, the promoter sequences defined as the 500 bp upstream of the predicted transcription start site (TSS) were retrieved from TAIR (version 10). *De novo* promoter motifs were identified by applying the motif-finding programs MEME (Bailey and Elkan, 1994) and XXmotif (Hartmann et al., 2013) to the promoters of all genes present in a given coexpression cluster. This approach exploited the strengths of different motif-finding strategies, which has been demonstrated to improve the

quality of motif detection (Tompa et al., 2005). Both algorithms searched for motifs on the forward and reverse strands and used the zero-or-one occurrences per sequence (ZOOPS) motif distribution model. MEME was run using a 3rd-order Markov model learned from the promoter sequences of all genes in the Arabidopsis genome, using parameter settings: '-minw 8 -maxw 12 -nmotifs 10'. XXmotif was run using a 3rd-order Markov model and the medium similarity threshold for merging motifs, with all other parameters kept as default. This analysis yielded a large number of motifs, many of which were highly similar. To reduce redundancy amongst motifs, a post-processing step was performed using the TAMO software package (Gordon et al., 2005). Motifs were converted to TAMO format, clustered using the UPGMA algorithm, and merged to produce consensus motifs. The set of processed motifs was converted to MEME format for all subsequent analyses using the tamo2meme function available in the MEME Suite (Bailey et al., 2009). For the analysis of known motifs originating from protein-binding microarray (PBM) studies (Franco-Zorrilla et al., 2014; Weirauch et al., 2014), the published weight matrices were converted into MEME format.

The presence or absence of a given motif within a promoter was determined using FIMO (Grant et al., 2011). A promoter was considered to contain a motif if it had at least one match with a *P* value ≤ 10^{-4}. For each *de novo*- and PBM-derived motif, the statistical enrichment of each motif within the promoters of coexpression gene clusters or transcriptional phases was tested using the cumulative hypergeometric distribution. This test computed the probability that a motif was present within a set of promoter sequences at a frequency greater than would be expected if the promoters were selected at random from the Arabidopsis genome.

Analysis of the *ORA47* DNA-binding motif conservation across different plant species was performed using the promoters of genes orthologous to Arabidopsis *AOC2*, *AOS*, *OPR3* and *LOX3.* Orthologs were identified in *Vitis vinifera*, *Populus trichocarpa* and *Brassica rapa* genomes (Ensembl database release 25) using the reciprocal best BLAST hit method (Tatusov et al., 1997). Presence or absence of the *ORA47* motif in the promoters (500 bp upstream of predicted TSS) of these orthologous genes was determined using FIMO as described above.

Gene Ontology analysis

Gene ontology (GO) enrichment analysis on gene clusters was performed using GO term finder (Boyle et al., 2004) and an Arabidopsis gene association file downloaded from ftp.geneontology.org on 2nd May 2013. Overrepresentation for the GO categories 'Biological Process' and 'Molecular Function' was identified by computing a *P* value

using the hypergeometric distribution and false discovery rate for multiple testing ($P \leq 0.05$).

Identification of chronological phases in MeJA-induced gene expression

To identify phases of MeJA-induced changes in transcription we first divided all DEGs depending on whether they were either up- or down-regulated in response to MeJA and then further according to their function as either a transcriptional regulator (termed regulator genes) or having a different function (termed regulated genes). To identify DEGs that encode transcriptional regulators, we used the comprehensive list of Arabidopsis TFs and transcriptional regulators described by Pruneda-Paz et al., (2014) and subjected it to minor additional manual literature curation. This filtering yielded four mutually exclusive sets of MeJA-responsive genes (i.e. regulator genes up and down, regulated genes up and down). For each of the four gene sets, the depth-normalized expression values (see above) for all pairs of time points were compared pairwise using the Pearson correlation measure. Each resulting correlation matrix was then clustered using the Euclidean distance measure with average linkage. The resulting dendrograms were used to infer distinct phases of MeJA-induced transcription, where each phase had a start and end time. Each gene present in one of the four final gene sets was assigned to a transcriptional phase based on its time point of first differential expression (Supplemental Figure 5). All genes that were for the first time differentially expressed before, or equal to, the final time point in a given phase (clustered group of time points), and after the final time point of a preceding phase, were assigned to that transcriptional phase (see Supplemental Figure 6 for overview of the method).

Network construction

The identification of potential regulatory network connections between TFs and transcriptional phases was performed with a set of TFs that met two criteria: (1) They were differentially expressed in response to application of MeJA (and thus belonged to a phase). (2) They had an annotated DNA-binding motif (as described in "TF family and promoter motif analyses"). Each set of genes that constituted a transcriptional phase (10 phases in total) was tested for overrepresentation of each motif using the hypergeometric distribution as described above. A directional edge was drawn from a TF to a phase when its cognate binding motif was overrepresented in the promoters of genes belonging to that phase (hypergeometric distribution; $P \leq 0.005$). The resulting network was visualized using Cytoscape (Shannon et al., 2003).

Quantitative RT-PCR analysis

For quantitative RT-PCR (qRT-PCR), RNA was extracted as previously described (Oñate-Sánchez and Vicente-Carbajosa, 2008) and subsequently treated with DNaseI (Fermentas, St. Leon-Rot, Germany) to remove genomic DNA. Genomic DNA-free total RNA was reverse transcribed by using RevertAid H minus Reverse Transcriptase (Fermentas, St. Leon-Rot, Germany). PCR reactions were performed in optical 384-well plates with a ViiA 7 realtime PCR system (Applied Biosystems, Carlsbad, CA, USA), with SYBR® Green (Applied Biosystems, Carlsbad, CA, USA). A standard thermal profile was used: 50°C for 2 min, 95°C for 10 min, followed by 40 cycles of 95°C for 15 s and 60°C for 1 min. Amplicon dissociation curves were recorded after cycle 40 by heating from 60 to 95°C with a ramp speed of 0.05°C/sec. All primers used for qRT-PCR are listed in Supplemental Table 1. The gene *At1g13320* was used as reference for normalization of expression (Czechowski et al., 2004).

Generation of the Y2H prey library and bait constructs

RNA originating from 15-day-old Arabidopsis seedlings was isolated using phenol/chloroform extraction and cDNA library was constructed using Invitrogen Custom Services (Invitrogen, Carlsbad, CA). A three-open reading frame, uncut cDNA library integrated into pENTR222 was created from 2 mg RNA using Gateway cloning technology. The library was subcloned into Y2H destination vector pDEST22 to generate GAL4-AD-fused constructs. Full-length *bHLH27* and truncated forms were amplified from cDNA and cloned into entry vector pENTR/D-TOPO (Invitrogen). Entry vectors were recombined with pDEST32 using LR Clonase (Invitrogen) to generate GAL4-BD-bHLH27 fusion constructs.

Yeast strains and transformation

To create competent yeast, cells were grown o/n in 250 ml YEPD at 28 °C and 200 rpm to an OD_{600} of 0.2-0.8. Cells were centrifuged at 1800 rpm for 5 min, washed with 50 ml sterile ddH_2O, centrifuged again and washed a final time with 50 ml TE/LiAc (100 mM LiAc, 10 mM Tris, 1 mM EDTA, pH 8.0). After a final centrifugation step, yeast cells were resuspended in TE/LiAc and diluted to an OD_{600} of 0.2. For single construct transformation, 20 µl of competent yeast cells were incubated with 200 ng plasmid and 20 µl salmon sperm DNA (Sigma #D1626; 2 mg/ml in TE, heated at 95 °C for 5 min and transferred to ice) in 11 µl 10xTE buffer (100 mM Tris, 10 mM EDTA, pH 8.0), 13 µl 1 M LiAc, 82 µl 60% PEG at 30 °C for 30 min, and then to a water bath at 42 °C for 15 min. To each transformation reaction 1 ml ddH_2O was added and centrifuged at 5000 rpm for 30 sec and resuspended in ddH_2O. Bait strains were selected on synthetic complete (Sc) –Leu medium and prey strains were selected on Sc –Trp medium. For

library transformation the protocol was scaled up to 3200 µl competent yeast cells and 90 µg plasmid DNA. Yeast colonies were harvested in YEPD medium + 20% (v/v) glycerol and 1 ml aliquots with an OD_{600} of 40 were frozen at -80 °C. The yeast prey library consisted of 1.1 x 10^6 – 1.5 x 10^6 individual colonies. Yeast strain Y8800 (genotype MATa trp1−901 leu2−3,112 ura3−52 his3− 200 gal4Δ gal80Δ cyh2R GAL1::HIS3@LYS2 GAL2::ADE2 GAL7::LacZ@met2) was used for prey and yeast strain Y8930 (genotype MATα trp1−901 leu2−3,112 ura3−52 his3−200 gal4Δ gal80Δ cyh2R GAL1::HIS3@LYS2 GAL2::ADE2 GAL7::LacZ@met2) was used for bait. Bait strains that grew on Sc –Leu –His plates in the absence of prey were considered auto-activating and discarded (Schiestl and Gietz, 1989).

Library screening

Library screening was performed using the mating method (Fromont-Racine et al., 2002). A 1 ml yeast library aliquot was used to inoculate 100 ml YEPD medium, and incubated with shaking at 28 °C for 1 h, after which the yeast cells were centrifuged at 1800 rpm for 5 min and washed twice with ddH_2O. Yeast were resuspended in YEPD medium to OD_{600} = 1. Six ml of yeast library was combined with an equal amount of overnight-cultured bait-strain cells, collected by centrifugation, resuspended in 300 µl ddH_2O and plated on YEPD medium supplemented with 100 µg/ml ampicillin. After incubation at 30 °C for 4 h, 2 ml ddH_2O was added to the plate to resuspend the yeast, which were collected by centrifugation and resuspended in 600 µl ddH_2O. Yeast was plated on Sc –Leu –Trp –His + amp medium and incubated at 30 °C for four days. The yeast suspension was diluted 10^5-fold and plated on Sc –Leu –Trp + amp medium to determine the number of diploid yeast screened. For each bait a minimum of 10^6 diploid cells were screened. Up to 96 colonies per Sc –Leu –Trp –His + amp plate were picked, resuspended in 25 µl ddH_2O and spotted on fresh Sc –Leu –Trp –His + amp medium in duplo. After incubation at 30 °C for two days, one plate was used for replica plating and the other for colony PCR. Yeast was replica plated on Sc –Leu –Trp –His + 2 mM 3-amino-1,2,4-triazole (3AT) (Formedium) + amp medium and Sc –Leu –Trp –His +5 mM 3AT + amp medium followed by incubation at 30 °C for two days, and plated on Sc –Leu –Trp –Ade + amp medium followed by incubation at 20 °C for five days. For colony PCR, yeast patches from a Sc –Leu –Trp –His + amp plate were touched with a pipette tip, resuspended in 30 µl 0.02 M NaOH and boiled at 99 °C for 10 min. Lysates were spun down briefly and 1 µl of the supernatant was used for a 10 µl PCR reaction with DreamTaq DNA polymerase (ThermoScientific) and primers pDEST22 and pDEST22/32 (Supplemental table 1). Prey PCR products were purified using Agencourt AMPure XP beads according to the manufacturer's protocol and Sanger sequenced.

Accession numbers

RNA-Seq data, including gene accession numbers, are available in the NCBI SRA under accession numbers PRJNA224133 (MeJA time series) and PRJNA395645 (Col-0 and *myb48 myb59*).

Supplemental Data

Additional supporting information Supplemental File 1, Supplemental Figures S1 to S9, and Supplemental Data S1 to S16 may be found in the online version of Hickman *et al.,* (2017): http://www.plantcell.org/content/29/9/2086

Figure S1. SplineCluster analysis of MeJA-responsive gene expression profiles**.**

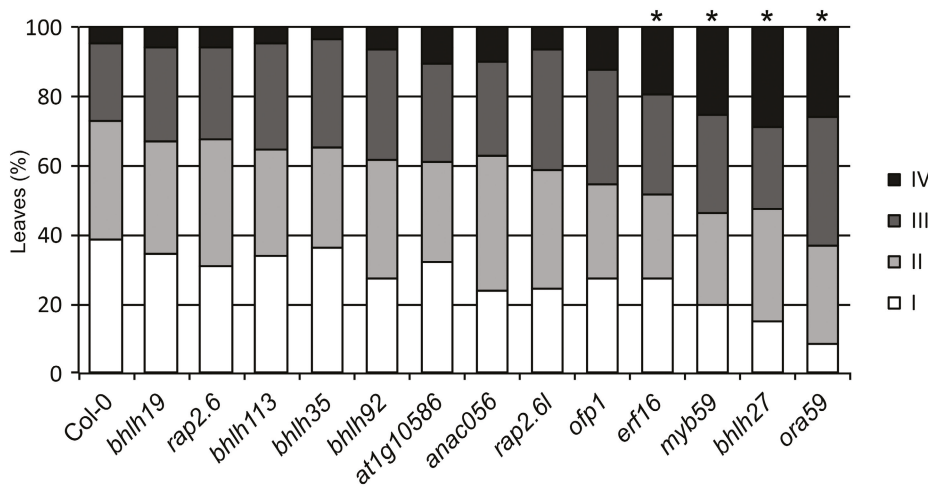

Figure S2. *B. cinerea* disease severity assay with selected mutant lines.

Quantification of *B. cinerea* disease severity at 3 days after inoculation of T-DNA insertion lines for selected genes encoding predicted early regulators of the JA pathway. *bHLH19*, *RAP2.6*, *bHLH027* belong to Cluster 1; *AT1G10586*, *RAP2.6L*, *OFP1*, *ERF16* belong to Cluster 2; *MYB59* belongs to Cluster 4; *bHLH92* belongs to Cluster 6; *bHLH35* belongs to Cluster 7; *ANAC056* belongs to Cluster 13; *bHLH113* belongs to Cluster 14. Disease severity of inoculated leaves was scored in four classes ranging from restricted lesion (class I), non-spreading lesion (class II), spreading lesion (class III), up to severely spreading lesion (class IV). The percentage of leaves in each class was calculated per plant (n=20). Asterisk indicates statistically significant difference from Col-0 (Chi-squared test; $P \leq 0.05$). Most genotypes were tested multiple times.

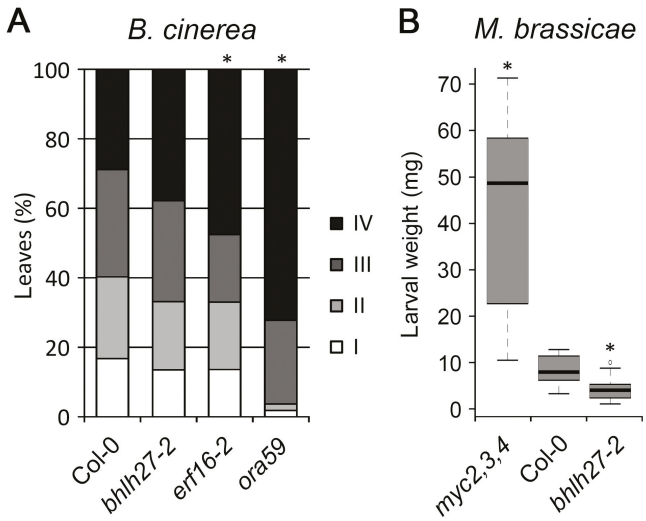

Figure S3. *B. cinerea* disease severity and growth of *M. brassicae* larvae on additional mutant alleles.

(A) Quantification of *B. cinerea* disease severity at 3 days after inoculation of T-DNA insertion lines harboring an *bHLH27* or *ERF16* mutation (*bhlh27-2, erf16-2*) different from that in the mutant lines tested in main Figure 2 (and Supplemental Figures 3 and 5). Disease severity of inoculated leaves was scored in four classes ranging from restricted lesion (class I), non-spreading lesion (class II), spreading lesion (class III), up to severely spreading lesion (class IV). The percentage of leaves in each class was calculated per plant (n=20). Asterisk indicates statistically significant difference from Col-0 (Chi-squared test; $P \leq 0.05$). **(B)** Larval fresh weight of *M. brassicae* was determined after 8 days of feeding on *bhlh27-2*. Asterisk indicates statistically significant difference from Col-0 (two-tailed Student's *t* test for pairwise comparisons; $P \leq 0.05$; n > 10; error bars are SE).

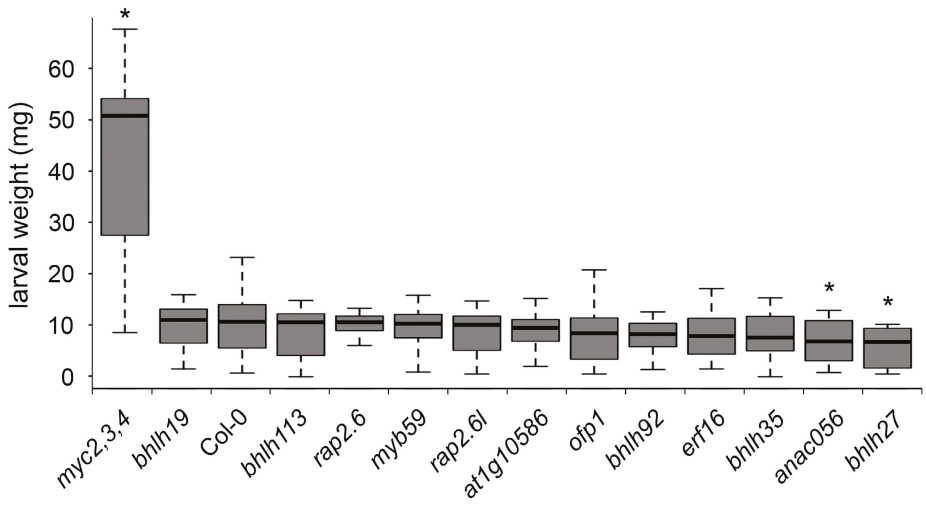

Figure S4. Growth of *M. brassicae* larvae on selected mutant lines.

T-DNA insertion lines were chosen based on the MeJA-induced expression of the TF genes they are mutated in. See for information on which coexpression gene cluster the genes belong to the Legend to Supplemental Figure 3. Larval fresh weight was determined after 8 days of feeding on T-DNA insertion lines for selected genes encoding predicted regulators of the JA pathway. Values represent mean weight (±SE) of the larvae. Asterisk indicates statistically significant difference from Col-0 (two-tailed Student's *t* test for pairwise comparisons; $P \leq 0.05$; n=30; error bars are SE). Most genotypes were tested multiple times.

Figure S5. Timing of differential expression for all differentially expressed genes.

Figure S6. Identification of transcriptional phases induced in response to MeJA treatment.

Table S1. List of primers used for genotyping of T-DNA mutants, qRT-PCR analysis and promoter cloning for Y2H assays.

Primers used for genotyping T-DNA mutants		
T-DNA line	Forward primer (5'-3')	Reverse primer (5'-3')
SALK_111492C	ATTGGGCCGAAAACATATAGG	CGACCGCATTCTAAGTCTCAC
GK-627C09	AAGAGGAATGCCATAGGTTCC	AGTGGGTGGTGATTTTTGATG
SALK_137131C	GGCACTGCGTCGTTATATAGG	AGACTCCACCATTGATGCAAC
SALK_051006C	TTCGGTTCGTGTGTTTTTCA	TATGCTGATCGGTGGTTCAA
SAIL_1225G09	TCAATCAACGTGTCATGAAGG	TCAGACTGAAGTTGTATTGGGAG
SALK_053563C	GCCACGGCTCATTTATTTTAAG	CGGCTCTTTACTGTCTTCGTG
SALK_027725C	GATGAATGTCCTTGCTATCGC	TTTATTGGCACCAACAGTTGC
GABI_461E05	ATCAAATGCATTTTGAGTGCC	CACGAAACGATTGTGTCAATG
SALK_049808C	AAACAAAAATTGCTGGTGACG	GGCCATAATCATTACGTACGC
SALK_100300C	CCAAGAAAAAGTAAAAGGGAACC	TAGCAATTGCAATCTGCTGC
SALK_033657C	AAATTTTGTTGCCAAGACACG	AATCTCATCCACGGCTTTTTC
GK_892H04	CCCCTCTAAAAAGGTACACATTG	AAGGAGTAACGAGCTTCTCCG
Primers used for qRT-PCR		
Gene	Forward primer (5'-3')	Reverse primer (5'-3')
ORA47	TCCACCGTCGATCTCCGTAGAAAA	GCGAATCTAGCAGCAGCTTCCTGA
LOX2	ACAGCCAAGGGCACTTCATT	TGATTCTGGGGAGCAGAGGT
LOX3	AACACAACCACATGGTCTTAAACTC	GGAGCTCAGAGTCTGTTTTGATAAG
AOS	TCCGATTTCTCTCCACCCAAA	TGACCCGGAAGCTTTGATCG
AOC1	CTCTCAGAACTTGGGAAATAC	GATCTCCGAGACCAAAACCTA
AOC2	ATCGAAAACCCTAGACCAAGC	CGAGACCGAACATTAAGCTGA
AOC3	CGAAGGAGATAGAAACAGTCCAGC	CCGAGACAAAGCTCTGTTGGTT
OPR3	CCGGCGGTTTTCTCATCTC	GCTTCCATGCTTCTACTTGT
JAR1	GGGTTGTATCGATACCGGCTTGG	CTTCTGAGAGTCTCTTTGCAGCCG
Primers used for cloning for Y2H assay		
Promoter	Primer (5'-3')	
bHLH27 - FW	ATGGAAGATCTCGACCATGAGTACAAGA	
bHLH27 - RV	TTAGAAGTTGATAAGACAATTTGGATCATTATAAGC	
Δ51 – RV	TTACGCCTGGAGGAAGAGGGTGGT	
Δ52 – RV	TTACTTGCTACATGTTATGCATACCACTACCGT	
Δ53 – RV	TTAGTGTTGTACTCTAGTACTGTAATCCATCTG	
Δ54 – RV	TTAGCAATCGTAATCTCTTACCGGATTTTCTAG	
Δ55 – FW	GCGTTTTCGGGTTCCGGCGAG	
Δ56 – FW	GCTCTCCGGTCAGTTGTTCCCAAT	

Table S1. Continued

Primers used for cloning for Y2H assay	
Δ57 – FW	GACTATATGCAAGAACTTATTGATCAAGAGAAGACT
Δ58 - FW	GATTGCAATTTTGCGGAAACTCATCTGCAA
pDEST22 - FW	TATAAGCCGTTTGGAATCACT
pDEST22/32- RV	AGCCGACAACCTTGATTGGAGAC

Supplemental Data Set 1. Time series experimental setup and mRNA sequencing details.

Supplemental Data Set 2. Median-count ratio normalized expression values of all genes and biological replicates for t = 0 h and the 14 time points after MeJA and mock treatments.

Supplemental Data Set 3. Mean expression values for all genes across the time series following MeJA treatment.

Supplemental Data Set 4. Arabidopsis Gene Identifier codes for members of each of the 27 gene coexpression clusters identified by SplineCluster.

Supplemental Data Set 5. GO terms overrepresented in each of the 27 coexpression gene clusters.

Supplemental Data Set 6. Lists of genes differentially expressed *in myb48 myb59* compared with Col-0.

Supplemental Data Set 7. GO terms overrepresented in the upregulated and downregulated *myb48 myb59* differentially expressed gene sets.

Supplemental Data Set 8. Enrichment of known TF DNA binding motifs in each of the 27 coexpression gene clusters.

Supplemental Data Set 9. De novo-derived motif enrichment in each of the 27 gene coexpression clusters.

Supplemental Data Set 10. De novo-derived sequence motifs in Weblogo and position weight matrix format.

Supplemental Data Set 11. Arabidopsis Gene Identifier codes for members of each of the 10 transcriptional phases that are initiated after MeJA treatment.

Supplemental Data Set 12. GO terms overrepresented in each of the 10 transcriptional phases that are initiated after MeJA treatment.

Supplemental Data Set 13. Known TF DNA binding motif enrichment in each of the 10 transcriptional phases that are initiated after MeJA treatment.

Supplemental Data Set 14. De novo-derived motif enrichment in each of the 10 transcriptional phases that are initiated after MeJA treatment.

Supplemental Data Set 15. List of differentially expressed TF genes and enrichment of their corresponding TF DNA binding motif in the promoters of genes within a transcriptional phase.

Supplemental File 1. Gene ID-searchable significance of differential expression over time for all DEGs in the 27 clusters of coexpressed genes in response to MeJA treatment.

3

Architecture and dynamics of the salicylic acid gene regulatory network infers a novel role for NAC transcription factors in plant immunity

Richard Hickman[1], Marciel Pereira Mendes[1], Marcel C. Van Verk[1,2], Anja J.H. Van Dijken[1], Jacopo Di Sora[1], Katherine Denby[3], Corné M.J. Pieterse[1], Saskia C.M. Van Wees[1]

[1]Plant-Microbe Interactions, Department of Biology, Science4Life, Utrecht University, P.O. Box 800.56, 3508 TB, Utrecht, the Netherlands

[2]Bioinformatics, Department of Biology, Science4Life, Utrecht University, P.O. Box 800.56, 3508 TB, Utrecht, the Netherlands

[3]Department of Biology, University of York, York, YO10 5DD, UK

The work described in Chapter 3 is a large study with important contributions of different authors. Marciel Pereira Mendes was one of the main contributors to this story, which includes the screening of transcription factor mutants in bioassays (Fig. 7), and all work (bioassays, RNA-seq, coexpression analysis, RT-qPCR) related to NAC61 NAC90 (Fig. 8, 9, and 10; Supplemental Fig. S2).

ABSTRACT

The phytohormone salicylic acid (SA) is a central regulator of plant immunity. To better understand SA-mediated transcriptional reprogramming, we performed high-resolution RNA-seq time series of Arabidopsis leaves treated with SA. Analysis of this large-scale, information-rich data set revealed that approximately one-third of the Arabidopsis genome was differentially expressed in response to SA over a 16-h period. The temporal changes in gene expression occurred in well-defined process-specific waves of induction or repression that partitioned into distinct clusters representing coregulated genes covering a broad-range of biological processes. Promoter analysis of these clusters generated novel insights into the underlying regulatory mechanisms recruited by the specific SA network. Finally, we demonstrated the utility of our dataset for the identification of novel defense regulators by demonstrating that knockout of the predicted SA pathway regulators *ANAC061* and *ANAC090* resulted in increased disease resistance and enhanced SA signaling in specific sectors. Collectively, our data provide an unprecedented level of detail about transcriptional changes during the SA response, revealing previously unknown regulators, and serving as a valuable resource for functional studies on SA network components in plant defense.

INTRODUCTION

In plants, like all complex organisms, the execution of specific gene expression programs is required to ensure proper development and appropriate responses to environmental perturbations and stresses. Phytohormones play important roles in regulation of gene expression programs. Direct and indirect interactions between genes and their molecular regulators, such as transcription factors (TFs), determine the complexity of the global large-scale reprogramming of gene activity (MacNeil and Walhout, 2011). Understanding the organization of these gene regulatory networks (GRNs) and how they ultimately drive specific biological outputs are key questions in plant biology, with the resulting knowledge important for driving improvement of agronomically important traits in crops (Ferrier et al., 2011; Krouk et al., 2013; Lavarenne et al., 2018).

To understand the dynamic organization and regulation of complex gene expression programs plant biologists are increasingly seeking to study systems in their entirety rather than focus on a small number of genes (Long et al., 2008). Such systems biology approaches are being driven by high-throughput omics technologies that can monitor different aspects of gene expression on a whole-genome scale. In particular, the accumulation of mature mRNA as determined by microarrays and high-throughput RNA sequencing (RNA-seq) analyses has emerged as the leading method for systems level gene expression profiling. Moreover, most biological processes are dynamic, and by collecting transcriptome data of high-resolution time series the regulatory networks and their sub-modules underlying gene expression programs can be more accurately deciphered. Several of these large-scale transcriptome studies have generated key biological and regulatory insights into a wide-range of plant responses, including for example, development, hormone signaling, and abiotic and biotic stresses (Chapter 2; Brady et al., 2007; Krouk et al., 2010; Breeze et al., 2011; Bechtold et al., 2016; Hickman et al., 2017; Hillmer et al., 2017; Mine et al., 2018). While many studies used time series mRNA data alone to successfully infer plant GRN models (Krouk et al., 2010; Breeze et al., 2011; Windram et al., 2014; Lewis et al., 2015; Bechtold et al., 2016; Walker et al., 2017), a small number of recent studies have combined dynamic time series data with protein–DNA interaction data (Song et al., 2016; Varala et al., 2018), which typically enhance the confidence of reconstructed GRN models and their regulatory predictions.

Phytohormones are key regulators of GRNs that are essential for a wide range of biological processes, including plant growth, development, reproduction, and survival. Changes in hormone concentration or sensitivity, as triggered among others by biotic stresses, induce gene expression programs that orchestrate a range of adaptive plant

responses (Pieterse et al., 2012). Salicylic acid (SA) and jasmonic acid (JA) are major players in plant defense (Pieterse et al., 2012; Howe et al., 2018). While the JA pathway is generally induced by and effective against necrotrophic pathogens and herbivorous insects, the SA pathway is generally regulating resistance against (hemi-)biotrophic pathogens that feed and reproduce on living host tissue, such as *Pseudomonas syringae* and *Hyaloperonospora arabidopsidis* on *Arabidopsis thaliana* (hereafter Arabidopsis). SA has a well-established central role in the two major layers of plant immunity: pathogen-associated molecular pattern (PAMP)-triggered immunity (PTI), which is activated after pattern recognition receptors recognize conserved microbial patterns, and effector-triggered immunity (ETI), which is activated when the host detects perturbations in host cells caused by pathogen effector molecules (Klessig et al., 2018). Also, SA is involved in the broad-spectrum induced immune mechanism, well-known as systemic acquired resistance (SAR) (Fu and Dong, 2013). Numerous studies, many of which utilized mutant screens, have revealed a diverse set of pathways, effector genes and host cellular processes as regulatory targets of SA (Vlot et al., 2009), including the production of antimicrobial pathogenesis-related (PR) proteins that promote immunity against diverse pathogens (Van Loon et al., 2006). In addition to its role in defense, SA also plays important roles in plant growth, development, thermotolerance, leaf senescence, responses to ultraviolet light and shade avoidance (Vlot et al., 2009; Nozue et al., 2018).

Over the past decade, studies in the reference plant Arabidopsis have dramatically enhanced our understanding of how SA is perceived and how this perception leads to changes in defense gene expression. Recent studies support a model in which the regulatory protein NONEXPRESSOR OF PR GENES1 (NPR1), and two close relatives, NPR3 and NPR4 each function as SA receptors (Fu et al., 2012; Wu et al., 2012; Ding et al., 2018; Innes, 2018). In the absence of a pathogen, when SA levels are low, NPR3- and NPR4-containing complexes are active and suppress the transcription of defense-related genes, while the activity of NPR1, which is a positive regulator of defense-related gene expression, is constrained at low levels of SA. Following pathogen detection, elevated SA levels and increased binding of SA by all three NPR proteins leads to reverses in NPR activity. Binding of SA to NPR3 and NPR4 inactivates the co-transcriptional complexes, relieving their repressive activities (Ding et al., 2018), while NPR1 is activated by SA binding, leading to enhanced transcription of downstream target genes (Wu et al., 2012; Ding et al., 2018). NPR1 has been shown to be critical for the activation of a large fraction of SA-responsive genes, with a minority being regulated by an NPR1-independent mechanism (Wang et al., 2006).

Transcriptional reprogramming is a major feature of the SA response, and several studies have identified thousands of Arabidopsis transcripts that change in expression after treatment with either SA or benzothiadiazole S-methylester (BTH; a functional analog of SA) (Wang et al., 2006; Goda et al., 2008; Blanco et al., 2009), pointing to the existence of a complex GRN of TFs and target genes downstream of the core NPR-TGA transcriptional complexes. Several groups of TFs have been identified as regulators of the SA-mediated response. The role of members of the WRKY TF family in host immunity is firmly established, and several of them have been implicated in the regulation of SA-mediated transcriptional reprogramming by functioning as either positive or negative regulators of SA-responsive genes, including SA biosynthesis genes (Fu and Dong, 2013; Tsuda and Somssich, 2015). Selected members from other TF families, including NAC, TCP, CAMTA and E2F, have also been reported to regulate SA-responsive genes (Du et al., 2009; Zheng et al., 2012; Chandran et al., 2014; Wang et al., 2015c; Zheng et al., 2015).

Different combinations of phytohormones organize the plant's reaction to multiple environmental inputs it perceives at the same time. Crosstalk between hormone signaling pathways generates an extra layer of complexity in the GRNs, which finetunes the adaptation responses in a cost-efficient manner (Spoel and Dong, 2008; Vos et al., 2013a; Vos et al., 2015). In particular, the SA response is influenced by the antagonistic or synergistic action of other defense-associated hormones, like JA, ABA, and auxin (Pieterse et al., 2012; Caarls et al., 2015). Antagonistic cross-communication between the SA and JA pathways, in both directions, is a paradigm for hormone pathway crosstalk, and has been demonstrated in several plant species (Pieterse et al., 2012). Attackers can exploit this antagonistic relationship to rewire the host immune response for their own benefit by the production of effector molecules that specifically activate either the SA or JA pathway to attenuate otherwise effective JA- or SA-mediated defenses, respectively (Brooks et al., 2005; El Oirdi et al., 2011; Gimenez-Ibanez et al., 2014). Recent studies have begun to provide insights into the mechanisms underlying crosstalk between the SA and JA pathways. The ERF TF ORA59 had reduced transcript and protein levels upon activation of the SA pathway (Van der Does et al., 2013; Zander et al., 2014). The SA response was antagonized by three closely related JA-induced NAC TFs, which affected SA biosynthesis and metabolism (Zheng et al., 2012).

Despite the major role of the SA pathway in mediating plant immunity, relatively little is known about the organization of the GRNs that operate downstream of SA perception and the NPR signaling module, and which members from the diverse TF families orchestrate the elaborate gene expression programs that lead to SA-mediated immunity. Moreover, the dynamics of SA responses, such as which genes are targeted

when, affecting which biological processes, and what are the underlying regulatory mechanisms, remains poorly understood. Previously, we used high temporal resolution transcriptome profiling of MeJA-treated Arabidopsis leaves (Chapter 2; Hickman et al., 2017). In the present study, we profiled the dynamics of the transcriptional response to treatment with of Arabidopsis leaves with SA to (1) obtain a detailed understanding of the architecture and dynamics of the GRN that underlie the SA response, and (2) predict and validate novel regulators of the SA-controlled GRN and SA-mediated immunity.

RESULTS

A time course of SA-elicited transcriptional reprogramming

We performed high-resolution transcriptional profiling of the SA response in Arabidopsis by using RNA-seq to measure mRNA levels in leaves harvested just before the treatments (t = 0 h) and at 14 consecutive time points (15 and 30 min, and 1, 1.5, 2, 3, 4, 5, 6, 7, 8, 10, 12 and 16 h) following treatment with SA or a mock control. True leaf 6 from four independent 5-week-old Col-0 plants that were rosette-dipped in the SA or mock solution, was sampled in quadruplicate, providing four biological replicates per time point, per treatment. This leaf tissue was treated and harvested simultaneously with the material used in our previously published time series study of the JA response (Chapter 2; Hickman et al., 2017). Also, the RNA-seq libraries preparation and sequencing was performed in parallel with that of the MeJA study, and therefore the mock-treated control samples are shared between the two studies. To identify genes that responded to SA, we fitted a generalized linear model (GLM) to our transcription data, which led to the identification of 9524 differentially expressed genes (DEGs) between SA and mock treatments over the time course (Supplemental Data Set S1; see Methods). Many of these genes were not previously described as SA responsive in earlier array-based studies, where one to three time points were assayed in seedlings treated with SA (Goda et al., 2008; Blanco et al., 2009) or whole plants treated with benzothiadiazole S-methylester (BTH; a functional analog of SA) (Wang et al., 2006). Moreover, in our experiment the SA treatment clearly had a greater effect on the overall gene expression than MeJA treatment that changed the expression of 3611 genes (Chapter 2; Hickman et al., 2017).

Inspection of the expression profiles for known SA responsive genes revealed a variety of dynamic expression patterns, including genes that showed transient responses, sustained induction/repression, and some with complex behavior. To achieve this, we estimated the time at which each gene first became differentially expressed using a previously outlined strategy (Chapter 2; Hickman et al., 2017) and we divided the

genes in two sets of up- and downregulated DEGs (based on agglomerative hierarchical clustering, described in greater detail below). Plotting of the time point of first differential expression for all up- and downregulated DEGs indicated key time points of transcriptional change, which pointed to distinct transcriptional waves (Figure 1). Three waves of upregulation and two waves of downregulation were identified. For both gene sets the first wave of expression (0–2 h after SA treatment), representing the immediate transcriptional response to SA, contains a far greater number of DEGs than the subsequent waves, representing the intermediate/late SA response.

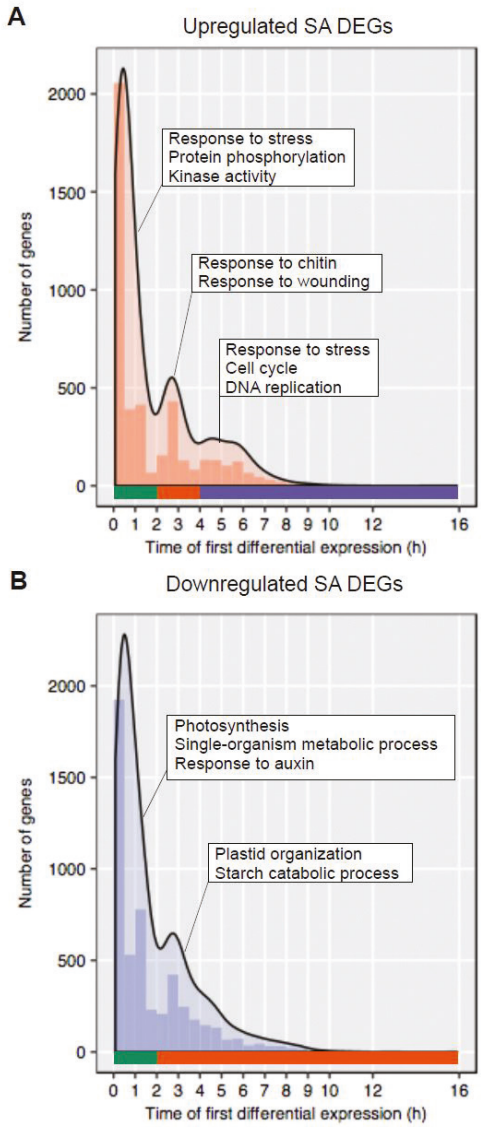

Figure 1. Major transcriptional waves of the SA response.

Shown is the number of genes estimated to be first differentially expressed in 30 min time windows for genes upregulated (**A**) and downregulated (**B**) in Arabidopsis leaves following exogenous application of SA. Colored bars indicate waves of transcription, with green, orange and purple indicating the first, second and third waves respectively. Transcriptional waves are annotated with the most significant functional categories in each wave together with additional selected significant terms.

To investigate the biological relevance of these transcriptional waves, the genes assigned to each wave were tested for overrepresented functional categories using Gene Ontology (GO) term enrichment analysis. Interestingly, we found that each wave was enriched for distinct annotations, indicating a chronology in the regulation of different biological processes mediated by SA signaling. The first and largest wave of gene upregulation (Figure 1A) was linked to immune signaling, such as 'protein phosphorylation', 'signal transduction', 'vesicle mediated transport' and 'programmed cell death'. Genes upregulated in the second wave (2–4 h) were enriched for JA-related defensive functions such as 'response to chitin' and 'response to wounding'. The third, and final, wave of upregulation (4 h onwards) was associated with cell cycle and DNA repair. Both waves of downregulated gene expression by SA (Figure 1B) were overrepresented for terms related to photosynthesis and include genes related to photosystem I and II, and chlorophyll biosynthesis. Distinct term enrichment was also apparent; for example, the terms 'response to auxin' and 'starch metabolism' were selectively enriched in the first and second waves, respectively. Concluding, this analysis showed that distinct pathways became active at different times during the SA response, which makes these transcriptome data more suitable than previously generated data sets for delineating the transcriptional programs induced by SA.

Coherent functional modules of coexpressed genes

To characterize the key patterns of gene regulation during the SA response, we used the time-series clustering algorithm SplineCluster to group the 9524 DEGs into 45 clusters of coexpressed genes that share similar expression profiles (Figure 2A; Supplemental Data Set S2). To investigate the biological significance of the distinct dynamic expression patterns, the genes in each cluster were tested for overrepresented functional categories using GO term enrichment analysis (Supplemental Data Set S2). Many of the clusters showed enrichment for coherent functional annotations and showed a wide range of distinct biological processes to be regulated by SA (Figure 2B).

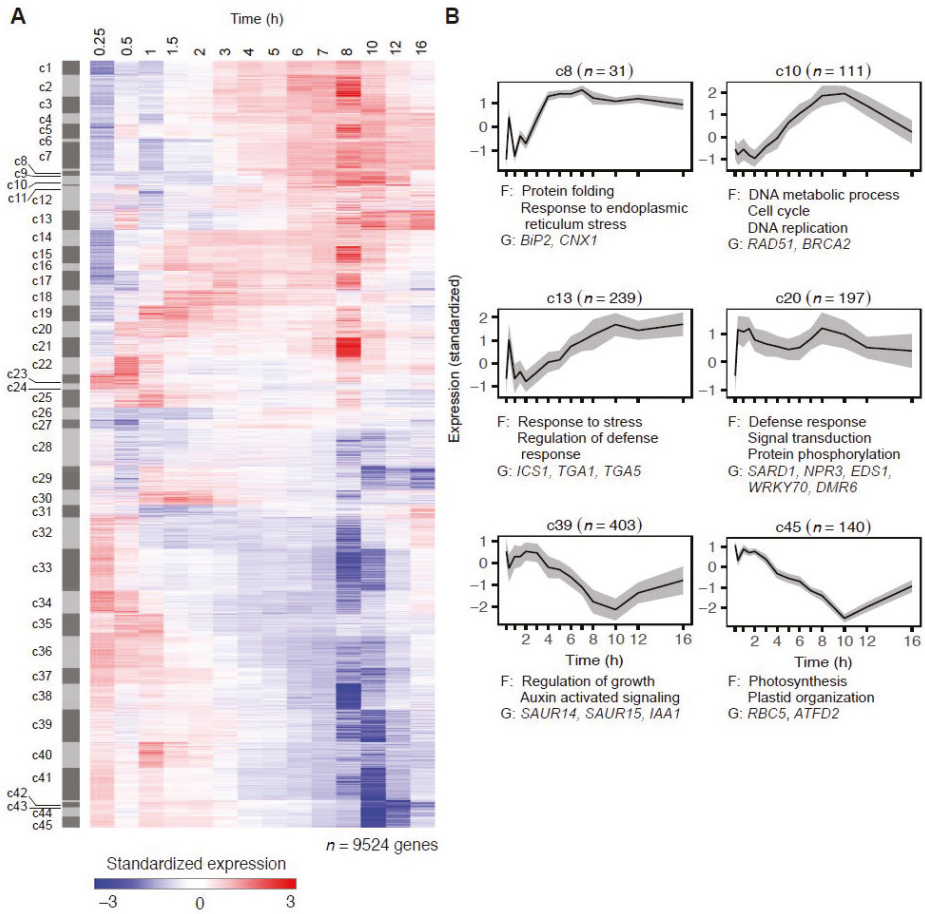

Figure 2. Temporal analysis of SA-responsive genes reveals coherent functional modules of coexpressed genes.

(**A**) The set of 9524 genes showing differential expression in response to SA were partitioned into 45 (c1–c45) distinct coexpressed gene clusters using SplineCluster. Each row of the heatmap represents an individual gene and indicates level of expression, with red and blue indicating increased and decreased expression (standardized on a per gene basis across mock and SA treatments), respectively. (**B**) Representative coexpression modules with distinct functional enrichment. Shown is the mean expression profile for a module (black line), with grey areas indicating median absolute deviation. Cluster number and size (*n*) is indicated above each plot. Selected overrepresented functional categories (F) and representative genes (G) are denoted.

As expected, several upregulated coexpression clusters were enriched in immune-related annotations (e.g., c13, c19, c20), and correlate with many previously described primary SA-responsive genes, including genes involved in SA metabolism (*ICS1, PBS3, EDS5, DMR6, CBP60g, and SARD1*), and known regulators of the SA pathway (*TGA1*, *TGA5*, *NPR4*, *NIMIN1, NIMIN2, WRKY18*, *WRKY51*, *WRKY54* and *WRKY70*). Some

coexpression modules were enriched for other defined SA-regulated biological pathways and processes. For example, c8 was associated with the protein folding response (Wang et al., 2005), and c10 was highly enriched for genes involved in DNA replication and cell cycle regulation (Wang et al., 2010; Wang et al., 2014).

Downregulated clusters showed how SA may regulate the switch from normal growth to defense with broad overrepresentation for functional terms associated with growth and development, and primary metabolism. Strikingly, there was strong enrichment of genes associated with photosynthesis among downregulated genes. Clusters c41–c45, all of which showed a marked decrease in transcript levels following SA treatment, were overrepresented for photosynthesis and plastid-related genes. Distinct enrichment of genes associated with development was also evident; for example, c35 and c39 are specifically overrepresented for genes associated with cell wall organization/biogenesis and auxin signaling, respectively. SA-mediated suppression of the auxin pathway has been shown to be an important component of plant defense (Wang et al., 2006).

Thus, our information-rich time series expression profiles revealed in unprecedented detail the broad range of biological processes differentially regulated by SA and refines the breadth of the SA-responsive gene expression program. The specific and coherent functional enrichment of genes in both up- and downregulated gene clusters suggests an elaborate GRN controlling the phasing of the changes in expression of these genes and biological processes to ultimately favor defense over normal growth and development.

Transcriptional control of the SA response

To investigate mechanisms of gene regulation underlying the SA response, we analyzed the coregulation of transcriptional response of Arabidopsis to SA at two levels of granularity. First, we created a set of coarse-grain SA-response modules, which we defined as the unions of upregulated (c1–c25) and downregulated (c26–c45) gene clusters, and analyzed these large gene list for enriched TF-families and *cis*-regulatory elements in order to capture broad mechanisms of coregulation.

Within the SA-upregulated coarse-grained module, genes encoding members of the WRKY and NAC TF families were significantly overrepresented (Figure 3A). In line with the enhanced activity of genes encoding these TFs, motifs corresponding to DNA binding sites of WRKY and NAC TFs were also overrepresented in the group of upregulated genes, suggesting that these TF families dominate the onset of SA-induced gene expression (Figure 3B). Genes in the downregulated coarse-grained module were overrepresented for members of the HD-ZIP, CO-like and bHLH TF-families (Figure 3A), which have been

shown to regulate processes associated with development, photosynthesis, and JA-dependent responses (Ariel et al., 2007; Leivar and Quail, 2011; Gangappa and Botto, 2014). The SA-mediated downregulation of genes associated with these processes, may be achieved through SA suppressing members of these TF families. Interestingly, bHLH and bZIP TF binding motifs, which both share the same G-box core, are both similarly enriched in up and downregulated coarse-grained modules, and may reflect both positive and negative roles for members of these TF families in the regulation of the SA response.

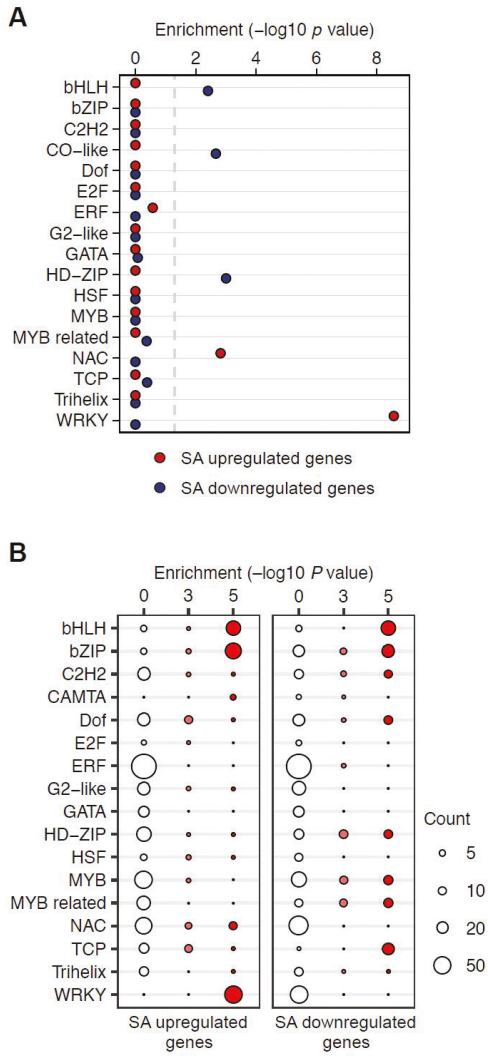

Figure 3. Enriched TFs and DNA-binding motifs in genes upregulated and downregulated in response to SA.

(**A**) Significantly overrepresented genes of TF families within the unified upregulated (c1–25; red or downregulated (c25–45; blue) gene clusters in response to SA treatment. Corrected *P* value < 0.01 (indicated by dashed grey line) (hypergeometric test). (**B**) Significantly overrepresented DNA-binding motifs in the promoters of genes upregulated or downregulated in response to SA treatment. Motifs are grouped according to cognate TF family. The size and color of each circle represent the per-family motif count and enrichment *P* value range (hypergeometric test), respectively. Significantly enriched motif frequencies are indicated by red coloring.

Next, we investigated more specific regulatory mechanisms that may control the smaller subsets of process-specific SA-responsive genes, by analyzing motif enrichment within each of the 45 fine-grained coexpression modules identified by the SplineCluster analysis (Figure 4). This revealed promoter elements that were selectively enriched in specific clusters, and offered a more precise link between motifs and module-specific expression patterns. DNA-binding motifs associated with WRKY TFs were highly enriched in many upregulated coexpression clusters, further demonstrating the importance of this TF family and its cognate binding sites in the regulation of the SA response. Binding sites for NAC TFs were also significantly and selectively overrepresented in a number of upregulated clusters. For both the WRKY and NAC DNA-binding motifs, the broad pattern of enrichment is consistent with the large-scale induction of genes that encode TFs from these families following SA treatment (Figure 3A). Despite its prevalence among upregulated clusters, several upregulated clusters lacked enrichment for the WRKY binding motif (W-box), suggesting additional TFs and *cis*-elements primarily regulate genes in these groups. For example, c9 and c10 are enriched for E2F TF DNA-binding motifs, while c12 and c22 are enriched for binding sites for HSF and CAMTA TF families, respectively. Consistent with the functional term analysis results, TF families implicated with regulation of growth and development are enriched in several downregulated clusters. For example, TCP and HD-ZIP TF DNA-binding motifs are selectively enriched in downregulated clusters, and members of both of these families are linked with regulation of growth and development (Martín-Trillo and Cubas, 2010). Binding sites for bHLH and bZIP TF families (both of which can bind DNA sites that contain the core G-box motif) were enriched in both selected upregulated and downregulated clusters, suggesting that G-box motifs play an important role in directing both the activation and suppression of target genes as part of the SA response.

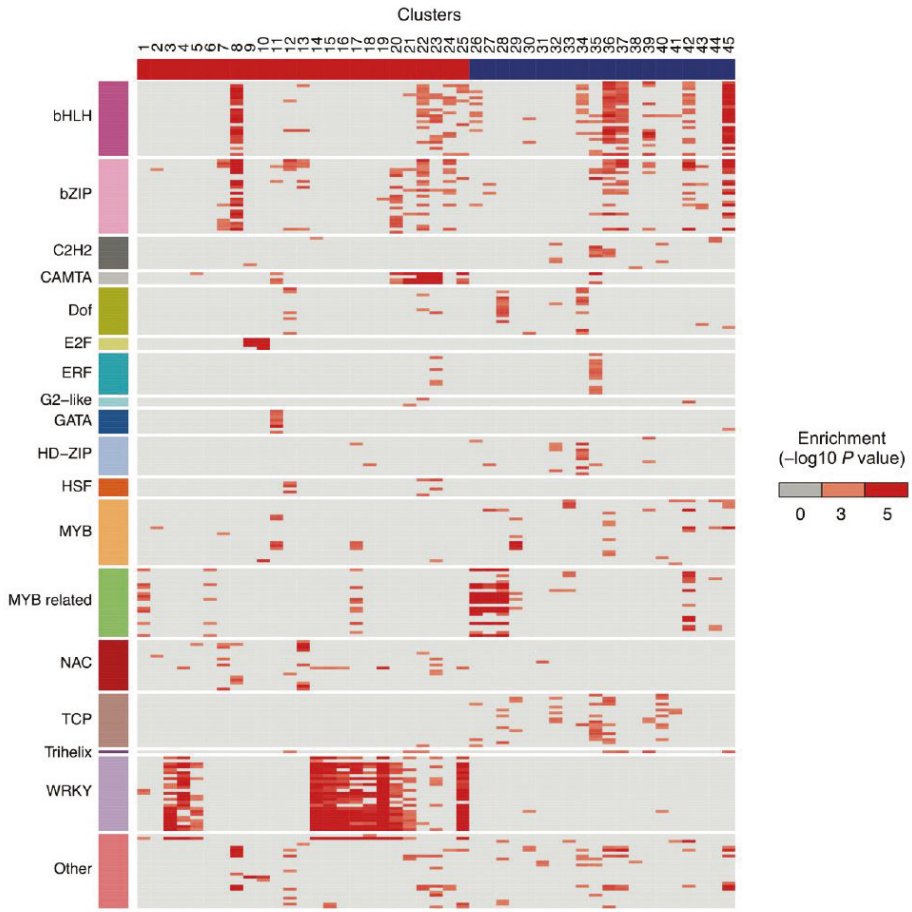

Figure 4. Enriched cis-regulatory motifs in SA-responsive gene coexpression clusters.

Known TF DNA-binding motifs are differentially enriched in the promoters of genes clustered on the basis of their expression following application of SA. Rows indicate motifs and are colored by corresponding TF family. A maximum of 25 motifs are shown per family. Columns indicate coexpression clusters, with red and blue column colors differentiating between up and downregulated clusters respectively. Red boxes indicate a motif that is significantly overrepresented (hypergeometric test).

To complement the motif analysis, we also tested clusters for enrichment of TF targets inferred from DNA affinity purification sequencing (DAP-seq) data (O'Malley et al., 2016) (Supplemental Figure S1). Target genes (inferred from TF-binding peaks) for a total of 349 Arabidopsis TFs were available in the Plant Cistrome Database (http://neomorph.salk.edu/PlantCistromeDB). The patterns of enrichment across clusters were in broad agreement with the promoter motif analysis, however, some notable differences were also apparent. This included overrepresentation for targets of some

ERF family TFs among several coexpression clusters. ERF DNA-binding motifs were not detected as widely enriched in our promoter analysis, which may reflect additional complexity in TF-DNA binding that is not accounted for in the weight matrix models of TF binding specificities. These findings highlight the potential added value of utilizing complimentary TF interaction data sets.

Regulation of gene expression often occurs through the coordinated action of multiple TFs. To obtain insight into this multi-factorial transcriptional control of the SA-induced response, we next used the DAP-seq data to determine the overlap in SA-induced target genes by the SA-induced TFs. For the 129 SA-responsive TFs for which DAP-seq DNA binding profile data were available, we computed the Jaccard similarity index (i.e., the fraction of shared target genes) over all possible pairs of target genes. Unsupervised hierarchical clustering largely grouped TFs according to their family, but weaker overlap was observed between the members within the different families (Figure 5). The WRKY family displayed the highest degree of within-family overlap, targeting broadly similar sets of genes. Differences among TFs belonging to the same family were also evident, as shown for the NAC, the ERF, and the bZIP TFs, for clear differences in the degree of similarity between family members was highlighted, suggesting within-family specificity targeting distinct sets of SA response genes.

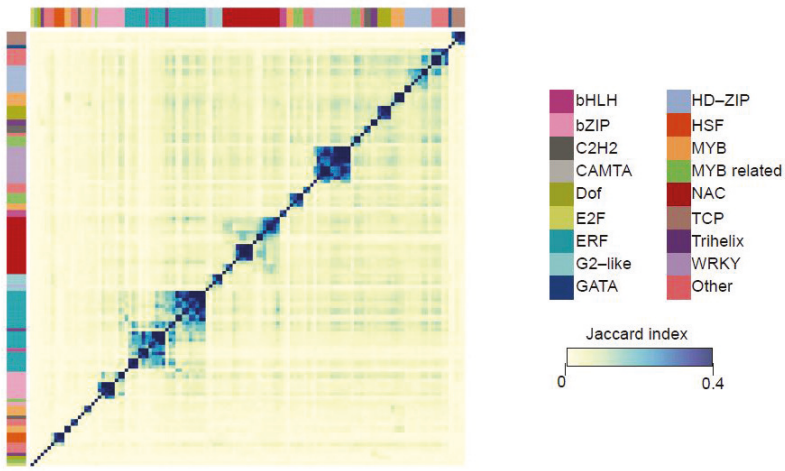

Figure 5. Overlap between the target genes of SA-responsive TFs.

Heatmap depicting the overlap in TF target genes by different members of TF families (inferred from DAP-seq data) as measured by the Jaccard similarity index, where both TF and target genes were differentially expressed in response to SA treatment. The pairwise matrix of Jaccard indices are organized via unsupervised hierarchical clustering. Sidebars indicate TF family membership.

In summary, our analyses suggest a complex array of different *cis*-regulatory motifs, their combinations and cognate TFs that allow SA to coordinate the expression of distinct gene modules that comprise the SA response.

Chronology of SA-mediated transcriptional reprogramming

The above analyses clearly showed that the SA response is associated with waves of distinct transcriptional signatures. To investigate the temporal regulation driving dynamic expression patterns during the SA response, we used Dynamic Regulatory Events Miner (DREM) (Schulz et al., 2012) to model the SA gene regulatory network. DREM integrates static protein–DNA interaction with time course expression data by searching the time series for bifurcation events, which are time points where subsets of coexpressed genes diverge from each other and predicting the TFs that regulate these routes. Figure 6 shows the reconstructed temporal transcriptional network, built with the 129 SA-responsive TFs where interaction information could be inferred from DAP-seq data (O'Malley et al., 2016).

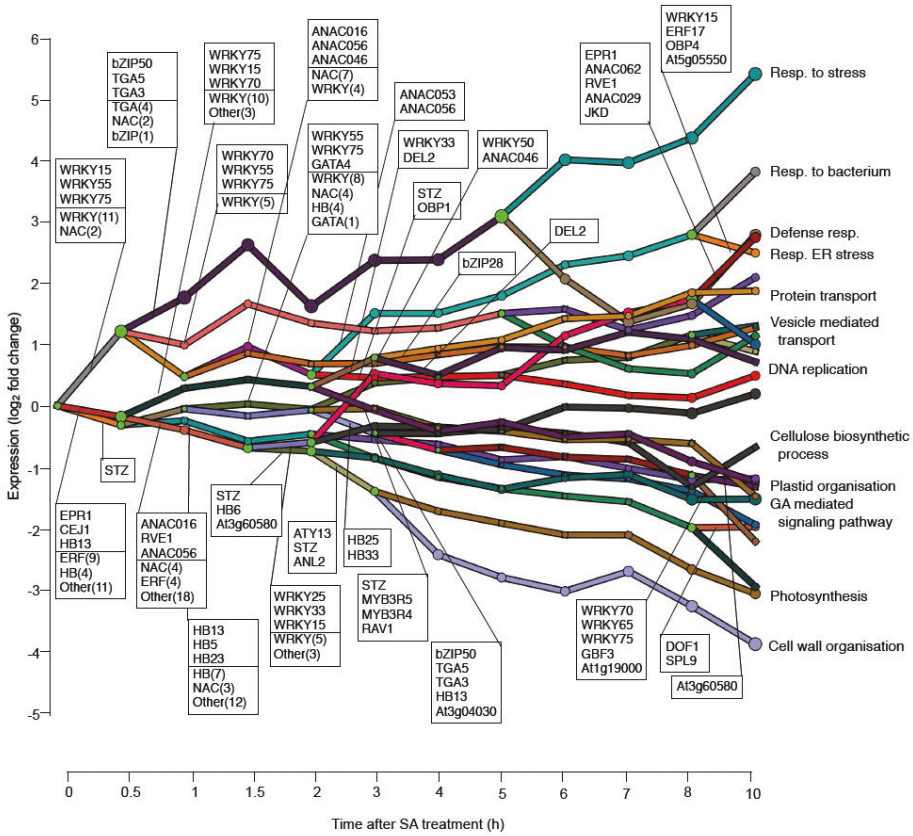

Figure 6. Modeling the SA pathway TF network (GRN).

Simplified DREM model annotated with TFs based on DAP-seq data. Each path corresponds to a set of genes that were coexpressed. Green nodes represent a bifurcation point where coexpressed genes diverge in expression. Only the top three TFs (strongest associations) and summary of TF families involved are shown. In order to improve readability, only time points until 10 h are shown as no additional path splits were identified after this time. Selected paths are annotated with the most significant functional category overrepresented among the genes assigned to a given path.

This SA GRN model contains 27 unique paths controlled by a wide range of TF families. Bifurcation points were identified at several time points and suggest complexity in the network. In line with our analysis of time of first differential expression (Figure 1), the majority of transcriptional switch points occur early on in the time course, within 4 h of SA treatment. The biological coherence of the identified paths was confirmed with GO term analysis, which revealed that most paths were enriched for distinct biological processes, with many of these being SA related and consistent with the SplineCluster analysis. Among the upregulated paths this included broad terms like ‘response to biotic stimulus’ and ‘response to stress’, as well more specific ones such as ‘vesicle

mediated transport' and 'DNA replication', whereas downregulated paths included 'photosynthesis' and 'cell wall organization'. Regulation of the first path upregulated by SA is enriched for WRKY TFs. Among these is the well-studied WRKY70, which plays an important role as a positive regulator of SA-mediated defense, but is also a negative regulator of SA accumulation (Li et al., 2004; Wang et al., 2006; Knoth et al., 2007). The model also predicted WRKY75 as a regulator of the immediate transcriptional response to SA. This is in line with the recent finding that WRKY75 positively regulates SA accumulation through direct activation of *ICS1* (Guo et al., 2017), but our model also predicts a broader role of WRKY75 in the immediate transcriptional regulation of genes induced following SA pathway stimulation. Two NAC TFs, ANAC075 and ANAC002/ATAF1 are also assigned to this first path of upregulation. Thus, our model suggests that WRKY and NAC TFs are the dominant regulators of genes that are induced in the first stage of the SA response. Interestingly, when this first upregulated path splits at 0.5 h, the WRKY and NAC TF families were assigned to different paths in the bifurcation point, suggesting specificity in regulatory roles at this time point. bZIP family-member TGA TFs also appeared on the same path as the NAC TFs, suggesting possible connective regulation of genes in this group. As time progresses, additional bifurcation points in the model give rise to an increasing number of paths, which are then annotated with distinct sets of TF members from different families, including WRKY, NAC, E2F and ERF. Downregulated gene paths were also annotated with coherent sets of TFs. For example, several early downregulated paths were annotated with homeobox (HB) TFs, and several of these TFs were themselves downregulated by SA treatment. Another notable prediction was the coordinated early downregulation of SA target genes by the SA-upregulated zinc finger TF STZ, which has been shown to function as a repressor of transcription (Saibo et al., 2009).

Thus, while static binding data are available for only a subset of SA-inducible Arabidopsis TFs, the dynamic network model that was inferred by DREM identified known regulators of the SA response and in addition, predicted many more. As the model is able to account for temporal regulatory binding it was able to differentiate between early and secondary response regulators of the dynamic SA transcriptional regulatory network. It is also noteworthy that many of the genes assigned to specific paths by DREM are enriched for similar sets of distinct annotations as present in the different coexpression clusters identified by the SplineCluster analysis. This is in spite of the genes being grouped together by expression behavior using two distinct theoretical models (SplineCluster uses Bayesian agglomerative clusters, while DREM uses input-output hidden Markov models). This observation underlines how our time series is sufficiently detailed to capture discrete sectors of the SA-controlled gene network that

represent specific pathways and processes, which are likely to have roles in SA-mediated immunity.

Network analysis identifies novel regulators of the SA response

Our analysis of SA-mediated transcriptional reprogramming uncovered known aspects of the SA gene regulatory network and predicted many more. For example, our coexpression clustering analysis identified coherent gene modules, which can be used to associate genes of unknown function with particular biological processes. This guilt-by-association approach is an often-used technique that we, and others, have previously demonstrated as a successful approach to uncover novel regulators of particular biological processes and pathways in Arabidopsis (Chapter 2; Lewis et al., 2013; Song et al., 2016; Hickman et al., 2017; Walker et al., 2017). To identify novel regulators of the SA response, we selected TF-encoding genes with no previously reported roles in the SA response pathway that were present in clusters that are enriched for terms related to defense responses. We paid particular attention to members of the NAC and WRKY TFs because these families were most significantly overrepresented in the SA-induced DEG set (Figure 6). In total we identified homozygous Arabidopsis T-DNA insertion lines for 18 thus far uncharacterized TF-encoding genes. In some cases, pairs of candidate TFs displayed high sequence similarity and we predicted that single mutants might not display the full effects on host immunity. To account for this possibility, we identified three pairs of genetically-unlinked paralogous genes from our candidate list and either generated double mutants by crossing the single mutants or obtained the double mutants from the GABI-DUPLO collection (Bolle et al., 2013).

We then functionally analyzed the selected single and double mutants for their resistance against the hemi-biotrophic bacterial pathogen *Pseudomonas syringae* pv. *tomato* DC3000 (*Pto* DC3000) that is controlled by SA-inducible defenses (Pieterse et al., 2012). A list of the 20 mutants examined for altered susceptibility to *Pto* is shown in Figure 7. Of the 20 TF mutants tested, the single mutant of the TF *ANAC090*, and the double mutant of *ANAC090* and its paralog *ANAC061*, had an altered level of resistance to *Pto* DC3000, being more resistant.

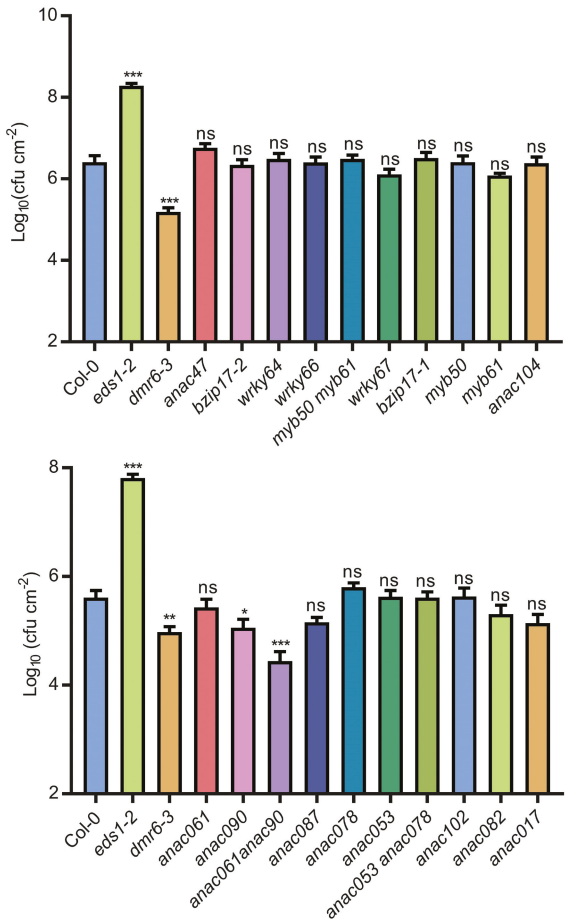

Figure 7. All mutant alleles for predicted SA pathway regulators and their *Pto* DC3000 disease resistance phenotypes.

Pto DC3000 resistance phenotypes of TF mutant lines based on bacterial growth in leaves 72 h after pressure infiltration. Mutants were tested in different batches together with Col-0 (WT). One-way Anova with Dunnett's post-hoc test was used to compare the $\log_{10}$-transformed cfu/cm^2 of leaf tissue of the different genotypes to WT.*P< 0.05; **P < 0.001; NS, no significant difference.

The expression kinetics of the *ANAC061* and *ANAC090* genes in wild-type Col-0 plants in response to SA was similar and both genes were therefore assigned to SA response cluster c22 (Figure 8A), which is enriched for genes associated with plant defense (see analysis of the SA coexpression clusters described above). Furthermore, a public database search using the Arabidopsis eFP Browser (Winter et al., 2007) revealed that both *ANAC061* and *ANAC090* were highly induced upon treatment with bacterial-

derived elicitors, flg22 or HrpZ (assayed 1 h post treatment), further supporting a role for these TFs in the immune response. The expression behavior of the *ANAC61* and *ANAC90* genes in the *anac061*, *anac090*, and *anac061 anac090* mutant lines was verified by qRT-PCR analysis (Supplemental Figure S2). This showed extremely low or undetectable expression levels if the (single and double) mutants carried the mutation in that gene, and overcompensation in expression of the homologous gene in the two single mutants.

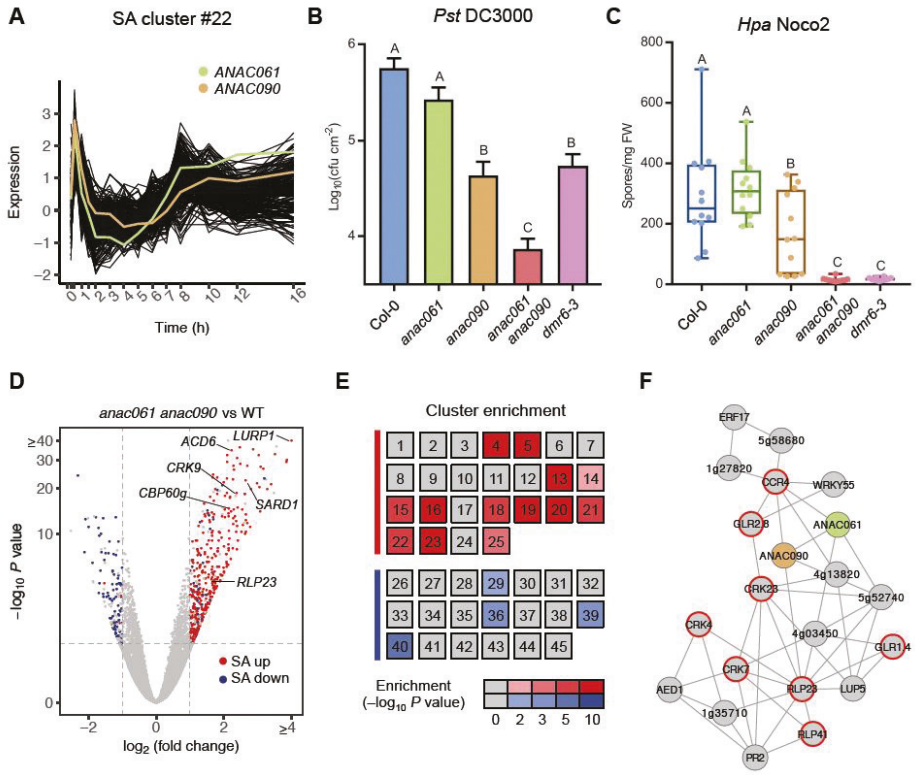

Figure 8. Identification of ANAC061 and ANAC090 as coexpressed homologous TFs that regulate resistance to *P. syringae* and *H. arabidopsidis*.

(**A**) *ANAC061* and *ANAC090* belong to the same coexpression cluster (c22) following SA treatment. (**B**) Quantification of bacterial growth in leaves of Col-0 (WT), *anac61, anac90, anac61 anac90*, and *dmr6-3* lines at 72 h after pressure infiltration with *P. syringae* pv. *tomato* (*Pto*) DC3000. One-way ANOVA and post-hoc Tukey test was used to compare the $\log_{10}$-transformed Pto growth data between different genotypes (n=8; error bars indicate SE). (**C**) Amount of *H. arabidopsidis* Noco2 spores on Col-0 (WT), *anac61, anac90, anac61 anac90*, and *dmr6-3* lines at 7 dpi. One-way ANOVA and post-hoc Tukey test was used to compare the count data of different genotypes to WT (n=10; error bars indicate SD). (**D**) Volcano plot depicting differentially expressed genes (FDR < 0.05, $|\log_2$ fold change$|$ > 1; indicated by dashed grey lines) in *anac61 anac90* compared to WT in basal conditions. Genes that are up- and downregulated following SA treatment of Col-0 (WT) are colored red and blue, respectively. Selected genes with defense-related functions are labeled.

(**E**) Heatmap indicating hypergeometric enrichment *P* value (after Bonferroni correction) of genes with significantly increased (red gradient) or decreased (blue gradient) transcript levels in *anac61 anac90* in each SA-responsive coexpression cluster (see Figure 2A). Clusters are grouped according to classification as upregulated (red bar) or downregulated (blue bar) following SA treatment. (**F**) Coexpression network obtained using public whole-genome transcriptome data sets with *ANAC061* and *ANAC090* as baits. Genes encoding receptor or receptor-like proteins are marked with a red border.

Figure 8B shows that the single *anac090* mutant displayed a reduction in the growth of *Pto* DC3000, while there was no difference with wild-type Col-0 plants in the *anac061* mutant. The *anac061 anac090* double mutant accomplished an even greater reduction of bacterial growth than the single *anac090* mutant, and was less diseased than the positive control mutant *dmr6-3* (Zeilmaker et al., 2015). A similar reduction in bacterial growth was also observed for *Pseudomonas syringae* pv. *maculicola* ES4326 (*Pma* ES4326) in the *anac090* single mutant and the *anac061 anac090* double mutant (Figure 9A). We then also tested the *anac061*, *anac090,* and *anac061 anac090* mutants for their resistance against the SA-controlled oomycete pathogen *Hyaloperonospora arabidopsidis* (*Hpa*) isolate Noco2. As shown in Figure 8C, the level of susceptibility to *Hpa* Noco2, based on quantification of sporulation, was reduced in the *anac090* mutant, whereas *anac061* developed symptoms similar to wild-type plants. Again, the *anac061 anac090* double mutant displayed even greater levels of resistance, reaching a similar reduction in *Hpa* sporulation as the *dmr6-3* mutant. Furthermore, we also tested the *anac* mutant for resistance to the JA-controlled necrotrophic fungal pathogen *B. cinerea* and chewing caterpillar *M. brassicae* and found these did not differ from wild-type plants (Figure 9B-C). Taken together, these results suggest that *anac061* and *anac090* have shared activities as negative regulators of immunity against biotrophic and hemi-biotrophic pathogens.

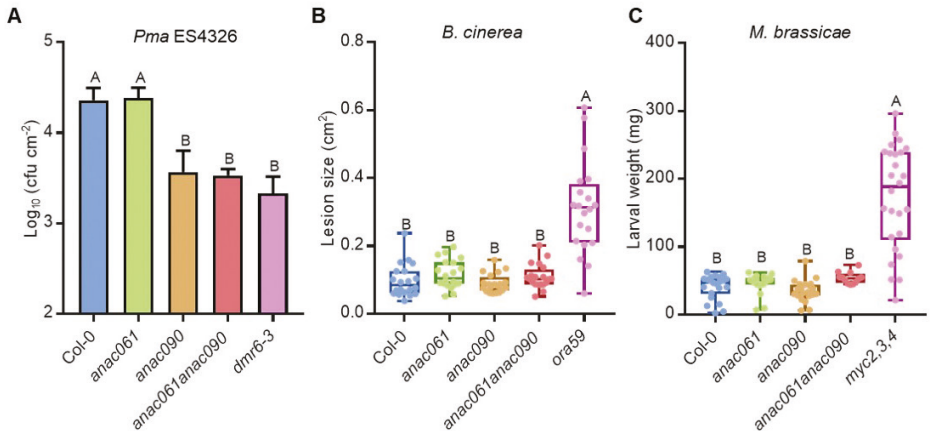

Figure 9. Arabidopsis ANAC061 and ANAC090 play overlapping roles in regulating resistance *Pma* ES4326, but without role in *B. cinerea* and *M. brassicae* resistance.

(A) Quantification of bacterial growth in leaves of Col-0, *anac061, anac090, anac061 anac090* and *dmr6-3* mutant lines 72 h after pressure infiltration with *Pma* ES4326. One-way ANOVA and post-hoc Tukey test was used to compare the $\log_{10}$-transformed data of different genotypes (n=8; error bars are SE). **(B)** Lesion size (cm^2) of *B. cinerea* in leaves of Col-0, *anac061, anac090, anac061 anac090* and highly susceptible *ora59* mutant lines 72 h after inoculation with *B. cinerea*. ANOVA and Tukey's test was used to compare the data of different genotypes (n=20; error bars are SD). **(C)** Performance of *M. brassicae* larvae on Col-0, *anac061, anac090, anac061 anac090* and highly susceptible triple bHLH TF mutant *myc2,3,4* mutant lines. The larval fresh weight was determined after 13 days of feeding. ANOVA and Tukey's test was used to compare fresh weight data of different genotypes (n=20; error bars are SD).

To provide insight into the biological processes contributing to reduced biotrophic pathogen performance on *anac061 anac090*, we performed RNA-seq analysis on leaves harvested from the double mutant and wild-type Col-0. A total of 592 genes were differentially expressed between *anac061 anac090* and wild-type plants (453 were upregulated and 139 were downregulated in the double mutant; Supplemental Data Set S3). Functional category analysis showed that for genes with upregulated expression in the double mutant versus wild type, processes such as "defense response" and "response to SA" were among the most significantly enriched terms, while downregulated genes were associated with primary metabolism (Supplemental Data Set S3). Volcano plot visualization demonstrated that the transcriptional signature of *anac061 anac090* was characterized by an upregulation of many genes that were also induced by SA in wild-type plants in our time series data set and include important regulators of SA signaling and immunity (e.g., *SARD1*, *CBP60g*, *ACD6*, *CRK9*, *LURP1*) (Figure 8D). Genes that were downregulated in *anac061 anac090* generally overlap with genes that were downregulated by SA. In accordance with these findings *anac061 anac090*-upregulated DEGs were specifically overrepresented in several

coexpression clusters of the SA-induced DEGs, and many of these are enriched for defense-related functions. Furthermore, *anac061 anac090*-downregulated DEGs were only overrepresented among downregulated coexpression clusters (Figure 8E). Thus, these RNA-seq data indicate that ANAC061 and ANAC090 are negative regulators of SA-mediated immunity and specifically target certain sectors with the SA network. This hypothesis was further supported by gene coexpression network analysis performed on public data sets of different perturbation experiments with Arabidopsis transcriptome data using ATTED-II (Obayashi et al., 2017), which demonstrated coregulation of the *ANAC061* and *ANAC090* genes with genes with immune annotations including a large proportion that encode receptor-like proteins (Figure 8F).

Role of NAC TFs in plant growth

Because enhanced resistance can often be accompanied by a growth penalty, we investigated this trait for Col-0, *anac061, anac090, anac061 anac090* single and double mutants and mutant *dmr6-3* (which shows reduced growth alongside enhanced disease resistance in the background of accession Col-0). We measured the rosette area at 3 different plant ages. Plant size measurements (Figure 10) showed that after 5 weeks of cultivation only the *dmr6-3* mutant had a slightly smaller size compared to Col-0. However, the differences between genotypes increased over time, and after 6 weeks of growth, also *anac090* and *anac061 anac090* plants were evidently smaller in size compared to wild type.

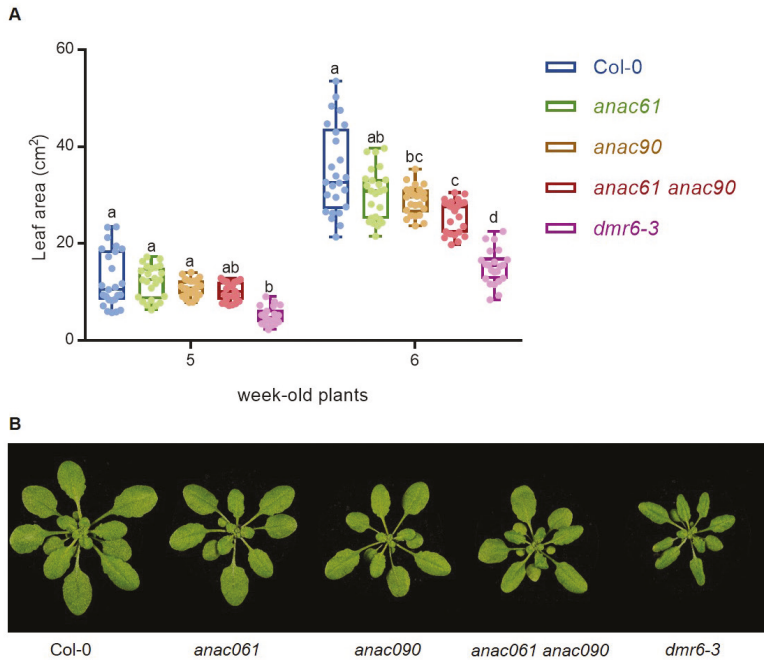

Figure 10. Arabidopsis *anac061, anac090* mutants and *anac061 anac090* double mutants growth development.

(**A**) Total leaf area was measured in 5- and 6-week-old plants. (**B**) Representative photos of 5-week-old plants for each of the assayed genotype. One-way ANOVA and post-hoc Tukey test was used to compare the data of different genotypes per plant age (*n*=29 error bars indicate SD).

DISCUSSION

Plant immunity is regulated by a complex network of cross-communicating signaling pathways that control gene expression programs responsible for mediating a range of adaptive defense responses. SA is a key immune signaling hormone that controls defense responses that are effective against pathogens with (hemi)-biotrophic lifestyles (Vlot et al., 2009).

Previous transcript profiling studies of the SA response in Arabidopsis have analyzed these processes with a limited number of time points after exogenous application of SA or BTH or tracked the effects of induced SA signaling by transcriptome profiling in a SA signaling mutant after pathogen stimulation (Goda et al., 2008; Kim et al., 2014; Hillmer et al., 2017). These studies gave a static picture of the overall changes in gene expression that occur in response to SA, and provided limited information on the timing

and sequence of transcriptional changes and related biological processes affected, and lack the resolution required to infer an in depth understanding of the dynamic GRN underlying the SA responses. To move knowledge beyond these previous studies, this chapter describes the generation and analysis of an information-rich, high-resolution time-course gene expression data set to analyze the response of Arabidopsis leaves to SA treatment.

Temporal transcription landscape and dynamic GRN modeling of the SA response

Analysis of this gene expression time series showed that SA induces large-scale transcriptional reprogramming with approximately one-third of the Arabidopsis genome changing in expression during the first 16 h following application of SA. Our analysis of differential gene expression greatly expanded the number of genes that respond in a SA-dependent manner, including hundreds of transcripts that could not have been detected previously with microarrays. From these data, we were able to make a series of detailed regulatory insights into the SA response, including the timing of transcriptional response, patterns of coregulation, and biological processes targeted.

One striking finding from our analysis was that SA-mediated differential expression occurs in clearly defined temporal waves, which were enriched for genes corresponding to distinct biological processes (Figure 1). The majority of gene expression changes (upregulation and downregulation) occurred rapidly within the first 2 h after SA treatment, taking place in the first wave (Figure 1). Within the first wave of gene upregulation were many well-established immune response genes. The second wave of upregulation (2–4 h) was associated with genes involved in the wounding response. Interestingly, within the third wave (4 h onwards) were many genes associated with cell cycle and DNA repair. The two discernable waves of downregulated genes were both associated with different categories of metabolism: photosynthesis and development (wave 1) and starch (wave 2). The ability to see these differences in transcriptional activity over time provides an unprecedently nuanced view of the genes and respective biological processes involved in the SA response. The cluster analysis identified groups of SA-responsive genes that had not been observed previously with more limited time series data (Figure 2). Analysis of the individual clusters identified groups of genes involved in a common process among both upregulated and downregulated genes. Annotations among upregulated clusters included classical immune responses (e.g., signal transduction, protein phosphorylation, etc), as well more specific terms, such as unfolded protein response and DNA repair; downregulated clusters were associated with processes related to primary metabolism and development, such as photosynthesis, chlorophyll metabolism, and auxin signaling.

It seems likely that genes involved in the same process, with similar expression profiles, are coregulated rather than simply coexpressed during the SA response, and this prediction is strengthened by the analysis of promoter motifs and TF binding. In general, we find significant correspondence among expression pattern, gene functions, and promoter enrichment for known TF motifs in and TF binding (DAP-seq data) (Figure 4 and S1). This combined analysis re-identified many known regulatory components and suggested additional roles for other *trans*- and *cis*-acting factors in regulation of the SA response.

Previous studies have highlighted several members of the WRKY TF family as components in a SA-mediated regulatory network that function as either positive or negative regulators of target genes (Wang et al., 2006). The importance of WRKY TF families in promoting the SA-response in Arabidopsis was clearly illustrated through the specific and highly significant enrichment for WRKY binding sites for these regulators in the promoters of multiple clusters of upregulated genes (Figure 4).

Upregulated gene clusters that were not enriched for WRKY binding motifs were typically enriched for motifs corresponding to other TF families, such as NAC, CAMTA, HSF, and E2F (Figure 4). The distribution of enrichment for these motifs suggests that they act to fine-tune the expression of dedicated sets of target genes in specific sectors of the SA GRN and demonstrates the diversity in regulation underlying the SA response.

Dynamic network modelling enables prediction of regulatory interactions

Efforts aimed at reconstructing GRNs can be greatly assisted by genome-wide TF-DNA binding data. However, until recently very few comprehensive studies of genome-wide DNA-binding of TFs were available for plants. Utilizing, recently published information on target genes derived a large-scale, genome-wide study of Arabidopsis TF-DNA binding profiles (O'Malley et al., 2016), we were able to leverage these data with our transcriptional time series to generate a dynamic transcriptional map of the SA response. To achieve this, we used DREM (Ernst et al., 2007), a tool specifically designed to integrate information on TF-gene interactions with time series gene expression data to identify patterns of temporal gene expression, the associated regulators and the dynamics of the interactions.

From the resulting temporal map (Figure 6) we could generate new insights and predictions about the regulation of the SA response. In line with current models of SA-signaling, the DREM model indicates that several different WRKY TFs act as master regulators of the SA pathway. For example, WRKY15, WRKY75 and WRKY55 were among

the top ranked TFs assigned to the first path of gene upregulation, suggesting important roles in regulating the immediate/early SA-response. Validating their importance to the SA-response and SA-mediated immunity through, for example, the use of mutant and transgenic TF lines, will be important focus of future research

Following the initial activation response, the network is subject to a series of splits, which represents divergence of genes that were co-regulated up until that point. Many of these expression paths are enriched for specific biological processes, and this set shares a high level of overlap with the different processes also found in SplineCluster analysis described above. While some WRKY TFs are predicted to regulate splits in gene expression trajectories, the model generally predicts a different set of secondary regulators to be responsible for determining the patterns of genes linked to specific pathways and processes, and include members of the bZIP, NAC and E2F families. Thus, by combining high-resolution expression time series with static TF-DNA binding, we were able to infer a temporal cascade of TFs that regulate the SA-response and highlights differences between master and secondary transcriptional regulators in the network.

An important caveat is that the DREM analysis was limited to the 349 Arabidopsis TFs for which high-quality binding profiles are currently in the DAP-seq database (O'Malley et al., 2016). Thus, hundreds of known and potentially important regulators of the SA pathway are missing from our analysis. The generation of genome-wide binding profiles for additional SA-regulated TFs will be required to identify the full complement of master and secondary TFs that orchestrate the SA response.

Obviously, transcriptional regulation is only one of several mechanisms of gene regulation in plants, and complex patterns of gene expression can also be controlled at posttranscriptional or posttranslational level. For example, the initial steps in the SA response are regulated through the posttranslational modifications of NPR1, NPR3 and NPR4 (Tada et al., 2008; Fu et al., 2012; Wu et al., 2012; Ding et al., 2018). The next challenge is to link non-transcriptional regulation such as mRNA stability, mRNA translation, and protein stability to transcriptional network models.

Emerging role for NAC TFs in the SA response

The plant-specific NAC family of TFs plays diverse roles regulating plant growth, development and responses to environmental stress. In recent years, the majority of studies have focused on the roles of NAC family members in the regulation of development processes such as cellular differentiation and senescence, and abiotic

stresses such as drought and high-salinity (Olsen et al., 2005; Nakashima et al., 2012; Kim et al., 2016). In recent years, several NAC TFs, including ANAC019, ANAC055 and ANAC032 have also been identified as important components of the SA pathway (Zheng et al., 2012; Allu et al., 2016). Several lines of evidence in this study pointed to the NAC TF family playing an extended role in regulating the SA response. First, our comprehensive cataloguing of SA-responsive genes revealed that, after the WRKY TF family, genes encoding NAC TFs displayed the most significant enrichment among those upregulated in response to SA (Figure 3A). Secondly, motif analysis of promoters of coexpressed genes identified NAC TF motifs as enriched within several clusters (Figure 3B and 4). Third, our dynamic regulatory model of the SA-response predicted several NAC TFs were responsible for regulating several dynamic paths of coexpression (Figure 6).

Using a guilt-by-association approach, we identified several NAC TFs as candidate regulators of the SA-response and screened their respective mutants, and in some cases, double mutants for altered resistance against SA-inducing pathogens. This reverse-genetic screen identified the single *anac090* mutant, and the double *anac061 anac090* mutant as displaying enhanced resistance to *Hpa* Noco2 and *Pto* DC3000 when compared to wild-type plants (Figure 8A-B). The *anac061 anac090* double mutant was the most resistant, indicating that this paralogous TF pair acts redundantly. Furthermore, we also tested the *anac* mutant for resistance to the JA-controlled necrotrophic fungal pathogen *B. cinerea* and chewing caterpillar *M. brassicae* and found these did not differ from wild-type plants (Figure 9B-C), suggesting that the NAC61 and NAC90 defense module plays no role in the control of these attackers. Transcriptome analysis of the double mutant confirmed upregulation of many SA pathway genes (Figure 8D-E), which likely explains the enhanced resistance against the (hemi)-biotrophic pathogens. In support of our findings, a recent study of a NAC TF network during developmental leaf senescence by (Kim et al., 2018) also linked ANAC090 to SA signaling. In that study, ANAC090 was identified as a negative regulator of SA-mediated leaf senescence and they showed that loss of ANAC090 led to increased SA levels and accelerated leaf senescence. Furthermore, using ChIP-qPCR technology they showed that ANAC090 binds upstream of several important SA-signaling genes, including *ICS1* and *EDS5*. We observed a reduced growth of the Arabidopsis *anac061 anac090* double mutant, but not to the same extent as the SA hydroxylase mutant *dmr6-3* (Figure 10).

High sequence similarity and genetic redundancy between TF family members can often mask the contribution of individual TFs towards regulation of a specific process. This may explain why most of other *ANAC* single mutants tested did not display significant

effects on host immunity in the above-described analyses, even if these individual TFs would constitute valid nodes in the SA GRN. An important step in future research will be to generate higher order mutants of related NAC TFs and others predicted to play a role in regulating the SA response.

METHODS

Plant materials and growth conditions

All wild type, mutant, and transgenic *Arabidopsis thaliana* plants used in this study are in the Columbia accession (Col-0) background. The following T-DNA insertion mutants and transgenic lines were obtained from the Nottingham Arabidopsis Stock Centre: *bzip17* (At2g40950; SALK_004048C), *anac017* (At1g34190; SALK_022174C), *anac047* (At3g04070; SALK_066615), *anac053* (At3g10500; SALK_009578), *anac061* (At3g44350; SALK_041446), *anac078* (At5g04410; SALK_040812), *anac082* (At5g09330; GK-282H08), *anac087* (At5g18270; SALK_079821) *anac090* (At5g22380; SALK_011849C), *anac104* (At5g64530; SALK_022552), *myb50* (At1g57560; SALK_035416C) *myb61* (At1g09540; SALK_106556C), *wrky64* (At1g66560; GABI_519C02), *wrky66* (At1g80590; SALK_055084C), *wrky67* (At1g66550; SALK_027849C), and *anac053 anac078* double mutant from the GABI-DUPLO collection (Bolle et al., 2013) (N2103080). The *myb50 myb61* and *anac061 anac090* double mutants were generated by crossing the single mutants listed above. Mutants *eds2-1* (Bartsch et al., 2006), *dmr6-3* (Van Damme et al., 2008), *ora59* (Zander et al., 2014), and *myc2 myc3 myc4* (Fernández-Calvo et al., 2011) were kind gifts from the Parker, Van den Ackerveken, Gatz, and Solano groups, respectively.

Plants were grown as described previously (Chapter 2; Hickman et al., 2017). In brief, seeds were stratified at 4°C for 48 h prior to sowing on river sand supplemented with modified half-strength Hoagland nutrient solution containing 10 mM Sequestreen (CIBA-GEIGY GmbH, Frankfurt, Germany). Two weeks after germination, the seedlings were transferred to 60-mL pots containing a soil:river sand mixture (12:5) that had been autoclaved twice for 1 h. Plants were cultivated in a growth chamber under a 10-h day (75 µmol/m^2/s^1) and 14-h night cycle at 21°C and 70% relative humidity. Plants were watered every other day and received the modified Hoagland solution once a week.

RNA-seq experimental setups

For the SA time series experiments, 5-week-old Arabidopsis Col-0 plants were treated by dipping the rosette leaves into a solution containing 0.015% (v/v) Silwet L77 (Van Meeuwen Chemicals BV) and either 1 mM SA (Mallinckrodt Baker). Subsequently,

developmental leaf six was harvested from four individual SA-treated plants at each of the following time points post-treatment: 15 min, 30 min and 1, 1.5, 2, 3, 4, 5, 6, 7, 8, 10, 12 and 16 h. The SA treated samples were harvested simultaneously with MeJA and mock-treated samples described in a previously published time series analysis of phytohormone responses (Chapter 2; Hickman et al., 2017). For the comparison of the *anac061 anac090* double mutant with wild-type Col-0, two mature leaves (number 6 and 7) were harvested per plant from two 5-week-old plants per genotype, resulting in two biological replicates.

RNA-seq library preparation and sequencing

Total RNA was extracted using the RNeasy Plant mini kit (Qiagen), including a DNase treatment step in accordance with the manufacturer's instructions. For the time series experiment, RNA-Seq library preparation and sequencing was performed as described previously (Chapter 2; Hickman et al., 2017). Libraries were prepared using the Illumina TruSeq mRNA Sample Prep Kit and sequenced on the Illumina HiSeq 2000 platform with read lengths of 50 bases. For the analysis of the *anac061 anac090* double mutant, RNA-Seq libraries were prepared using the Illumina Truseq mRNA Stranded Sample Prep Kit, and sequenced on the Illumina NextSeq 500 platform with read lengths of 75 bases. All raw RNA-Seq read data are deposited in the Sequence Read Archive (http://www.ncbi.nlm.nih.gov) with BioProject ID PRJNA224133 and PRJNA395645.

RNA-Seq analysis

Quantification of gene expression from RNA-seq data was performed as described previously (Chapter 2; Hickman et al., 2017). Sequencing reads were aligned to the Arabidopsis genome (TAIR version 10) using TopHat v2.0.4 (Trapnell et al., 2009), summarized over annotated gene models using HTSeq-count v0.5.3p9 (Anders et al., 2015) and normalized using the DESeq R package (Anders and Huber, 2010).

To identify genes whose transcript levels differed significantly over time between a given pair of hormone treatments we used the approach previously described in Chapter 2 (Hickman et al., 2017). Briefly, for each gene a negative binomial generalized linear model was fit to the normalized gene counts with treatment and time as covariates. We then used ANOVA to compare to the full model to a reduced model without the treatment variable. To adjust for multiple comparisons, we adjusted the resulting *P* values using the Bonferroni method. Genes with an adjusted *P* value < 0.05 and a fold change > 2 at one or more timepoints were called as DEGs. Genes differentially expressed between MeJA- and mock-treated leaves were described previously (Chapter 2; Hickman et al., 2017). Genes differentially expressed between Col-0 and *anac061*

anac090 (|log2-fold change| >1; false discovery rate < 0.05) were identified using DESeq2 (Love et al., 2014) with default settings.

Clustering of gene expression profiles

Clustering of DEGs was performed using SplineCluster (Heard et al., 2006). Genes for the SA vs mock comparison were clustered with a prior precision value of 10^{-5} on the basis of SA expression. An additional reallocation function (Heard, 2011) that redistributes cluster outliers into more appropriate clusters was also performed.

Gene Ontology analysis

GO enrichment analysis on gene clusters was performed using GO term finder (Boyle et al., 2004) and an Arabidopsis gene association file downloaded from ftp.geneontology.org on 10th Feb 2017. To remove generic GO terms, only GO categories at level three and above in the GO hierarchy were included in the GO analysis. Overrepresentation for the GO categories 'Biological Process', 'Molecular Function' and 'Cellular Component' were identified by computing a *P* value using the hypergeometric distribution and false discovery rate for multiple testing ($P < 0.05$). GO analysis of DREM paths was performed using DREM's in-built GO enrichment method (Schulz et al., 2012), using the gene association file described above.

TF family analysis

Overrepresented TF families within a set of genes were analyzed as described in Chapter 2 (Hickman et al., 2017). TF family annotations were retrieved from PlantTFDB version 3.0 (Jin et al., 2014) and tested for enrichment using the hypergeometric distribution with *P* values corrected for multiple testing with the Bonferroni method.

Promoter motif and transcription factor binding analysis

For the analysis of known Arabidopsis TF DNA-binding motifs we retrieved published position specific weight matrices from CIS-DB version 1.02 (Weirauch et al., 2014) and those described in Franco-Zorrilla et al. (2014). Promoter sequences defined as the 500 bp upstream of the transcription start site (TSS) were retrieved from TAIR (version 10). The occurrence of a motif within a promoter was determined using FIMO (Grant et al., 2011), where a promoter was considered to contain a motif if it had at least one match with a *P* value < 10^{-4}. Motif enrichment was assessed using the hypergeometric distribution against the background of all Arabidopsis genes.

TF-gene interactions were inferred from DAP-seq (DNA affinity purification sequencing) experiments, which provide the genome-wide binding profiles of in-vitro-expressed

TFs (O'Malley et al., 2016). DAP-seq peaks for 349 Arabidopsis TFs with a FRiP (fraction of reads in peaks) score ≥5% were retrieved from the Plant Cistrome DB (O'Malley et al., 2016). To improve the interpretability of our models we took an approach based on that outlined in Narsai et al. (2017), and reduced the size of the TF-gene interaction dataset by keeping the strongest 25% DAP-seq peaks for each TF and used ChIPpeakAnno to assign their target genes using a TSS distance threshold of -2000 with all other parameters kept as default (Zhu et al., 2010). The enrichment of TF targets within coexpressed gene clusters was assessed using the hypergeometric distribution as described above.

Coexpression network analysis

The coexpression network was obtained using the ATTED-II Network Drawer tool (http://atted.jp/cgi-bin/NetworkDrawer.cgi) (Obayashi et al., 2017) using *ANAC061* and *ANAC090* as query genes.

Disease bioassays and insect performance

Pseudomonas syringae pv. *tomato* DC3000 (*Pto* DC3000) was cultured in King's B medium supplemented with 50 mg/L rifampicin at 28°C overnight. Bacteria were collected by centrifugation for 10 min at 4000 rpm, and re-suspended in 10 mM $MgSO_4$. The suspension was adjusted to OD_{600}=0.005 and pressure infiltrated into three mature leaves of 5-week-old plants with a needleless syringe as described previously (Van Wees et al., 2013). After three days, leaf discs from infected leaves were harvested from two inoculated leaves per plant to give a single biological replicate. Eight biological replicates were harvested for each genotype. Subsequently, 500 µl of 10 mM $MgSO_4$ was added to the samples, after which they were macerated using a TissueLyser (Qiagen). Serial ten-fold dilutions were made in 10 mM $MgSO_4$, and 30 µl aliquots plated onto KB agar plates containing 50 mg/mL rifampicin. After 48 h incubation at 28°C, bacterial colonies were counted. Bacterial growth in the mutant lines was compared with that of the wild type (Col-0) using ANOVA followed by Dunnett's multiple comparison tests for mutant screening and ANOVA followed by Tukey's multiple comparison test for specific ANAC assays, as indicated in the figure legends.

Hyaloperonospora arabidopsidis isolate Noco2 (*Hpa* Noco2) spores were harvested from infected (*eds2* mutant) plants, eluted through Miracloth, and diluted in water to 50 spores/µl. For the disease bioassay, five-week-old plants were spray inoculated with this spore suspension. Plants were subsequently placed at 100% RH, under short day conditions (9 h light/15 h dark) at 16°C. After 9 days the spores from eight individual rosette plants were harvested in 5 ml of water and the number of spores per milligram

of plant tissue (fresh weight of aerial parts) was counted using a light microscope. Spore counts in the mutant lines were compared with that of the wild type (Col-0) using ANOVA followed by Tukey's multiple comparison test.

Pseudomonas syringae pv. *maculicola* ES4326 (*Pma* ES4326) was cultured in King's B medium supplemented with 50 mg/L streptomycin at 28 °C overnight. Bacteria were collected by centrifugation for 10 min at 4000 rpm, and re-suspended in 10 mM $MgSO_4$. The suspension was adjusted to OD_{600}=0.002 and pressure infiltrated into 2 mature leaves of 5-week-old plants with needleless syringe. The protocol as described above for *Pto* was followed, except that 30 µl aliquots of serial dilutions were plated onto KB agar plates containing 50 mg/mL streptomycin. After 48 h incubation at 28°C, bacterial colonies were counted. Statistical analyses were performed using ANOVA followed by Tukey's multiple comparison test for means of log_{10}-transformed colony counts.

Botrytis cinerea disease resistance was determined essentially as described previously (Van Wees et al., 2013). In brief, *B. cinerea* was grown on half-strength Potato Dextrose Agar (PDA; Difco BD Diagnostics, Franklin Lakes, NJ, USA) plates for 2 weeks at 22°C. Harvested spores were incubated in half-strength Potato Dextrose Broth (PDB; Difco) at a final density of 5 x 10^5 spores/ml for 2 h prior to inoculation. Five-week-old plants were inoculated by placing a 5-µl droplet of spore suspension onto the leaf surface. Five leaves were inoculated per plant. Plants were maintained under 100% relative humidity with the same temperature and photoperiod conditions. Disease severity was scored 3 days after inoculation in lesion area. Statistical analyses were performed using ANOVA and Tukey's test of the differences between means of lesion area.

Mamestra brassicae eggs were obtained from the laboratory of Entomology at Wageningen University where they were reared as described previously (Pangesti et al., 2015). Per 5-week-old Arabidopsis plant one freshly hatched first-instar (L1) larva was directly placed on a leaf using a fine paintbrush. Larval fresh weight was determined after 8–12 days of feeding. To confine the larvae, every plant was placed in a cup that was covered with an insect-proof mesh. Significant differences in larval weight between genotypes were determined using a statistical analysis were performed using ANOVA and Tukey's test of the differences between means of larval weight.

Rosette area quantification

To monitor plant growth, photographs of the same 29 plants for each genotype were taken once per week over a period of 2 weeks. Rosette area was measured using Image

J software. Significant differences in leaf surface area between genotypes was identified using ANOVA followed by Tukey's multiple comparison test.

Supplemental data

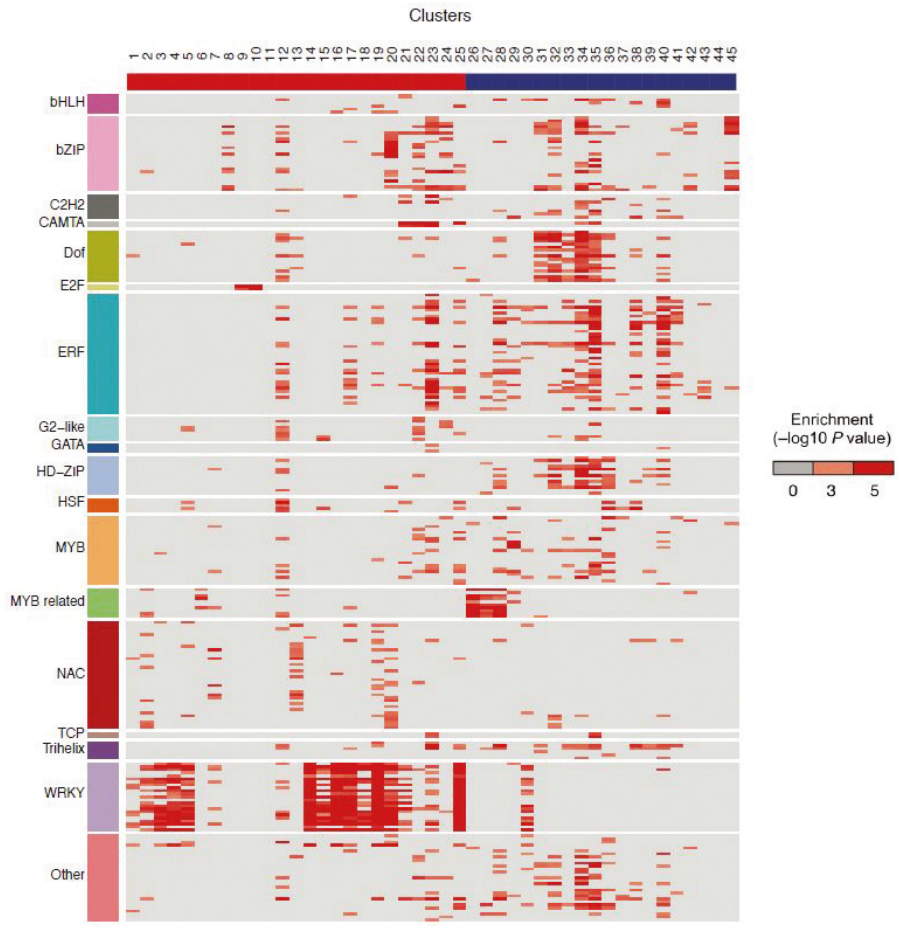

Figure S1. Enriched TF targets in SA-responsive gene coexpression clusters.

TF targets inferred from DAP-seq data are differentially enriched in the promoters of genes clustered on the basis of their expression following application of SA. Rows indicate TFs and are colored by corresponding family. Columns indicate coexpression clusters, with red and blue column colors differentiating between up- and downregulated clusters respectively. Red boxes indicate a TF targets are significantly overrepresented among genes in a given cluster (hypergeometric test).

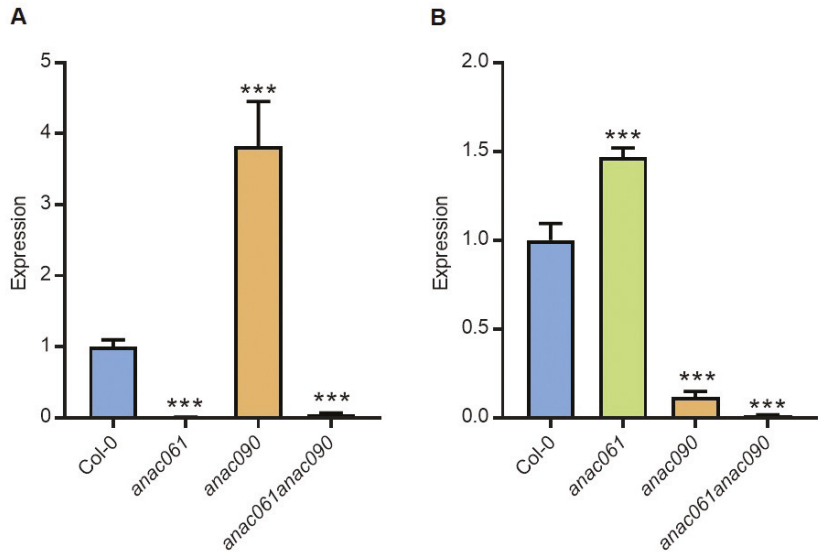

Figure S2. Expression of *ANAC061* and *ANAC090* in the wild type, *anac061*, *anac090* and *anac061 anac090*.

Transcript abundance of *ANAC061* **(A)** and *ANAC090* **(B)** in single mutant insertion alleles and corresponding double mutant determined using qRT-PCR, 1 h after leaves were syringe-inoculated with 1 µM of flg22. Transcript abundance is expressed relative to the wild type (Col-0) and is the average and SE of three biological replicates (***P value < 0.0001; Student's t test).

The following data sets are available upon request.

Supplemental Table 1. List of primers used for genotyping of T-DNA mutants and qRT-PCR analysis.

Supplemental Data Set 1. SA-responsive DEGs.

Supplemental Data Set 2. Cluster membership for SA-responsive DEGs following clustering using SA-treated gene expression profiles. GO terms overrepresented in the clusters.

Supplemental Data Set 3. List of DEGs in a*nac61 anac90* compared to wild-type Col-0.

4

A role for pathogen-induced cysteine-rich transmembrane proteins (PCMs) in defense against biotrophic pathogens

Marciel Pereira Mendes[1], Richard Hickman[1], Marcel C. Van Verk[1,2], Nicole Nieuwendijk[1], Christina Papastolopoulou[1], Anja Reinstädler[3], Ralph Panstruga[3], Corné M.J. Pieterse[1], Saskia C.M. Van Wees[1]

[1]Plant-Microbe Interactions, Department of Biology, Science4Life, Utrecht University, P.O. Box 800.56, 3508 TB, Utrecht, the Netherlands

[2]Bioinformatics, Department of Biology, Science4Life, Utrecht University, P.O. Box 800.56, 3508 TB, Utrecht, the Netherlands

[3]RWTH Aachen University, Institute for Biology I, Unit of Plant Molecular Cell Biology, Worringerweg 1, 52056, Aachen, Germany

ABSTRACT

The biological function of the majority of genes that are induced during a plant immune response is unknown. Here, a bioinformatics pipeline, using whole transcriptome time series data of *Arabidopsis thaliana* treated exogenously with the defense hormone salicylic acid (SA), unearthed more than a hundred groups of related, SA-responsive genes with no previously characterized functions in plant immunity. One of these gene families consists of eight members, encoding small proteins that contain a cysteine-rich transmembrane domain. To reflect their high levels of gene expression induced by various pathogens and their immune elicitors, we named them Pathogen-induced Cysteine-rich transMembrane proteins (PCMs). Coexpression network analysis revealed that the *PCM* genes were co-expressed with several known defense-related genes. Only one of the PCM members, also known as PCC1, has been reported to exert a role in immunity. Transient expression assays in *Nicotiana benthamiana* with PCMs tagged with fluorescent proteins revealed for most of the PCMs that they were localized at the plasma membrane. Stable PCM-overexpressing Arabidopsis lines displayed enhanced resistance against the (hemi-)biotrophic pathogen *Hyaloperonospora arabidopsidis* Noco2 and one of the PCM sub-families was also more resistant to the (hemi-)biotrophic pathogen *Pseudomonas syringae* pv. *tomato* DC3000. Transcriptome analysis of PCM-overexpressing lines revealed no enrichment of typical immune-related genes and processes. Instead, genes related to light signaling and development were induced. In accordance, PCM-overexpressing seedlings displayed elongated hypocotyl growth. These results point to a function of PCMs in both disease resistance and photomorphogenesis, connecting both biological processes, possibly via effects on membrane structure or activity of interacting proteins at the plasma membrane.

INTRODUCTION

In nature and in agriculture, plants are exposed to many different pathogenic microorganisms. To counter these threats, plants have evolved a complex immune system that can perceive pathogens and activate an appropriate response. These induced defense responses aim to fortify physical barriers against pathogen entry, of which callose deposition at the site of interaction with the invader is well studied (Luna et al., 2011). In addition, defensive compounds accumulate like secondary metabolites and pathogenesis-related proteins (PRs), some of which have been demonstrated to possess *in vitro* antimicrobial activity and it is associated with plant resistance (Van Loon et al., 2006; Sels et al., 2008; Gamir et al., 2017). Plants can choose from a rich repertoire of defense compounds to combat different infecting agents. Still, many of the induced genes during pathogen infection have an unknown function, even though a role in defense can be expected for many of them.

The upstream multi-layered and intertwined immune circuitry instructs which responses are expressed upon recognition of the invader. A combination of conserved microbe-associated molecular patterns (MAMPs) and specific pathogen effectors are perceived by plant receptors (Dodds and Rathjen, 2010), which activates diverse signaling cascades that require elevated levels of reactive oxygen species and calcium, modification of enzymes, and changes in hormone levels (Boller and Felix, 2009). The phytohormone salicylic acid (SA) plays a key role as signaling molecule in the regulation of plant immune responses, which are primarily effective to fight biotrophic pathogens (Fu and Dong, 2013). In SA-activated cells, the transcriptional cofactor NONEXPRESSOR OF PR GENES1 (NPR1) interacts with members of the TGA family of transcription factors, leading to transcriptional activation of different other transcription factors, like members of the WRKY family, and downstream SA-responsive defense genes (Tsuda and Somssich, 2015; Chapter 3). Microarray analysis of *Arabidopsis thaliana* (hereafter: Arabidopsis) plants expressing an NPR1-GR (glucocorticoid receptor) fusion protein (Wang et al., 2006) showed that several well-known SA-related genes, like *PR*s and *WRKY*s, were among the differentially expressed genes (DEGs) following SA treatment and dexamethasone-induced nuclear localization of NPR1. Almost 20% of the 64 direct target genes regulated by NPR1 (insensitive to cycloheximide) were described as having an unknown or uncharacterized function. The family of transmembrane cysteine-rich domain proteins that we characterize in this study was present in this group of NPR1-regulated direct target genes. Transmembrane cysteine-rich domain proteins have been predicted to be involved in biotic and abiotic stress responses (Venancio and Aravind, 2010). For one of the family members (PCC1) a role as positive regulator of defense to the biotroph

Hyaloperonospora arabidopsidis has been demonstrated (Sauerbrunn and Schlaich, 2004), while for another family member (CYSTM3) a role as a negative regulator of salt stress responses has been reported (Xu et al., 2019).

The set of SA-activated genes encode proteins with diverse functionality, and are associated with a variety of biological processes (Chapter 3). While the role of SA in regulating responses to pathogen infection is well established, it is also known to have a broader influence, regulating responses to abiotic stresses, such as cold, heat shock, drought, high salinity, UV radiation, and shade avoidance (Hayat et al., 2010; Nozue et al., 2018). SA also impacts plant growth by inhibiting auxin signaling (growth hormone) and contributes to developmental processes such as flower formation. The latter is delayed in SA-deficient Arabidopsis genotypes (*NahG, eds5*, and *sid2*), suggesting an interplay of SA with photoperiod and autonomous (flowering) pathways (Martinez et al., 2004; Rivas-San Vicente and Plasencia, 2011).

Even though the complete Arabidopsis genome has been known for nearly two decades (Arabidopsis Genome Initiative, 2000), a large fraction of the protein-coding genes is still lacking a meaningful characterization (Niehaus et al., 2015). A common starting point for gene characterization is to reveal the conditions under which genes are expressed. Transcriptome analysis has been extensively used to pinpoint genes that are active in specific tissue/cell types, at developmental stages or in response to different stimuli. Recently, several research groups, including our own, have utilized time-series transcriptome experiments in the model plant Arabidopsis under different conditions, which provides a wealth of functional and regulatory information regarding the complete set of genes that are differentially expressed during diverse situations (Chapters 2 and 3; Krouk et al., 2010; Breeze et al., 2011; Bar-Joseph et al., 2012; Windram et al., 2012; Lewis et al., 2015; Coolen et al., 2016; Hickman et al., 2017). In our recent study, we utilized high-resolution RNA sequencing (RNA-seq) time series to show that approximately one-third of the Arabidopsis genome was differentially expressed in leaves upon treatment with SA over a 16-h time course, with changes in gene expression occurring in well-defined process-specific waves of induction or repression (Chapter 3). Here, this SA-responsive gene set was analyzed with the comparative genomics tools OrthoMCL and JackHMMER to identify homologous groups of uncharacterized genes that may play a role in SA-associated immunity. This integrated analysis categorized over a hundred SA-responsive gene groups, including one group of 8 genes encoding short proteins that share a cysteine-rich transmembrane domain and are also responsive to various pathogens and immune elicitors, which we therefore named Pathogen-induced Cysteine-rich transMembrane proteins (PCMs). Analysis of Arabidopsis PCM-

overexpressing lines revealed a novel, positive role of these proteins in immunity against pathogens with biotrophic lifestyles. Furthermore, we expanded the potential scope of their function to a role in photomorphogenesis and hypocotyl development.

RESULTS

Analysis of uncharacterized SA-responsive genes identifies a family of cysteine-rich transmembrane proteins

Recently, we used high-throughput RNA-seq to profile genome-wide changes in mRNA abundance in Arabidopsis leaves following treatment with SA over a 16-h period. Analysis of these transcriptome data identified 9524 genes that were differentially expressed between mock- and SA-treated leaves (Chapter 3). Subsequent investigation of functional annotations associated with these differentially expressed genes (DEGs), revealed that 630 genes encode proteins of unknown or uncharacterized function. Because of SA's central role in defense against pathogen infection we hypothesized that among these would be genes with undiscovered roles in plant immunity. To simplify the analysis and functional interpretation of these uncharacterized genes, we first divided them in groups based on amino acid sequence similarity. To achieve this, we used OrthoMCL (Li et al., 2003), which is a tool for identifying homologous relationships between sets of proteins. This analysis resulted in a division of 101 groups of putative homologs (Supplemental Dataset 1; Figure 1A). Because we were specifically interested in genes that are involved in defense against pathogens, we analyzed gene behavior, using available gene expression data from Genevestigator (http://www.genevestigator.ethz.ch/) (Hruz et al., 2008). This pointed to a group of seven genes that were highly induced by a variety of immune-elicitors and pathogens (Figure 2A) and were responsive to SA in our RNA-seq experiment (Figure 2B).

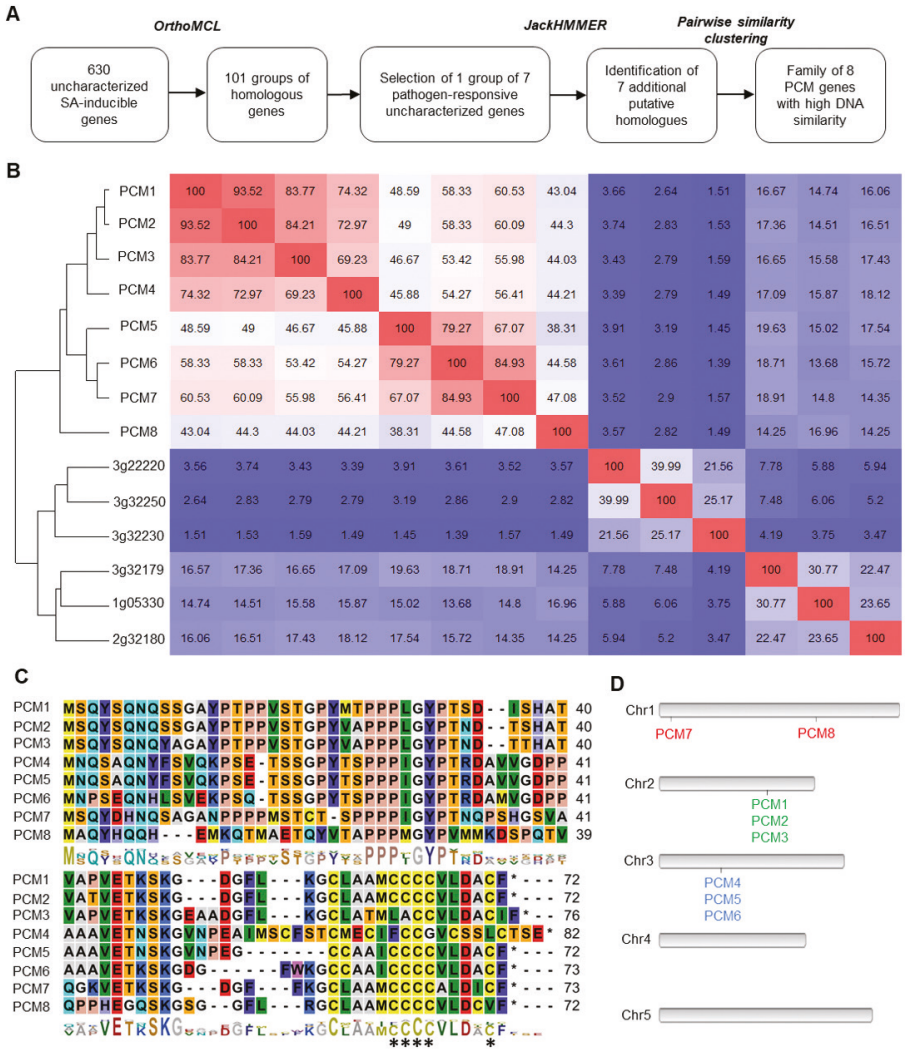

Figure 1. Identification of groups of homologous, uncharacterized SA-inducible genes; Selection of the PCM gene family.

(**A**) Workflow to identify groups of homologous, unknown SA-inducible genes. First, SA-induced DEGs were grouped by DNA similarity using OrthoMCL. One pathogen-responsive group was subjected for further analysis using JackHMMER, followed by pair-wise similarity clustering, revealing a distinct family of eight homologous *PCM* genes. (**B**) DNA similarity matrix showing the 14 genes identified by the JackHMMER search. Red and blue indicate high and low similarity, respectively. Unsupervised hierarchical clustering identified a distinct group of *PCM* genes with high DNA similarity. (**C**) Amino acid sequence alignment of the eight PCMs. The conserved cysteine-rich transmembrane domain is highlighted. (**D**) The locations of the eight *PCM* genes on the Arabidopsis chromosomes (Chr1 to Chr5). The different color gene names reflect *PCM* distribution across chromosomes.

To identify all possible paralogs (including remote paralogs), the seven genes were used as queries in JackHMMER (Finn et al., 2015) (www.ebi.ac.uk/Tools/hmmer/search/jackhmmer). JackHMMER is a highly sensitive homology detection tool that can identify shared protein domains among matched sequences, as defined according to Pfam domains (Finn et al., 2015). This analysis led to the prediction of seven additional paralogs (Supplemental Dataset 2). Next, we quantified the degree of nucleotide sequence identity between the 14 proteins by constructing a nucleotide sequence identity matrix (Figure 1B), which was followed by unsupervised clustering of the similarity matrix, leading to the identification of a distinct family of eight small genes (<82 AA) with high nucleotide identity (>38%). All the seven originally selected unknown genes belong to this group, including *PCC1* (*PCM4* in Figure 1), which has a reported role in defense and is regulated by the circadian clock (Sauerbrunn and Schlaich, 2004). One other member, *CYSTM3* (*PCM8* in Figure 1) has very recently also been characterized and shown to negatively influence salt stress resistance (Xu et al., 2019). Supplemental Table 1 lists all the *PCM* genes with their AGI number and alternative name. The genes in this family all encode short proteins (71-82 AA) with a conserved cysteine-rich transmembrane (CYSTM) domain, as predicted by the JackHMMER analyses (Figure 1C). To reflect their regulation and enrichment for cysteine residues, this eight-member gene family was named pathogen-induced cysteine-rich transmembrane proteins (PCMs). The *PCM* gene family contains two distinct gene clusters; the *PCM1*, *PCM2* and *PCM3* genes are situated in tandem on Arabidopsis chromosome 2, while *PCM4* (*PCC1*), *PCM5* and *PCM6* are tandemly arrayed on chromosome 3 (Figure 1D). Furthermore, *PCM7* and *PCM8* (*CYSTM3*) are positioned at distant locations on chromosome 1. The expression behavior of the eight *PCM* genes is broadly along the lines of the three subgroups, showing overlap but also differences with members of the other subgroups (Figure 2A and 2B). This is in accordance with varying overrepresentation of different transcription factor-binding DNA motifs in the promoters of the eight *PCM* genes (Figure 2C). The remainder of this paper explores the significance of the PCM protein family and its three subgroups in plant immunity.

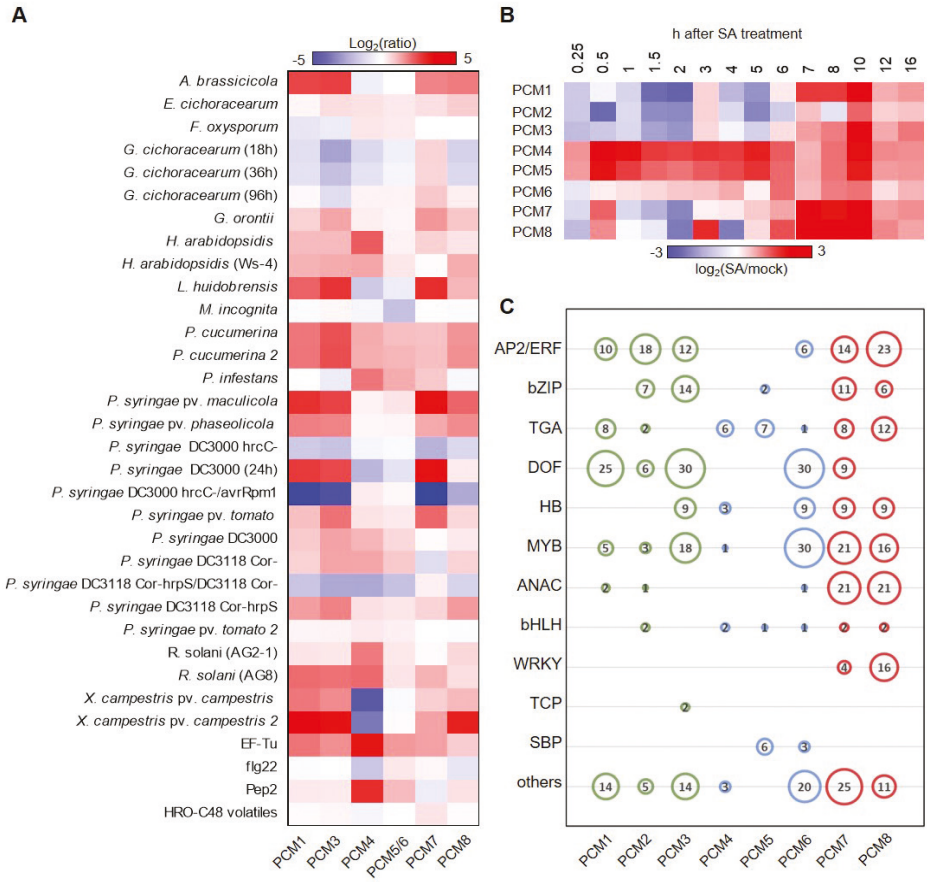

Figure 2. Expression behavior of *PCM* genes.

(**A**) Genevestigator expression analysis. Shown is a heatmap of expression ratios for the *PCM* genes following treatments with biotic stressors/elicitors. On the microarrays from which these data are derived ($P < 0.001$), probes for *PCM2* are missing, and the probes for *PCM5* and *PCM6* are shared. (**B**) Temporal expression of *PCM* genes over a 16-h time course upon exogenous application of SA. Red and blue indicate increased and decreased expression, respectively. (**C**) Representation of DNA-binding motifs in the promoters of the *PCM* genes. Motifs are grouped according to cognate transcription factor family. The size and number in each circle represent the per-family motif count.

Subcellular localization of PCMs

The characteristic CYSTM domain that resides in the PCM protein family is encoded by a total of 98 genes across 33 plant species (Supplemental Figure 1). Typically, a transmembrane domain plays a role in mediating responses between the interior and exterior of the cells (Luschnig and Vert, 2014), and such transmembrane domains are often conserved across kingdoms when it has a specialized function (e.g., photoreceptors in eyes of mammals and insects) (Fischer et al., 2004). To begin to characterize the PCMs, we determined their subcellular localization by fusing yellow fluorescent protein (YFP) to the C-terminus of all eight PCM proteins and expressing these fusion proteins under the control of the constitutively active CaMV 35S promoter. Expression of empty vector (EV-YFP) served as a control, and the dye FM 4-64 dye was used as a membrane marker. Confocal microscopy analysis of *Agrobacterium*-infiltrated *Nicotiana benthamiana* leaves transiently expressing the fusion proteins, confirmed plasma membrane localization for five of PCM-YFP variants (Figure 3). PCM1, PCM2, PCM3, PCM4 and PCM5 all localized exclusively at the plasma membrane, with YFP signals overlapping with the plasma membrane-localized FM 4-64 dye. The YFP-tagged family members PCM6, PCM7 and PCM8 were detected prevalently in the cytoplasm and nucleus.

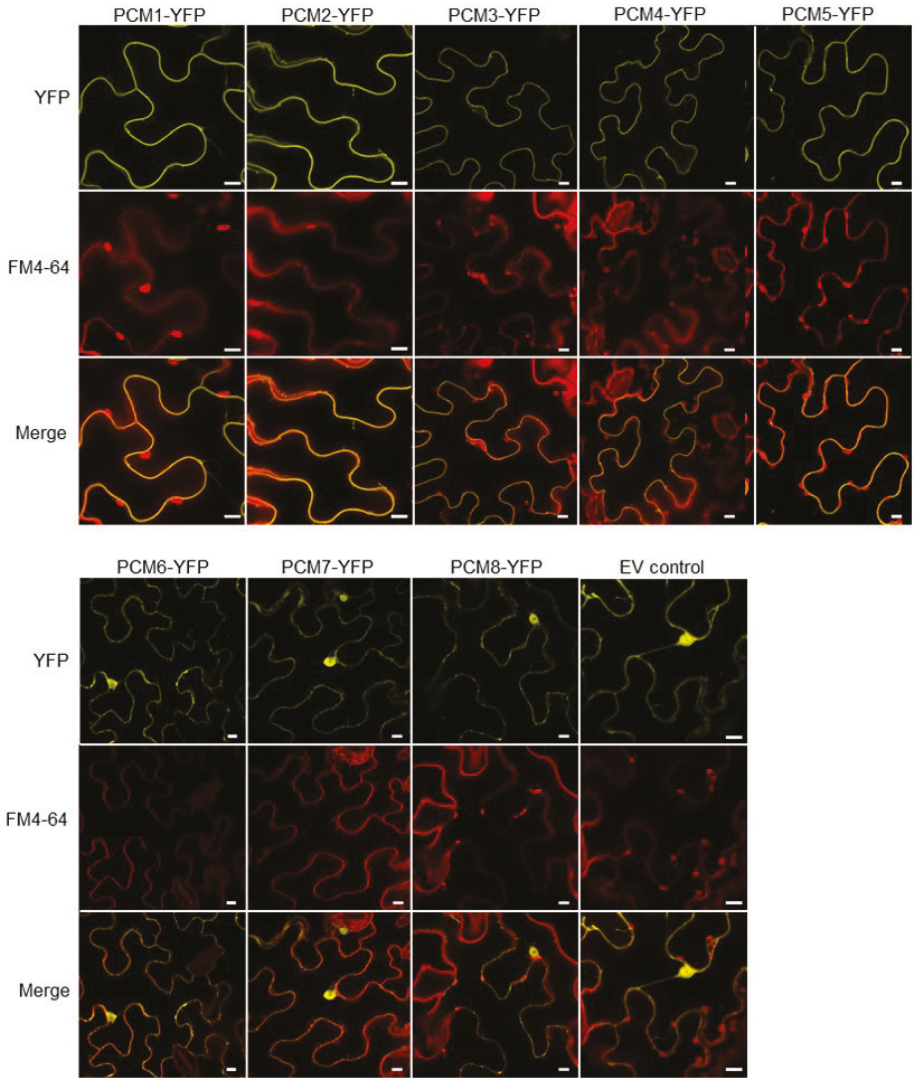

Figure 3. Subcellular localization of PCM-YFP fusions.

Confocal images of transiently transformed *N. benthamiana* epidermal leaf cells expressing the eight YFP-tagged PCM proteins under control of the 35S promoter. Representative fluorescence images are shown of PCM-YFP or free YFP (control) in the top panels, of FM 4-64 labelling of the membranes in the middle panels, and of the overlay of YFP and FM 4-64 in the bottom panels. Bar = 10 µm.

***PCM* coexpression analysis points to specificity in PCM function**

Because genes with related biological functions often have similar expression patterns, a well-established method to investigate gene function is by the construction and analysis of gene coexpression networks (Vandepoele et al., 2009). Using the eight *PCM* genes as query genes we generated *PCM* coexpression networks using publicly available microarray and RNA-seq datasets with the ATTED-II coexpression tool (Obayashi *et al*., 2018) (Figure 4). The *PCM* coexpression network was enriched for genes associated with defense responses ($P < 0.01$; hypergeometric test) and included known defense-related genes such as *LURP1*, *ACD6*, *RLP36*, *NTL6*, *NAC61*, *NAC90*, *ZFAR*, *PDR12*, *WRKY75* and *MPK11,* suggesting a role for the PCM protein family in plant defense. Within the *PCM* coexpression network, coexpression neighborhoods of members of the three *PCM* subgroups (Figure 2) overlap. Interestingly, the coexpression neighborhood occupied by subgroup *PCM4*, *PCM5* and *PCM6* was distinct from that of all other *PCM* genes. Also, *PCM7* was part of a relatively isolated coexpression subnetwork. On the other hand, *PCM8* shared its coexpression neighborhood to a large extent with that of subgroup *PCM1*, *PCM2* and *PCM3*. In sum, our coexpression network analysis suggests a role for all eight *PCM* genes in plant defense, and highlights subnetworks suggesting functional specificity and/or differential regulation of *PCM* subgroups. This is supported by the distinct gene expression behavior of the different *PCM* subgroups after treatment with pathogens or exogenous SA and the presence of different transcription factor binding sites in the promoters of the *PCM* genes (Figure 2).

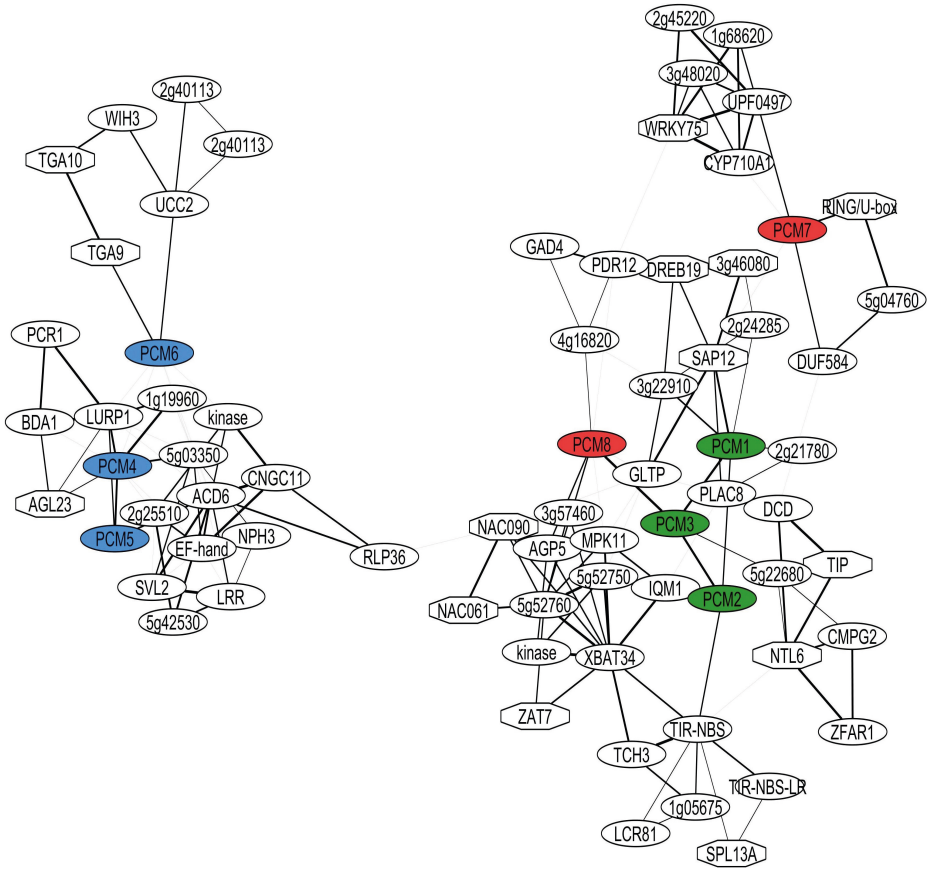

Figure 4. *PCM* coexpression networks.

Coexpression network obtained using the ATTED-II Network Drawer tool on whole-genome transcriptome data sets with *PCM* genes as bait. Hexagonal-shaped nodes indicate genes encoding transcriptional regulators. The thickness of the lines is proportional to the extent of coexpression of the linked gene.

PCM-overexpressing lines are enhanced resistant to (hemi)-biotrophic pathogens

To further investigate the hypothesis that members of the PCM protein family play a role in plant immunity, transgenic Arabidopsis lines expressing the individual *PCM* genes under the control of the CaMV 35S promoter were generated. Because the *PCM* gene family responded to exogenous SA treatment (Figure 2B), the *PCM*-overexpression lines (*PCM*-OX) were screened for an altered level of resistance to two pathogens that are controlled by SA-dependent defenses: the obligate biotrophic oomycete *H. arabidopsidis* Noco2 (*Hpa* Noco2) and the hemi-biotrophic bacterium *P. syringae* pv. *tomato* DC3000 (*Pto* DC3000). For both assays, the performance of the *PCM*-OX lines was compared to that of the wild-type (Col-0) and the enhanced susceptible mutant *eds1-2*. With the exception of *PCM6*, overexpression of all other *PCM* genes led to

reduced *Hpa* Noco2 spore formation when compared to wild-type plants (Figure 5A). *Pto* DC3000 growth was significantly decreased in the *PCM1*-OX, *PCM2*-OX, and *PCM3*-OX lines but not in the other lines (Figure 5B). These findings suggest that the vast majority of PCM family members is positively involved in host defense against *Hpa* Noco2, while a protective effect against *Pto* DC3000 is evident for subgroup PCM1, PCM2, and PCM3 of the PCM protein family.

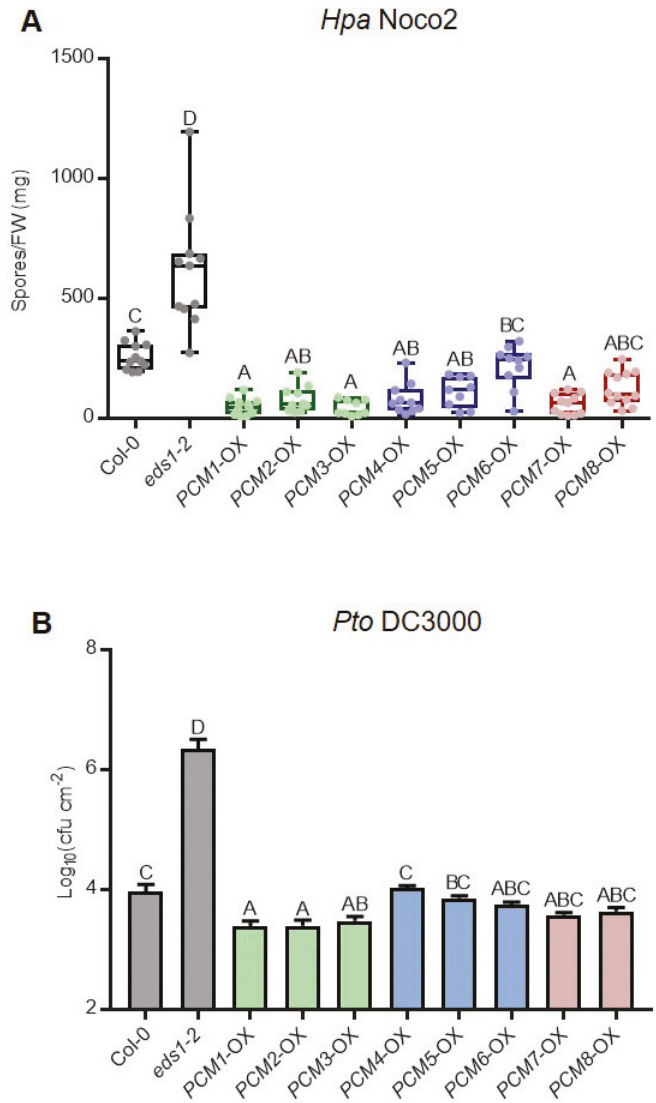

Figure 5. Overexpression of PCMs enhances resistance to *Hpa* and *Pto* DC3000.

(**A**), Quantification of *Hpa* Noco2 sporulation on 5-week-old wild-type (Col-0), *eds1-2* and transgenic lines

constitutively overexpressing individual *PCM* genes under the control of the CaMV 35S promoter (*PCM*-OX) at 10 dpi by spraying (n = 9-12*).* (**B**), Bacterial multiplication of *Pto* DC3000 in wild-type (Col-0), *eds1-2* and *PCM*-OX lines at 3 dpi by pressure infiltration (n = 8). Means ± SE (error bars) are shown. Letters denote significant differences between genotypes (one-way ANOVA, Tukey's post-hoc test, $P < 0.05$).

Transcriptome analysis of *PCM*-OX lines reveals no upregulation of typical immune responses

To gain insight into the mechanisms underlying the enhanced disease resistance obtained by overexpression of the *PCM* genes, we analyzed the transcriptome of three *PCM*-OX lines, each representing a member of the three PCM subgroups: *PCM1*-OX, *PCM5*-OX, and *PCM7*-OX represent the PCM1-PCM3, PCM4-PCM6, and PCM7-PCM8 subgroups, respectively. RNA-seq was performed on leaf tissue harvested from 5-week-old, non-treated plants. Differential expression analysis revealed that in the *PCM1*-OX, *PCM5*-OX and *PCM7*-OX lines 934, 873, and 515 genes, respectively, were differentially expressed in comparison to the wild-type Col-0 plants ($P < 0.05$, fold change > 2) (Supplemental Dataset 2). There was considerable overlap between the expression profiles of the three *PCM*-OX lines (Figure 6A). Of all DEGs, 27% were upregulated or downregulated in all three lines (in the same direction), whereas 44% were specifically up- or downregulated in a single overexpression line (Figure 6B). More genes were downregulated (60%) than upregulated (40%).

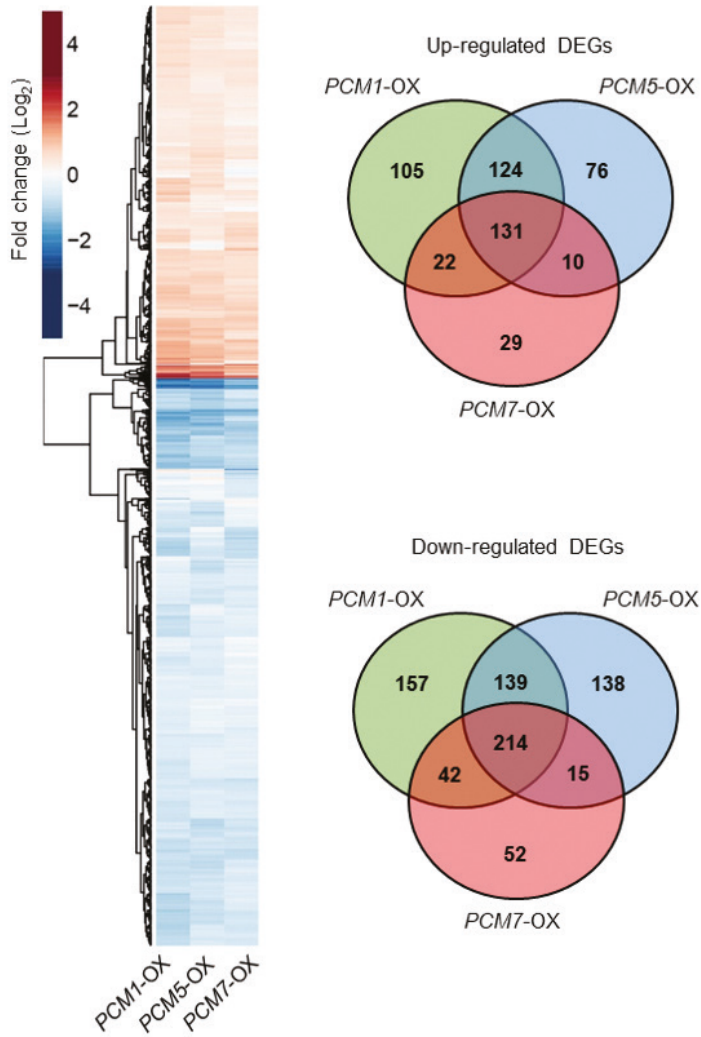

Figure 6. Transcriptome analysis of *PCM*-OX lines.

(**A**)**,** Heatmap (left) showing up- and downregulation of genes in the *PCM1*-OX, *PCM5*-OX or *PCM7*-OX lines in comparison to wild-type Col-0 plants, as revealed by RNA-seq analysis. (**B**)**,** Venn diagrams (right) indicating the overlap between DEGs in each of the PCM-OX lines.

The overlapping 131 upregulated DEGs shared by all three *PCM*-OX lines were not enriched for typical immunity-related functions (Figure 7). Instead, the term 'circadian rhythm' was the most significantly enriched specific category, with additional enriched terms including 'regulation of multicellular organismal development' 'plant cell wall loosening', and 'response to red or far red light'. The shared 214 downregulated DEGs by all three *PCM*-OX lines were associated with functional categories such as

'rRNA processing', 'response to cytokinin' and 'response to light stimulus' (Figure 7). There was also no enrichment of purely immunity-related categories DEGs that were specifically up- or downregulated in either one of the *PCM1*-OX, *PCM5*-OX or *PCM7*-OX lines. General terms like 'response to hormone' were overrepresented in different lines though, while 'glycosinolate process' was specifically enriched in up-regulated DEGs of *PCM7*-OX, and 'nucleolus' was overrepresent in *PCM7*-OX (up- and downregulated) and *PCM5*-OX (only downregulated). Based on these data, we hypothesize that pathogen-induced PCM production contributes to an increased level of defense through an impact on developmental processes in the cells may affect pathogen performance.

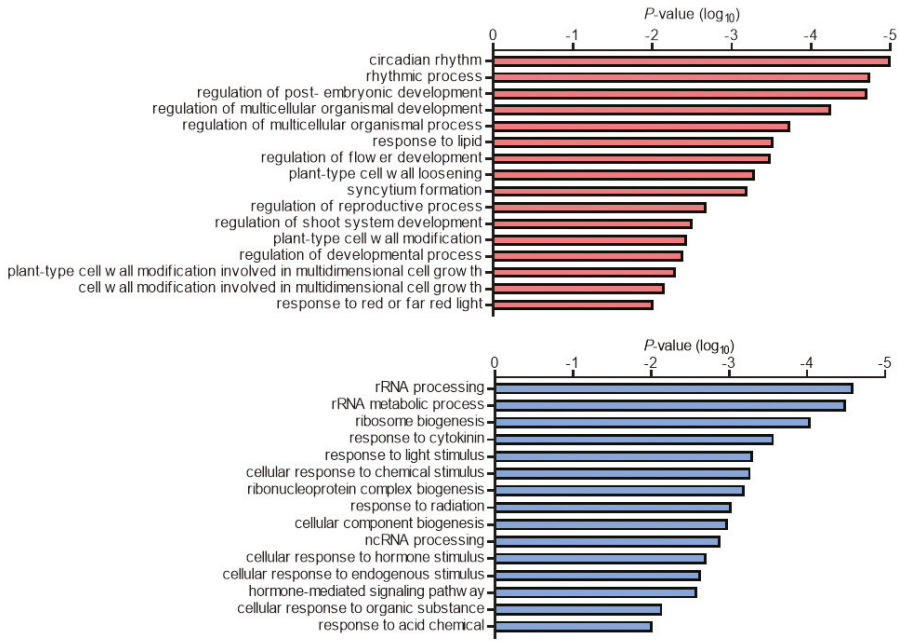

Figure 7. GO terms enriched among genes up- or downregulated in *PCM*-OX lines.

Shown are the GO terms significantly enriched among the genes that are significantly upregulated (top) or downregulated (bottom) in *PCM1*-OX, *PCM5*-OX and *PCM7*-OX, when compared to wild type.

Involvement of PCMs in hypocotyl elongation

There was no clear link to plant immunity among the genes differentially expressed in the three *PCM*-OX lines assayed, while the association with developmental processes and light responses was obvious. In all three *PCM*-OX lines, the *HY5* and *HYH* genes, which are master regulators of light signaling and also respond to pathogen infection (Genevestigator), were upregulated. This prompted us to investigate morphogenic responsiveness of the *PCM*-OX lines. In shade avoiding plants such as Arabidopsis,

perception of far-red light triggers morphological adaptations such as elongation of the hypocotyl and petioles in order to reach for better quality light (Ballaré, 2014). The *hy5 hyh* double mutant, which is affected in HY5 and its close relative HY5 homolog (HYH), displays such elongated hypocotyl growth compared to wild-type plants when cultivated in white light (Van Gelderen et al., 2018). Unexpectedly, the hypocotyl length of the *PCM1*-OX*, PCM5*-OX*,* and *PCM7*-OX lines was also greater than that of the wild type, and the hypocotyl of *PCM7*-OX was even of the same size as that of *hy5 hyh* (Figure 8). This points to a role for PCMs in growth and development. Possibly, the PCMs affect HY5 protein activity or stability, which is compensated by an enhanced expression level of the *HY5* gene. Altogether, our data suggest dual roles for PCMs in defense and in photomorphogenesis.

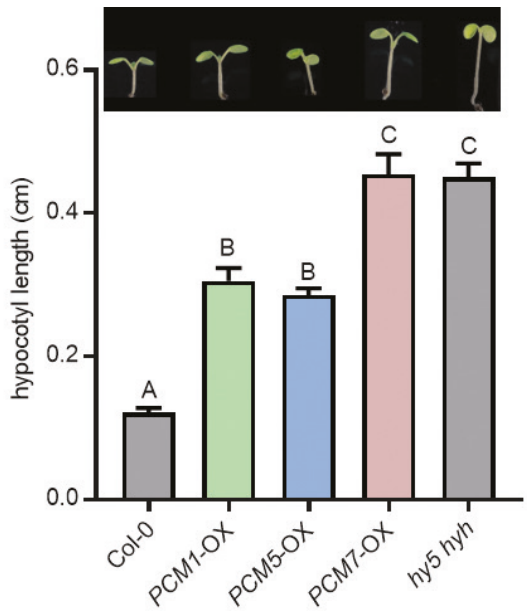

Figure 8. PCM1, PCM5, and PCM7 influence hypocotyl elongation.

Hypocotyl lengths of 7-day-old Col-0, *PCM1*-OX, *PCM5*-OX, *PCM7*-OX and *hy5hyh* seedlings grown *in vitro* in white light (n = 20). Means ± SE (error bars) are shown. Letters denote significant differences between genotypes (one-way ANOVA, Tukey's post-hoc test, $P < 0.05$). Inset: representative pictures of 7-day-old seedlings.

DISCUSSION

Despite over two decades of research efforts focused on the model plant Arabidopsis, a significant fraction of genes found in this plant are not characterized to any extent. Our analysis of SA-responsive genes in Arabidopsis leaves revealed that 630 genes encode proteins of unknown function at the beginning of our study. Using a protein homology search we grouped these uncharacterized genes into 101 groups of paralogs that likely encode proteins with similar functions (Figure 1A; Supplemental dataset 1). We validated whether such an approach could aid the functional annotation of such groups of unknown genes. Therefore, we selected and further characterized a novel family of eight pathogen-induced cysteine-rich transmembrane proteins (PCMs). The *PCM* genes formed three subgroups, based on their nucleotide similarity and chromosomal position (Figure 1B and 1D). The expression profiles of the PCM members under different biotic stress conditions and SA treatment broadly followed that of the three subgroups, showing overlap but also differences between the subgroups (Figure 2A and 2B). This is in agreement with the commonalities and dissimilarities in transcription factor binding sites detected in the promotor regions of the eight *PCM* genes (Figure 2C), and the overlap or isolation of the coexpression networks of the *PCM* genes (Figure 4). Moreover, overexpression of one *PCM* member of each of the three subgroups (*PCM1*-OX, *PCM5*-OX and *PCM7*-OX) revealed 27% overlap of all DEGs, and 44% specific expression by one of the *PCM* genes (Figure 6). A function for the PCMs in defense was evidenced by the enhanced resistance of *PCM* overexpression lines to the biotrophic pathogens *Hpa* Noco2 and *Pto* DC3000 (Figure 5). Moreover, *PCM* overexpression resulted in differential expression of genes related to light and development, and seedlings displayed elongated hypocotyl growth, suggesting an additional role for PCMs in photomorphogenesis (Figure 8).

The function of CYSTM domain-containing PCMs in plant defense

The PCMs are small proteins (<84 AA) that contain a cysteine-rich transmembrane C-terminus domain (CYSTM), which is a rare domain, but highly conserved among eukaryotic organisms. CYSTM domain-containing proteins are present in diverse species, including *Homo sapiens*, *Caenorhabditis elegans*, *Candia albicans*, *Mus musculus*, *Oryza sativa*, *Saccharomysces cerevisae*, *Zea mays* and Arabidopsis (Venancio and Aravind, 2010). The molecular mechanism by which the CYSTM module functions is not clear yet, but the proteins appear to play a role in stress tolerance for example by altering the redox potential of membranes thereby quenching radical species to protect the plant or changing membrane-associated protein functions (Kuramata et al., 2009; Venancio and Aravind, 2010).

The conserved cysteines may serve to interact with a ligand, which could be homodimerization with self or heterodimerization with other PCMs, as shown in yeast expression systems for several Arabidopsis family members (Xu et al., 2018; Mir and Leon, 2014). However, the PCMs can potentially also interact with other protein partners, as shown for PCM4/PCC1, which interacts with its N-terminal part (cytoplasm-faced, non-CYSTM containing) with the subunit 5 of the COP9 signalosome at the plasma membrane. This may lead to post-translational control of multiple protein targets involved in diverse biological processes such as light signaling, development, and immunity (Mir and Leon, 2014; Mir et al., 2013).

Furthermore, the tight association with lipids, that we have also experimentally shown for PCM1-PCM5 (Figure 3) confirms that these proteins are anchored to the plasma membrane, which could potentially change the lipid composition, as shown for PCM4/PCC1 (Mir et al., 2013), and the structure of the membrane. This may be related to the changes in gene expression observed in the PCM-OX lines that highlighted enrichments in GO terms related to 'response to lipid', cell wall modification', and 'regulation of development' (Figure 7). Moreover, membrane alterations may block the invasion of intracellular pathogens like *Hpa* (Figure 5A) that form an interface with the host membrane. There may also be consequences for membrane permeability or activity of (defense regulatory) proteins associated with the plasma membrane. While plasma membrane localization of PCM1-PCM5 was confirmed using YFP-tagged PCMs in transiently transformed *N. benthamiana* leaves, this was not the case for PCM6-PCM8 (Figure 3). We cannot exclude that the detected cytoplasmic localization is due to degradation of the PCM-YFP fusion protein in this experiment, but a recent study by Xu et al. (2018) also showed cytoplasmic localization of these proteins using the same study system. However, these authors also reported cytoplasmic localization for PCM1, PCM2, PCM3 and PCM5 for which we detected solely plasma membrane localization, which is in line with the expectations based on the presence of the CYSTM domain (Venancio and Aravind, 2010) and early reports on PCC1/PCM4 (Mir and Leon, 2014).

The *PCM4* gene is also known as *PCC1* and has previously been identified as an early-activated gene upon infection with the bacterial pathogen *Pto* carrying the avirulence gene AvrRpt2 and to be controlled by the circadian clock (Sauerbrunn and Schlaich, 2004). Microarray analysis of mutant *npr1-1* showed that in addition to several *PR* genes, the expression of *PCC1* was affected, as well as that of *PCM6* (Wang et al., 2006). Later, *PCC1* was identified to be induced by UV-C light in a SA-dependent manner, potentially playing a role as activator of stress-stimulated flowering in Arabidopsis (Segarra et al., 2010). Transgenic plants carrying the GUS reporter gene showed that

the expression of *PCC1* in the seedling stage was confined to the root vasculature and the stomata guard cells of cotyledons, but spread to the petioles and the whole limb of fully expanded leaves (Mir et al., 2013). *PCC1*-OX lines were enhanced resistant to *Hpa* (Sauerbrunn 2004; Figure 5A), while RNAi plants were more susceptible to the hemi-biotrophic oomycete pathogen *Phytophthora brassicae* and more resistant to the necrotrophic fungal pathogen *Botrytis cinerea* when compared with wild-type plants (Mir et al., 2013). We confirm that PCM4 (PCC1) overexpression lines are resistant to *Hpa* and extend this finding to additional PCMs: Overexpression of PCM1, PCM2, PCM3, PCM5, PCM7, and PCM8 also provided protection against *Hpa* infection (Figure 5A). This points to a common underlying defense mechanism that is activated by the PCMs, which we discussed in the previous paragraphs. This mechanism may also be responsible for the enhanced protection against *Pto* infection that we observed by overexpressing PCM1, PCM2, and PCM3 (Figure 5B). The lack of effect on *Pto* of the other PCM-OX lines however also points to divergent effects of the different PCMs, which is corroborated by the partly distinct DEG sets of the PCM1-, PCM5-, and PCM7-OX lines (Figure 7B). We also assayed the *PCM1*, *PCM5* and *PCM7* overexpressors for resistance to the biotrophic powdery mildew fungus *Golovinomyces orontii*, but found that our lines displayed the same disease development as the wild type, whereas the positive control triple mutant *mlo2 mlo6 mlo12* was highly resistant (Supplemental Figure 2). It may be that the protection mechanism provided by the PCMs is not effective against this pathogen strain, but it may also be that the strain was so virulent that it could have overcome the quantitative resistance accomplished by PCM overexpression.

Interplay between immunity and photomorphogenesis

Our transcriptome data revealed that the *PCM1-*, *PCM5-*, and *PCM7*-OX lines were enriched for genes and biological functions related to circadian rhythm, light signaling, and growth and development. The *PCM4*/*PCC1* gene had previously been reported to respond to circadian rhythm and UV-C light, and to have an effect on stress-induced flowering (Segarra et al., 2010). Here, we show that the *PCM1-*, *PCM5-*, and *PCM7*-OX lines exhibit elongated hypocotyl growth compared to wild-type plants (Figure 8). This phenotype is shared with the *hy5 hyh* double mutant, suggesting that the PCMs promote photomorphogenesis. Several studies have addressed the connection between plant defense and light signaling; e.g. UV-C induces SA-dependent defenses, and high levels of far red light (as in shade) repress both pathogen and insect defenses (reviewed by Ballaré (2014). A recent paper by Nozue et al. (2018) reported that SA pathway genes are key components of shade avoidance, and *PCM4* and *PCM5* were found to be downregulated by high far red levels, and to have an altered expression level in shade avoidance syndrome mutants. Therefore, a double role for the PCMs in defense and

photomorphogenesis is not unexpected. How the PCMs accomplish this double role is not clear yet. Like discussed earlier, the PCMs might influence membrane structure and activity of proteins that reside in the membrane or that bind to PCMs, like the subunit 5 of the COP9 signalosome (Mir 2013, Mir 2014). These diverse effects may independently influence defense and photomorphogenesis, but an interdependence between the two biological processes, where one is a consequence of the other, is also a possibility.

In conclusion, our approach led to the identification of the family of PCM proteins that carry the unique CYSTM module, and which have a broad biological impact on plant performance, as shown for enhanced protection against biotrophic pathogens and enhanced hypocotyl growth. We elucidated some molecular effects of the PCMs by showing that the majority of the PCM members localize to the plasma membrane, that the PCM genes are induced by SA and pathogen challenge, and that overexpression of PCMs leads to the induction of genes associated with light responses and development, but not typical defense-associated responses.

MATERIAL AND METHODS

Plant material and cultivation conditions

Arabidopsis thaliana accession Col-0 wild type, mutant *eds1-2* (Bartsch et al., 2006), triple mutant *mlo2 mlo6 mlo12* (Consonni et al., 2006), *hy5 hyh* (Van Gelderen et al., 2018) or PCM overexpression lines were used in this study. For whole plant assays with pathogen infection and SA treatment, the seeds were stratified for 48 h in 0.1% agar at 4°C prior to sowing them on river sand that was saturated with half-strength Hoagland nutrient solution containing 10 mM Sequestreen (CIBA-GEIGY GmbH, Frankfurt, Germany). After 2 weeks, the seedling were transferred to 60-mL pots containing a soil:river sand mixture (12:5 vol/vol) that had been autoclaved twice for 1 h. Plants were cultivated in standardized conditions under a 10-h day (75 µmol/m^2/s^1) and 14-h night cycle at 21°C and 70% relative humidity. Plants were watered every other day and received modified half-strength Hoagland nutrient solution containing 10 mM Sequestreen (CIBA-GEIGY GmbH, Frankfurt, Germany) once a week. To minimize within-chamber variation, all the trays, each containing a mixture of plant genotype or treatments, were randomized throughout the growth chamber once a week. For the hypocotyl elongation assay seeds were surface-sterilized and sown on MS plates (8 g l^{-1} agar and 1 g l^{-1} Murashige and Skoog (Duchefa Biochemie B.V., Haarlem, The Netherlands)). The seeds were stratified in the dark at 4°C for 2-3 days before being moved to a climate chamber with long-day conditions (16h light:8h dark). After 7 days

the plates were photographed and hypocotyl length was measured using ImageJ as described previously (de Wit et al., 2016).

The Arabidopsis PCM overexpression lines were generated by amplifying the coding sequence of genes *At2g32190* (*PCM1*), *At2g32200* (*PCM2*), *At2g32210* (*PCM3*), *At3g22231* (*PCM4*), *At3g22235* (*PCM5*), *At3g22240* (*PCM6*), *At1g05340* (*PCM7*) and *At1g56060* (*PCM8*) from accession Col-0. The *PCM* genes were part of a recent paper by Xu et al. (2018) and were named differently, as clarified in Supplemental Table S1. The primers used for cloning are also listed in Supplemental Table S1. The DNA sequence of the PCR fragments was verified and then cloned using Gateway® cloning (Invitrogen) in the pENTR vector, and subsequently in the pFAST-GO2 Gateway® (Shimada et al., 2010) compatible binary vector under control of the 35S promoter, followed by sequence verification. Binary vectors were transformed into *Agrobacterium tumefaciens* strain C58C1 containing pGV2260, which was used to transform accession Col-0 using the floral dip method (Clough and Bent, 1998). Transformants were selected by growth on ½ MS plates containing DL-Phosphinothricin BASTA, and resistant T_1 seedlings were transplanted to soil for seed production. T_2 lines were selected for single insertion of the transgenes using BASTA resistance. Finally, T_3 seeds were screened for homozygosity using GFP signal in dry seeds. Experiments were performed using T_3 or T_4 seeds.

RNA-seq library preparation and sequencing

The experimental design of the RNA-seq time series experiment with SA-treated Arabidopsis has been described previously (Caarls et al., 2017). In brief, the rosette of five-week-old Arabidopsis accession Col-0 plants was dipped into a solution containing 1 mM SA (Mallinckrodt Baker) and 0.015% (v/v) Silwet L77 (Van Meeuwen Chemicals BV). For mock treatments, plants were dipped into a solution containing 0.015% (v/v) Silwet L77. The sixth leaf (counted from the oldest to the youngest) was harvested from four individual SA- or mock-treated plants at each of the following time points post-treatment: 15 min, 30 min and 1, 1.5, 2, 3, 4, 5, 6, 7, 8, 10, 12 and 16 h. Total RNA was extracted using the RNeasy Mini Kit (Qiagen), including a DNase treatment step in accordance with the manufacturer's instructions. RNA-seq library preparation and sequencing was performed by UCLA Neuroscience Genomics Core (Los Angeles, CA, USA). Sequencing libraries were prepared using the Illumina TruSeq RNA Sample Prep Kit, and sequenced on the Illumina HiSeq 2000 platform with single read lengths of 50 bases.

For the comparison of the *PCM1*-OX, *PCM5*-OX and *PCM7*-OX lines with wild-type Col-0, two mature leaves (developmental leaf number six and seven) were harvested from

two 5-week-old plants per genotype, resulting in two biological replicates. RNA-seq library preparation and sequencing was performed by the Utrecht Sequencing Facility (Utrecht, Netherlands). Sequencing libraries were prepared using the Illumina Truseq mRNA Stranded Sample Prep Kit, and sequenced on the Illumina NextSeq 500 platform with read lengths of 75 bases.

RNA-seq analysis

Quantification of gene expression from RNA-seq data was performed as described previously (Chapters 2 and 3; Caarls et al., 2017; Hickman et al., 2017). Reads were mapped to the Arabidopsis genome (TAIR version 10) using TopHat version 2.0.4 (Trapnell et al., 2009) and aligned reads summarized over annotated gene models using HTseq-count (Anders et al., 2015). Genes that were significantly altered over time in response to SA in comparison to the mock treatment were identified using a generalized linear model implemented with the R statistical environment (www.r-project.org). Genes that were differentially expressed between Col-0 and *PCM1*-OX, *PCM5*-OX, or *PCM7*-OX were identified using DESeq2 (Anders and Huber, 2010; Love et al., 2014).

Identification of uncharacterized gene families

Protein sequences of the 630 SA-responsive DEGs with unknown/uncharacterized function (based on gene annotations retrieved from TAIR version 10 (retrieved in 2016) were run through OrthoMCL with default parameters (www.orthomcl.org) (Li et al., 2003). JackHMMER (www.ebi.ac.uk/Tools/hmmer/search/jackhmmer) was then used to identify additional paralogs belonging to the groups identified with OrthoMCL. The phylogenetic tree of PCM homologs was generated using PLAZA v4.0 (https://bioinformatics.psb.ugent.be/plaza/) with the *PCM1* gene as a query (Van Bel et al., 2018).

Determination of transcription factor binding motifs

TF-gene interactions were inferred from DAP-seq (DNA affinity purification sequencing) experiments, which provide the genome-wide binding profiles of in-vitro-expressed TFs (O'Malley et al., 2016). DAP-seq peaks for 349 Arabidopsis TFs with a FRiP (fraction of reads in peaks) score ≥5% were retrieved from the Plant Cistrome DB (O'Malley et al., 2016). DAP-seq peaks were used to infer representation of DNA-binding motifs in the promoters of the PCM genes. Motifs are grouped according to cognate transcription factor family.

Coexpression network analysis

The PCM coexpression network was obtained using the ATTED-II Network Drawer tool with the Ath-r platform (http://atted.jp/cgi-bin/NetworkDrawer.cgi) (Obayashi et al., 2017) using the *PCM* genes as query genes. Coexpression networks were visualized using Cytoscape v.3.5.1 (Shannon et al., 2003).

Functional enrichment analysis

GO-term enrichment analysis on gene lists was performed using the GO term finder tool (Boyle et al., 2004). Where indicated, generic GO terms were removed from the analysis by limiting the maximum size of functional categories to 1500 genes.

Construction of YFP-tagged PCMs and visualization by confocal microscopy

For in planta localization experiments, cDNA extracted from Arabidopsis was used to amplify the CDSs without the stop codon of PCMs using the primers listed in the supplemental table 1. The PCR products containing *att*B sequence were cloned into the Gateway pDONR221, then the resulting entry vectors containing *PCM* genes were recombined into the Gateway expression vector pB7WGY2 which contain venus fluorescent protein (YFP).

Competent cells of *A. tumefaciens* were transformed with the Gateway expression vector described in the previous paragraph made for protein localization. Transformed colonies were selected using the antibiotic resistance of vector and with rifampicin carried by *A. tumefaciens*. Single colonies were grown for 2 days at 28^{O}C in 20 ml LB medium under shaking conditions. After, the OD_{600} was measured, the cells were pelleted and resuspended to a final OD_{600} of 0.5 with a ½ MS medium (Duchefa Biochemie) supplemented with 10 mM MES hydrate (Sigma-Aldrich), 20 g/L sucrose (Sigma-Aldrich), 200 µM acetosyringone (Sigma-Aldrich) at pH 5.6 and incubated in darkness for at least 1 h. The solutions were used to agroinfiltrated the abaxial side of 4-5-week-old *N. benthamiana* leaves using a 1 ml syringe. The plants were left to grow in normal light conditions and after 2 days leaf sections were taken from agroinfiltrated regions and visualized with confocal microscope.

Microscopy was performed using a Zeiss LM 700 (Zeiss, Germany) confocal laser-scanning microscope. Fresh leaf material was prepared on glass slide with cover slip. Excitation of YFP and RFP (plasma membrane FM4-46 dye (Sigma-Aldrich) plus autofluorescence of chlorophyll were done at 488 nm. Light emission of YFP was detected at 493-550 nm and RFP at 644-800 nm. Analyses of the images were performed with ZEN lite (blue edition).

Pathogen cultivation and bioassays

Hyaloperonospora arabidopsidis isolate Noco2 (*Hpa* Noco2) spores were harvested from infected (*eds2* mutant) plants, eluted through Miracloth, and diluted in water to 50 spores/µL. For the disease bioassay, five-week-old plants were spray inoculated with this spore suspension. Plants were subsequently placed at 100% RH, under short day conditions (9 h light/15 h dark) at 16°C. After 9 days the spores from eight individual rosette plants were harvested in 5 mL of water and the number of spores per milligram of plant tissue (fresh weight of aerial parts) was counted using a light microscope. Spore counts in the mutant and overexpression lines were compared using ANOVA followed by Tukey's multiple comparison tests.

Pseudomonas syringae pv. *tomato* (*Pto*) DC3000 was cultured in King's B medium supplemented with 50 mg/L rifampicin at 28°C overnight. Bacteria were collected by centrifugation for 10 min at 4000 rpm, and re-suspended in 10 mM $MgSO_4$. The suspension was adjusted to OD_{600}=0.0005 and pressure infiltrated into 3 mature leaves of 5-week-old plants with a needleless syringe. After 3 days, leaf discs of 5-mm diameter were harvested from two inoculated leaves per plant, representing a single biological replicate. Eight biological replicates were harvested for each genotype. Subsequently, 500 µl of 10 mM $MgSO_4$ was added to the leaf discs, after which they were ground thoroughly with metal beads using a TissueLyser (Qiagen). Serial ten-fold dilutions were made in 10 mM $MgSO_4$, and 30 µl aliquots plated onto KB agar plates containing 50 mg/mL rifampicin. After 48 h of incubation at 28°C, bacterial colonies were counted. Statistical analyses were performed using ANOVA followed by Tukey's multiple comparison test for means of log_{10}-transformed colony counts.

For powdery mildew assays, Arabidopsis plants were inoculated with powdery mildew at roughly 2.5 cm (radius) rosette size at four to five weeks after germination. *Golovinomyces orontii* is adapted to infection of Arabidopsis (Kuhn et al., 2016) and was cultivated on susceptible *eds1-2* plants. Inoculation was conducted by leaf-to-leaf transfer of conidiospores. Leaves from five individual plants were collected at 48 hpi and bleached in 80% ethanol at room temperature for at least two to three days. Prior to microscopic analysis, fungal structures were stained by submerging the leaves in Coomassie staining solution (100% v/v ethanol acid, 0.6% w/v Coomassie blue R-250; Carl Roth, Karlsruhe, Germany) twice for 15-30 s and shortly washed in tap water thereafter. The samples were analyzed with an Axiophot microscope (Carl Zeiss AG, Jena, Germany). The fungal penetration rate was determined as the percentage of spores successfully developing secondary hyphae over all spores that attempted penetration, visible by an appressorium (Haustorium index). Macroscopic pictures of

G. orontii-infected plants were taken at 7 dpi with a Coolpix P600 camera (Nikon). Susceptible Col-0 and the fully resistant *mlo2-5 mlo6-2 mlo12-1* triple mutant (Consonni et al., 2006) served as positive and negative control, respectively. Haustorium index in the mutant and overexpression lines were compared using ANOVA followed by Tukey's multiple comparison tests.

Supplemental data

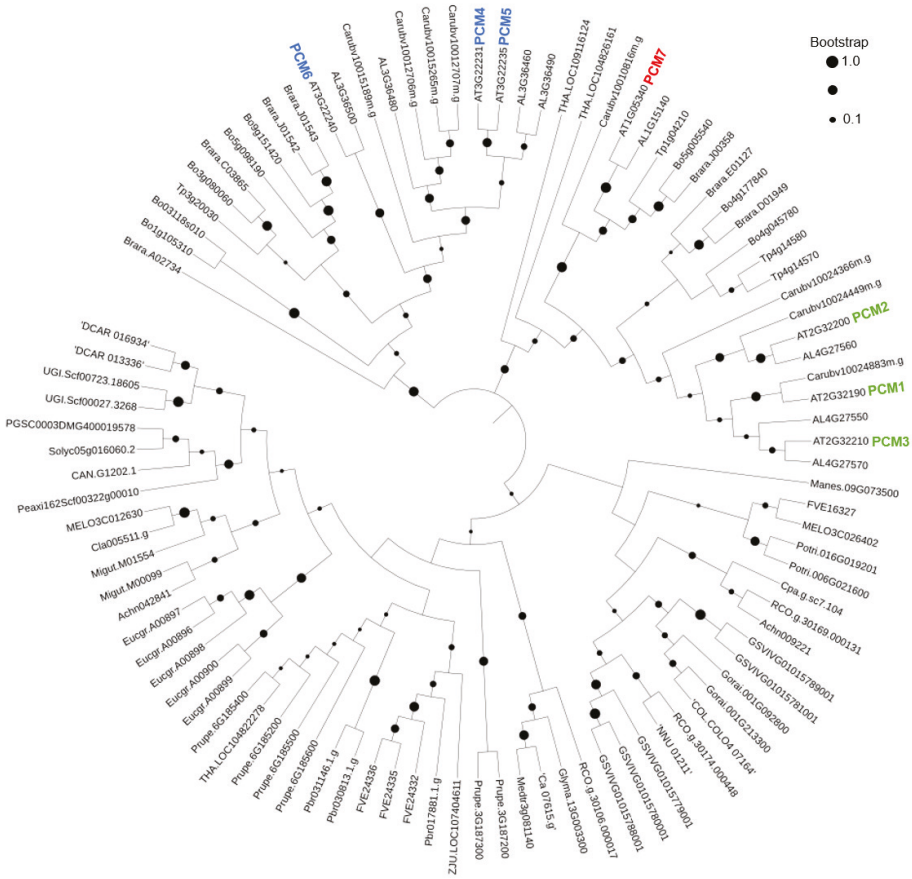

Supplemental Figure S1.

Phylogenetic relationship of closely related homologs of the PCM gene family in Arabidopsis and 32 other plant species. The PLAZA platform included the isoform of PCM8 in which the CYSTM domain is excised, for this reason, PCM8 is not included in the phylogenetic tree.

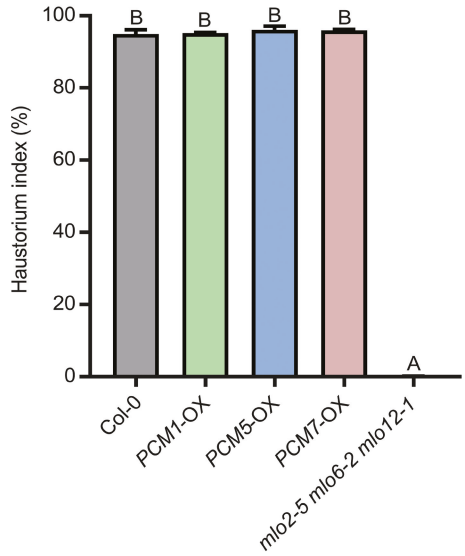

Supplemental Figure S2.

Powdery mildew infection in *PCM*-OX lines. Quantitative analysis of host cell entry (after 48 hpi) on wild-type Col-0, fully resistant *mlo2-5 mlo6-2 mlo12-1* triple mutant and *PCM1*-OX, *PCM5*-OX and *PCM7*-OX. Letters denote significant differences between genotypes (one-way ANOVA, Tukey's post-hoc test, $P < 0.05$).

Supplemental Table S1.
List *PCM* genes, their AGI numbers (ID) and alternative names. Primer sequences used for cloning**.**

	ID	Other name	Forward and reverse primers (5' – 3')
PCM1	AT2G32190	ATCYSTM4	F: ATGAGCCAATACAGCCAAAACCAATCTTC R: GAAGCAGGCGTCGAGGACACAA
PCM2	AT2G32200	ATCYSTM5	F: ATGAGCCAATACAGTCAAAACCAATATGCAG R: GAAAATGCATGCGTCGAGGACGCAA
PCM3	AT2G32210	ATCYSTM6	F: ATGAGTCAATACAGCCAAAACCAATCTTCAG R: GAAGCATGCGTCGAGGACACAACAA
PCM4	AT3G22231	PCC1	F: ATGAATCAATCCGCGCAAAATTACTTTTCCG R: CTCTGATGTACAGAGGCTGGAGCAT
PCM5	AT3G22235	ATCYSTM8	F: ATGAATCAATCCGCGCAAAATTACTTTTCCG R: GAAGCATGCATCCAGGACACAACAG
PCM6	AT3G22240	ATCYSTM9	F: ATGAATCCATCCGAGCAGAATCACTTGTC R: GAAGCATGCATCCAGGACACAACAG
PCM7	AT1G05340	ATCYSTM1	F: ATGAGCCAGTACGATCACAACCAGTC R: GAAGCAAATGTCCAGGGCACAACAG
PCM8	AT1G56060	ATCYSTM3	F: ATGGCTCAGTATCATCAACAGCATGAAATG R: GAAGACACAATCCAAAACGCAGCAGC

The following data sets are available upon request.

Supplemental Dataset S1. Set of 103 groups of putative homologs among the set of uncharacterized SA-induced genes, identified using OrthoMCL.

Supplemental Dataset S2. Genes differentially expressed in *PCM1*-OX, *PCM5*-OX and *PCM7*-OX lines in comparison to wild-type plants.

Supplemental Dataset S3. GO terms overrepresented in the upregulated and downregulated DEGs sets of *PCM1*-OX, *PCM5*-OX and *PCM7*-OX.

5

Summarizing discussion

Activation of the innate immune system is essential for a plant's survival in hostile environments. The plant immune system relies on an expanded repertoire of immune receptors on the cell surface or inside the cell to detect molecular signatures associated with microbial invasion or pest attack. Conserved pathogen-associated molecular patterns (PAMPs), such as bacterial flagellin, or endogenous damage-associated molecular patterns (DAMPs) derived from pathogen- or insect-caused damage of host cells, or possibly herbivore-associated molecular patterns (HAMPs) are perceived by cell surface localized pattern recognition receptors (PRRs), which leads to activation of PAMP-triggered immunity (PTI) (Boller and Felix, 2009; Erb and Reymond, 2019). Successful pathogens and insects can overcome this immune activation by delivering effector molecules into host cells that inhibit defense signaling. To counteract pathogen threat, plants in turn evolved intracellular nucleotide-binding site leucine-rich repeat (NLR; also known as NBS-LRR) receptors that recognize pathogen-derived effector molecules, which activates the second layer of immunity, called effector-triggered immunity (ETI) (Jones and Dangl, 2006). PTI and ETI both activate a variety of signaling pathways, which trigger a range of adaptive responses to restrict microbial infection and herbivorous insect proliferation. The network of complex interactions between the diverse sets of different immune receptors, and downstream immune signaling components and hormone networks is collectively defined as the plant immune network (Nobori et al., 2018). Phytohormone signaling networks play a critical role in regulating large-scale changes in gene expression that lead to an array of physical and chemical defensive outputs. Almost all known phytohormones contribute towards modulation of the immune signaling networks in some capacity, either by positive regulation of defense gene expression or via antagonistic or synergistic crosstalk with defense-related hormone pathways (Pieterse et al., 2012; Caarls et al., 2015).

Following pathogen or insect attack plants accumulate a blend of hormones that is largely specific to the attacker present (De Vos et al., 2005). Research over the past two decades has highlighted the role of jasmonic acid (JA) and salicylic acid (SA) as major defense hormones that form the backbone of the plant immune signaling network. In general, JA and SA regulate defenses against different types of attackers, whereby JA is induced by and activates defenses against necrotrophic pathogens and herbivorous insects, whereas SA induction and signaling plays a key role in regulating responses to biotrophic pathogens (Pieterse et al., 2012). While these hormones have been implicated in regulating distinct defenses, both JA and SA can accumulate following infection by the same pathogen (Van Wees et al., 1999; Betsuyaku et al., 2018). The JA and SA pathways can antagonize each other's activity, but synergistic effects on downstream responses also exist (Mur et al., 2006). Other hormones with important functions in

regulation of the plant immune network are ethylene (ET) and abscisic acid (ABA), which fine-tune the activation of JA-dependent defenses against necrotrophic pathogens and herbivorous insects, respectively, and also affect SA-dependent defense signaling against pathogens (Pieterse et al., 2012). Because induction of immune responses comes with fitness costs, fine tuning of defense signaling via defense hormone crosstalk is essential to optimize both defense and maintain plant growth (Vos et al., 2013a; Vos et al., 2013b). Hormones associated with the promotion of growth and reproduction, such as auxin, brassinosteroids, and gibberellin, are typically antagonized by immune hormone pathways as a mechanism to balance tradeoffs between growth and defense (Lozano-Duran and Zipfel, 2015).

The regulation of gene expression can be controlled at several levels, including transcription, mRNA stability, mRNA translation, and protein stability. While all these layers of control have been implicated in the modulation of hormone pathways, hormone-responsive genes are predominantly regulated at the level of mRNA synthesis, whereby TFs control gene expression by directly interacting with *cis*-regulatory DNA sequences that are typically located adjacent to their target genes. Transcription factors (TFs) may act in combination with transcriptional co-regulators via protein-protein interactions. Over the past couple of decades, several master transcriptional regulators of both JA and SA response pathways have been elucidated. Many of these master regulators were identified through mutant screens and reverse genetics studies, with the identified mutants often resulting in severe misregulation of the relevant hormone pathway response. Examples of master regulators of JA signaling discovered in this way include COI1, MYC2 and the JAZ repressors (Xie et al., 1998; Lorenzo et al., 2004; Chini et al., 2007), whilst NPR1 was identified as a master regulator of the SA response (Cao et al., 1994; Glazebrook et al., 1996). Yet, the wide range of biological processes and pathways that are activated by JA and SA at the transcriptional level imply that many additional regulators function in a complex manner downstream of the master regulators that sit at the very top of regulatory hierarchy to orchestrate the regulation of specific sets of genes.

Previous attempts to identify JA- and SA-responsive genes and their possible regulators have typically used microarrays to monitor genome-wide changes in gene expression in response to phytohormone treatment. However, these studies were often limited in their temporal resolution, therefore lacking the power to identify the complete set genes responding to a particular hormone, including genes that display transient changes in expression; this limited temporal information also does not suffice to detect tightly coregulated genes, thereby restricting the insights that can be gained into

underlying regulatory mechanisms. Chapters 2 and 3 describe the generation of high temporal transcriptional time series data sets of Arabidopsis in response to the immune hormones JA (Chapter 2) and SA (Chapter 3). By sampling Arabidopsis leaves at 14 time points over a 16-h period following treatment with either MeJA (rapidly converted into JA by the plant) or SA, the goal of these experiments was to move knowledge beyond previous transcriptome studies of these two hormones, in which typically single or a few time points were analyzed. The resulting high-information transcript profiles allowed us to investigate multiple aspects of the JA and SA responses, including: chronology of transcriptional events and their biological functions triggered, dynamic patterns of gene co-regulation, and possible regulatory mechanisms underlying these expression patterns. Using the "guilt-by-association" principle, Chapters 2 and 3 also describe the prediction and validation of novel TFs with a role in JA and SA signaling and in resistance against pathogens or insects.

Transcriptional networks ultimately lead to the expression of proteins that perform physical or biochemical functions as part of the defense response. JA-associated defense outputs include the production of anti-insect or anti-microbial compounds, comprising proteins such as thionins, chitinases and proteinase inhibitors, and secondary metabolites such as glucosinolates, anthocyanins, and camalexin (De Geyter et al., 2012; War et al., 2012). SA-associated defense outputs include pathogenesis-related (PR) proteins with anti-microbial activity, such as sterol-sequestering proteins and glucanases, chemicals such as anti-microbial phytoalexins, and the cell wall fortifying polysaccharide callose (Sels et al., 2008; Luna et al., 2011; Gamir et al., 2017; Klessig et al., 2018). Since sequencing of the Arabidopsis genome in the year 2000 and the identification of approximately 27,000 protein-coding genes, hundreds of proteins have been shown to play significant roles in plant defense. Yet, despite almost two decades of post-genome research it is estimated that around a third of all known protein coding genes in Arabidopsis have uncharacterized or unknown functions (Niehaus et al., 2015). The thousands of JA- and SA-inducible genes that we identified in our transcriptome time series analysis as described in Chapters 2 and 3 included many genes with uncharacterized functions that may potentially have important defensive functions that can be targeted in plant breeding or engineering approaches aiming the development of improved resistant crops. In Chapter 4, starting from a pool of 630 uncharacterized genes that were induced by SA, we identified a family of genes encoding pathogen-inducible cysteine rich transmembrane proteins (PCMs), for which we validated their role in defense to biotrophic pathogens, and investigated their mode of action.

Novel regulators of defense hormone-controlled immune regulatory networks

In Chapters 2 and 3 the computational analysis of high-density time series of RNA-Seq data obtained from leaves of Arabidopsis treated with MeJA or SA are described. This provided an unprecedented detailed insight into the dynamics of JA- and SA-mediated transcriptional reprogramming. Our study showed that over a time course of 16 h, JA significantly altered the expression of 3611 genes, while SA affected far more genes, namely 9524. For both JA and SA, a wide variety of transcript profiles were observed. Some genes displayed transient up or down-regulation, whereas others displayed sustained changes, and some showed more complex expression patterns. The first time of differential expression varied per hormone treatment: 90% of all JA-inducible genes were differentially expressed within 2 h, but it took 5 h for 90% of the SA-inducible gene set to become differentially expressed. Clustering of the diverse expression profiles of the JA- and SA-inducible gene sets revealed the main patterns of coregulation, and identified groups of genes that share common biological processes.

Analysis of the upstream regulatory regions of coexpressed genes revealed potential TF DNA binding motifs that are likely to contribute to the coregulation of genes involved in the JA and SA responses. Certain known TF motifs were clearly enriched in the promoters of genes that shared similar expression profiles, with some TF families represented across broad sets of clusters, while others appeared in more specific clusters. From this analysis, it became clear that two major types of *cis* motifs largely discriminate between JA and SA up-regulated genes: the G-box motif (consensus CACGTG) was enriched among many of the clusters of genes upregulated in response to JA, while this motif was not enriched in SA-upregulated gene clusters; the W-box motif (TTGAC[C|T]) displayed the opposite pattern, as it was highly enriched among the promoters of genes falling in clusters that were upregulated in response to SA, but absent from the JA-upregulated gene clusters. This pattern of motif enrichment also correlates with the gene expression activity of the TF families that recognize each of these discriminating motifs. The master regulators of JA signaling, MYC2, MYC3 and MYC4 are members of the bHLH TF family that specifically bind to G-box motif elements in the promoters of target genes. WRKY family TFs such as WRKY18, WRKY51, WRKY54 and WRKY70 play key roles in the regulation of the SA response (Wang et al., 2006; Pandey and Somssich, 2009). Strikingly, in line with the antagonistic relationship between the JA and SA pathways, genes that were downregulated by JA were found to be enriched for the W-box motif, whereas SA-downregulated genes were enriched for G-box motifs. Collectively, these findings suggest that the G-box and W-box *cis*-regulatory elements are highly specialized in regulating activation and suppression of JA- and SA-induced responses. Because a large fraction of each TF family that can bind

to the core G-box and W-box motifs, and many of the genes encoding such TFs are JA or SA responsive, a key future challenge will be to pinpoint the exact set of TFs that bind to a given motif occurrence and regulate target gene expression. Flanking sequences can play an important role in defining motif specificity, as has been recently shown for the G-box motif family (Ezer et al., 2017). Such investigations of flanking sequences are reliant on experimental TF-DNA interaction data, and will therefore require the use of relevant techniques like chromatin immunoprecipitation (ChIP) assays with sequencing or yeast-1-hybrid assays.

Besides the domination by the bHLH and WRKY TF families of the JA and SA regulatory networks, respectively, we could also identify enrichment of binding motifs for a wide range of other TF families in specific coexpression clusters. In particular, ERF and MYB TFs appeared to regulate the expression of dedicated sets of target genes in specific sectors of the JA network. Motif enrichment among the SA coexpression clusters was more diverse than for the JA response, and pointed to engagement of members of the bZIP, CAMTA, E2F, MYB, HSF, and NAC TF families in the SA network. Thus, it appears that both JA and SA pathways recruit specific sets of TFs from different families to regulate distinct sectors of the immune regulatory network controlling specific biological responses.

The identification of sets of tightly co-regulated genes also provided an opportunity to predict novel regulatory factors within the hormone response networks. The key assumption in this approach is that coexpressed neighbors of important immune regulators are likely to perform a similarly important function. The so-called “guilt-by-association” paradigm is a long-used technique with a strong track record of successfully annotating genes to biological processes (Lee et al., 2011). For each hormone treatment dataset, we explored upregulated gene clusters and identified biological process-unknown TF encoding genes among clusters that were enriched for functional terms associated with immunity or plant defense. Subsequent, screening of the respective mutants for dozens of candidate TFs in resistance bioassays using relevant JA- or SA-inducing pathogens or insects confirmed the role of some as regulators of hormone-mediated immunity. When considering single gene insertion mutants, four of the JA pathway candidate TFs (bHLH27, ERF16, MYB59, and ANAC056) tested were found to play a role in resistance against the assayed pathogen *Botrytis cinerea* and/or the insect *Mamestra brassicae*, whilst only one of the tested candidate regulatory TFs in the SA pathway (ANAC090) displayed a disease phenotype against the assayed pathogen *Pseudomonas syringae* DC3000. Thus, while our approach could clearly identify TFs

with novel roles in regulating resistance, we did not observe phenotypes for many of these single order mutants, especially for the SA candidates.

Functional redundancy, whereby closely related TFs target the same or highly overlapping sets of genes is a likely explanation for the low score of disease phenotypes by the single mutants tested. This can be attributed to genetic redundancy arising from segmental duplications within the Arabidopsis genome. A study by Armisén et al. (2008) reported that more than 90% of genes in the Arabidopsis genome have at least one additional homolog. Full redundancy of duplicated genes prevents deleterious effects if one copy is lost (Figure 1). However, if two gene copies that originate from one ancestral gene undergo different mutations, then this may lead to functional divergence between the two, which may result in differential sub-functionalization for each of the gene copies, or in the acquirement of completely novel functions (Rutter et al., 2012; Bolle et al., 2013) (Figure 1). Often, gene duplications lead to partly redundant but also distinct functions, as is shown for the different members of the JAZ protein family that regulate JA signaling (Howe et al., 2018).

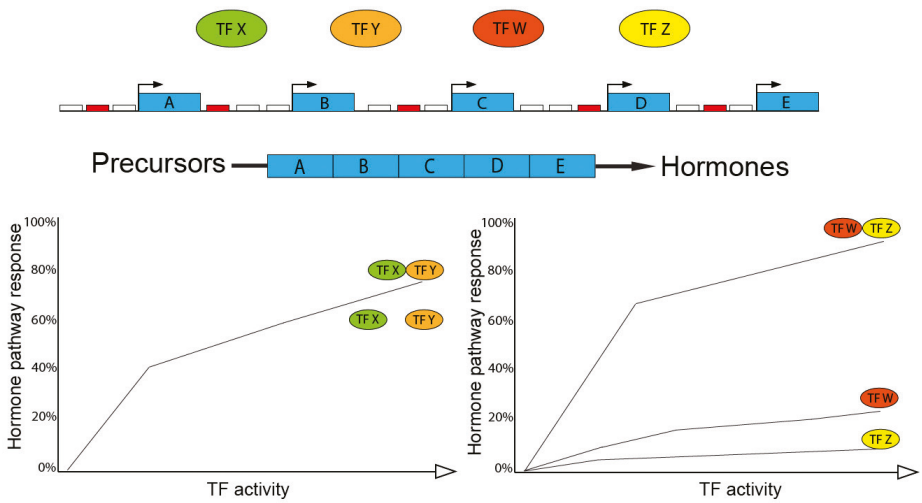

Figure 1. TFs redundancy model.
Homologous TFs sharing function in hormone biosynthesis, by binding to the same or different TF binding sites (TF activity). White and red boxes indicate different *cis*-elements, which affect the TF activity. In the case of full redundancy, as exemplified by TFs X and Y, both TFs have exactly the same function and bind to the same *cis*-element (white box in the different genes A to E, encoding precursors for the hormone production), so that either one of the TFs suffices. In case of neofunctionalization, as exemplified by TFs W and Z, the combination of the TFs is more active, e.g. by binding to different *cis*-elements (white and red box in the genes), so that together they have a synergistic effect on the hormone response.

By specifically targeting highly similar TF-encoding gene pairs from both JA- and SA-candidate lists, we were able to generate double mutants that displayed more severe perturbation of host defenses compared to either single mutant alone. The double mutant for JA-responding paralogous TF genes *MYB48* and *MYB59* displayed highly elevated resistance to caterpillar feeding, and the double mutant for SA-responding *ANAC061* and *ANA090* displayed highly increased resistance to both bacterial and oomycete biotrophic pathogens, when compared to the performance of the corresponding single mutants. These findings demonstrate the importance of utilizing higher-order mutants for the understanding of TF regulatory functions and their role within the wider gene regulatory networks. Future research will increasingly necessitate the generation of higher order mutants that knockout or knockdown two or more homologous TFs in order to shed light on TF function. In particular, the use of CRISPR/Cas9-based gene editing to generate knock-out alleles for several related TF encoding genes will be particularly powerful in this endeavor (Swinnen et al., 2016).

Two homologous NAC TFs function in SA signaling

In Chapter 3, we show how analysis of the transcriptional response to SA led to the characterization of a NAC TF double mutant, *anac61 anac90,* that displayed increased resistance to the biotrophic pathogens *P. syringae* and *Hyaloperonospora arabidopsidis*. The single mutants of the respective genes showed an intermediate (*anac090*) or no significant (*anac061*) effect on the resistance level compared to that of the wild type against both pathogens, pointing to functional redundancy of these two homologous TFs. Interestingly, the growth penalty of the *anac061 anac090*, as measured by leaf area, was relatively small. Mutant *dmr6*, that contains elevated SA levels due to impaired SA hydroxylase activity, is also enhanced resistant to these biotrophic pathogens (Zeilmaker et al., 2015; Zhang et al., 2017a), but in the background of accession Col-0 the mutation in DMR6 causes a more severe growth reduction phenotype than the NAC double mutation (Chapter 3). We also tested the *anac061 anac090* double mutant for resistance to the JA defense-inducing necrotrophic fungal pathogen *B. cinerea* and found this did not differ from wild-type plants (Chapter 3). Transcriptome analyses of the *anac61 anac90* mutants, under non-stress conditions, revealed that several SA-related processes were upregulated. This observation is in line with a recent publication that pointed to ANAC90 as a negative regulator of senescence, which was associated with repression of multiple downstream-targeted *NAC* genes and of SA content (Kim et al., 2018). Both *ANAC061* and *ANAC090* genes were found to be upregulated during infection by different pathogens and their elicitors (publicly available data in the Genevestigator database), indicating that they are an integral part of the plant response to pathogens. In recent literature, different NAC TFs from several species have

been reported as a new class of positive and negative regulators of hormone-regulated networks, influencing development (Kim et al., 2018) and immunity (Yoshii et al., 2010; McLellan et al., 2013; Wang et al., 2015b; Wang et al., 2016).

The NAC family of TFs, which is comprised of 117 members in Arabidopsis, is among one of the largest plant-specific TF families. NAC TF family members contain two key protein domains: a highly conserved N-terminal DNA-binding domain, and a highly variable C-terminal transcriptional activation region (TER) that plays a major role in transcriptional regulation (Olsen et al., 2005). A phylogenetic study of NAC proteins divided family members into 14 specific subgroups (Ooka et al., 2003). The majority of NAC TFs that have been implicated in regulating stress responses fall within the SNAC subgroup (Nuruzzaman et al., 2013). Interestingly, phylogenetic analysis performed by Wang et al. (2016; Figure 2) assigned ANAC061 and ANAC090 to the TERN subfamily, which also contains the tobacco TF TERN (the name giver of the subfamily), the rice TF ONAC012, and an ortholog in cotton, GbNAC1, that was demonstrated to confer resistance against the soil-borne pathogen *Verticillium dahliae* when overexpressed in cotton. This suggests a role for members of the TERN subfamily in plant immunity. Wang et al. (2016) reported that the TERN subfamily members contain a conserved motif at the NAC subdomain C (Figure 2A), which differentiates them from SNAC subfamily members (Figure 2B).

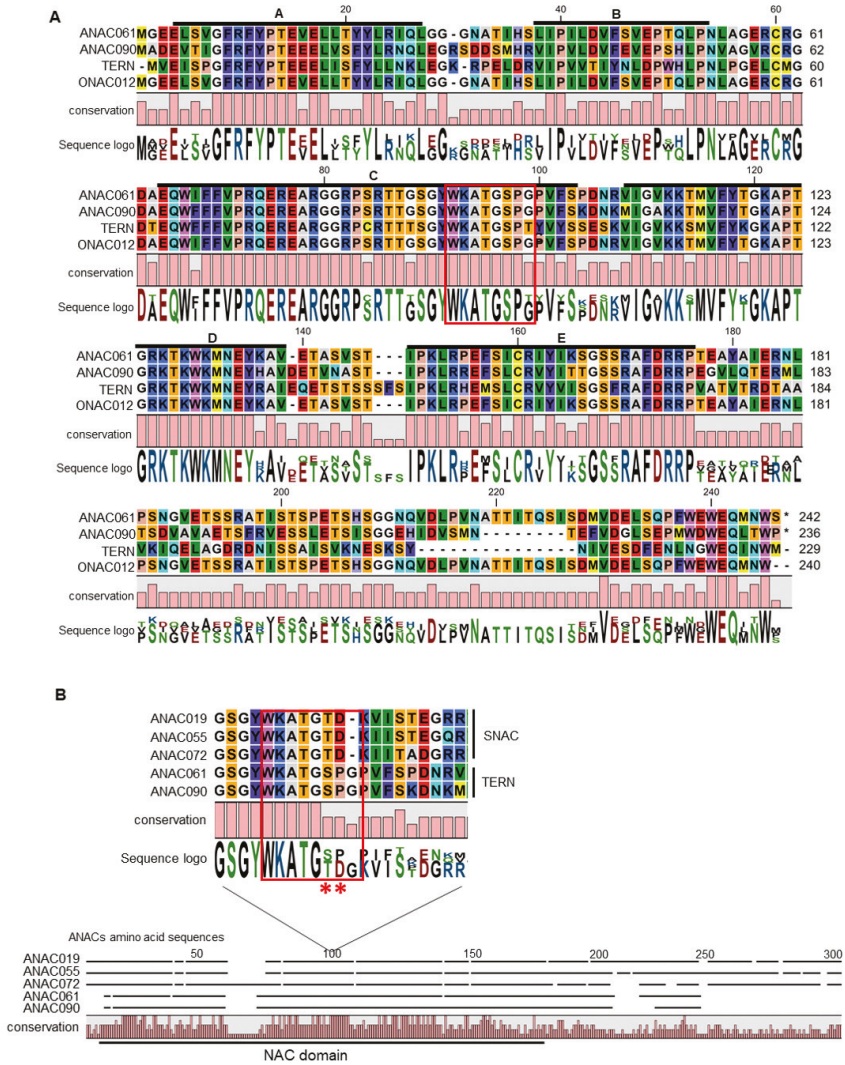

Figure 2. Amino acid alignment of the TERN subfamily of NAC TFs in different plant species (A) and of the TERN and SNAC ANAC representatives from Arabidopsis (B);

(**A**) ANAC61, ANAC90, TERN (*N. benthamiana*) and representative orthologs of TERN sub-family member ONAC12 from rice (*Oryza sativa*). The NAC sub domains are indicated with the letters A to E. The red box indicates the highly conserved amino acids in the TERN subgroup (Adapted from Wang et al., 2016). (**B**) Amino acid alignment of the Arabidopsis ANACs TFs comparing TERN and SNAC subgroups: ANAC061 and ANAC090 represent TERN, while ANAC019, ANAC055 and ANAC072 represent SNAC. The TERN conserved motif is not present in the SNAC subgroup. The red asterisks (*) indicate the position of distinct amino acids between the TERN and SNAC subfamilies. Lower panel indicates full protein sequence alignment of ANAC061, ANAC090, ANAC019, ANAC055 and ANAC017, in which the NAC domain is highlighted.

Little is known about the contribution of the TERN sub family and the role of their characteristic protein domain in plant defense, which may define an important role in defense signaling. A future challenge will be to identify how TERN subfamily domain structure defines functionality of these TFs and how this differs from other members of the NAC family.

Novel defensive outputs of the SA response

While it is the concerted action of many transcriptional regulators such as TFs and their co-activators/repressors that underlies immune hormone gene regulatory networks, the defense outputs are ultimately the changed expression levels of genes that encode proteins that have either direct anti-microbial properties, or are responsible for production or transport of such proteins or other antimicrobial compounds. For example, SA activates not only expression of antimicrobial *PR* genes, but also that of ER resident genes to facilitate the correct folding and secretion of the PR proteins (Wang et al., 2005). For a fraction of all SA-responsive genes, their role in defense is known, but many proteins with novel immune-associated functionality have remained undiscovered.

In Chapter 4 we studied this problem by deliberately targeting SA-activated genes that were lacking meaningful functional characterization. We identified 630 biological process-unknown genes and based on sequence similarity divided them over groups of homologous proteins. As a proof of concept, we focused on one of the largest identified groups, which we defined as a family of eight cysteine-rich polypeptides with a transmembrane domain, ranging in size from 71 to 82 amino acids. Because the expression of many of these family members is also induced by a range of pathogens or pathogen-derived elicitors we named this group the pathogen-induced cysteine-rich transmembrane protein (PCM) family. Interestingly, the PCM family also contains PCC1 (PCM4), a protein that has been described previously as regulated by both pathogen infection and the circadian clock and overexpression was demonstrated to result in enhanced resistance against *H. arabidopsidis* (Sauerbrunn and Schlaich, 2004). A recent publication showed a role for PCM8 (named CYSTM3) in salt stress resistance (Xu et al., 2019). Yet, the remaining six PCM family members had not been characterized to any significant degree. By using transgenic Arabidopsis lines that overexpress each of the PCM family members, we showed plasma membrane localization for PCM1 to PCM5, while PCM6 to PCM8 were detected in the cytoplasm, but we had not determined whether this could be due to degradation of the YFP-tagged protein. A number of *PCM*-OX lines was found to be more resistant to the biotrophic pathogens *P. syringae* (PCM1, PCM2 and PCM3) and *H. arabidopsidis* (PCM1, PCM2, PCM3, PCM4, PCM5 and

PCM7). Moreover, we showed that subgroups of the PCMs had overlapping coexpression networks, in which several known defense-related genes were present. RNA-Seq analysis of three of the overexpression lines (*PCM1*-OX, *PCM5*-OX, and *PCM7*-OX, representing the three subgroups) pointed to enrichment of light- and development-related genes being differentially expressed, while no typical defense-related genes were induced. While we were able to demonstrate that this family of proteins likely plays an important role in plant immunity, the exact functional mechanism that underlies this positive effect on resistance remains enigmatic. We hypothesize that PCM overexpression can change membrane structure, which may affect infection structures, or PCMs may interact with other proteins, which has multiple consequences on different biological functions of the plant. The creation of knock-out lines for the PCMs, although difficult because of their high sequence similarity, should be conducted to prove more insight in their roles. Future work on the mechanistic basis of PCMs' role in pathogen defense may lead to insights that can be applied to crops, since the CYSTM family, to which the PCMs belong are a very widespread family among organisms, suggesting they have a conserved and important role (Venancio and Aravind, 2010; Xu et al., 2018). The fact that the PCMs also seem to play an important role in tolerance to abiotic stresses (Xu et al., 2018; Xu et al., 2019) and in plant growth (Chapter 4), impacts their applicability.

CONCLUDING REMARKS

The importance of plant hormones as key regulators of induced plant immune responses is well established. In this thesis, the complexity of the gene regulatory networks, as induced by the two major defense hormones, JA and SA, is revealed using RNA-Seq data and computational analyses. We have predicted and validated novel components in these networks. Several JA- and SA-responsive TFs were characterized, allowing us to add small pieces to the big puzzle representing the complex plant immune regulatory network. However, their effective transcriptional activity still needs to be validated by experimental approaches such as protein-DNA interactions methods. *In vivo* binding of TFs to DNA is dependent on chromatin accessibility, DNA methylation, TF cooperativity, and TF interactions with non-binding cofactors and the transcription machinery. For instance, ChIP-seq would be an optimal technique to identify the binding sites (motifs) of DNA-associated proteins (TFs) predicted in this thesis. Furthermore, analysis of genome-wide gene expression changes in SA or/and JA accumulation at multiple regulatory steps would definitely add to our understanding of how the plant immune regulatory network functions. The recently developed assay for transposase-accessible chromatin (ATAC)-seq provides detailed information on nucleosome position and how chromatin compaction and DNA-binding proteins regulate gene expression at high resolution

in planta. Its application to single cells offers a look at the variability in chromatin organization and TF binding sites in different cell types (Sullivan et al., 2014; Buenrostro et al., 2013; Cusanovich et al., 2015). Once transcription is initiated, a variety of critical and highly-regulated co- and post-transcriptional pre-mRNA processing steps occur in the nucleus, prior to export of mature mRNA to the cytoplasm. Among these processes are transcript elongation, which can be determined by Global Run-On sequencing (GRO-seq), measuring nascent RNA that is undergoing transcription by RNA polymerase in the nucleus. Comparison of GRO-seq data with RNA-seq data exposes differences in the contribution of different co- and post-transcription processes. Furthermore, translation efficiency of mRNA into protein can be an important step in the regulation of immune responses. The Ribo-seq methodology determines which mRNAs are undergoing translation. Collectively, the wealth of data on the JA and SA gene regulatory networks and the possible roles of their players in plant immunity form a rich reservoir of knowledge that in the future may be utilized via e.g. gene editing technologies to improve or rewire defense-related signaling pathways in future crop that can maximize both growth and defense.

REFERENCES

Allu, A.D., Brotman, Y., Xue, G.P., and Balazadeh, S. (2016). Transcription factor ANAC032 modulates JA/SA signalling in response to *Pseudomonas syringae* infection. EMBO reports **17,** 1578-1589.

Alon, U. (2007). Network motifs: theory and experimental approaches. Nature Reviews Genetics **8,** 450-461.

Anders, S., and Huber, W. (2010). Differential expression analysis for sequence count data. Genome Biology **11,** R106.

Anders, S., Pyl, P.T., and Huber, W. (2015). HTSeq—a Python framework to work with high-throughput sequencing data. Bioinformatics **31,** 166-169.

Arabidopsis Genome Initiative, C. (2000). Analysis of the genome sequence of the flowering plant *Arabidopsis thaliana*. Nature **408,** 796-815.

Arabidopsis Interactome Mapping, C. (2011). Evidence for network evolution in an Arabidopsis interactome map. Science **333,** 601-607.

Armisén, D., Lecharny, A. and Aubourg, S. (2008) Unique genes in plants: specificities and conserved features throughout evolution. BMC Evolutionary Biology. **8**, 280.

Ariel, F.D., Manavella, P.A., Dezar, C.A., and Chan, R.L. (2007). The true story of the HD-Zip family. Trends in Plant Science **12,** 419-426.

Attaran, E., Major, I.T., Cruz, J.A., Rosa, B.A., Koo, A.J.K., Chen, J., Kramer, D.M., He, S.Y., and Howe, G.A. (2014). Temporal dynamics of growth and photosynthesis suppression in response to jasmonate signaling. Plant Physiology **165,** 1302-1314.

Attard, A., Gourgues, M., Callemeyn-Torre, N., and Keller, H. (2010). The immediate activation of defense responses in Arabidopsis roots is not sufficient to prevent *Phytophthora parasitica* infection. New Phytologist **187,** 449-460.

Baba, K., Nakano, T., Yamagishi, K., and Yoshida, S. (2001). Involvement of a nuclear-encoded basic helix-loop-helix protein in transcription of the light-responsive promoter of psbD. Plant Physiology **125,** 595-603.

Baek, D., Nam, J., Koo, Y.D., Kim, D.H., Lee, J., Jeong, J.C., Kwak, S.S., Chung, W.S., Lim, C.O., Bahk, J.D., Hong, J.C., Lee, S.Y., Kawai-Yamada, M., Uchimiya, H., and Yun, D.J. (2004). Bax-induced cell death of Arabidopsis is meditated through reactive oxygen-dependent and -independent processes. Plant Molecular Biology **56,** 15-27.

Bailey, T.L., and Elkan, C. (1994). Fitting a mixture model by expectation maximization to discover motifs in biopolymers. Proceedings of the 8th International Conference on Intelligent Systems for Molecular Biology **2,** 28-36.

Bailey, T.L., Boden, M., Buske, F.A., Frith, M., Grant, C.E., Clementi, L., Ren, J.Y., Li, W.W., and Noble, W.S. (2009). MEME SUITE: tools for motif discovery and searching. Nucleic Acids Research **37,** W202-W208.

Bakker, P.A.H.M., Ran, L.X., and Mercado-Blanco, J. (2014). Rhizobacterial salicylate production provokes headaches!. Plant and Soil **382,** 1-16.

Bakker, P.A.H.M., Pieterse, C.M.J., de Jonge, R., and Berendsen, R.L. (2018). The soil-borne legacy. Cell **172,** 1178-1180.

Ballaré, C.L. (2014). Light regulation of plant defense. Annual Review of Plant Biology **65,** 335-363.

Bar-Joseph, Z., Gitter, A., and Simon, I. (2012). Studying and modelling dynamic biological processes using time-series gene expression data. Nature Reviews Genetics **13,** 552-564.

Bartsch, M., Gobbato, E., Bednarek, P., Debey, S., Schultze, J.L., Bautor, J., and Parker, J.E. (2006). Salicylic acid-independent ENHANCED DISEASE SUSCEPTIBILITY1 signaling in Arabidopsis immunity and cell death is regulated by the monooxygenase FMO1 and the Nudix hydrolase NUDT7. Plant Cell **18,** 1038-1051.

Bechtold, U., Penfold, C.A., Jenkins, D.J., Legaie, R., Moore, J.D., Lawson, T., Matthews, J.S.A., Vialet-Chabrand, S.R.M., Baxter, L., and Subramaniam, S. (2016). Time-series transcriptomics reveals that AGAMOUS-LIKE22 affects primary metabolism and developmental processes in drought-stressed Arabidopsis. Plant Cell **28,** 345-366.

Beck, M., Wyrsch, I., Strutt, J., Wimalasekera, R., Webb, A., Boller, T., and Robatzek, S. (2014). Expression patterns of flagellin sensing 2 map to bacterial entry sites in plant shoots and roots. Journal of Experimental Botany **65,** 6487-6498.

Bemer, M., Van Dijk, A.D.J., Immink, R.G.H., and Angenent, G.C. (2017). Cross-family transcription factor interactions: an additional layer of gene regulation. Trends in Plant Science **22,** 66-80.

Berendsen, R.L., Pieterse, C.M., and Bakker, P.A. (2012). The rhizosphere microbiome and plant health. Trends in Plant Science **17,** 478-486.

Berendsen, R.L., Vismans, G., Yu, K., Song, Y., de Jonge, R., Burgman, W.P., Burmolle, M., Herschend, J., Bakker, P., and Pieterse, C.M.J. (2018). Disease-induced assemblage of a plant-beneficial bacterial consortium. ISME Journal **12,** 1496-1507.

Berens, M.L., Berry, H.M., Mine, A., Argueso, C.T., and Tsuda, K. (2017). Evolution of hormone signaling networks in plant defense. Annual Review of Phytopathology **55,** 401-425.

Berens, M.L., Wolinska, K.W., Spaepen, S., Ziegler, J., Nobori, T., Nair, A., Kruler, V., Winkelmuller, T.M., Wang, Y., Mine, A., Becker, D., Garrido-Oter, R., Schulze-Lefert, P., and Tsuda, K. (2019). Balancing trade-offs between biotic and abiotic stress responses through leaf age-dependent variation in stress hormone cross-talk. Proceedings of the National Academy of Sciences of the United States of America **116,** 2364-2373.

Berrocal-Lobo, M., Molina, A., and Solano, R. (2002). Constitutive expression of *ETHYLENE-RESPONSE-FACTOR1* in Arabidopsis confers resistance to several necrotrophic fungi. Plant Journal **29,** 23-32.

Betsuyaku, S., Katou, S., Takebayashi, Y., Sakakibara, H., Nomura, N., and Fukuda, H. (2018). Salicylic acid and jasmonic acid pathways are activated in spatially different domains around the infection site during effector-triggered immunity in *Arabidopsis thaliana*. Plant & Cell Physiology **59,** 8-16.

Blanco, F., Salinas, P., Cecchini, N.M., Jordana, X., Van Hummelen, P., Alvarez, M.E., and Holuigue, L. (2009). Early genomic responses to salicylic acid in Arabidopsis. Plant Molecular Biology **70,** 79–102.

Bolle, C., Schneider, A., and Leister, D. (2011). Perspectives on systematic analyses of gene function in *Arabidopsis thaliana*: new tools, topics and trends. Current Genomics **12,** 1.

Bolle, C., Huep, G., Kleinbölting, N., Haberer, G., Mayer, K., Leister, D., and Weisshaar, B. (2013). GABI-DUPLO: a collection of double mutants to overcome genetic redundancy in *Arabidopsis thaliana*. Plant Journal **75,** 157-171.

Boller, T., and Felix, G. (2009). A renaissance of elicitors: perception of microbe-associated molecular patterns and danger signals by pattern-recognition receptors. Annual Review of Plant Biology **60,** 379-406.

Boutrot, F., and Zipfel, C. (2017). Function, discovery, and exploitation of plant pattern recognition receptors for broad-spectrum disease resistance. Annual Review of Phytopathology **55,** 257-286.

Bowers, J.E., Chapman, B.A., Rong, J., and Paterson, A.H. (2003). Unravelling angiosperm genome evolution by phylogenetic analysis of chromosomal duplication events. Nature **422,** 433-438.

Boyle, E.I., Weng, S.A., Gollub, J., Jin, H., Botstein, D., Cherry, J.M., and Sherlock, G. (2004). GO::TermFinder - open source software for accessing Gene Ontology information and finding significantly enriched Gene Ontology terms associated with a list of genes. Bioinformatics **20,** 3710-3715.

Brady, S.M., Orlando, D.A., Lee, J.Y., Wang, J.Y., Koch, J., Dinneny, J.R., Mace, D., Ohler, U., and Benfey, P.N. (2007). A high-resolution root spatiotemporal map reveals dominant expression patterns. Science **318,** 801-806.

Breeze, E., Harrison, E., McHattie, S., Hughes, L., Hickman, R., Hill, C., Kiddle, S., Kim, Y.S., Penfold, C.A., Jenkins, D., Zhang, C.J., Morris, K., Jenner, C., Jackson, S., Thomas, B., Tabrett, A., Legaie, R., Moore, J.D., Wild, D.L., Ott, S., Rand, D., Beynon, J., Denby, K., Mead, A., and Buchanan-Wollaston, V. (2011). High-resolution temporal profiling of transcripts during Arabidopsis leaf senescence reveals a distinct chronology of processes and regulation. Plant Cell **23,** 873-894.

Brooks, D.M., Bender, C.L., and Kunkel, B.N. (2005). The *Pseudomonas syringae* phytotoxin coronatine promotes virulence by overcoming salicylic acid-dependent defences in *Arabidopsis thaliana*. Molecular Plant Pathology **6,** 629-639.

Bu, Q., Jiang, H., Li, C.B., Zhai, Q., Zhang, J., Wu, X., Sun, J., Xie, Q., and Li, C. (2008). Role of the *Arabidopsis thaliana* NAC transcription factors ANAC019 and ANAC055 in regulating jasmonic acid-signaled defense responses. Cell Research **18,** 756-767.

Buenrostro, J.D., Giresi, P.G., Zaba, L.C., Chang, H.Y., and Greenleaf, W.J. (2013). Transposition of native chromatin for fast and sensitive epigenomic profiling of open chromatin, DNA-binding proteins and nucleosome position. Nature Protocol **10,** 1213-1218.

Caarls, L., Pieterse, C.M.J., and Van Wees, S.C.M. (2015). How salicylic acid takes transcriptional control over jasmonic acid signaling. Frontiers in Plant Science **6,** 170.

Caarls, L., Van der Does, D., Hickman, R., Jansen, W., Verk, M.C., Proietti, S., Lorenzo, O., Solano, R., Pieterse, C.M.J., and Van Wees, S.C.M. (2017). Assessing the role of ETHYLENE RESPONSE FACTOR transcriptional repressors in salicylic acid-mediated suppression of jasmonic acid-responsive genes. Plant & Cell Physiology **58,** 266-278.

Campos, M.L., Kang, J.H., and Howe, G.A. (2014). Jasmonate-triggered plant immunity. Journal of Chemical Ecology **40,** 657–675.

Cao, H., Bowling, S.A., Gordon, A.S., and Dong, X. (1994). Characterization of an Arabidopsis mutant that is nonresponsive to inducers of systemic acquired resistance. Plant Cell **6,** 1583-1592.

Carvalhais, L.C., Dennis, P.G., Badri, D.V., Tyson, G.W., Vivanco, J.M., and Schenk, P.M. (2013). Activation of the jasmonic acid plant defence pathway alters the composition of rhizosphere bacterial communities. PLoS ONE **8,** e56457.

Chandran, D., Rickert, J., Huang, Y., Steinwand, M.A., Marr, S.K., and Wildermuth, M.C. (2014). Atypical E2F transcriptional repressor DEL1 acts at the intersection of plant growth and immunity by controlling the hormone salicylic acid. Cell Host & Microbe **15,** 506-513.

Chang, K.N., Zhong, S., Weirauch, M.T., Hon, G., Pelizzola, M., Li, H., Huang, S.S., Schmitz, R.J., Urich, M.A., Kuo, D., Nery, J.R., Qiao, H., Yang, A., Jamali, A., Chen, H., Ideker, T., Ren, B., Bar-Joseph, Z., Hughes, T.R., and Ecker, J.R. (2013). Temporal transcriptional response to ethylene gas drives growth hormone cross-regulation in Arabidopsis. Elife **2,** e00675.

Chen, H., Chen, J., Li, M., Chang, M., Xu, K., Shang, Z., Zhao, Y., Palmer, I., Zhang, Y., McGill, J., Alfano, J.R., Nishimura, M.T., Liu, F., and Fu, Z.Q. (2017). A bacterial type III effector targets the master regulator of salicylic acid signaling, NPR1, to subvert plant immunity. Cell Host & Microbe **22,** 777-788 e777.

Chen, H.Y., Hsieh, E.J., Cheng, M.C., Chen, C.Y., Hwang, S.Y., and Lin, T.P. (2016). ORA47 (octadecanoid-responsive AP2/ERF-domain transcription factor 47) regulates jasmonic acid and abscisic acid biosynthesis and signaling through binding to a novel *cis*-element. New Phytologist **211,** 599-613.

Chen, Z., Agnew, J.L., Cohen, J.D., He, P., Shan, L., Sheen, J., and Kunkel, B.N. (2007). *Pseudomonas syringae* type III effector AvrRpt2 alters *Arabidopsis thaliana* auxin physiology. Proceedings of the National Academy of Sciences of the United States of America **104,** 20131-20136.

Cheng, Z., Sun, L., Qi, T., Zhang, B., Peng, W., Liu, Y., and Xie, D. (2011). The bHLH transcription factor MYC3 interacts with the jasmonate ZIM-domain proteins to mediate jasmonate response in Arabidopsis. Molecular Plant **4,** 279–288.

Chini, A., Gimenez-Ibanez, S., Goossens, A., and Solano, R. (2016). Redundancy and specificity in jasmonate signalling. Current Opinion in Plant Biology **33,** 147-156.

Chini, A., Fonseca, S., Fernandez, G., Adie, B., Chico, J.M., Lorenzo, O., Garcia-Casado, G., Lopez-Vidriero, I., Lozano, F.M., Ponce, M.R., Micol, J.L., and Solano, R. (2007). The JAZ family of repressors is the missing link in jasmonate signalling. Nature **448,** 666–671.

Clough, S.J., and Bent, A.F. (1998). Floral dip: a simplified method forAgrobacterium-mediated transformation ofArabidopsis thaliana. The Plant Journal **16,** 735-743.

Coego, A., Brizuela, E., Castillejo, P., Ruiz, S., Koncz, C., del Pozo, J.C., Pineiro, M., Jarillo, J.A., Paz-Ares, J., Leon, J., and Transplanta Consortium. (2014). The TRANSPLANTA collection of *Arabidopsis* lines: a resource for functional analysis of transcription factors based on their conditional overexpression. Plant Journal **77,** 944-953.

Consonni, C., Humphry, M.E., Hartmann, H.A., Livaja, M., Durner, J., Westphal, L., Vogel, J., Lipka, V., Kemmerling, B., Schulze-Lefert, P., Somerville, S.C., and Panstruga, R. (2006). Conserved requirement for a plant host cell protein in powdery mildew pathogenesis. Nature Genetics **38,** 716-720.

Coolen, S., Proietti, S., Hickman, R., Davila Olivas, N.H., Huang, P.P., Van Verk, M.C., Van Pelt, J.A., Wittenberg, A.H., De Vos, M., Prins, M., Van Loon, J.J., Aarts, M.G., Dicke, M., Pieterse, C.M.J., and Van Wees, S.C.M. (2016). Transcriptome dynamics of Arabidopsis during sequential biotic and abiotic stresses. Plant Journal **86,** 249-267.

Cordovez, V., Dini-Andreote, F., Carrion, V.J., and Raaijmakers, J.M. (2019). Ecology and evolution of plant microbiomes. Annual Review of Microbiology**,** 10.1146/annurev-micro-090817-062524.

Couto, D., and Zipfel, C. (2016). Regulation of pattern recognition receptor signalling in plants. Nature Reviews Immunology **16,** 537-552.

Cui, H., Tsuda, K., and Parker, J.E. (2015). Effector-triggered immunity: from pathogen perception to robust defense. Annual Review of Plant Biology **66,** 487-511.

Cusanovich, D.A., Daza, R., Adey, A., Pliner, H.A., Christiansen, L., Gunderson, K.L., Steemers, F.J., Trapnell, C., and Shendure, J. (2015). Multiplex single cell profiling of chromatin accessibility by combinatorial cellular indexing. Science **348,** 910-914.

Czechowski, T., Bari, R.P., Stitt, M., Scheible, W.R., and Udvardi, M.K. (2004). Real-time RT-PCR profiling of over 1400 Arabidopsis transcription factors: unprecedented sensitivity reveals novel root- and shoot-specific genes. Plant Journal **38,** 366–379.

Dangl, J.L., Horvath, D.M., and Staskawicz, B.J. (2013). Pivoting the plant immune system from dissection to deployment. Science **341,** 746-751.

De Coninck, B., Timmermans, P., Vos, C., Cammue, B.P., and Kazan, K. (2015). What lies beneath: belowground defense strategies in plants. Trends in Plant Science **20,** 91-101.

De Geyter, N., Gholami, A., Goormachtig, S., and Goossens, A. (2012). Transcriptional machineries in jasmonate-elicited plant secondary metabolism. Trends in Plant Science **17,** 349–359.

De Vos, M., Van Oosten, V.R., Van Poecke, R.M., Van Pelt, J.A., Pozo, M.J., Mueller, M.J., Buchala, A.J., Metraux, J.P., Van Loon, L.C., Dicke, M., and Pieterse, C.M.J. (2005). Signal signature and transcriptome changes of Arabidopsis during pathogen and insect attack. Molecular Plant-Microbe Interactions **18,** 923-937.

Ding, Y., Sun, T., Ao, K., Peng, Y., Zhang, Y., Li, X., and Zhang, Y. (2018). Opposite roles of salicylic acid receptors NPR1 and NPR3/NPR4 in transcriptional regulation of plant immunity. Cell **173,** 1454-1467. e1415.

Dodds, P.N., and Rathjen, J.P. (2010). Plant immunity: towards an integrated view of plant-pathogen interactions. Nature Reviews Genetenics **11,** 539-548.

Dombrecht, B., Xue, G.P., Sprague, S.J., Kirkegaard, J.A., Ross, J.J., Reid, J.B., Fitt, G.P., Sewelam, N., Schenk, P.M., Manners, J.M., and Kazan, K. (2007). MYC2 differentially modulates diverse jasmonate-dependent functions in Arabidopsis. Plant Cell **19,** 2225–2245.

Du, L., Ali, G.S., Simons, K.A., Hou, J., Yang, T., Reddy, A.S.N., and Poovaiah, B.W. (2009). Ca^{2+}/calmodulin regulates salicylic-acid-mediated plant immunity. Nature **457,** 1154-1158.

El Oirdi, M., El Rahman, T.A., Rigano, L., El Hadrami, A., Rodriguez, M.C., Daayf, F., Vojnov, A., and Bouarab, K. (2011). *Botrytis cinerea* manipulates the antagonistic effects between immune pathways to promote disease development in tomato. Plant Cell **23,** 2405–2421.

Erb, M., and Reymond, P. (2019). Molecular interactions between plants and insect herbivores. Annual Review of Plant Biology **70,** 527-557.

Ernst, J., Vainas, O., Harbison, C.T., Simon, I., and Bar-Joseph, Z. (2007). Reconstructing dynamic regulatory maps. Molecular Systems Biology **3,** 74.

Ezer, D., Shepherd, S.J.K., Brestovitsky, A., Dickinson, P., Cortijo, S., Charoensawan, V., Box, M.S., Biswas, S., Jaeger, K.E., and Wigge, P.A. (2017). The G-Box transcriptional regulatory code in Arabidopsis. Plant Physiology **175,** 628-640.

Fernández-Calvo, P., Chini, A., Fernández-Barbero, G., Chico, J.M., Gimenez-Ibanez, S., Geerinck, J., Eeckhout, D., Schweizer, F., Godoy, M., Franco-Zorrilla, J.M., Pauwels, L., Witters, E., Puga, M.I., Paz-Ares, J., Goossens, A., Reymond, P., De Jaeger, G., and Solano, R. (2011). The Arabidopsis bHLH transcription factors MYC3 and MYC4 are targets of JAZ repressors and act additively with MYC2 in the activation of jasmonate responses. Plant Cell **23,** 701–715.

Ferrier, T., Matus, J.T., Jin, J., and Riechmann, J.L. (2011). Arabidopsis paves the way: genomic and network analyses in crops. Current Opinion in Biotechnology **22,** 260-270.

Feys, B.J., Moisan, L.J., Newman, M.A., and Parker, J.E. (2001). Direct interaction between the Arabidopsis disease resistance signaling proteins, EDS1 and PAD4. EMBO Journal **20,** 5400–5411.

Finn, R.D., Clements, J., Arndt, W., Miller, B.L., Wheeler, T.J., Schreiber, F., Bateman, A., and Eddy, S.R. (2015). HMMER web server: 2015 update. Nucleic Acids Research **43,** W30-38.

Fischer, J.A., Acosta, S., Kenny, A., Cater, C., Robinson, C., and Hook, J. (2004). Drosophila klarsicht has distinct subcellular localization domains for nuclear envelope and microtubule localization in the eye. Genetics **168,** 1385-1393.

Fonseca, S., Chini, A., Hamberg, M., Adie, B., Porzel, A., Kramell, R., Miersch, O., Wasternack, C., and Solano, R. (2009). (+)-7-iso-Jasmonoyl-L-isoleucine is the endogenous bioactive jasmonate. Nature Chemical Biology **5,** 344-350.

Foo, M., Gherman, I., Zhang, P., Bates, D.G., and Denby, K.J. (2018). A framework for engineering stress resilient plants using genetic feedback control and regulatory network rewiring. ACS Syntheic Biology **7,** 1553-1564.

Franco-Zorrilla, J.M., and Solano, R. (2017). Identification of plant transcription factor target sequences. Biochimica et Biophysica Acta **1860,** 21-30.

Franco-Zorrilla, J.M., López-Vidriero, I., Carrasco, J.L., Godoy, M., Vera, P., and Solano, R. (2014). DNA-binding specificities of plant transcription factors and their potential to define target genes. Proceedings of the National Academy of Sciences of the United States of America **111,** 2367–2372.

Fu, Z.Q., and Dong, X. (2013). Systemic acquired resistance: Turning local infection into global defense. Annual Review of Plant Biology **64,** 839-863.

Fu, Z.Q., Yan, S., Saleh, A., Wang, W., Ruble, J., Oka, N., Mohan, R., Spoel, S.H., Tada, Y., Zheng, N., and Dong, X. (2012). NPR3 and NPR4 are receptors for the immune signal salicylic acid in plants. Nature **486,** 228–232.

Gamir, J., Darwiche, R., Van't Hof, P., Choudhary, V., Stumpe, M., Schneiter, R., and Mauch, F. (2017). The sterol-binding activity of PATHOGENESIS-RELATED PROTEIN 1 reveals the mode of action of an antimicrobial protein. Plant Journal **89,** 502-509.

Gangappa, S.N., and Botto, J.F. (2014). The BBX family of plant transcription factors. Trends in Plant Science **19,** 460-470.

Gigolashvili, T., Yatusevich, R., Berger, B., Muller, C., and Flugge, U.I. (2007). The R2R3-MYB transcription factor HAG1/MYB28 is a regulator of methionine-derived glucosinolate biosynthesis in *Arabidopsis thaliana*. Plant Journal **51,** 247-261.

Gimenez-Ibanez, S., Boter, M., Fernandez-Barbero, G., Chini, A., Rathjen, J.P., and Solano, R. (2014). The bacterial effector HopX1 targets JAZ transcriptional repressors to activate jasmonate signaling and promote infection in Arabidopsis. PLoS Biology **12,** e1001792.

Glazebrook, J., Rogers, E.E., and Ausubel, F.M. (1996). Isolation of Arabidopsis mutants with enhanced disease susceptibility by direct screening. Genetics **143,** 973-982.

Goda, H., Sasaki, E., Akiyama, K., Maruyama-Nakashita, A., Nakabayashi, K., Li, W., Ogawa, M., Yamauchi, Y., Preston, J., Aoki, K., Kiba, T., Takatsuto, S., Fujioka, S., Asami, T., Nakano, T., Kato, H., Mizuno, T., Sakakibara, H., Yamaguchi, S., Nambara, E., Kamiya, Y., Takahashi, H., Hirai, M.Y., Sakurai, T., Shinozaki, K., Saito, K., Yoshida, S., and Shimada, Y. (2008). The AtGenExpress hormone and chemical treatment data set: experimental design, data evaluation, model data analysis and data access. Plant Journal **55,** 526–542.

Gomez-Gomez, L., and Boller, T. (2000). FLS2: An LRR receptor-like kinase involved in the perception of the bacterial elicitor flagellin in Arabidopsis. Molecular Cell **5,** 1003-1012.

Gordon, D.B., Nekludova, L., McCallum, S., and Fraenkel, E. (2005). TAMO: a flexible, object-oriented framework for analyzing transcriptional regulation using DNA-sequence motifs. Bioinformatics **21,** 3164-3165.

Gourion, B., Berrabah, F., Ratet, P., and Stacey, G. (2015). Rhizobium-legume symbioses: the crucial role of plant immunity. Trends in Plant Science **20,** 186-194.

Grant, C.E., Bailey, T.L., and Noble, W.S. (2011). FIMO: scanning for occurrences of a given motif. Bioinformatics **27,** 1017–1018.

Greene, G.H., and Dong, X. (2018). To grow and to defend. Science **361,** 976-977.

Guo, P., Li, Z., Huang, P., Li, B., Fang, S., Chu, J., and Guo, H. (2017). A tripartite amplification loop involving the transcription factor WRKY75, salicylic acid, and reactive oxygen species accelerates leaf senescence. Plant Cell **29,** 2854-2870.

Gust, A.A., and Felix, G. (2014). Receptor like proteins associate with SOBIR1-type of adaptors to form bimolecular receptor kinases. Current Opinion in Plant Biology **21,** 104-111.

Hacquard, S., Spaepen, S., Garrido-Oter, R., and Schulze-Lefert, P. (2017). Interplay between innate immunity and the plant microbiota. Annual Review of Phytopathology **55,** 565-589.

Hammargren, J., Rosenquist, S., Jansson, C., and Knorpp, C. (2008). A novel connection between nucleotide and carbohydrate metabolism in mitochondria: sugar regulation of the Arabidopsis nucleoside diphosphate kinase 3a gene. Plant Cell Reports **27,** 529-534.

Haney, C.H., and Ausubel, F.M. (2015). Plant microbiome blueprints. Science **349,** 788-789.

Hartmann, H., Guthohrlein, E.W., Siebert, M., Luehr, S., and Soding, J. (2013). P-value-based regulatory motif discovery using positional weight matrices. Genome Research **23,** 181-194.

Hayat, Q., Hayat, S., Irfan, M., and Ahmad, A. (2010). Effect of exogenous salicylic acid under changing environment: A review. Environmental and Experimental Botany **68,** 14-25.

Heard, N.A. (2011). Iterative reclassification in agglomerative clustering. Journal of Computational and Graphical Statistics **20,** 920-936.

Heard, N.A., Holmes, C.C., and Stephens, D.A. (2006). A quantitative study of gene regulation involved in the immune response of anopheline mosquitoes: An application of Bayesian hierarchical clustering of curves. Journal of the American Statistical Association **101,** 18-29.

Heil, M., and Baldwin, I.T. (2002). Fitness costs of induced resistance: emerging experimental support for a slippery concept. Trends in Plant Science **7,** 61-67.

Hickman, R., Van Verk, M.C., Van Dijken, A.J.H., Pereira Mendes, M., Vroegop-Vos, I.A., Caarls, L., Steenbergen, M., Van der Nagel, I., Wesselink, G.J., Jironkin, A., Talbot, A., Rhodes, J., De Vries, M., Schuurink, R.C., Denby, K., Pieterse, C.M.J., and Van Wees, S.C.M. (2017). Architecture and dynamics of the jasmonic acid gene regulatory network. Plant Cell **29,** 2086-2105.

Hillmer, R.A., Tsuda, K., Rallapalli, G., Asai, S., Truman, W., Papke, M.D., Sakakibara, H., Jones, J.D.G., Myers, C.L., and Katagiri, F. (2017). The highly buffered Arabidopsis immune signaling network conceals the functions of its components. PLoS Genetics **13,** e1006639.

Howe, G.A., and Yoshida, Y. (2019). Evolutionary origin of JAZ proteins and jasmonate signaling. Molecular Plant **12,** 153-155.

Howe, G.A., Major, I.T., and Koo, A.J. (2018). Modularity in jasmonate signaling for multistress resilience. Annual Review of Plant Biology **69,** 387-415.

Hruz, T., Laule, O., Szabo, G., Wessendorp, F., Bleuler, S., Oertle, L., Widmayer, P., Gruissem, W., and Zimmermann, P. (2008). Genevestigator V3: a reference expression database for the meta-analysis of transcriptomes. Advances in Bioinformatics **2008: 420747**.

Innes, R. (2018). The positives and negatives of NPR: A unifying model for salicylic acid signaling in plants. Cell **173,** 1314-1315.

Jiang, S., Yao, J., Ma, K.W., Zhou, H., Song, J., He, S.Y., and Ma, W. (2013). Bacterial effector activates jasmonate signaling by directly targeting JAZ transcriptional repressors. PLoS Pathogens **9,** e1003715.

Jin, J.P., Zhang, H., Kong, L., Gao, G., and Luo, J.C. (2014). PlantTFDB 3.0: a portal for the functional and evolutionary study of plant transcription factors. Nucleic Acids Research **42,** D1182-D1187.

Jones, J.D., and Dangl, J.L. (2006). The plant immune system. Nature **444,** 323-329.

Kazan, K. (2018). A new twist in SA signalling. Nature Plants **4,** 327-328.

Kazan, K., and Manners, J.M. (2008). Jasmonate signaling: Toward an integrated view. Plant Physiology **146,** 1459-1468.

Kazan, K., and Manners, J.M. (2013). MYC2: the master in action. Molecular Plant **6,** 686-703.

Kazan, K., and Lyons, R. (2014). Intervention of phytohormone pathways by pathogen effectors. Plant Cell **26,** 2285-2309.

Kim, H.J., Nam, H.G., and Lim, P.O. (2016). Regulatory network of NAC transcription factors in leaf senescence. Current Opinion in Plant Biology **33,** 48-56.

Kim, H.J., Park, J.H., Kim, J., Kim, J.J., Hong, S., Kim, J., Kim, J.H., Woo, H.R., Hyeon, C., Lim, P.O., Nam, H.G., and Hwang, D. (2018). Time-evolving genetic networks reveal a NAC troika that negatively regulates leaf senescence in Arabidopsis. Proceedings of the National Academy of Sciences of the United States of America **115,** 4930-4939.

Kim, Y., Tsuda, K., Igarashi, D., Hillmer, R.A., Sakakibara, H., Myers, C.L., and Katagiri, F. (2014). Mechanisms underlying robustness and tunability in a plant immune signaling network. Cell Host & Microbe **15,** 84-94.

Klessig, D.F., Choi, H.W., and Dempsey, D.A. (2018). Systemic acquired resistance and salicylic acid: past, present, and future. Molecular Plant-Microbe Interactions **31,** 871-888.

Kloepper, J.W., Ryu, C.-M., and Zhang, S.A. (2004). Induced systemic resistance and promotion of plant growth by *Bacillus* spp. Phytopathology **94,** 1259-1266.

Knoth, C., Ringler, J., Dangl, J.L., and Eulgem, T. (2007). Arabidopsis WRKY70 is required for full RPP4-mediated disease resistance and basal defense against *Hyaloperonospora parasitica*. Molecular Plant-Microbe Interactions **20,** 120-128.

Koroney, A.S., Plasson, C., Pawlak, B., Sidikou, R., Driouich, A., Menu-Bouaouiche, L., and Vicre-Gibouin, M. (2016). Root exudate of Solanum tuberosum is enriched in galactose-containing molecules and impacts the growth of Pectobacterium atrosepticum. Annals of Botany.

Krouk, G., Mirowski, P., LeCun, Y., Shasha, D.E., and Coruzzi, G.M. (2010). Predictive network modeling of the high-resolution dynamic plant transcriptome in response to nitrate. Genome Biology **11,** R123.

Krouk, G., Lingeman, J., Colon, A.M., Coruzzi, G.M., and Shasha, D.E. (2013). Gene regulatory networks in plants: learning causality from time and perturbation. Genome Biology **14,** 1.

Kuhn, H., Kwaaitaal, M., Kusch, S., Acevedo-Garcia, J., Wu, H., and Panstruga, R. (2016). Biotrophy at its best: novel findings and unsolved mysteries of the Arabidopsis-powdery mildew pathosystem. Arabidopsis Book **14,** e0184.

Kuramata, M., Masuya, S., Takahashi, Y., Kitagawa, E., Inoue, C., Ishikawa, S., Youssefian, S., and Kusano, T. (2009). Novel cysteine-rich peptides from *Digitaria ciliaris* and *Oryza sativa* enhance tolerance to cadmium by limiting its cellular accumulation. Plant & Cell Physiology **50,** 106-117.

Lakshmanan, V., Kitto, S.L., Caplan, J.L., Hsueh, Y.-H., Kearns, D.B., Wu, Y.-S., and Bais, H.P. (2012). Microbe-associated molecular patterns-triggered root responses mediate beneficial rhizobacterial recruitment in Arabidopsis. Plant Physiology **160,** 1642-1661.

Lavarenne, J., Guyomarc'h, S., Sallaud, C., Gantet, P., and Lucas, M. (2018). The spring of systems biology-driven breeding. Trends in Plant Science.

Lebeis, S.L., Paredes, S.H., Lundberg, D.S., Breakfield, N., Gehring, J., McDonald, M., Malfatti, S., Glavina del Rio, T., Jones, C.D., Tringe, S.G., and Dangl, J.L. (2015). Salicylic acid modulates colonization of the root microbiome by specific bacterial taxa. Science **349,** 860-864.

Lee, I., Blom, U.M., Wang, P.I., Shim, J.E., and Marcotte, E.M. (2011). Prioritizing candidate disease genes by network-based boosting of genome-wide association data. Genome Research **21,** 1109-1121.

Leivar, P., and Quail, P.H. (2011). PIFs: pivotal components in a cellular signaling hub. Trends in Plant Science **16,** 19-28.

Lewis, D.R., Olex, A.L., Lundy, S.R., Turkett, W.H., Fetrow, J.S., and Muday, G.K. (2013). A kinetic analysis of the auxin transcriptome reveals cell wall remodeling proteins that modulate lateral root development in Arabidopsis. Plant Cell, tpc. 113.114868.

Lewis, L.A., Polanski, K., de Torres-Zabala, M., Jayaraman, S., Bowden, L., Moore, J., Penfold, C.A., Jenkins, D.J., Hill, C., Baxter, L., Kulasekaran, S., Truman, W., Littlejohn, G., Prusinska, J., Mead, A., Steinbrenner, J., Hickman, R., Rand, D., Wild, D.L., Ott, S., Buchanan-Wollaston, V., Smirnoff, N., Beynon, J., Denby, K., and Grant, M. (2015). Transcriptional dynamics driving MAMP-triggered immunity and pathogen effector-mediated immunosuppression in Arabidopsis leaves following infection with *Pseudomonas syringae* pv *tomato* DC3000. Plant Cell **27,** 3038–3064.

Li, J., Brader, G., and Palva, E.T. (2004). The WRKY70 transcription factor: a node of convergence for jasmonate-mediated and salicylate-mediated signals in plant defense. Plant Cell **16,** 319–331.

Li, L., Stoeckert, C.J.J., and Roos, D.S. (2003). OrthoMCL: identification of ortholog groups for eukaryotic genomes. Genome Research **13,** 2178-2189.

Liu, L., Sonbol, F.M., Huot, B., Gu, Y., Withers, J., Mwimba, M., Yao, J., He, S.Y., and Dong, X. (2016). Salicylic acid receptors activate jasmonic acid signalling through a non-canonical pathway to promote effector-triggered immunity. Nature Communications **7,** 13099.

Long, T.A., Rady, S.M., and Benfey, P.N. (2008). Systems approaches to identifying gene regulatory networks in plants. Annual Review of Cell and Developmental Biology **24,** 81-103.

Lorenzo, O., and Solano, R. (2005). Molecular players regulating the jasmonate signalling network. Current Opinion in Plant Biology **8,** 532-540.

Lorenzo, O., Piqueras, R., Sánchez-Serrano, J.J., and Solano, R. (2003). ETHYLENE RESPONSE FACTOR1 integrates signals from ethylene and jasmonate pathways in plant defense. Plant Cell **15,** 165–178.

Lorenzo, O., Chico, J.M., Sanchez-Serrano, J.J., and Solano, R. (2004). *JASMONATE-INSENSITIVE1* encodes a MYC transcription factor essential to discriminate between different jasmonate-regulated defense responses in Arabidopsis. Plant Cell **16,** 1938–1950.

Love, M.I., Huber, W., and Anders, S. (2014). Moderated estimation of fold change and dispersion for RNA-seq data with DESeq2. Genome Biology **15,** 550.

Lozano-Duran, R., and Zipfel, C. (2015). Trade-off between growth and immunity: role of brassinosteroids. Trends in Plant Science **20,** 12-19.

Luna, E., Pastor, V., Robert, J., Flors, V., Mauch-Mani, B., and Ton, J. (2011). Callose deposition: a multifaceted plant defense response. Molecular plant-microbe interactions **24,** 183-193.

Luschnig, C., and Vert, G. (2014). The dynamics of plant plasma membrane proteins: PINs and beyond. Development **141,** 2924-2938.

MacNeil, L., and Walhout, A.J.M. (2011). Gene regulatory networks and the role of robustness and stochasticity in the control of gene expression. Genome Research **21,** 645-657.

Marcel, S., Sawers, R., Oakeley, E., Angliker, H., and Paszkowski, U. (2010). Tissue-adapted invasion strategies of the rice blast fungus *Magnaporthe oryzae.* Plant Cell **22,** 3177-3187.

Margolin, A.A., Nemenman, I., Basso, K., Wiggins, C., Stolovitzky, G., Dalla Favera, R., and Califano, A. (2006). ARACNE: an algorithm for the reconstruction of gene regulatory networks in a mammalian cellular context. BMC bioinformatics **7,** S7.

Martín-Trillo, M., and Cubas, P. (2010). TCP genes: a family snapshot ten years later. Trends in Plant Science **15,** 31-39.

Martinez-Medina, A., Flors, V., Heil, M., Mauch-Mani, B., Pieterse, C.M.J., Pozo, M.J., Ton, J., Van Dam, N.M., and Conrath, U. (2016). Recognizing plant defense priming. Trends in Plant Science **21,** 818-822.

Martinez, C., Pons, E., Prats, G., and Leon, J. (2004). Salicylic acid regulates flowering time and links defence responses and reproductive development. Plant Journal **37,** 209-217.

McClerklin, S.A., Lee, S.G., Harper, C.P., Nwumeh, R., Jez, J.M., and Kunkel, B.N. (2018). Indole-3-acetaldehyde dehydrogenase-dependent auxin synthesis contributes to virulence of *Pseudomonas syringae* strain DC3000. PLoS Pathogens **14,** e1006811.

McLellan, H., Boevink, P.C., Armstrong, M.R., Pritchard, L., Gomez, S., Morales, J., Whisson, S.C., Beynon, J.L., and Birch, P.R. (2013). An RxLR effector from *Phytophthora infestans* prevents re-localisation of two plant NAC transcription factors from the endoplasmic reticulum to the nucleus. PLoS Pathogens **9,** e1003670.

Mendes, R., Garbeva, P., and Raaijmakers, J.M. (2013). The rhizosphere microbiome: significance of plant beneficial, plant pathogenic, and human pathogenic microorganisms. FEMS Microbiology Reviews **37,** 634-663.

Millet, Y.A., Danna, C.H., Clay, N.K., Songnuan, W., Simon, M.D., Werck-Reichhart, D., and Ausubel, F.M. (2010). Innate immune responses activated in Arabidopsis roots by microbe-associated molecular patterns. Plant Cell **22,** 973-990.

Mine, A., Seyfferth, C., Kracher, B., Berens, M.L., Becker, D., and Tsuda, K. (2018). The defense phytohormone signaling network enables rapid, high-amplitude transcriptional reprogramming during effector-triggered immunity. Plant Cell **30,** 1199-1219.

Mine, A., Nobori, T., Salazar-Rondon, M.C., Winkelmuller, T.M., Anver, S., Becker, D., and Tsuda, K. (2017a). An incoherent feed-forward loop mediates robustness and tunability in a plant immune network. EMBO Reports **18,** 464-476.

Mine, A., Berens, M.L., Nobori, T., Anver, S., Fukumoto, K., Winkelmuller, T.M., Takeda, A., Becker, D., and Tsuda, K. (2017b). Pathogen exploitation of an abscisic acid- and jasmonate-inducible MAPK phosphatase and its interception by Arabidopsis immunity. Proceedings of the National Academy of Sciences of the United States of America **114,** 7456-7461.

Mir, R., Hernandez, M.L., Abou-Mansour, E., Martinez-Rivas, J.M., Mauch, F., Metraux, J.P., and Leon, J. (2013). Pathogen and Circadian Controlled 1 (PCC1) regulates polar lipid content, ABA-related responses, and pathogen defence in Arabidopsis thaliana. Journal of Experimental Botany **64,** 3385-3395.

Mur, L.A.J., Kenton, P., Atzorn, R., Miersch, O., and Wasternack, C. (2006). The outcomes of concentration-specific interactions between salicylate and jasmonate signaling include synergy, antagonism, and oxidative stress leading to cell death. Plant Physiology **140,** 249-262.

Nakashima, K., Takasaki, H., Mizoi, J., Shinozaki, K., and Yamaguchi-Shinozaki, K. (2012). NAC transcription factors in plant abiotic stress responses. Biochimica et Biophysica Acta (BBA)-Gene Regulatory Mechanisms **1819,** 97-103.

Nakata, M., Mitsuda, N., Herde, M., Koo, A.J.K., Moreno, J.E., Suzuki, K., Howe, G.A., and Ohme-Takagi, M. (2013). A bHLH-type transcription factor, ABA-INDUCIBLE BHLH-TYPE TRANSCRIPTION FACTOR/JA-ASSOCIATED MYC2-LIKE1, acts as a repressor to negatively regulate jasmonate signaling in Arabidopsis. Plant Cell **25,** 1641–1656.

Narsai, R., Gouil, Q., Secco, D., Srivastava, A., Karpievitch, Y.V., Liew, L.C., Lister, R., Lewsey, M.G., and Whelan, J. (2017). Extensive transcriptomic and epigenomic remodelling occurs during Arabidopsis thaliana germination. Genome Biology **18,** 172.

Nickstadt, A., Thomma, B.P.H.J., Feussner, I., Kangasjarvi, J., Zeier, J., Loeffler, C., Scheel, D., and Berger, S. (2004). The jasmonate-insensitive mutant *jin1* shows increased resistance to biotrophic as well as necrotrophic pathogens. Molecular Plant Pathology **5,** 425-434.

Niehaus, T.D., Thamm, A.M., de Crecy-Lagard, V., and Hanson, A.D. (2015). Proteins of unknown biochemical function: a persistent problem and a roadmap to help overcome it. Plant Physiology **169,** 1436-1442.

Nobori, T., Mine, A., and Tsuda, K. (2018). Molecular networks in plant-pathogen holobiont. FEBS Letters **592,** 1937-1953.

Nozue, K., Devisetty, U.K., Lekkala, S., Mueller-Moulé, P., Bak, A., Casteel, C.L., and Maloof, J.N. (2018). Network analysis reveals a role for salicylic acid pathway components in shade avoidance. Plant Physiology **178,** 1720-1732.

Nuruzzaman, M., Sharoni, A.M., and Kikuchi, S. (2013). Roles of NAC transcription factors in the regulation of biotic and abiotic stress responses in plants. Frontiers in Microbiology **4,** 248.

O'Malley, R.C., Huang, S.C., Song, L., Lewsey, M.G., Bartlett, A., Nery, J.R., Galli, M., Gallavotti, A., and Ecker, J.R. (2016). Cistrome and epicistrome features shape the regulatory DNA landscape. Cell **165,** 1280-1292.

O'Malley, R.C., Huang, S.-s.C., Song, L., Lewsey, M.G., Bartlett, A., Nery, J.R., Galli, M., Gallavotti, A., and Ecker, J.R. (2016). Cistrome and epicistrome features shape the regulatory DNA landscape. Cell **165,** 1280-1292.

Obayashi, T., Aoki, Y., Tadaka, S., Kagaya, Y., and Kinoshita, K. (2017). ATTED-II in 2018: a plant coexpression database based on investigation of the statistical property of the mutual rank index. Plant and Cell Physiology **59,** e3-e3.

Okazaki, S., Kaneko, T., Sato, S., and Saeki, K. (2013). Hijacking of leguminous nodulation signaling by the rhizobial type III secretion system. Proceedings of the National Academy of Sciences of the United States of America **110,** 17131-17136.

Olsen, A.N., Ernst, H.A., Leggio, L.L., and Skriver, K. (2005). NAC transcription factors: structurally distinct, functionally diverse. Trends in Plant Science **10,** 79-87.

Oñate-Sánchez, L., and Vicente-Carbajosa, J. (2008). DNA-free RNA isolation protocols for *Arabidopsis thaliana,* including seeds and siliques. BMC Research Notes **1,** 93.

Ooka, H., Satoh, K., Doi, K., Nagata, T., Otomo, Y., Murakami, K., Matsubara, K., Osato, N., Kawai, J., Carninci, P., Hayashizaki, Y., Suzuki, K., Kojima, K., Takahara, Y., Yamamoto, K., and Kikuchi, S. (2003). Comprehensive analysis of NAC family genes in *Oryza sativa* and *Arabidopsis thaliana*. DNA Research **10,** 239-247.

Pandey, S.P., and Somssich, I.E. (2009). The role of WRKY transcription factors in plant immunity. Plant Physiology **150,** 1648-1655.

Pangesti, N., Pineda, A., Dicke, M., and van Loon, J.J.A. (2015). Variation in plant-mediated interactions between rhizobacteria and caterpillars: potential role of soil composition. Plant Biology **17,** 474–483.

Papadopoulou, G.V., Maedicke, A., Grosser, K., van Dam, N.M., and Martinez-Medina, A. (2018). Defence signalling marker gene responses to hormonal elicitation differ between roots and shoots. AoB Plants **10,** ply031.

Pauwels, L., Morreel, K., De Witte, E., Lammertyn, F., Van Montagu, M., Boerjan, W., Inzé, D., and Goossens, A. (2008). Mapping methyl jasmonate-mediated transcriptional reprogramming of metabolism and cell cycle progression in cultured Arabidopsis cells. Proceedings of the National Academy of Sciences of the United States of America **105,** 1380–1385.

Penfold, C.A., and Wild, D.L. (2011). How to infer gene networks from expression profiles, revisited. Interface Focus **1,** 857-870.

Pieterse, C.M., Zamioudis, C., Berendsen, R.L., Weller, D.M., Van Wees, S.C., and Bakker, P.A. (2014). Induced systemic resistance by beneficial microbes. Annual Review of Phytopathology **52,** 347-375.

Pieterse, C.M.J., Leon-Reyes, A., Van der Ent, S., and Van Wees, S.C.M. (2009). Networking by small-molecule hormones in plant immunity. Nature Chemical Biology **5,** 308-316.

Pieterse, C.M.J., Van der Does, D., Zamioudis, C., Leon-Reyes, A., and Van Wees, S.C.M. (2012). Hormonal modulation of plant immunity. Annual Review of Cell and Developmental Biology **28,** 489–521.

Pineda, A., Dicke, M., Pieterse, C.M.J., and Pozo, M.J. (2013). Beneficial microbes in a changing environment: are they always helping plants to deal with insects? Functional Ecology **27,** 574-586.

Plancot, B., Santaella, C., Jaber, R., Kiefer-Meyer, M.C., Follet-Gueye, M.L., Leprince, J., Gattin, I., Souc, C., Driouich, A., and Vicre-Gibouin, M. (2013). Deciphering the responses of root border-like cells of Arabidopsis and flax to pathogen-derived elicitors. Plant Physiology **163,** 1584-1597.

Plett, J.M., Daguerre, Y., Wittulsky, S., Vayssieres, A., Deveau, A., Melton, S.J., Kohler, A., Morrell-Falvey, J.L., Brun, A., Veneault-Fourrey, C., and Martin, F. (2014). Effector MiSSP7 of the mutualistic fungus Laccaria bicolor stabilizes the Populus JAZ6 protein and represses jasmonic acid (JA) responsive genes. Proceedings of the National Academy of Sciences of the United States of America **111,** 8299-8304.

Poncini, L., Wyrsch, I., Denervaud Tendon, V., Vorley, T., Boller, T., Geldner, N., Metraux, J.P., and Lehmann, S. (2017). In roots of *Arabidopsis thaliana,* the damage-associated molecular pattern AtPep1 is a stronger elicitor of immune signalling than flg22 or the chitin heptamer. PLoS One **12,** e0185808.

Pozo, M.J., and Azcon-Aguilar, C. (2007). Unraveling mycorrhiza-induced resistance. Current Opinion in Plant Biology **10,** 393-398.

Pré, M., Atallah, M., Champion, A., De Vos, M., Pieterse, C.M.J., and Memelink, J. (2008). The AP2/ERF domain transcription factor ORA59 integrates jasmonic acid and ethylene signals in plant defense. Plant Physiology **147,** 1347–1357.

Pruneda-Paz, J.L., Breton, G., Para, A., and Kay, S.A. (2009). A functional genomics approach reveals CHE as a component of the Arabidopsis circadian clock. Science **323,** 1481-1485.

Pruneda-Paz, J.L., Breton, G., Nagel, D.H., Kang, S.E., Bonaldi, K., Doherty, C.J., Ravelo, S., Galli, M., Ecker, J.R., and Kay, S.A. (2014). A genome-scale resource for the functional characterization of Arabidopsis transcription factors. Cell Reports **8,** 621-631.

Raaijmakers, J.M., and Mazzola, M. (2016). Soil immune responses Soil microbiomes may be harnessed for plant health. Science **352,** 1392-1393.

Rivas-San Vicente, M., and Plasencia, J. (2011). Salicylic acid beyond defence: its role in plant growth and development. Journal of Experimental Botany **62,** 3321-3338.

Robert-Seilaniantz, A., Grant, M., and Jones, J.D. (2011). Hormone crosstalk in plant disease and defense: more than just jasmonate-salicylate antagonism. Annual Review of Phytopathology **49,** 317-343.

Rodriguez, P.A., Rothballer, M., Chowdhury, S.P., Nussbaumer, T., Gutjahr, C., and Falter-Braun, P. (2019). Systems biology of plant-microbiome interactions. Molecular Plant **12,** 804-821.

Rutter, M.T., Cross, K.V., and Van Woert, P.A. (2012). Birth, death and subfunctionalization in the Arabidopsis genome. Trends in Plant Science **17,** 204-212.

Saibo, N.J., Lourenco, T., and Oliveira, M.M. (2009). Transcription factors and regulation of photosynthetic and related metabolism under environmental stresses. Annals of Botany **103,** 609-623.

Sasaki-Sekimoto, Y., Jikumaru, Y., Obayashi, T., Saito, H., Masuda, S., Kamiya, Y., Ohta, H., and Shirasu, K. (2013). Basic Helix-Loop-Helix transcription factors JA-ASSOCIATED MYC2-LIKE 1 (JAM1), JAM2 and JAM3 are negative regulators of jasmonate responses in Arabidopsis. Plant Physiology **163,** 291–234.

Sauerbrunn, N., and Schlaich, N.L. (2004). PCC1: a merging point for pathogen defence and circadian signalling in Arabidopsis. Planta **218,** 552-561.

Schiestl, R.H., and Gietz, R.D. (1989). High efficiency transformation of intact yeast cells using single stranded nucleic acids as a carrier. Current Genetics **16,** 339-346.

Schulz, M.H., Devanny, W.E., Gitter, A., Zhong, S., Ernst, J., and Bar-Joseph, Z. (2012). DREM 2.0: Improved reconstruction of dynamic regulatory networks from time-series expression data. BMC Systems Biology **6,** 104.

Schweizer, F., Bodenhausen, N., Lassueur, S., Masclaux, F.G., and Reymond, P. (2013). Differential contribution of transcription factors to *Arabidopsis thaliana* defense against *Spodoptera littoralis*. Frontiers in Plant Science **4**.

Segarra, S., Mir, R., Martinez, C., and Leon, J. (2010). Genome-wide analyses of the transcriptomes of salicylic acid-deficient versus wild-type plants uncover Pathogen and Circadian Controlled 1 (PCC1) as a regulator of flowering time in Arabidopsis. Plant Cell & Enviroment **33,** 11-22.

Sels, J., Mathys, J., De Coninck, B.M., Cammue, B.P., and De Bolle, M.F. (2008). Plant pathogenesis-related (PR) proteins: a focus on PR peptides. Plant Physiology and Biochemistry **46,** 941-950.

Shannon, P., Markiel, A., Ozier, O., Baliga, N.S., Wang, J.T., Ramage, D., Amin, N., Schwikowski, B., and Ideker, T. (2003). Cytoscape: A software environment for integrated models of biomolecular interaction networks. Genome Research **13,** 2498-2504.

Sheard, L.B., Tan, X., Mao, H.B., Withers, J., Ben-Nissan, G., Hinds, T.R., Kobayashi, Y., Hsu, F.F., Sharon, M., Browse, J., He, S.Y., Rizo, J., Howe, G.A., and Zheng, N. (2010). Jasmonate perception by inositol-phosphate-potentiated COI1-JAZ co-receptor. Nature **468,** 400–405.

Shen, Q., Liu, Y., and Naqvi, N.I. (2018). Fungal effectors at the crossroads of phytohormone signaling. Current Opinion in Microbiology **46,** 1-6.

Shimada, T.L., Shimada, T., and Hara-Nishimura, I. (2010). A rapid and non-destructive screenable marker, FAST, for identifying transformed seeds of Arabidopsis thaliana. Plant Journal **61,** 519-528.

Shoresh, M., Harman, G.E., and Mastouri, F. (2010). Induced systemic resistance and plant responses to fungal biocontrol agents. Annual Review of Phytopathology **48,** 21-43.

Smakowska-Luzan, E., Mott, G.A., Parys, K., Stegmann, M., Howton, T.C., Layeghifard, M., Neuhold, J., Lehner, A., Kong, J., Grunwald, K., Weinberger, N., Satbhai, S.B., Mayer, D., Busch, W., Madalinski, M., Stolt-Bergner, P., Provart, N.J., Mukhtar, M.S., Zipfel, C., Desveaux, D., Guttman, D.S., and Belkhadir, Y. (2018). An extracellular network of Arabidopsis leucine-rich repeat receptor kinases. Nature **553,** 342-346.

Song, L., Huang, S.S.C., Wise, A., Castanon, R., Nery, J.R., Chen, H.Y., Watanabe, M., Thomas, J., Bar-Joseph, Z., and Ecker, J.R. (2016). A transcription factor hierarchy defines an environmental stress response network. Science **354,** aag1550.

Song, S., Qi, T., Fan, M., Zhang, X., Gao, H., Huang, H., Wu, D., Guo, H., and Xie, D. (2013). The bHLH subgroup IIId factors negatively regulate jasmonate-mediated plant defense and development. PLoS Genetics **9,** e1003653.

Spoel, S.H., and Dong, X. (2008). Making sense of hormone crosstalk during plant immune responses. Cell Host & Microbe **3,** 348-351.

Spoel, S.H., and Dong, X. (2012). How do plants achieve immunity? Defence without specialized immune cells. Nature Reviews Immunology **12,** 89-100.

Spoel, S.H., Johnson, J.S., and Dong, X. (2007). Regulation of tradeoffs between plant defenses against pathogens with different lifestyles. Proceedings of the National Academy of Sciences of the United States of America **104,** 18842-18847.

Spoel, S.H., Koornneef, A., Claessens, S.M.C., Korzelius, J.P., Van Pelt, J.A., Mueller, M.J., Buchala, A.J., Métraux, J.-P., Brown, R., Kazan, K., Van Loon, L.C., Dong, X., and Pieterse, C.M.J. (2003). NPR1 modulates cross-talk between salicylate- and jasmonate-dependent defense pathways through a novel function in the cytosol. Plant Cell **15,** 760–770.

Stein, E., Molitor, A., Kogel, K.H., and Waller, F. (2008). Systemic resistance in Arabidopsis conferred by the mycorrhizal fungus *Piriformospora indica* requires jasmonic acid signaling and the cytoplasmic function of NPR1. Plant and Cell Physiology **49,** 1747-1751.

Stringlis, I.A., de Jonge, R., and Pieterse, C.M.J. (2019). The age of coumarins in plant-microbe interactions: an ironic love story. Plant Cell Physiology **60 (7)**, 1405-1419.

Stringlis, I.A., Proietti, S., Hickman, R., Van Verk, M.C., Zamioudis, C., and Pieterse, C.M.J. (2018). Root transcriptional dynamics induced by beneficial rhizobacteria and microbial immune elicitors reveal signatures of adaptation to mutualists. Plant Journal **93,** 166-180.

Sullivan, A.M., Arsovski, A.A., Lempe, J., Bubb, K.L., Weirauch, M.T., Sabo, P.J., Sandstrom, R., Thurman, R.E., Neph, S., Reynolds, A.P., Stergachis, A.B., Vernot, B., Johnson, A.K., Haugen, E., Sullivan, S.T., Thompson, A., Neri, F.V., 3rd, Weaver, M., Diegel, M., Mnaimneh, S., Yang, A., Hughes, T.R., Nemhauser, J.L., Queitsch, C., and Stamatoyannopoulos, J.A. (2014). Mapping and dynamics of regulatory DNA and transcription factor networks in *A. thaliana*. Cell Reports **8,** 2015-2030.

Sun, Y., Detchemendy, T.W., Pajerowska-Mukhtar, K.M., and Mukhtar, M.S. (2018). NPR1 in JazzSet with Pathogen Effectors. Trends in Plant Science **23,** 469-472.

Swinnen, G., Goossens, A., and Pauwels, L. (2016). Lessons from domestication: Targeting *cis*-regulatory elements for crop improvement. Trends in Plant Science **21,** 506-515.

Tada, Y., Spoel, S.H., Pajerowska-Mukhtar, K., Mou, Z., Song, J., Wang, C., Zuo, J., and Dong, X. (2008). Plant immunity requires conformational changes of NPR1 via S-nitrosylation and thioredoxins. Science **321,** 952–956.

Tan, S.T., Dai, C., Liu, H.T., and Xue, H.W. (2013). Arabidopsis casein kinase1 proteins CK1.3 and CK1.4 phosphorylate cryptochrome2 to regulate blue light signaling. Plant Cell **25,** 2618-2632.

Tatusov, R.L., Koonin, E.V., and Lipman, D.J. (1997). A genomic perspective on protein families. Science **278,** 631-637.

Thines, B., Katsir, L., Melotto, M., Niu, Y., Mandaokar, A., Liu, G.H., Nomura, K., He, S.Y., Howe, G.A., and Browse, J. (2007). JAZ repressor proteins are targets of the SCF^{COI1} complex during jasmonate signalling. Nature **448,** 661–665.

Tompa, M., Li, N., Bailey, T.L., Church, G.M., De Moor, B., Eskin, E., Favorov, A.V., Frith, M.C., Fu, Y.T., Kent, W.J., Makeev, V.J., Mironov, A.A., Noble, W.S., Pavesi, G., Pesole, G., Regnier, M., Simonis, N., Sinha, S., Thijs, G., van Helden, J., Vandenbogaert, M., Weng, Z.P., Workman, C., Ye, C., and Zhu, Z. (2005). Assessing computational tools for the discovery of transcription factor binding sites. Nature Biotechnology **23,** 137-144.

Torres-Zabala, M., Truman, W., Bennett, M.H., Lafforgue, G., Mansfield, J.W., Rodriguez Egea, P., Bogre, L., and Grant, M. (2007). *Pseudomonas syringae* pv. *tomato* hijacks the Arabidopsis abscisic acid signalling pathway to cause disease. EMBO Journal **26,** 1434-1443.

Tran, T.M., MacIntyre, A., Hawes, M., and Allen, C. (2016). Escaping underground nets: extracellular DNases degrade plant extracellular traps and contribute to virulence of the plant pathogenic bacterium *Ralstonia solanacearum*. PLoS Pathogens **12,** e1005686.

Trapnell, C., Pachter, L., and Salzberg, S.L. (2009). TopHat: discovering splice junctions with RNA-Seq. Bioinformatics **25,** 1105–1111.

Tsuda, K., and Somssich, I.E. (2015). Transcriptional networks in plant immunity. New Phytologist **206,** 932-947.

Tsuda, K., Sato, M., Stoddard, T., Glazebrook, J., and Katagiri, F. (2009). Network properties of robust immunity in plants. PLoS Genetics **5,** e1000772.

Van Bel, M., Diels, T., Vancaester, E., Kreft, L., Botzki, A., Van de Peer, Y., Coppens, F., and Vandepoele, K. (2018). PLAZA 4.0: an integrative resource for functional, evolutionary and comparative plant genomics. Nucleic Acids Research **46,** D1190-D1196.

Van Damme, M., Huibers, R.P., Elberse, J., and Van den Ackerveken, G. (2008). Arabidopsis DMR6 encodes a putative 2OG-Fe(II) oxygenase that is defense-associated but required for susceptibility to downy mildew. Plant Journal **54,** 785-793.

Van der Does, D., Leon-Reyes, A., Koornneef, A., Van Verk, M.C., Rodenburg, N., Pauwels, L., Goossens, A., Körbes, A.P., Memelink, J., Ritsema, T., Van Wees, S.C.M., and Pieterse, C.M.J. (2013). Salicylic acid suppresses jasmonic acid signaling downstream of SCF^{COI1}-JAZ by targeting GCC promoter motifs via transcription factor ORA59. Plant Cell **25,** 744–761.

Van Gelderen, K., Kang, C., Paalman, R., Keuskamp, D., Hayes, S., and Pierik, R. (2018). Far-red light detection in the shoot regulates lateral root development through the HY5 transcription factor. Plant Cell **30,** 101-116.

Van Loon, L.C., Rep, M., and Pieterse, C.M.J. (2006). Significance of inducible defense-related proteins in infected plants. Annual Review of Phytopathology **44,** 135-162.

Van Verk, M.C., Hickman, R., Pieterse, C.M.J., and Van Wees, S.C.M. (2013). RNA-Seq: revelation of the messengers. Trends in Plant Science **18,** 175–179.

Van Wees, S.C.M., Van Pelt, J.A., Bakker, P.A.H.M., and Pieterse, C.M.J. (2013). Bioassays for assessing jasmonate-dependent defenses triggered by pathogens, herbivorous insects, or beneficial rhizobacteria. Methods in Molecular Biology **1011,** 35–49.

Van Wees, S.C.M., Luijendijk, M., Smoorenburg, I., Van Loon, L.C., and Pieterse, C.M.J. (1999). Rhizobacteria-mediated induced systemic resistance (ISR) in Arabidopsis is not associated with a direct effect on expression of known defense-related genes but stimulates the expression of the jasmonate-inducible gene Atvsp upon challenge. Plant Molecular Biology **41:** 537.

Vandenkoornhuyse, P., Quaiser, A., Duhamel, M., Le Van, A., and Dufresne, A. (2015). The importance of the microbiome of the plant holobiont. New Phytologist **206,** 1196-1206.

Vandepoele, K., Quimbaya, M., Casneuf, T., De Veylder, L., and Van de Peer, Y. (2009). Unraveling transcriptional control in Arabidopsis using cis-regulatory elements and coexpression networks. Plant Physiology **150,** 535-546.

Varala, K., Marshall-Colón, A., Cirrone, J., Brooks, M.D., Pasquino, A.V., Léran, S., Mittal, S., Rock, T.M., Edwards, M.B., and Kim, G.J. (2018). Temporal transcriptional logic of dynamic regulatory networks underlying nitrogen signaling and use in plants. Proceedings of the National Academy of Sciences of the United States of America **115,** 6494-6499.

Venancio, T.M., and Aravind, L. (2010). CYSTM, a novel cysteine-rich transmembrane module with a role in stress tolerance across eukaryotes. Bioinformatics **26,** 149-152.

Verhage, A., van Wees, S.C.M., and Pieterse, C.M.J. (2010). Plant immunity: It's the hormones talking, but what do they say? Plant Physiology **154,** 536-540.

Verhage, A., Vlaardingerbroek, I., Raaymakers, C., Van Dam, N., Dicke, M., Van Wees, S.C.M., and Pieterse, C.M.J. (2011). Rewiring of the jasmonate signaling pathway in Arabidopsis during insect herbivory. Frontiers in Plant Science **2,** 47.

Vlot, A.C., Dempsey, D.A., and Klessig, D.F. (2009). Salicylic acid, a multifaceted hormone to combat disease. Annual Review of Phytopathology **47,** 177–206.

Vos, I.A., Pieterse, C.M.J., and Van Wees, S.C.M. (2013a). Costs and benefits of hormone-regulated plant defences. Plant Pathology **62,** 43–55.

Vos, I.A., Moritz, L., Pieterse, C.M.J., and Van Wees, S.C.M. (2015). Impact of hormonal crosstalk on plant resistance and fitness under multi-attacker conditions. Frontiers in Plant Science **6,** 639.

Vos, I.A., Verhage, A., Schuurink, R.C., Watt, L.G., Pieterse, C.M.J., and Van Wees, S.C.M. (2013b). Onset of herbivore-induced resistance in systemic tissue primed for jasmonate-dependent defenses is activated by abscisic acid. Frontiers in Plant Science **4,** 539.

Walker, L., Boddington, C., Jenkins, D., Wang, Y., Grønlund, J.T., Hulsmans, J., Kumar, S., Patel, D., Moore, J.D., and Carter, A. (2017). Changes in gene expression in space and time orchestrate environmentally mediated shaping of root architecture. Plant Cell **29,** 2393-2412.

Wang, C., Liu, Y., Li, S.S., and Han, G.Z. (2015a). Insights into the origin and evolution of the plant hormone signaling machinery. Plant Physiology **167,** 872-886.

Wang, D., Amornsiripanitch, N., and Dong, X. (2006). A genomic approach to identify regulatory nodes in the transcriptional network of systemic acquired resistance in plants. PLoS Pathogens **2,** e123.

Wang, D., Weaver, N.D., Kesarwani, M., and Dong, X. (2005). Induction of protein secretory pathway is required for systemic acquired resistance. Science **308,** 1036-1040.

Wang, D., Pajerowska-Mukhtar, K., Hendrickson Culler, A., and Dong, X. (2007). Salicylic acid inhibits pathogen growth in plants through repression of the auxin signaling pathway. Current Biology **17,** 1784–1790.

Wang, F., Lin, R., Feng, J., Chen, W., Qiu, D., and Xu, S. (2015b). TaNAC1 acts as a negative regulator of stripe rust resistance in wheat, enhances susceptibility to *Pseudomonas syringae*, and promotes lateral root development in transgenic *Arabidopsis thaliana*. Frontiers in Plant Science **6,** 108.

Wang, S., Durrant, W.E., Song, J., Spivey, N.W., and Dong, X. (2010). Arabidopsis BRCA2 and RAD51 proteins are specifically involved in defense gene transcription during plant immune responses. Proceedings of the National Academy of Sciences of the United States of America **107,** 22716–22721.

Wang, S., Gu, Y., Zebell, S.G., Anderson, L.K., Wang, W., Mohan, R., and Dong, X. (2014). A noncanonical role for the CKI-RB-E2F cell-cycle signaling pathway in plant effector-triggered immunity. Cell host & microbe **16,** 787-794.

Wang, W., Yuan, Y., Yang, C., Geng, S., Sun, Q., Long, L., Cai, C., Chu, Z., Liu, X., Wang, G., Du, X., Miao, C., Zhang, X., and Cai, Y. (2016). Characterization, expression, and functional analysis of a novel *NAC* gene associated with resistance to verticillium wilt and abiotic stress in cotton. G3: Genes, Genomes, Genetics **6,** 3951-3961.

Wang, X., Gao, J., Zhu, Z., Dong, X., Wang, X., Ren, G., Zhou, X., and Kuai, B. (2015c). TCP transcription factors are critical for the coordinated regulation of isochorismate synthase 1 expression in Arabidopsis thaliana. Plant Journal **82,** 151-162.

War, A.R., Paulraj, M.G., Ahmad, T., Buhroo, A.A., Hussain, B., Ignacimuthu, S., and Sharma, H.C. (2012). Mechanisms of plant defense against insect herbivores. Plant Signaling & Behavior **7,** 1306-1320.

Wasternack, C. (2015). How jasmonates earned their laurels: past and present. Journal of Plant Growth Regulation **34,** 761-794.

Wasternack, C., and Hause, B. (2013). Jasmonates: biosynthesis, perception, signal transduction and action in plant stress response, growth and development. An update to the 2007 review in Annals of Botany. Annals of Botany **111,** 1021–1058.

Wasternack, C., and Song, S. (2017). Jasmonates: biosynthesis, metabolism, and signaling by proteins activating and repressing transcription. Journal of Experimental Botany **68,** 1303-1321.

Wasternack, C., and Feussner, I. (2018). The oxylipin pathways: biochemistry and function. Annual Review of Plant Biology 2018 69:1, 363-386.

Weirauch, M.T., Yang, A., Albu, M., Cote, A.G., Montenegro-Montero, A., Drewe, P., Najafabadi, H.S., Lambert, S.A., Mann, I., Cook, K., Zheng, H., Goity, A., Van Bakel, H., Lozano, J.C., Galli, M., Lewsey, M.G., Huang, E., Mukherjee, T., Chen, X., Reece-Hoyes, J.S., Govindarajan, S., Shaulsky, G., Walhout, A.J.M., Bouget, F.Y., Ratsch, G., Larrondo, L.F., Ecker, J.R., and Hughes, T.R. (2014). Determination and inference of eukaryotic transcription factor sequence specificity. Cell **158,** 1431–1443.

Windram, O., and Denby, K.J. (2015). Modelling signaling networks underlying plant defence. Current Opinion in Plant Biology **27,** 165-171.

Windram, O., Penfold, C.A., and Denby, K.J. (2014). Network modeling to understand plant immunity. Annual Review of Phytopathology **52,** 93-111.

Windram, O., Madhou, P., McHattie, S., Hill, C., Hickman, R., Cooke, E., Jenkins, D.J., Penfold, C.A., Baxter, L., Breeze, E., Kiddle, S.J., Rhodes, J., Atwell, S., Kliebenstein, D.J., Kim, Y.S., Stegle, O., Borgwardt, K., Zhang, C.J., Tabrett, A., Legaie, R., Moore, J., Finkenstadt, B., Wild, D.L., Mead, A., Rand, D., Beynon, J., Ott, S., Buchanan-Wollaston, V., and Denby, K.J. (2012). Arabidopsis defense against *Botrytis cinerea*: Chronology and regulation deciphered by high-resolution temporal transcriptomic analysis. Plant Cell **24,** 3530-3557.

Winter, D., Vinegar, B., Nahal, H., Ammar, R., Wilson, G.V., and Provart, N.J. (2007). An "Electronic Fluorescent Pictograph" browser for exploring and analyzing large-scale biological data sets. PloS one **2,** e718.

Wu, Y., Zhang, D., Chu, J.Y., Boyle, P., Wang, Y., Brindle, I.D., De Luca, V., and Després, C. (2012). The Arabidopsis NPR1 protein is a receptor for the plant defense hormone salicylic acid. Cell Reports **1,** 639–647.

Wyrsch, I., Dominguez-Ferreras, A., Geldner, N., and Boller, T. (2015). Tissue-specific *FLAGELLIN-SENSING 2* (*FLS2*) expression in roots restores immune responses in Arabidopsis *fls2* mutants. New Phytologist **206,** 774-784.

Xie, D.X., Feys, B.F., James, S., Nieto-Rostro, M., and Turner, J.G. (1998). COI1: An Arabidopsis gene required for jasmonate-regulated defense and fertility. Science **280,** 1091–1094.

Xin, X.F., Kvitko, B., and He, S.Y. (2018). *Pseudomonas syringae*: what it takes to be a pathogen. Nature Reviews Microbiology **16,** 316-328.

Xu, Y., Yu, Z., Zhang, S., Wu, C., Yang, G., Yan, K., Zheng, C., and Huang, J. (2019). CYSTM3 negatively regulates salt stress tolerance in Arabidopsis. Plant Molecular Biology **99,** 395-406.

Xu, Y., Yu, Z., Zhang, D., Huang, J., Wu, C., Yang, G., Yan, K., Zhang, S., and Zheng, C. (2018). CYSTM, a novel non-secreted cysteine-rich peptide family, involved in environmental stresses in *Arabidopsis thaliana*. Plant & Cell physiology **59,** 423-438.

Yang, L., Teixeira, P.J., Biswas, S., Finkel, O.M., He, Y., Salas-Gonzalez, I., English, M.E., Epple, P., Mieczkowski, P., and Dangl, J.L. (2017). *Pseudomonas syringae* type III effector HopBB1 promotes host transcriptional repressor degradation to regulate phytohormone responses and virulence. Cell Host & Microbe **21,** 156-168.

Yosef, N., and Regev, A. (2011). Impulse control: temporal dynamics in gene transcription. Cell **144,** 886-896.

Yoshii, M., Yamazaki, M., Rakwal, R., Kishi-Kaboshi, M., Miyao, A., and Hirochika, H. (2010). The NAC transcription factor RIM1 of rice is a new regulator of jasmonate signaling. Plant Journal **61,** 804-815.

Yuan, J., Zhao, J., Wen, T., Zhao, M., Li, R., Goossens, P., Huang, Q., Bai, Y., Vivanco, J.M., Kowalchuk, G.A., Berendsen, R.L., and Shen, Q. (2018). Root exudates drive the soil-borne legacy of aboveground pathogen infection. Microbiome **6,** 156.

Zamioudis, C., and Pieterse, C.M.J. (2012). Modulation of host immunity by beneficial microbes. Molecular Plant-Microbe Interactions **25,** 139-150.

Zander, M., Thurow, C., and Gatz, C. (2014). TGA transcription factors activate the salicylic acid-suppressible branch of the ethylene-induced defense program by regulating *ORA59* expression. Plant Physiology **165,** 1671–1683.

Zeilmaker, T., Ludwig, N.R., Elberse, J., Seidl, M.F., Berke, L., Van Doorn, A., Schuurink, R.C., Snel, B., and Van den Ackerveken, G. (2015). DOWNY MILDEW RESISTANT 6 and DMR6-LIKE OXYGENASE 1 are partially redundant but distinct suppressors of immunity in Arabidopsis. Plant Journal **81,** 210–222.

Zhang, F., Yao, J., Ke, J., Zhang, L., Lam, V.Q., Xin, X.F., Zhou, X.E., Chen, J., Brunzelle, J., and Griffin, P.R. (2015a). Structural basis of JAZ repression of MYC transcription factors in jasmonate signalling. Nature **525,** 269-273.

Zhang, L., Zhang, F., Melotto, M., Yao, J., and He, S.Y. (2017a). Jasmonate signaling and manipulation by pathogens and insects. Journal of Experimental Botany **68,** 1371-1385.

Zhang, L., Yao, J., Withers, J., Xin, X.F., Banerjee, R., Fariduddin, Q., Nakamura, Y., Nomura, K., Howe, G.A., Boland, W., Yan, H., and He, S.Y. (2015b). Host target modification as a strategy to counter pathogen hijacking of the jasmonate hormone receptor. Proceedings of the National Academy of Sciences of the United States of America **112,** 14354-14359.

Zhang, W., Corwin, J.A., Copeland, D., Feusier, J., Eshbaugh, R., Chen, F., Atwell, S., and Kliebenstein, D.J. (2017b). Plastic transcriptomes stabilize Immunity to pathogen diversity: the jasmonic acid and salicylic acid networks within the Arabidopsis/Botrytis pathosystem. Plant Cell **29,** 2727-2752.

Zhang, Y., Fan, W., Kinkema, M., Li, X., and Dong, X. (1999). Interaction of NPR1 with basic leucine zipper protein transcription factors that bind sequences required for salicylic acid induction of the *PR-1* gene. Proceedings of the National Academy of Sciences of the United States of America **96,** 6523–6528.

Zheng, X.-Y., Zhou, M., Yoo, H., Pruneda-Paz, J.L., Spivey, N.W., Kay, S.A., and Dong, X. (2015). Spatial and temporal regulation of biosynthesis of the plant immune signal salicylic acid. Proceedings of the National Academy of Sciences of the United States of America **112,** 9166-9173.

Zheng, X.-Y., Spivey, N.W., Zeng, W., Liu, P.-P., Fu, Z.Q., Klessig, D.F., He, S.Y., and Dong, X. (2012). Coronatine promotes *Pseudomonas syringae* virulence in plants by activating a signaling cascade that inhibits salicylic acid accumulation. Cell Host & Microbe **11,** 587–596.

Zhou, Z., Wu, Y., Yang, Y., Du, M., Zhang, X., Guo, Y., Li, C., and Zhou, J.M. (2015). An Arabidopsis plasma membrane proton ATPase modulates JA signaling and is exploited by the *Pseudomonas syringae* effector protein AvrB for stomatal invasion. Plant Cell **27,** 2032-2041.

Zhu, L.J., Gazin, C., Lawson, N.D., Pagès, H., Lin, S.M., Lapointe, D.S., and Green, M.R. (2010). ChIPpeakAnno: a Bioconductor package to annotate ChIP-seq and ChIP-chip data. BMC Bioinformatics **11,** 237.

Zhu, Z., An, F., Feng, Y., Li, P., Xue, L., Mu, A., Jiang, Z., Kim, J.-M., To, T.K., Li, W., Zhang, X., Yu, Q., Dong, Z., Chen, W.-Q., Seki, M., Zhou, J.-M., and Guo, H. (2011). Derepression of ethylene-stabilized transcription factors (EIN3/EIL1) mediates jasmonate and ethylene signaling synergy in Arabidopsis. Proceedings of the National Academy of Sciences of the United States of America **108,** 12539–12544.

SAMENVATTING

Om optimaal te kunnen functioneren moeten planten, net zoals alle andere organismen, anticiperen op veranderingen in hun omgeving. Ter verdediging tegen ziekten en plagen brengen planten hun immuunsysteem in stelling. Moleculen die afkomstig zijn van micro-organismen of insecten, of moleculen die vrijkomen bij beschadiging van plantendelen als gevolg van infectie of vraat, worden herkend door de plant als tekens van potentieel gevaar. Daarop volgend reageert de plant met een adequate afweerreactie die kwaadaardige belagers bestrijdt, of goedaardige organismen juist toegang biedt om een langdurige samenwerking met de plant aan te gaan. De efficiëntie waarmee de plant op de grote verscheidenheid aan micro-organismen en insecten reageert, is bepalend voor hoe goed hij zich kan handhaven in een wisselende omgeving.

Plantenhormonen, en met name de hormonen jasmonzuur (JA) en salicylzuur (SA), zijn belangrijke regelaars van het cellulaire signaleringsnetwerk wat het immuunsysteem van planten aanstuurt. Het hormoon JA is essentieel voor het activeren van de afweer tegen insecten die de plant aanvreten en tegen necrotrofe schimmels en bacteriën die plantencellen vernielen om zich zo toegang tot de nutriënten van de plant te verschaffen. Het hormoon SA activeert met name afweerreacties die gericht zijn tegen biotrofe pathogenen (schimmels, bacteriën, oomyceten), die het geïnfecteerde plantenweefsel intact laten om zo nutriënten uit de plant te onttrekken. Herkenning van micro-organismen of insecten leidt tot veranderingen in hormoonconcentratie en/of -gevoeligheid. Hierdoor worden bepaalde sectoren van de ingenieuze hormoon-gestuurde signaleringsnetwerken geactiveerd of onderdrukt. Via regulatie van genexpressie door onder meer transcriptiefactor eiwitten leidt dit tot productie van specifieke fysische of chemische afweerstoffen die gericht zijn tegen de belagers. Anderszijds wordt doelgericht de groei van de plant tijdelijk afgeremd om afweer te kunnen prioriteren.

Om meer inzicht te krijgen in de verschillende mechanismen in het genreguleringsnetwerk dat aangestuurd wordt door de afweerhormonen SA en JA, is in dit proefschrift op detailniveau bestudeerd hoe de modelplant *Arabidopsis thaliana* (zandraket) reageert op deze hormonen. Hiertoe hebben we de verandering in expressie van alle ~27.000 genen van Arabidopsis bladeren gemeten over een tijdspanne van 16 uur op 14 tijdstippen na toediening van SA of JA. Met behulp van bioinformatische methodieken hebben we vervolgens nauwkeurig de architectuur en dynamiek van de SA en JA genreguleringsnetwerken gekarakteriseerd en beschreven. Met behulp van deze aanpak waren we in staat om te voorspellen welke genen en hun regulerende

transcriptiefactoren op welk moment een belangrijke rol spelen in de door SA en JA aangestuurde immuun signaleringsnetwerken van de plant. Een aantal van deze nieuwe componenten is nader experimenteel onderzocht en hun functie in het afweersysteem van de plant is blootgelegd. Deze expressiestudies zijn een waardevolle bron van nog vele andere voorheen onbekende regulatoren, waarvan we de doelgenen kunnen voorspellen, en potentieel bijdragen aan de immuunrespons.

We hebben 3611 genen geïdentificeerd die werden geactiveerd of onderdrukt door JA toediening over de periode van 16 uur waarin we hebben gemeten (Hoofdstuk 2). SA behandeling leidde tot verandering in expressieniveau van 9524 genen (Hoofdstuk 3). De reactie op de hormonen was zeer snel geïnduceerd: 90% van alle genen die reageerden deed dat binnen 2 uur op JA behandeling en binnen 5 uur op SA behandeling. Door de genen te clusteren volgens overeenkomstige expressieprofielen over de tijd konden we voorspellen welke transcriptiefactoren verantwoordelijk zijn voor veranderingen in het expressiepatroon. De dynamische JA en SA genreguleringsnetwerken die we op basis van deze informatie hebben geconstrueerd geven inzicht in hoe en wanneer verschillende sectoren binnen het netwerk gereguleerd worden door JA of SA. De bHLH- en WRKY-klasse van transcriptiefactoren bleken dominante regulaars te zijn van respectievelijk de activering en onderdrukking van de JA reactie, en vice versa voor de SA reactie. We vonden echter ook dat specifieke andere transcriptiefactoren, zoals van de ERF-, MYB-, en NAC-klasse, specifieke sectoren in de JA en SA netwerken reguleerden. Voor sommige transcriptiefactoren, zoals MYB59, bHLH27, ERF16, ANAC56 en ANAC90, konden we middels biotoetsen met mutanten van deze transcriptiefactoren een rol in afweer tegen pathogenen of insecten bevestigen. Dubbelmutanten van homologe genen, zoals *myb48 myb59* en *anac61 anac90* vertoonden nog grotere effecten op afweer, wat aangeeft dat effecten van genen vaak gemaskeerd worden door functionele redundantie, en dat het belangrijk kan zijn om homologe genen tegelijkertijd uit te schakelen om de rol van een eiwit (zoals een transcriptiefactor) in een bepaald proces te bestuderen.

Van veel genen is de functie nog onbekend. De gezamenlijke ativiteit van transcriptiefactoren en co-regulatoren orkestreert het signaleringsnetwerk, maar de doelgenen van deze regulatoren, die bijvoorbeeld belangrijk zijn voor de biosynthese of transport van anti-microbiële stoffen, vormen het afweergeschut tegen de belager. In Hoofdstuk 4 onthullen we de functie van een familie van acht kleine genen met een grotendeels onbekende functie, die worden geïnduceerd door SA behandeling en infectie met verschillende pathogenen: de Pathogeen-geïnduceerde Cysteïnerijke transMembraan eiwitten (PCM). Stabiele PCM-overexpressie Arabidopsis-lijnen

vertoonden verhoogde resistentie tegen bepaalde biotrofe pathogenen. Verder hebben transcriptoomanalyses van PCM-overexpressie lijnen een mogelijk verband met ontwikkeling en lichtsignalering blootgelegd. Het werkingsmechanisme van PCM in afweer zou verband kunnen houden met hun cysteïnerijke transmembraan domein waarmee ze zich in de plasmamembraan vestigen en daar misschien de membraanstructuur veranderen of met andere eiwitten interacteren, maar dit behoeft verder onderzoek.

Het werk wat in dit proefschrift beschreven staat biedt nieuwe inzichten in hoe planten hun afweerreactie reguleren na inductie van JA of SA signalering. Een rol voor nieuwe transcriptiefactoren en PCM eiwitten in verdediging tegen verschillende type belagers is vastgesteld. We hebben aangetoond dat onze onderzoeksmethode heel effectief is voor het ontdekken van nieuwe eigenschappen van de plant die een bijdrage kunnen leveren aan ziekteresistentie. De nieuwe ontdekkingen geven een goede basis voor verder onderzoek en kunnen leiden tot toekomstige gewassen die beter bestand zijn tegen ziekten en plagen.

ACKNOWLEDGEMENTS

This is the part of my thesis where I will try to express my gratitude with words for those who contributed to my professional and personal development. Words are not enough to express all my thankfulness, but I will use them in this acknowledgment.

Corné, many thanks for replying to my email and accepting me in your group five years ago. During our first meeting through Skype, I told you I did not have any molecular background, but you said it was not a problem and that you could easily teach me. And now, here I am. Moreover, your support during my entire PhD journey was speechless. Your patience and generosity with "the foreigners" are really important for those who are so far away from home. Nowadays, I even appreciate your insults because, somehow, they let me grow. I wish you all the best in the world, It was an honor to work with you.

I also would like to thank Saskia, for all the patience and helping with my writing, you were always trying to help me to improve my skills and showing that I still have a lot to learn. I also appreciate all your spontaneity. Unfortunately, our NAC project did not work (for now), but our work together is not finished, and we can always start a new project again.

I owe most of my scientific lab skills to Marcel, there are not enough words for that, you trained me in the beginning with advanced techniques, you had the patience and the teaching skills to instruct me with many complicated protocols, but the most important lesson was quite simple, just keep doing until you learned, thank you for all of that.

I also would like to say some words to my "British brother", Richard, your help, and supervision were very important to finish my thesis, especially for the bioinformatic support and translating the "jungle English" for the "Royal Queen's English". Also thank you for showing me the British etiquette and the "cuckoo" coffee/lunch breaks.

Peter, Roeland, Ronnie and Guido thank you for your advice during my half-year reports and for nice scientific discussions. Peter thank you for a simple way to see life. Guido, thank you for sharing your experience with the companies. Ronnie thank you for making me think outside of the box and give me different perspective of the facts. Roeland, thanks for your friendship when I just arrived in PMI, showing me the Primus and teaching me how to count in Dutch, together with Nora. Also, thanks to all other PMI staff, Hans thank you for your willingness to always solve the problems in the lab and

for taking beautiful pictures. Anja, Miek, Joyce and Kim thank you for answering my questions about how things run in the lab and about the rules I need to follow so that everything stays organized. I also would like to thanks Fred in the greenhouse for all support and nice conversation and all the cleaning ladies for all their hard work in cleaning the offices and the lab.

Thanks to PMI, I met my other family, Ke, Silvia and Giannis. We were split by the oceans, but we were together again in Utrecht. It were unforgettable times, so much fun and fights, as a family should be, we tolerated each other, because we love each other. Ke, your hard work was always an example, also your responsibility with the family and your sense of justice was always an inspiration. Silvietta, mi hai reso una persona migliore, ero un ragazzo della giungla e ora sono una persona pronta a vivere nella società, grazie mille per avermi salvato la vita in Italia e per tutta la gentilezza. Te avrai sempre un posto nel mio cuore. Giannis, file, thank you for guiding me since the beginning of my PhD, your experience was always helpful, thanks for the cultural discussions and enlighten me with ancient Greek knowledge. I also would like to thank "La compagnia" (the EvP girls) for the nice moments we had, all the dinners, trips, and parties. Chrysa, thank you for all the food you cooked and nice parties you gave in your house, Elaine thanks for all the kindness and nice gifts from USA. Sara, brigidina, sei una persona che è arrivata nella mia vita da poco, ma sembra che noi già ci conosciamo da molto tempo. Siamo stati insieme nella difficoltà, ma mal comune mezzo gaudio. Il tuo aiuto e tutto il tuo sostegno sono stato fondamentale per finire la mia tese, ho molto da ringraziare, mi hai accolto nel 34C e mi hai aiutato nel momento difficile. Por ora vado un po' lontano da te, ma non tanto! ma la nostra camminata è solo all'inizio e di sicuro torneremo a stare vicino di nuovo.

Thanks for The Basis, Ivan (aka el cojo matador), Roeland, Giannis, Richard, Diederik, Pim (the first) and many others. Those were legendary times of The Basis, also unforgettable moments in third half at Olympos, thank you all.

I am also grateful to my students: Pedro, Max, Stijn, Vera, Cristina, Nicole, Jacopo and Raquel. Due to your efforts, my project progressed, and you also helped me to become a better person, you helped me to improve my ideas and supervision skills. Thank you all and good luck with your future.

I would like to thank the other PMI members, Aster, Dharani, Eline, Erqin, Gilles, Hao, Juan, Joel, Marjolein, Manon, Merel, Niels, Pim (the new), Sanne, Sarah, Sebastian,

Sietske, Shu-Hua, Tijmen, Yang for all the good times we had in the lab and outside of the lab.

I also want to thanks all the previous PMI members: Ainhoa, Alberto, Alexandra, Colette, Claudia, Dongping, Irene, Lotte, Marco, Nicole, Nora, Pauline, Paul, Pim (the first), Tom and Yeling for the nice time in the lab when I started my PhD.

I would also like to thank people from other labs such as Chrysa, Sarah (from EvP), Simone, Amber (from E&B), Paul, Nikkita (from MPF) and Freek (from Microbiology) for all nice discussion and interaction in my two years of IEB council.

Esta parte da tese dedicarei a todos os colegas, amigos e familiares brasileiros. Gostaria de agradecer aos meus orientadores das instituições brasileiras pela as quais tive a honra de estudar; professor Walber, agradeço pelo incentivo pela busca de uma formação no exterior, agradeço também ao professor Machado e Flávio pela ajuda em obter minha posição de doutorado na Holanda.

Gostaria de agradecer também a todos os familiares e amigos que foram sempre de grande ajuda para o alcance desse sonho. Valdeir e Liliane, que considero como segundos pais, os quais foram fundamentais em todo o meu processo educativo e moral, não há palavras pelo quanto sou grato. Aos meus irmãos de coração, Victor e Renan, sua amizade foi sempre de grande valor sendo uma base solidada para o resto da vida. Gostaria também de agradecer ao meu padrinho Adonias, pelo exemplo de seriedade e caráter, os meus primos Anderson e Alex e ao meu tio Marcilio por toda ajuda no começo dos meus estudos e a todos meus demais familiares, muito obrigado.

Por fim, tem um agradecimento especial a minha Avó falecida que foi fundamental na minha criação, ao meu pai, Paulo, que apesar de nosso pouco contato, esteve presente nos momentos de necessidade, e a minha mãe, Marceli, na qual palavras não podem descrever toda minha admiração e gratidão, sua determinação na minha educação me levou onde eu estou hoje, acredito que esta tese também é sua. Por fim, agradeço a Deus, doador de toda a vida.

CURRICULUM VITAE

Marciel Pereira Mendes was born 6 November 1989 in Dourados, Mato Grosso do Sul, Brazil. He started his bachelor study in March 2007 at the Federal University of Grande Dourados (UFGD), Mato Grosso do Sul, Brazil. In the first year of his bachelor, he received a fellowship to start an internship at the Laboratory of Phytopathology laboratory under supervision of Prof. Walber Luiz Gavassoni. For his work on soybean rust he was honored with the best junior scientist prize by the UFGD. In the last year of his bachelor study he performed a final internship at the Federal University of Viçosa (UFV), Viçosa, Minas Gerais, Brazil, at the Laboratory of Nematology under supervision of Prof. Rosângela D'Arc de Lima Oliveira. After he finished his bachelor in 2011, he started to work as a research assistant at Syngenta until 2012. In the same year, he started his master in Phytopathology at the Federal University of Lavras (UFLA), Lavras, Minas Gerais, Brazil, under supervision of Prof. José da Cruz Machado to work on seed pathology. In 2014 he was granted with a PhD fellowship from the Brazilian Federal Government, Science Without Borders program to start his PhD research at the Plant-Microbe Interactions at Utrecht University under supervision of Prof. Corné Pieterse, Dr. Saskia van Wees and Dr. Richard Hickman. His PhD research on the molecular and functional analysis of novel regulators of plant defense hormone signaling is described in this thesis. After his graduation, he will continue working as a postdoctoral researcher at the Catholic University of Leuven (KU Leuven) in Leuven, Belgium.

LIST OF PUBLICATIONS

Nascimento, J.M., Gavassoni, W.L., Bacchi, L.M.A., Zuntini, B., **Pereira Mendes, M.**, Leonel, R.K., Pontim, B.C.A. (2012). Association of adjuvants with picoxystrobin + cyproconazole for Asian soybean rust control. *Summa Phytopathologica***,** vol. 38, no.3.

Hickman, R., Van Verk, M.C., Van Dijken, A.J.H., **Pereira Mendes, M.**, Vroegop-Vos, I.A., Caarls, L., Steenbergen, M., Van der Nagel, I., Wesselink, G.J., Jironkin, A., Talbot, A., Rhodes, J., De Vries, M., Schuurink, R.C., Denby, K., Pieterse, C.M.J., and Van Wees, S.C.M. (2017). Architecture and dynamics of the jasmonic acid gene regulatory network. *The Plant Cell* 29**,** 2086-2105.

Nascimento, J.M., Gavassoni, W.L., Bacchi, L.M.A., Oliveira, J.L., Laborde M.C., Pontim, B.C.A and **Pereira Mendes, M.** (2018). Asian soybean rust control with fungicide sprays initiated at pathogen detection or later. *Agrarian*, v.11, n.39, p. 42-49: 1984-2538.

Pereira Mendes, M., Hickman, R., Pieterse, C.M.J., Van Wees, S.C.M. Hormonal signaling in the plant holobiont. *solicited review, in preparation*.

Hickman, R., **Pereira Mendes, M.**, Van Verk, M.C., Van Dijken, A.J.H., Vroegop-Vos, I.A., Denby, K., Pieterse, C.M.J., and Van Wees, S.C.M. Transcriptional dynamics of the salicylic acid response and its interplay with the jasmonic acid pathway, *in preparation*.

Pereira Mendes, M., Hickman R., Van Verk M.C., Nieuwendijk N., Pieterse, C.M.J., and Van Wees., S.C.M. A role for pathogen-induced cysteine-rich transmembrane proteins (PCMs) in defense against biotrophic pathogens, *in preparation*.